



Durham E-Theses

Comparative analyses of rodent and human brain in ageing and disease using novel NMDAR-2B selective probes

Sheahan, Rebecca Louise

How to cite:

Sheahan, Rebecca Louise (2007) *Comparative analyses of rodent and human brain in ageing and disease using novel NMDAR-2B selective probes*, Durham theses, Durham University. Available at Durham E-Theses Online: <http://etheses.dur.ac.uk/2290/>

Use policy

The full-text may be used and/or reproduced, and given to third parties in any format or medium, without prior permission or charge, for personal research or study, educational, or not-for-profit purposes provided that:

- a full bibliographic reference is made to the original source
- a [link](#) is made to the metadata record in Durham E-Theses
- the full-text is not changed in any way

The full-text must not be sold in any format or medium without the formal permission of the copyright holders.

Please consult the [full Durham E-Theses policy](#) for further details.

Chapter 4

Ligand Autoradiographical Comparison of Ro 25,6981 and CP-101,606 in Normal Human Ageing and Dementia with Lewy Bodies

4.1. Introduction

The NMDA receptor is implicated in normal neuronal development (section 1.12), normal ageing (section 1.11) and neurological diseases (section 1.15, 1.16, 1.17) where changes in learning and memory may occur. Neurotoxicity may occur by over stimulation of the NMDA receptor due to excess excitatory amino acids, consequently raising intracellular calcium to damaging levels (Piggott *et al.*, 1994).

A number of NMDA receptor antagonists have been developed and used for the treatment of neurological diseases in patients. However, all of these drugs have been failed in clinical trials either because of intolerable side effects or lack of medical efficacy (Wang & Shuaib, 2005). Understanding of the molecular structure of NMDA receptors has considerably increased, thus providing a new generation of NR2B subtype-selective antagonist congeners, based on the basic structure of Ifenprodil and Eliprodil. It is hoped that these NR2B subtype-specific antagonists will have superior therapeutic implications in disorders such as epilepsy, stroke, traumatic brain injury, Alzheimer's disease, Parkinson's disease, neuropathic pain and psychiatric disorders such as anxiety and depression, but which lack the unwanted cognitive and motor side-effects (Nikam & Meltzer, 2002). NMDA receptor inhibition is used as a therapeutic strategy to prevent dramatic increases in extracellular glutamate levels resulting from prolonged over-activation of the receptors, which ultimately leads to neuron death. Neuronal apoptosis in this manner plays a major role in the



pathophysiology of PD, AD and DLB, and the NR2B subtype-selective antagonists CP-101,606 and Ro 25,6981 compounds have therefore been chosen for this study.

In PD, glutamatergic hyperactivity, secondary to the primary loss of dopamine, is thought to play a role in the pathophysiology of the disease. Evidence suggests glutamatergic pathways involving the subthalamic nucleus, medial globus pallidus, substantia nigra pars reticula, basal ganglia and corticostriatal structures become overactive (DeLong, 1990; Calabresi *et al.*, 1993; Tossman *et al.*, 1986). NMDA receptors are widespread throughout these structures and thus may mediate many of the pathophysiological side-effects (Nikam & Meltzer, 2002). Recent studies provide evidence for the ability of NMDA receptor blockade to alleviate the symptoms of parkinsonism and augment the effectiveness of dopaminergic therapy. They have also demonstrated that in some paradigms NMDA antagonists can prevent or reverse the induction of levodopa-related motor complications.

Dementia with lewy bodies (DLB) is a primary, neurodegenerative dementia sharing clinical and pathological characteristics with both PD and AD (McKeith *et al.*, 2003) (see 1.16). The presenting feature for DLB patients is usually cognitive decline (Barber *et al.*, 2001) but there is often a relative preservation of short-term memory (McKeith, 2002). NMDA receptor antagonists maybe used as drug therapies to alleviate cognitive, psychiatric and motor disabilities, using the same rationale as for PD patients (Hallet & Standaert, 2004). Several studies have implicated the NR2B subunit to be an important target in the treatment of the dementia component of DLB. For example, a preliminary study by Piggott *et al* (1992) provided evidence that NMDA receptors with pharmacological properties indicative of the NR1/NR2B subtype also decrease, in comparison to other subtypes, in aged humans. Clayton *et al* (2002) used animal models to demonstrate that reduced LTP and inferior cognitive performance correlated with a

decreased NR2B subunit expression with age. Over-expression of the forebrain NR2B subunit in transgenic mice (see 1.6.2) has been shown to have profound beneficial effects upon cognitive performance (Tang *et al.*, 1999). *In situ* hybridisation experiments carried out by Bai *et al* (2004), showed a significant overall decrease in the mRNA expression of the NR2B subunit in the prefrontal cortex and caudate nucleus between young and old macaque monkeys. Magnusson & Cotman (1993) showed similar results using aged mice.

Structure-activity relationship (SAR) studies of Ifenprodil analogues aimed at increasing potency and selectivity for NMDA receptors led to some second generation highly potent and selective NR2B antagonists. The work of Pfizer and Roche produced considerable advancement in this field, providing amongst others, the compounds CP-101,606 and Ro 25,6981 respectively. CP-101,606 has been shown to be a potent neuroprotectant selective for forebrain neurons. Autoradiography indicated the CP-101,606 binding site is located in forebrain, most notably in hippocampus and the outer layers of cortex (Menniti *et al.*, 1997). The systemic administration of CP-101,606 reduced parkinsonian symptoms in both haloperidol-treated rats and MPTP-lesioned non-human primates (Steece-Collier *et al.*, 2000). Its pharmacological profile has been widely reviewed (Nikam & Meltzer, 2002; Chazot *et al.*, 2002; Chazot, 2000; Menniti *et al.*, 1998; Chenard & Menniti, 1999).

Fischer *et al.* (1997) studied the characteristics of the interaction between Ro 25,6981 and NMDA receptors in a variety of different tests *in vitro*. They demonstrated that Ro 25,6981 is a highly selective, activity-dependant blocker of NMDA receptors that contain the NR2B subunit, with potent neuroprotective effects *in vitro*. Mutel *et al* (1998) studied the *in vitro* binding properties of [³H]Ro 25,6981 in rat brain using autoradiography. They detected a high density of binding sites in several layers of the cerebral cortex, in the hippocampus, dentate gyrus, caudate putamen, medium densities in the globus pallidus, thalamus, spinal cord dorsal horn and motoneurons, whereas the cerebellum, pons and medulla were poorly

labelled. Previous studies by Hawkins *et al.* (1999) have shown that Ro 25,6981 binds both NR1/NR2B and NR1/NR2A/NR2B receptors with similar high affinities, suggesting that Ro 25,6981 is an NR2B-selective compound, irrespective whether complexed with other NR2 subunit types. Preliminary evidence from studies by Brimecombe *et al.* (1997) and Chazot *et al.* (2002) suggest that CP-101,606 is NR2B selective and displays distinct pharmacological selectivity to Ro 25,6981, in that it may be influenced by the presence of other NR2 subunit types within the receptor complex.

Autoradiography of slide mounted post-mortem brain tissue provides a high resolution image of localised receptor binding, showing neuroanatomical detail between brain regions. In this study, autoradiographical techniques (Mutel *et al.*, 1998) were carried out on a series of human control and diseased brain slices using the radiolabelled ligands [³H]CP-101,606 [(1S,2S)-(4-[³H]hydroxyphenyl)-2-(4-hydroxy-4-phenylpiperidino)-1-propanol], and [³H]Ro 25,6981 (R-(R*,S*)-α-(4-[³H]hydroxyphenyl)-β-methyl-4-(phenylmethyl)-1-piperidine propanol]. The slices were taken from striatal and cortical sections of the brain. Spermidine, used to define specific binding of the radioligand (Hawkins *et al.* 1999), is an endogenous polyamine. Yoneda *et al.* (1991) showed that [³H]spermidine binds specifically to brain membranes and that this binding is displaced totally by unlabelled spermine and spermidine (Nicolas & Carter, 1994).

The aim of this study was to investigate the abundance and distribution of the NMDA NR2B subunit protein in DLB, PDD, DLBPDD, AD cases and respective controls, as well as any differences between the two NR2B radioligands used. The binding levels of Ro 25,6981 would be predicted to be higher in general than those of CP-101,606 due to their suggested distinct NR2B subtype selectivities previously described. The aim was to show any binding site distribution patterns between control and diseased tissue, and also any age-related changes there may be. The hypothesis was that the number of NR2B receptors

would decrease with age in control cases and the diseased cases would display lower NR2B subunit levels than the respective age-matched controls, and there would be a correlation with MMSE scores.

4.2 Methods

4.2.1 Cases used

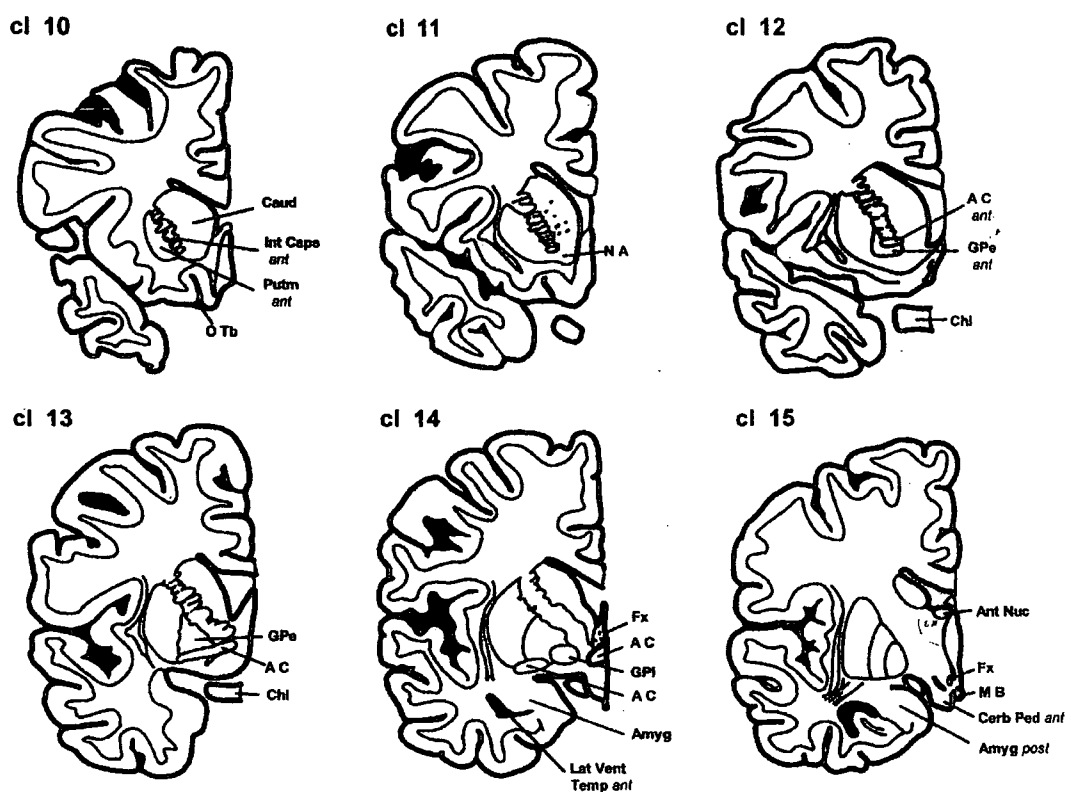
The 83 cases chosen for this study were at the level of the striatum (caudate nucleus and putamen) corresponding to coronal brain levels 9-15 using the Coronal Map of Brodmann Areas in the Human Brain (Perry 1993) (see figure 4.1). 29 of these were control cases showing no evidence of neurological or neuropathological disorder. 22 of these were DLB cases, 12 were DLBPDD cases, 9 were PDD cases, while 11 were AD cases each determined by pathological and clinical diagnosis (see Table 4.1). See also Table 4.2 for age-adjusted data sets for more accurate comparisons between the disease states.

	<u>n =</u>			<u>Age (years)</u>			<u>PM Delay (hours)</u>		
	<u>Total</u>	<u>Females</u>	<u>Males</u>	<u>Range</u>	<u>Mean</u>	<u>SD</u>	<u>Range</u>	<u>Mean</u>	<u>SD</u>
Control	29	17	12	62-91	77.79	7.69	8-96	39.57	23.48
DLB	22	7	15	69-92	81.27	6.22	4-65	38.25	21.29
DLBPDD	12	7	5	64-89	75.83	6.34	10-85	42.42	25.83
PDD	9	2	7	65-86	75.56	7.35	7-77	36.75	20.65
AD	11	7	4	78-91	84.18	4.29	10-82	30.73	20.84

Table 4.1 Summary of the 83 cases chosen for the study. (SD = standard deviation of either age or PM delay values. PM delay = post mortem delay, that is, time between death and freezing of the tissue, to allow for post-mortem examination).

	<u>n =</u>			<u>Age (years)</u>		
	<u>Total</u>	<u>Females</u>	<u>Males</u>	<u>Range</u>	<u>Mean</u>	<u>SD</u>
Control	26	15	11	67-91	79.39	6.36
DLB	22	7	15	69-92	81.27	6.22
DLBPDD	10	7	3	72-89	77.7	4.95
PDD	7	1	6	71-86	78	6.27
AD	10	6	4	78-87	83.5	3.84

Table 4.2 Summary of Cases with adjusted age-ranges and mean age values for comparison between control and disease state data sets.



Reproduced with kind permission of IAH Newcastle-upon-Tyne.

Figure 4.1: Coronal levels of striatum, 0.5 cm apart. AC = anterior commissure; Amyg = amygdala; Ant Nuc = anterior nucleus of thalamus; *ant* = anterior; Caud = caudate; Cerb Ped = cerebral peduncle; Chi = optic chiasma; cl = coronal level; Fx = fornix; GPe = external globus pallidus; Gpi = internal globus pallidus; Int Caps = internal capsule; Lat Vent Temp = temporal horn of lateral ventricle; MB = mammillary body; NA = nucleus accumbens; O Tb = olfactory tubercle; *post* = posterior; Putm = putamen

4.2.2 Tissue Isolation

At post-mortem, brains were divided into two hemispheres. The right hemisphere was fixed in formalin for neuropathological assessment and the left hemisphere was sliced coronally into 1cm slices. The slices were sealed in airtight polythene, rapidly frozen in Arcton at -70°C and cooled further over liquid nitrogen. The frozen tissue slices were stored at -80°C . Prior to sectioning, tissue slices were warmed to 15°C and blocks containing the striatum were sub-dissected and mounted onto cryostat chucks with 8% carboxymethylcellulose. Coronal sections were cryostat sectioned at a thickness of 20 microns using a Brights OTF cryostat, from a total of 83 dissected post-mortem brains obtained from the Newcastle-Upon-Tyne brain bank. Slides were prepared so that adjacent sections from each case were exposed to each of the two ligands used. For each case, 5 replicates were cut to measure 3 total and 2 non-specific radioligand binding. Cryostat sections from snap-frozen human brain tissue were thaw mounted onto Vectabond-coated glass slides, air dried for 1-2 hours and stored at -80°C prior to receptor autoradiography.

4.2.3 NMDA R2B receptor autoradiography

The autoradiographical method used was that essentially described by Mutel *et al.* (1998), with some modifications made. Tissue sections were brought to room temperature (1 hour) and incubated in approximately 4 litres of pre-incubation buffer (section 2.3.15) for 2 x 10 minutes at room temperature. Each section was then incubated in a total volume of 1.7ml buffer (medium size slides) or 1.4ml buffer (small size slides) containing 2 x K_D (10nM) (Chazot *et al.* 2002) [^3H]CP-101,606 (specific activity = 29.6Ci/mmol, stored at -20°C) from Dr. Menniti (Pfizer, Groton, USA), or 2 x K_D (18.8nM) (Hawkins *et al.* 1999) [^3H]Ro 25,6981 (specific activity = 25.6 Ci/mmol, stored at -20°C) from Dr. J. Kemp and

colleagues (Hoffmann LaRoche, Switzerland) for 90 minutes at 4°C, until equilibrium is reached. Non-specific binding was determined in the presence of 10mM unlabelled spermidine, an endogenous polyamine (as used by Chazot *et al.*, 2002, rather than 10µM Ro 04, 5595, as by Mutel *et al.*, 1998). The reaction was terminated by three washes in 50mM Tris-HCL buffer pH 7.4 at 4°C (2 x 5 minutes and 1 x 15 minutes) using approximately 1 litre of buffer per wash. This was the optimal rinse time to produce the maximal relative specific binding. After the three buffer washes, slides were briefly dipped in ice-cold distilled water (2 seconds) and then dried in a stream of cold air for 1-2 hours. The sections were then transferred to X-ray cassettes, each including tritium autoradiographic microscales as calibration standards, and exposed against tritium-sensitive Hyperfilm for 6 weeks at 4°C. The exposed films were then developed in D-19 developer (Kodak) for 5 minutes at room temperature, fixed for 6 minutes in Unifix (Kodak), washed under running tap water for 20 minutes and dried.

4.2.4 [³H]Ro 25,6981 and [³H]CP-101,606

The radioligand concentrations used were greater than those stated by Mutel *et al.* (1998). Preliminary unpublished studies by M. Lake (2002) were carried out using a range of radioligand concentrations. The concentrations of the radioligands used were chosen so they were twice the affinity (K_D) of their specific binding to ensure that each autoradiography run measured an acceptable number of receptor binding sites. The K_D of CP-101,606 is 5nM, and Ro 25,6981 is 9.4nM (Chazot *et al.*, 2002). Therefore 10nM and 18.8nM concentrations were used respectively. Before starting the experiment, the concentration of the incubation buffer containing the radioligand was checked by taking a 100µl aliquot into a scintillation vial with 2ml scintillation fluid (Packard Ultima Gold) and

measuring the dpm (disintegrations per minute) value in a Packard tri-carb 1900CA scintillation counter. All 83 cases were analysed using the [³H]Ro 25,6981 ligand and 25 of these (7 controls, 12 DLB, 3 PDD, 1 DLBPDD and 2 AD cases) were analysed using the [³H]CP-101,606 ligand. The lower numbers of cases used were due to limited supply of [³H]CP-101,606.

4.2.5 Image Analysis

The resulting brain images on the films were captured using a Dage 72 MTI CCD72S video camera and were quantitatively analysed by computer-assisted densitometry using Microcomputer Imaging Device (MCID Elite) version 7.0 software from Imaging research Inc., Ontario, Canada. The radioactive tritium standards were used to calculate a standard curve for each autoradiogram, which allowed the conversion from optical density values to units of concentration (femtomoles per mg of tissue protein), for each brain region analysed. The non-specific tissue sections were present on the same film as each of the corresponding total binding tissue sections for the same case. Specific binding was determined by subtracting mean non-specific binding from mean total binding. Brain structures were identified by reference to the Atlas of the Human Brain (Mai *et al.*, 1997) and the mean and standard deviations for each brain structure in each section were calculated. Inter-assay variability was eliminated by using ligand concentrations that were at least twice the ligand affinity, using ligand from the same batch for each autoradiographical run, and by standardising each film using calibration microscopes.

4.2.6 Statistical Analysis

Statistical analysis performed involved correlation analysis and students unpaired *t*-test, indicated with the use of Microsoft Excel and GraphPad Prism to analyse individual regions of the brain. Statistical significance was set at the $p < 0.05$ level for the correlation analysis, with a minimum *n* value of 5 or more, and at the $p < 0.05$ level for the *t*-tests with a minimum *n* value of 4 or more for each data set. Graphs were constructed using GraphPad Prism version 4. One-way Anova tests were also performed using GraphPad Prism version 4 to analyse statistical differences across data sets. Statistical significance was set at the $p < 0.05$.

4.3 The Mini Mental State Examination (MMSE)

The Mini Mental State Examination (MMSE), validated and widely used since its creation in 1975, is an effective tool for assessing cognitive mental status. The MMSE is used to detect cognitive impairment and monitor response to treatment. It is an eleven question test covering five areas of cognitive function: orientation, attention/calculation, recall and language, and the ability to follow simple verbal and written commands. A score of 23 or below, from a possible 30, indicates cognitive impairment. The test is effective but does have limitations, for example, patients that are hearing and visually impaired or who have low English literacy, or with communication disorders may perform poorly even when cognitively intact (Folstein *et al.*, 1975). The test provides a total score that places the individual on a scale of cognitive function. The values used in this study were those taken at the last assessment before death of the patient.

4.3.1 Mental Test Score (MTS)

The mental test score is used in the psychological assessment of elderly patients, and attempts to quantify the patients' capabilities by assessing a variety of memory and cognition functions. The main areas of assessment are orientation, registration, attention and calculation, recall and language. A 37-item test is used, and is referred to as the Roth-Hopkins test, taking its name from the creators of the test in 1953. An abbreviated 10-item Roth-Hopkins test is also widely used. This is a quicker and better tolerated test, useful in assessing mental impairment in patients in the community as well as in institutional care. A score of less than six in the 10-item test suggests dementia. A score in the range 0-30 in the 37-item list suggests dementia.

4.4 Unified Parkinson Disease Rating Scale (UPDRS)

The UPDRS is a rating tool to follow the longitudinal course of Parkinson's Disease. It is made up of the 1) Mentation, Behaviour and Mood, 2) Activities of Daily Living (ADL) and 3) Motor sections. These are evaluated by interview. Some sections require multiple grades assigned to each extremity. A total of 199 points are possible, where 199 represents the worst (total) disability, and 0 represents no disability. The values used in this study were those taken at the last assessment before death of the patient.

<u>Case</u>	<u>Type</u>	<u>Age</u> (Years)	<u>Sex</u>	<u>Coronal</u> <u>Level</u>	<u>Agonal State</u> 1 = Rapid Death 2 = Prolonged	<u>PM</u> <u>Delay</u> (Hours)
528	control	81	f	10	1	22
980	control	85	m	10	1	23
64.96	control	72	f	13	1	28
975	control	70	m	10	1	50
828	control	80	f	10	1	48
163.9	control	91	f	14	1	48
879	control	85	f	15+	1	96
814	control	86	f	15	1	50
122.94	control	72	f	12	1	32
823	control	85	f	14	1	50
208.95	control	85	m	14	2	10
1010	control	84	m	14	1	76
144.94	control	86	f	13	2	38
909	control	66	f	14	1	24
843	control	76	m	14	1	48
986	control	78	m	10	1	42
839	control	71	m	14	1	96
926	control	78	m	13	2	11
913	control	77	f	14	1	48
97.97	control	71	m	14	2	31
1014	control	67	m	15	1	10
125.94	control	75	f	15	2	31
922	control	84	f	15	1	43
959	control	82	f	9-10	1	15
288.99	control	62	f	11	2	
123.03	control	64	m	13	1	63
907	control	81	f	14	1	51
71.92	control	75	f	10	1	16
96.02	control	87	m	10	1	8

Table 4.3 Details of Control Cases used in the study (n = 29).

In all tables (4.3 – 4.7) all cases were labelled with [³H]Ro 25,6981, only those in red were labelled with [³H]CP-101,606 due to limited ligand availability.

<u>Case</u>	<u>Type</u>	<u>Age</u> (Years)	<u>Sex</u>	<u>Coronal</u> <u>Level</u>	<u>Agonal State</u> 1 = Rapid Death 2 = Prolonged	<u>PM</u> <u>Delay</u> (Hours)
47.98	DLB	70	m	12	1	58
205.95	DLB	85	f	10	1	18
60.98	DLB	77	f	15	1	48
192.96	DLB	79	m	14	1	16
3.98	DLB	87	f	15	1	13
110.96	DLB	84	m	11	1	51
19.98	DLB	79	m	14	1	26
2.01	DLB	87	m	8	1	4
96.93	DLB	75	m	14	1	52
125.97	DLB	86	m	13	1	60
146.97	DLB	84	f	11	1	48
113.03	DLB	77	m	10	1	
155.03	DLB	79	m	11	1	
7.03	DLB	88	f	11	1	
103.03	DLB	73	f	12	1	
80.01	DLB	92	m	10	1	
25.01	DLB	81	m	11	1	
295.99	DLB	89	m	10	1	65
111.03	DLB	81	m	11	1	
4.03	DLB	69	f	14	1	
74.01	DLB	87	m	10	1	
22.04	DLB	79	m	12	1	

Table 4.4 Details of Dementia with Lewy Bodies (DLB) Cases used in the study (n = 22).

<u>Case</u>	<u>Type</u>	<u>Age</u> (Years)	<u>Sex</u>	<u>Coronal</u> <u>Level</u>	<u>Agonal State</u> 1 = Rapid Death 2 = Prolonged	<u>PM</u> <u>Delay</u> (Hours)
991	PDD	86	m	13	1	48
711	PDD	72	m	14	1	7
1030	PDD	84	m	11	1	77
578	PDD	71	f	12	1	36
338.9	PDD	65	f	12	1	24
183.91	PDD	77	m	10	1	36
65.98	PDD	73	m	8	1	24
80.02	PDD	69	m	12	1	
109.91	PDD	83	m	12	1	42

Table 4.5 Details of Parkinson's Disease with Dementia (PDD) Cases used in the study (n = 9).

<u>Case</u>	<u>Type</u>	<u>Age</u> (Years)	<u>Sex</u>	<u>Coronal</u> <u>Level</u>	<u>Agonal State</u> 1 = Rapid Death 2 = Prolonged	<u>PM</u> <u>Delay</u> (Hours)
131.96	DLBPDD	77	f	14	1	23
19.95	DLBPDD	72	f	12	1	10
171.96	DLBPDD	72	f	8	1	24
26.98	DLBPDD	69	m	15	1	11
124.96	DLBPDD	77	m	11	1	60
123.97	DLBPDD	76	f	11	1	24
136.98	DLBPDD	77	m	11	1	33
75.97	DLBPDD	82	f	14	1	75
59.96	DLBPDD	89	f	10	1	64
153.96	DLBPDD	79	f	10	1	64
17.99	DLBPDD	76	m	14	1	85
151.98	DLBPDD	64	m	15	1	36

Table 4.6 Details of Dementia with Lewy Bodies + PDD symptoms (DLBPDD) Cases used in the study (n = 12).

<u>Case</u>	<u>Type</u>	<u>Age</u> (Years)	<u>Sex</u>	<u>Coronal</u> <u>Level</u>	<u>Agonal State</u> 1 = Rapid Death 2 = Prolonged	<u>PM</u> <u>Delay</u> (Hours)
136.95	AD	87	f	14	1	10
194.97	AD	87	m	14	1	15
131.98	AD	83	f	10	1	10
35.97	AD	87	f	11	1	35
172.95	AD	87	f	12	1	28
116.96	AD	78	f	10	1	41
291.99	AD	78	m	9	1	20
279.99	AD	91	f	12	1	17
10.97	AD	84	m	14	1	40
183.96	AD	85	m	11	1	40
19.96	AD	79	f	11	1	82

Table 4.7 Details of the Alzheimer's Disease (AD) Cases used in the study (n = 11).

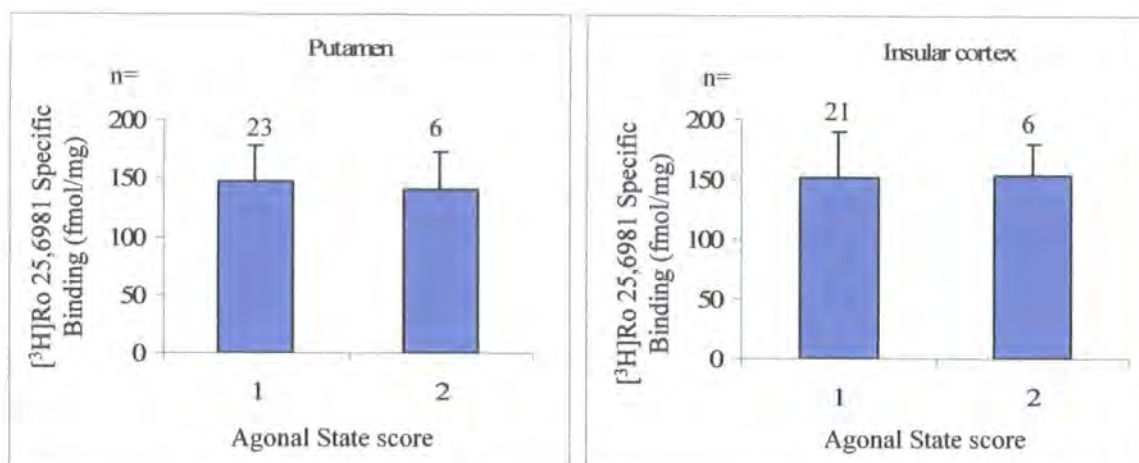


Figure 4.1(a) Agonal State score against [³H]Ro 25,6981 specific binding (fmol/mg) for Control cases, showing (A) Putamen and (B) Insular Cortex. 1=rapid death, 2=prolonged death.

All DLB, PDD, DLBPDD and AD cases had agonal state scores of 1, indicating a rapid death. Therefore there was no comparison to be made between these cases. However, in the control data set, there was a mix of agonal state scores 1 and 2. Figure 4.1(a) shows a comparison of the [³H]Ro 25,6981 binding densities in two representative brain areas (putamen and insular cortex) for both agonal state scores. There was no significant difference seen in the binding densities between agonal state scores and this would suggest that agonal state is not a significant factor in determining density of NR2B-containing NMDA receptors in post-mortem tissue. Rapid or prolonged death does not appear to affect the receptor population in this way.

<u>Case</u>	<u>Type</u>	<u>Age</u> (Years)	<u>Sex</u>	<u>MMSE</u>	<u>UPDRS</u>	<u>Depression</u>	<u>Delusions</u>	<u>Dementia</u>	<u>Vis Hall</u>
47.98	DLB	70	m	9	12		1	2	2
205.95	DLB	85	f	0	0	0	2	2	2
60.98	DLB	77	f	16	12	0	1	1	1
192.96	DLB	79	m		16	1	0	1	2
3.98	DLB	87	f	19	6	0	0	1	0
110.96	DLB	84	m	18	0	0	1	1	2
19.98	DLB	79	m	25	13	0	0	1	1
2.01	DLB	87	m	10	0	0	1	2	1
96.93	DLB	75	m	15	10	0	1	1	1
125.97	DLB	86	m	20	0		0	1	0
146.97	DLB	84	f	20	0	0	0	1	0
113.03	DLB	77	m						
155.03	DLB	79	m						
7.03	DLB	88	f						
103.03	DLB	73	f						
80.01	DLB	92	m						
25.01	DLB	81	m						
295.99	DLB	89	m						
111.03	DLB	81	m						
4.03	DLB	69	f						
74.01	DLB	87	m						
22.04	DLB	79	m						

Table 4.8 Clinical Details of DLB cases.

MMSE = Mini mental state examination score. UPDRS = Unified Parkinson disease rating scale

Depression: 0 = none, 1 = mild, 2 = severe. Delusions: 0 = none, 1 = mild, 2 = severe. Dementia: 0 = none, 1 = mild, 2 = severe.

Vis Hall (visual hallucinations): 0 = none, 1 = mild, 2 = severe.

<u>Case</u>	<u>Type</u>	<u>Age</u> (Years)	<u>Sex</u>	<u>MMSE</u>	<u>UPDRS</u>	<u>Depression</u>	<u>Delusions</u>	<u>Dementia</u>	<u>Vis Hall</u>	<u>MTS</u>
991	PDD	86	m		5			1	0	25
711	PDD	72	m					1		29
1030	PDD	84	m					1	1	33
578	PDD	71	f		5			1	0	
338.9	PDD	65	f					2	1	20
183.91	PDD	77	m				1	1	1	24
65.98	PDD	73	m	21	10		0	1	1	
80.02	PDD	69	m							
109.91	PDD	83	m					2	1	11

<u>Case</u>	<u>Type</u>	<u>Age</u> (Years)	<u>Sex</u>	<u>MMSE</u>	<u>UPDRS</u>	<u>Depression</u>	<u>Delusions</u>	<u>Dementia</u>	<u>Vis Hall</u>
131.96	DLBPDD	77	f	3	9	2	1	2	2
19.95	DLBPDD	72	f	12	15	0	0	2	2
171.96	DLBPDD	72	f	0	10	1	2	2	2
26.98	DLBPDD	69	m	10	7	0	2	2	2
124.96	DLBPDD	77	m	15	9	0	2	1	2
123.97	DLBPDD	76	f	11	10	0	1	2	2
136.98	DLBPDD	77	m		12		1	1	0
75.97	DLBPDD	82	f	1	12	1	2	2	2
59.96	DLBPDD	89	f	1	8	1	1	2	2
153.96	DLBPDD	79	f	22	11	0	0	1	2
17.99	DLBPDD	76	m	21	10	1	0	1	0
151.98	DLBPDD	64	m	14	19		0	1	0

Table 4.9 (above) Clinical Details of PDD cases. Table 4.10 (below) Clinical Details of DLBPDD cases

MMSE = Mini mental state examination score. UPDRS = Unified Parkinson disease rating scale

Depression: 0 = none, 1 = mild, 2 = severe. Delusions: 0 = none, 1 = mild, 2 = severe. Dementia: 0 = none, 1 = mild, 2 = severe.

Vis Hall (visual hallucinations): 0 = none, 1 = mild, 2 = severe.

<u>Case</u>	<u>Type</u>	<u>Age</u> (Years)	<u>Sex</u>	<u>MMSE</u>	<u>UPDRS</u>	<u>Depression</u>	<u>Delusions</u>	<u>Dementia</u>	<u>Vis Hall</u>
136.95	AD	f	87	1	14	0	2	1	2
194.97	AD	m	87						0
131.98	AD	f	83				0	1	2
35.97	AD	f	87	5	4	0	2	1	2
172.95	AD	f	87	14	7	2	0	1	0
116.96	AD	f	78	6	2	2	0	1	0
291.99	AD	m	78	18	2	0	1	1	1
279.99	AD	f	91						
10.97	AD	m	84	16	5	0	2	1	0
183.96	AD	m	85	14	6	0	2	0	2
19.96	AD	f	79	0	2	2	0	1	0

Table 4.11 Clinical Details of AD cases.

MMSE = Mini mental state examination score. UPDRS = Unified Parkinson disease rating scale

Depression: 0 = none, 1 = mild, 2 = severe. Delusions: 0 = none, 1 = mild, 2 = severe. Dementia: 0 = none, 1 = mild, 2 = severe.

Vis Hall (visual hallucinations): 0 = none, 1 = mild, 2 = severe.

4.5 Results

4.5.1 Results (Figure 4.2 to Figure 4.8)

The first section of the results (Figure 4.2 – 4.8) shows a qualitative analysis of the binding data, which is followed in the second section by quantitative analysis of the binding levels in each tissue. Figure 4.2 is given as an example showing the typical pattern of radioligand binding seen in many of the brain sections analysed, in this instance [³H]CP-101,606 has been used. The darker areas indicate those which have been labelled by the radioligands, the greater the intensity, the higher the binding density in that tissue. The section is cut at coronal level 11, see figure 4.1, where the striatal caudate and putamen areas are beginning to separate and the nucleus accumbens is clearly visible. The globus pallidus is not yet apparent at this level. The claustrum can be seen along the outer curved edge of the putamen, and can be used as a good indicator for the orientation of the section. The insular cortex is also well labelled, and has been divided into two, the outer insular cortex has been analysed as a separate region since many sections showed an interesting clearly visible higher binding level than that seen in the insular cortex as a whole. The cingulate cortex is also well labelled and is located on the same side of the striatum as the caudate.

Figures 4.3 to 4.8 show digital photographic examples of both [³H]Ro 25,6981 (left hand side) and [³H]CP-101,606 (right hand side) binding in control, DLB, PDD, and AD cases respectively. In each case figures A and B show the total binding of the radioligand, and the figures C and D show the non-specific binding, defined by 10mM spermidine. As described in section 4.2.5, the specific value is calculated by subtracting mean non-specific binding from mean total binding. In each of the examples shown, ligand binding was seen in the caudate, putamen, nucleus accumbens, insular, outer insular and cingulate cortex regions

and the claustrum. Binding was also observed in the globus pallidus when present in the tissue. The following table is a summary of the images shown.

<u>Figure</u>	<u>Group</u>	<u>Case no.</u>	<u>Coronal level</u>	<u>Age</u>	<u>Sex</u>
4.3	Control	96.02	10	87	m
4.4	Control	959	9 to 10	82	f
4.5	DLB	80.01	10	92	m
4.6	DLB	146.97	11	84	f
4.7	PDD	80.02	12	69	m
4.8	AD	183.96	11	85	m

Table 4.12 Summary of example cases showing digitally photographed images from the autoradiographic films.

4.5.2 Results (Figure 4.9 (A-C) to Figure 4.19). Refer to legends below each figure.

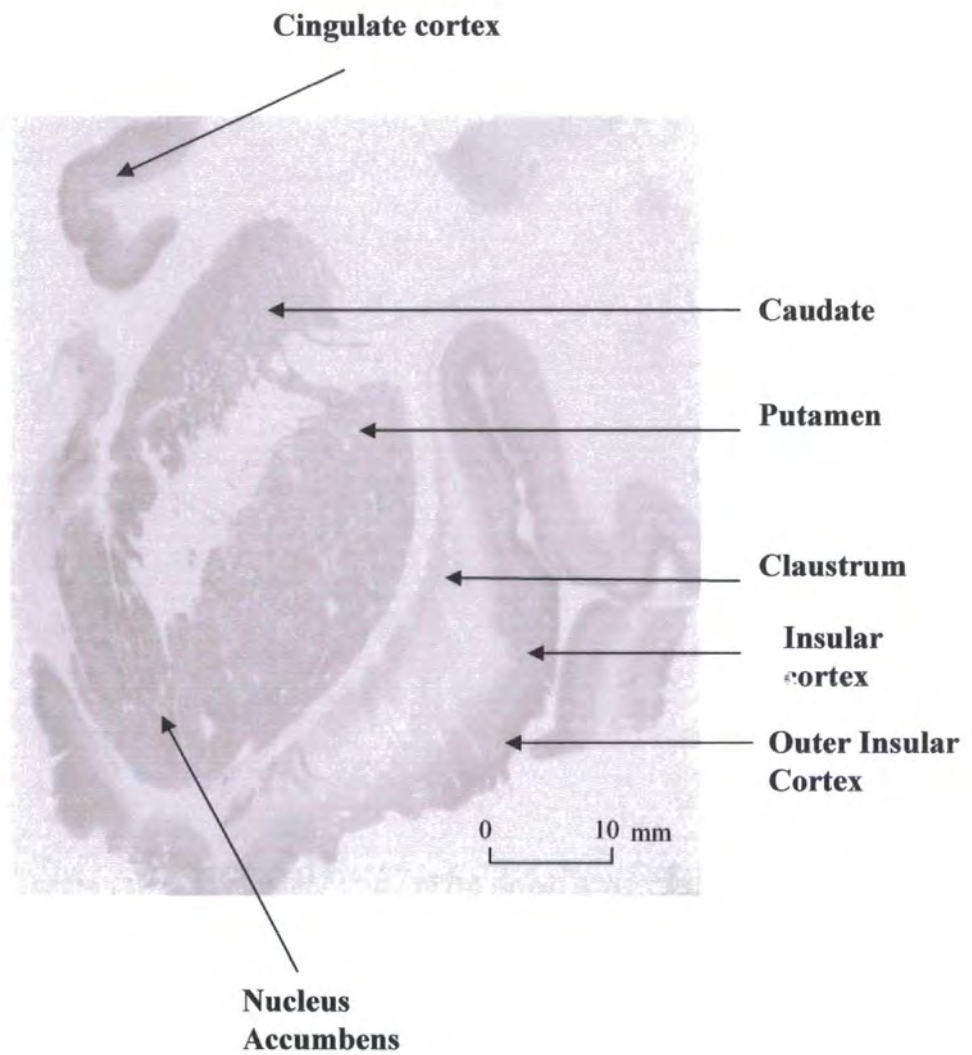


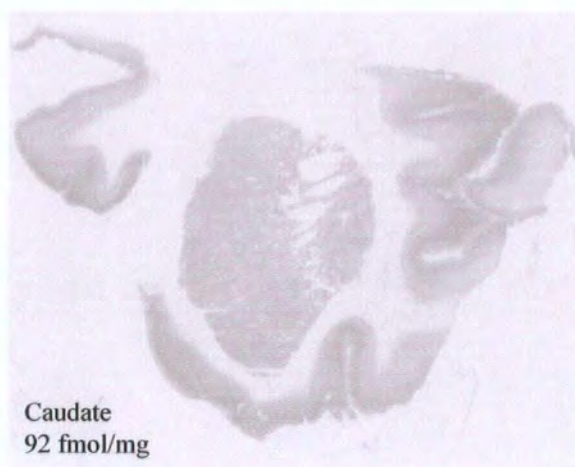
Figure 4.2 Representative Example of a Human brain section (84 years, female) . NR1/NR2B receptors labelled by $[^3\text{H}]\text{CP-101,606}$. Specific binding defined using 10mM spermidine.

[³H]Ro 25, 6981

[³H]CP-101,606

A

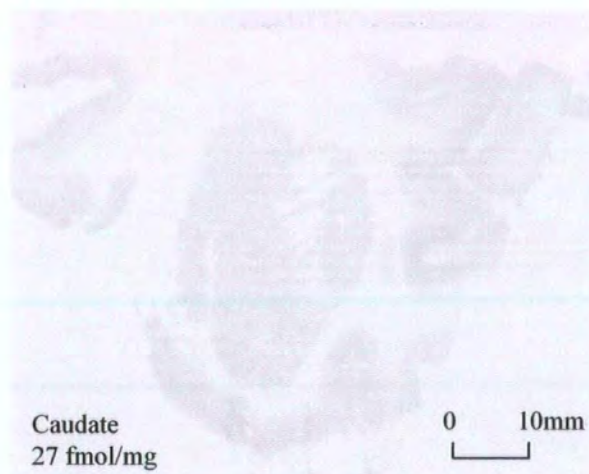
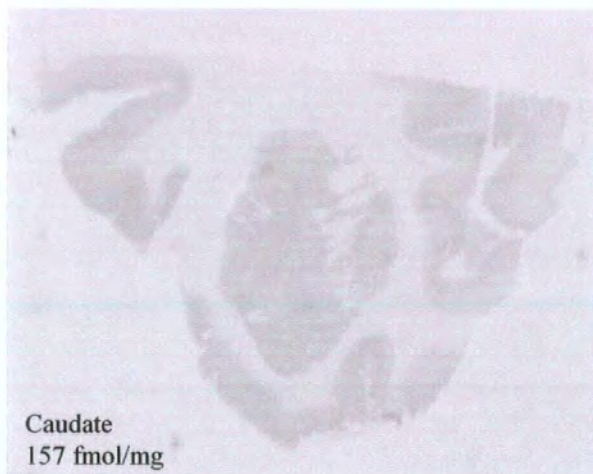
B



Total

C

D



Non-specific

Figure 4.3 (A-D) Autoradiography of Control Human Brain Slices (87 years, male). (A) Total binding [³H]Ro 25,6981, (B) Total binding [³H]CP-101,606, (C) Non-specific binding [³H]Ro 25,6981 and (D) Non-specific binding [³H]CP-101,606. Specific binding defined using 10mM spermidine.

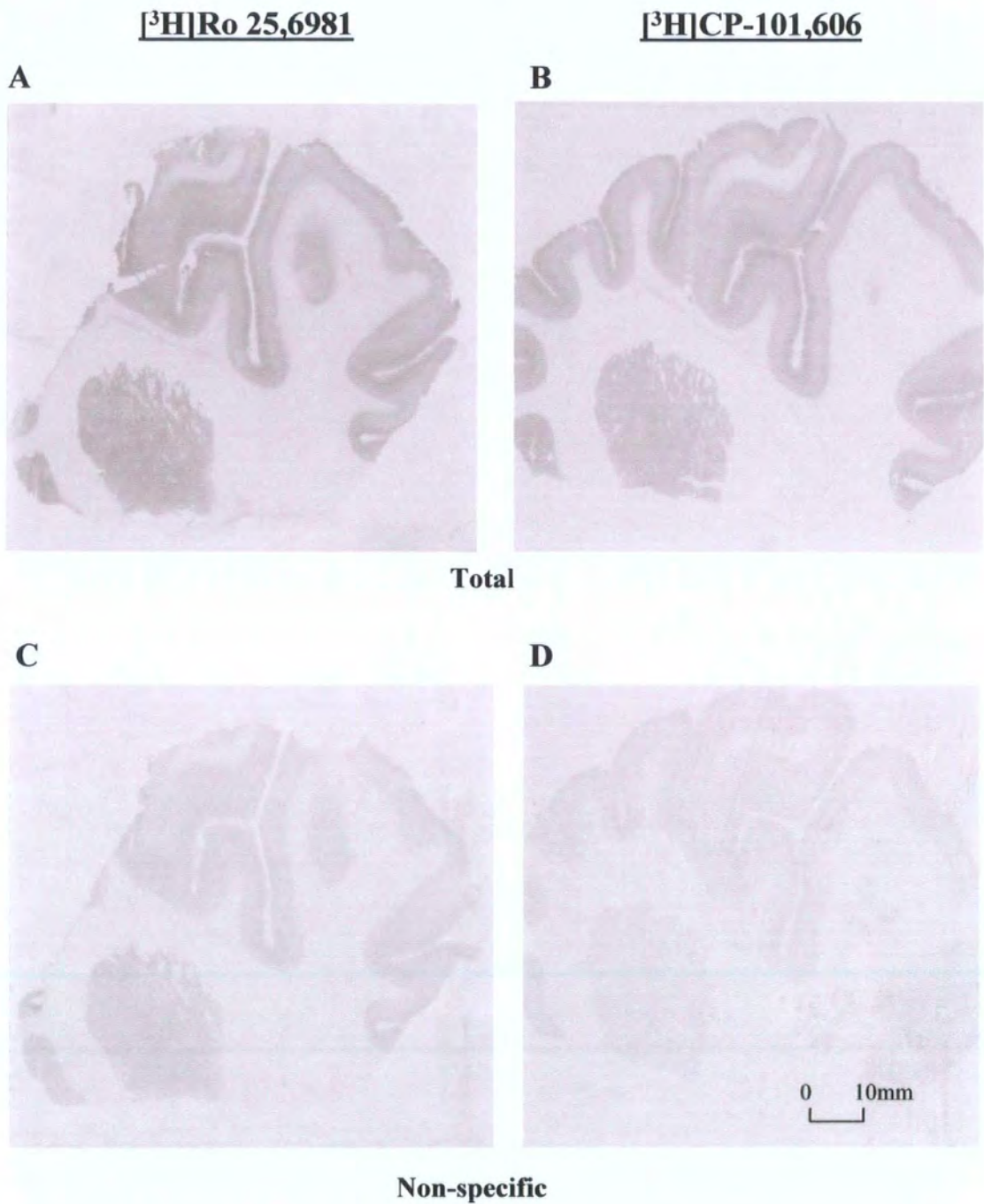


Figure 4.4 (A-D) Autoradiography of Control Human Brain Slices (82 years, female). (A) Total binding [³H]Ro 25,6981, (B) Total binding [³H]CP-101,606, (C) Non-specific binding [³H]Ro 25,6981 and (D) Non-specific binding [³H]CP-101,606. Specific binding defined using 10mM spermidine.

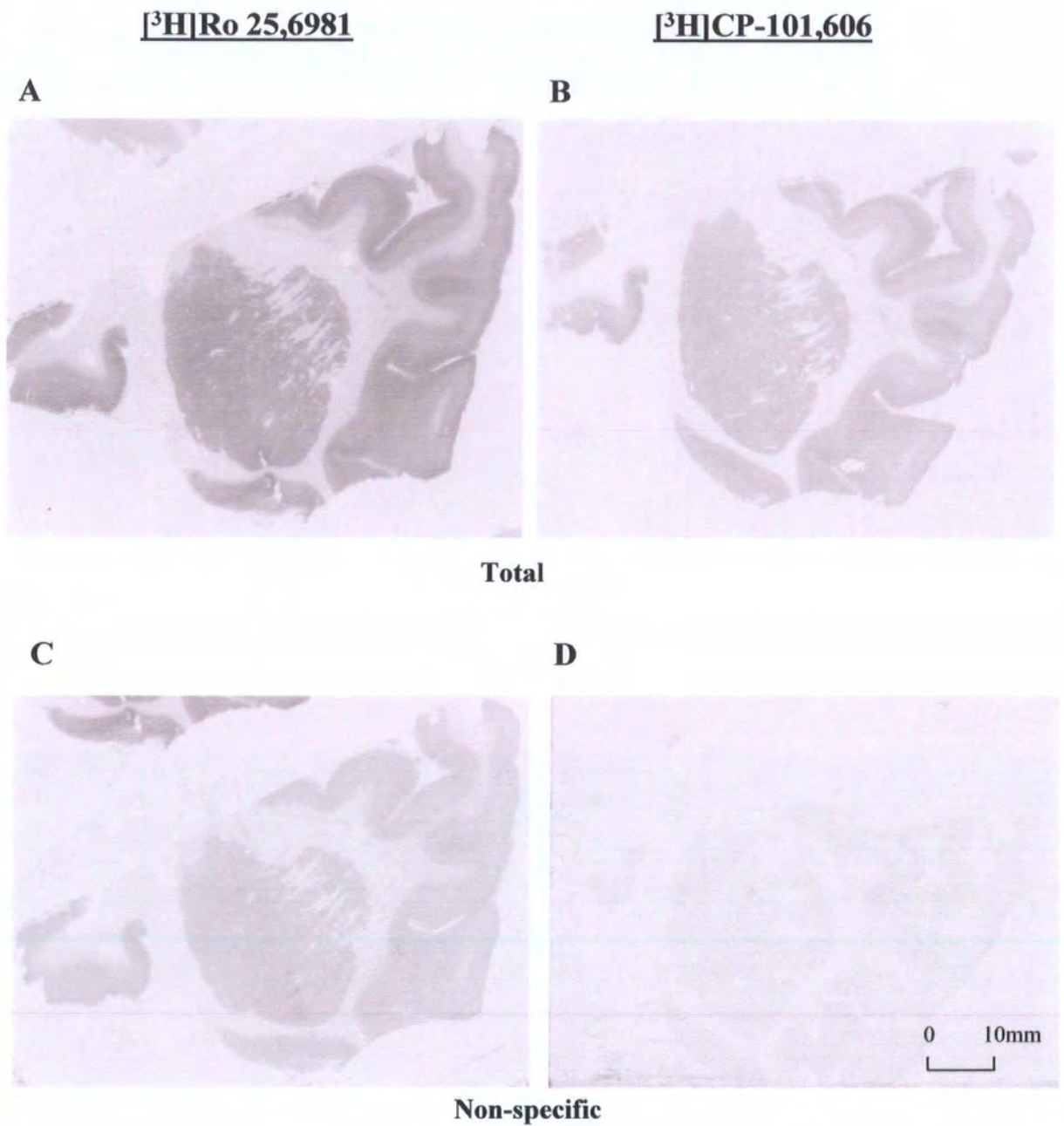


Figure 4.5 (A-D) Autoradiography of DLB Human Brain Slices (92 years, male). (A) Total binding [³H]Ro 25,6981, (B) Total binding [³H]CP-101,606, (C) Non-specific binding [³H]Ro 25,6981 and (D) Non-specific binding [³H]CP-101,606. Specific binding defined using 10mM spermidine.

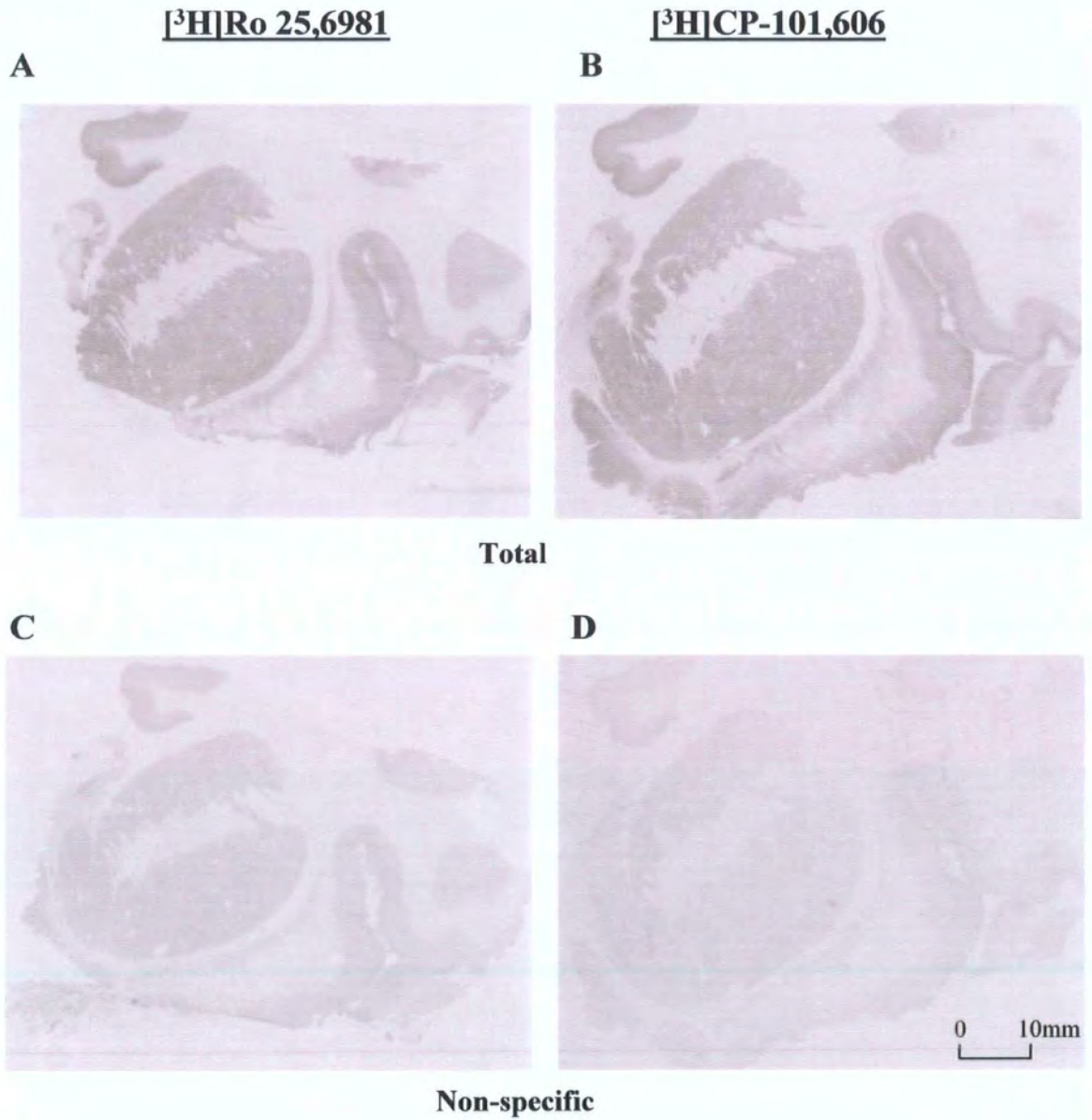


Figure 4.6 (A-D) Autoradiography of DLB Human Brain Slices (84 years, female). (A) Total binding [³H]Ro 25,6981, (B) Total binding [³H]CP-101,606, (C) Non-specific binding [³H]Ro 25,6981 and (D) Non-specific binding [³H]CP-101,606. Specific binding defined using 10mM spermidine.

[³H]Ro 25,6981

[³H]CP-101,606

A



B

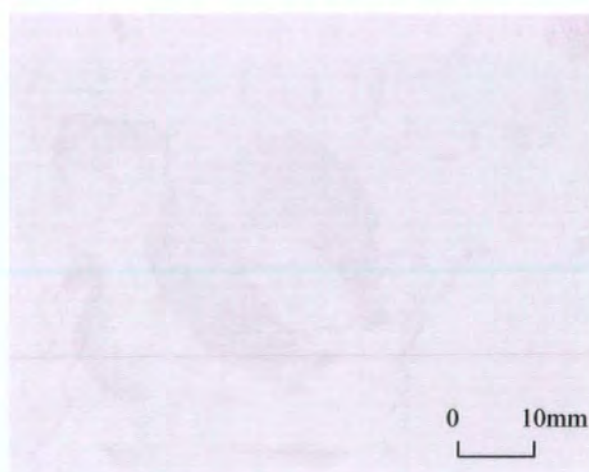


Total

C



D



Non-specific

Figure 4.7 (A-D) Autoradiography of PDD Human Brain Slices (69 years, male). (A) Total binding [³H]Ro 25,6981, (B) Total binding [³H]CP-101,606, (C) Non-specific binding [³H]Ro 25,6981 and (D) Non-specific binding [³H]CP-101,606. Specific binding defined using 10mM spermidine.

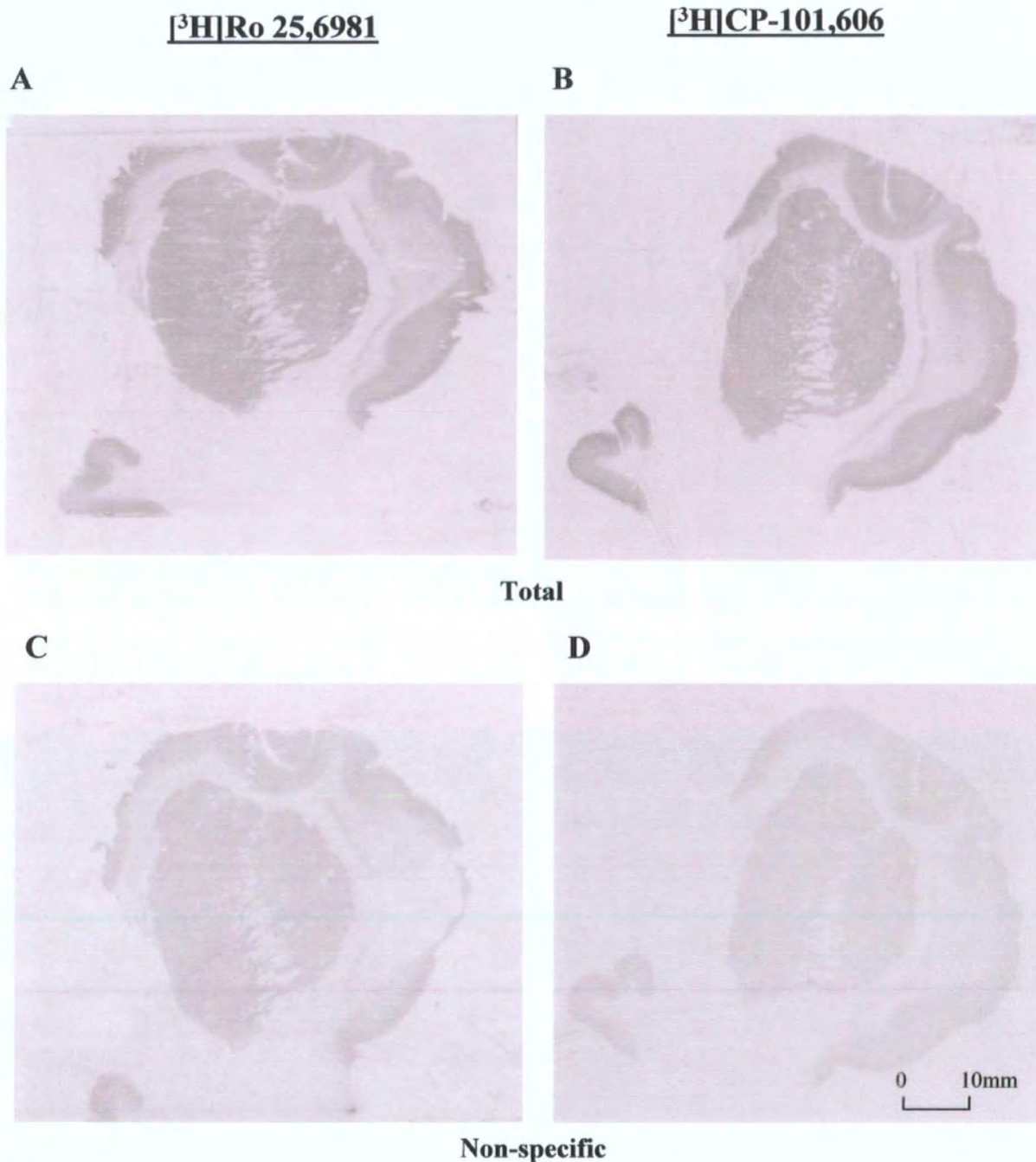


Figure 4.8 (A-D) Autoradiography of AD Human Brain Slices (85 years, male). (A) Total binding [³H]Ro 25,6981, (B) Total binding [³H]CP-101,606, (C) Non-specific binding [³H]Ro 25,6981 and (D) Non-specific binding [³H]CP-101,606. Specific binding defined using 10mM spermidine.

A

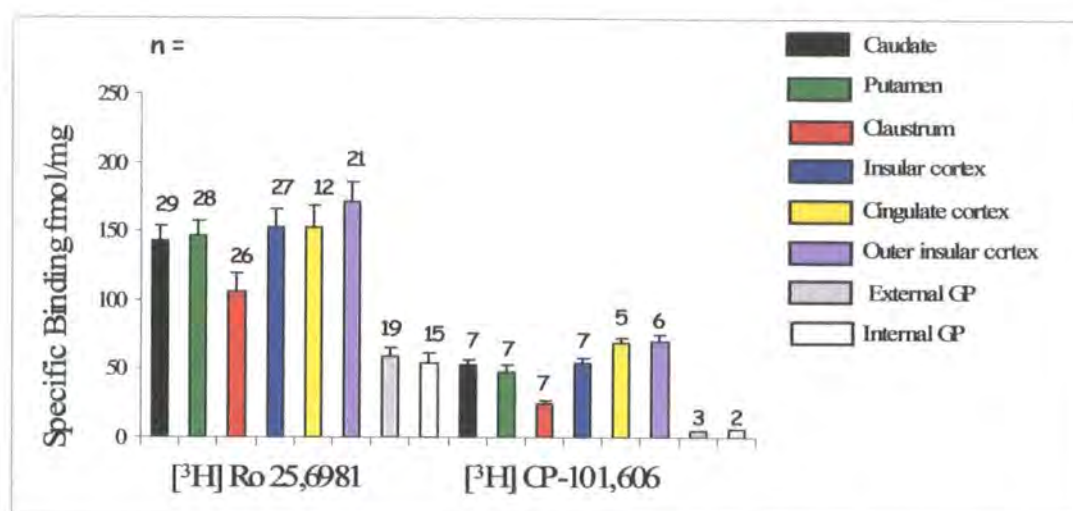


Figure 4.9 (A). Graph showing the significant differences in specific binding (fmol/mg) densities (mean \pm SEM for n determinations) between [³H]Ro 25,6981 and [³H]CP-101,606 in pooled male and female Control cases.

Brain tissue samples from the 29 control cases described in section 4.2.1 and summarised in table 4.1 were assayed for radiolabelled Ro 25,6981 and CP-101,606 binding by autoradiography. As shown in figure 4.9(A), there were significantly higher levels of binding with [³H]Ro 25,6981 than with [³H]CP-101,606 ($p \leq 0.0001$, two-tailed distribution, unpaired t-test) in all 8 brain regions defined. Binding of both radioligands showed differences between the regions analysed, with binding levels in the claustrum, external globus pallidus and internal globus pallidus consistently lower than all other regions for [³H]Ro 25,6981 and [³H]CP-101,606. These data were further analysed for gender differences, see figure 4.9(B,C). Due to low n values in the [³H]CP-101,606 male and female cohorts, external and internal globus pallidus data were excluded. A similar pattern of binding was seen for male and female cases to that of the total cases, showing significantly more binding of [³H]Ro 25,6981 than [³H]CP-101,606 (females $p \leq 0.0003$, males $p \leq 0.004$, two-tailed distribution, unpaired t-test) in all 6 regions defined. There was no evidence for gender bias. Male cases for [³H]CP-101,606 showed similar absolute binding levels to female cases although were not statistically valid due to low n values. All cases were statistically valid where ($n \geq 5$).

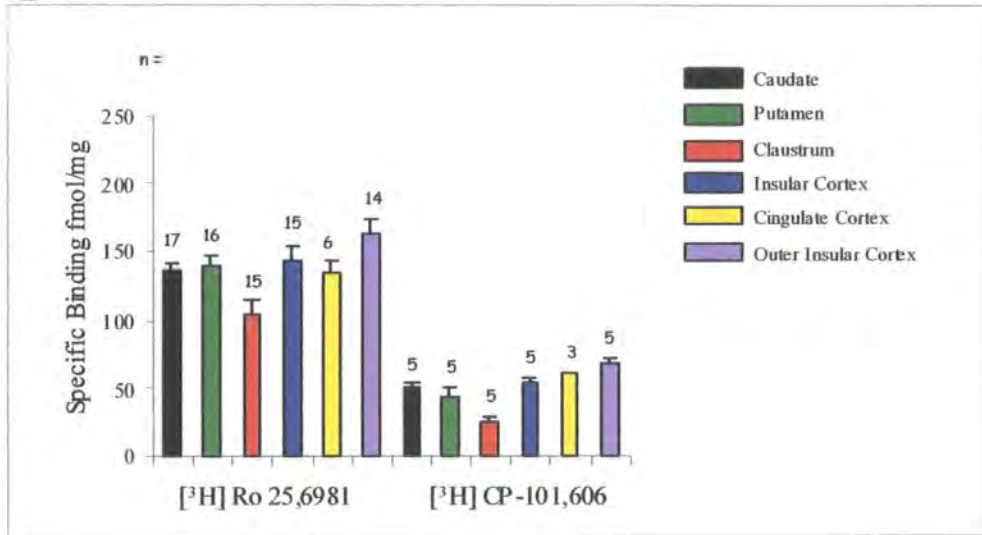
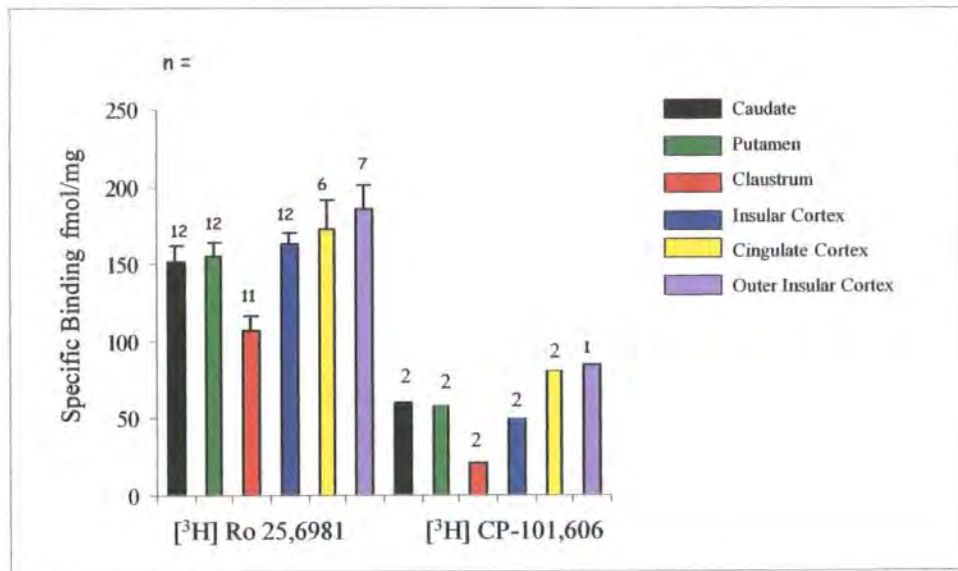
B**C**

Figure 4.9 (B,C) Graph showing the significant differences in specific binding (fmol/mg) densities (mean \pm SEM for n determinations) between [³H]Ro 25,6981 and [³H]CP-101,606 in (B) female and (C) male Control cases.

A

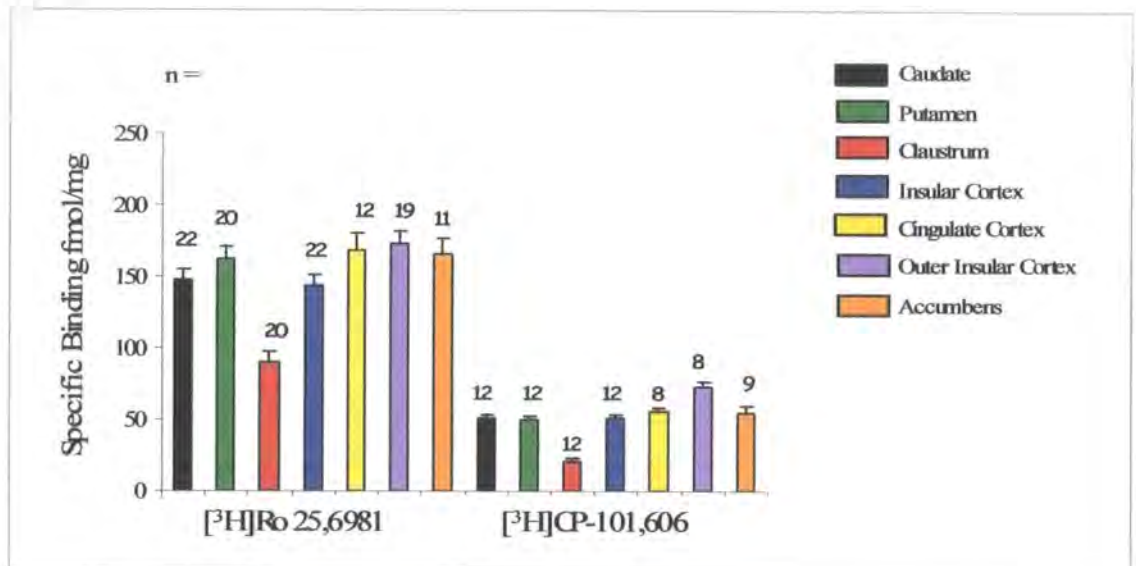
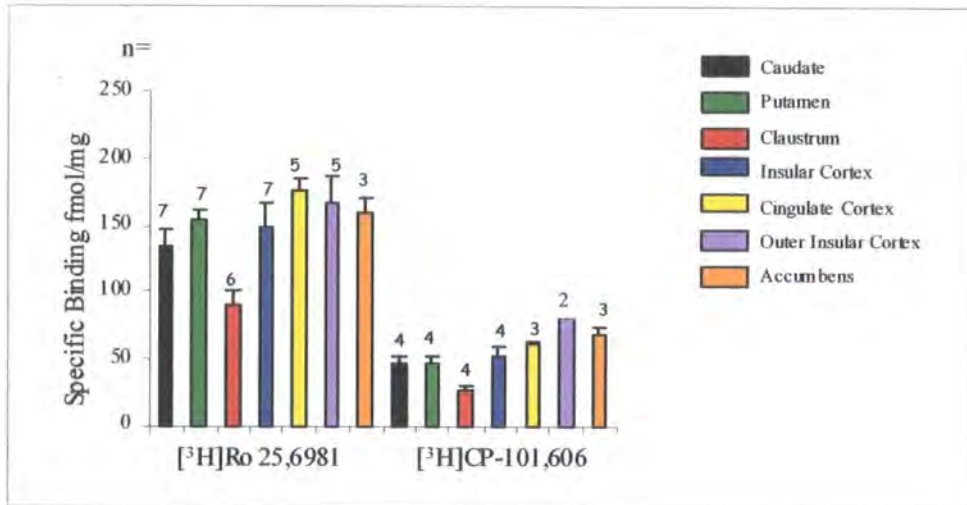


Figure 4.10 (A). Graph showing the significant differences in specific binding (fmol/mg) densities (mean \pm SEM for n determinations) between [³H]Ro 25,6981 and [³H]CP-101,606 in pooled male and female DLB cases.

Brain tissue samples from the 22 DLB cases described in section 4.2.1 and summarised in table 4.1 were assayed for radiolabelled Ro 25,6981 and CP-101,606 binding by autoradiography. As shown in figure 4.10(A), there were significantly higher levels of binding with [³H]Ro 25,6981 than with [³H]CP-101,606 ($p \leq 0.0001$, two-tailed distribution, unpaired t-test) in all 7 brain regions defined. Binding of both radioligands showed differences between the regions analysed, with binding levels in the claustrum consistently lower than all other regions for [³H]Ro 25,6981 and [³H]CP-101,606. These data were further analysed for gender differences, see figure 4.10(B,C). A similar pattern of binding was seen for male and female cases to that of the total cases, showing significantly more binding of [³H]Ro 25,6981 than [³H]CP-101,606 (females $p \leq 0.02$, males $p \leq 0.001$, two-tailed distribution, unpaired t-test) in all 7 regions defined. There was no evidence for gender bias. Female cases for [³H]CP-101,606 showed similar absolute binding levels to male cases although were not statistically valid due to low n values. All cases were statistically valid where ($n \geq 5$).

B



C

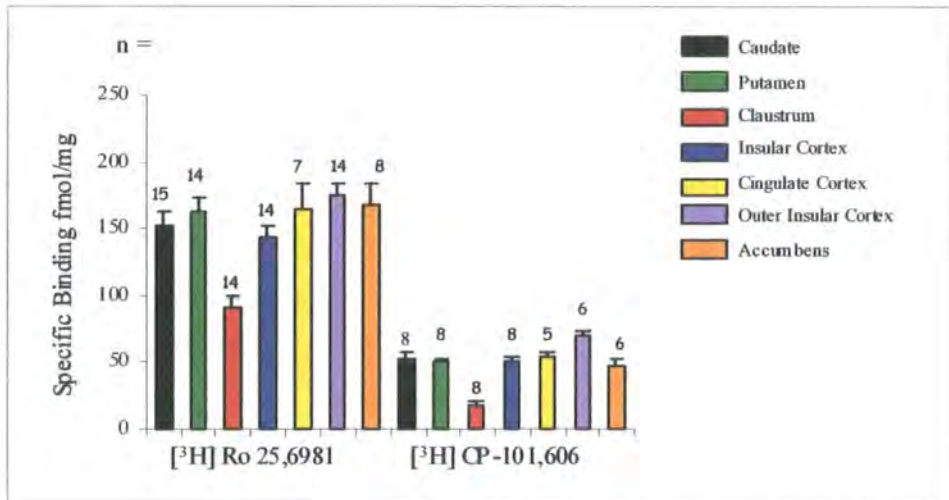


Figure 4.10 (B,C) Graph showing the significant differences in specific binding (fmol/mg) densities (mean \pm SEM for n determinations) between [³H]Ro 25,6981 and [³H]CP-101,606 in (B) female and (C) male DLB cases.

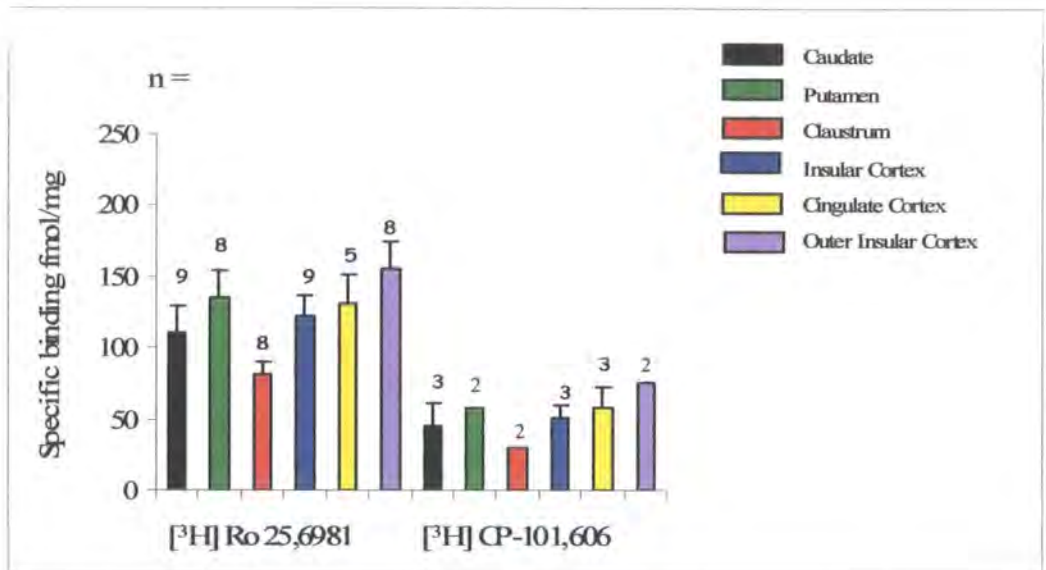


Figure 4.11. Graph showing the significant differences in specific binding (fmol/mg) densities (mean \pm SEM for n determinations) between [³H]Ro 25,6981 and [³H]CP-101,606 in pooled male and female PDD cases.

Brain tissue samples from the 9 PDD cases described in section 4.2.1 and summarised in table 4.1 were assayed for radiolabelled Ro 25,6981 and CP-101,606 binding by autoradiography. As shown in figure 4.11, there were significantly higher levels of binding with [³H]Ro 25,6981 than with [³H]CP-101,606 ($p \leq 0.03$, two-tailed distribution, unpaired t-test) in all 6 brain regions defined. Binding of both radioligands showed differences between the regions analysed, with binding levels in the caudate and claustrum consistently lower than all other regions for [³H]Ro 25,6981 and [³H]CP-101,606. A similar pattern of binding levels was observed across the range of brain regions for [³H]Ro 25,6981 and [³H]CP-101,606. Due to low n values in the CP-101,606 male and female cohorts these data were not further analysed for gender differences as results would not be statistically relevant. All cases were statistically valid where ($n \geq 5$).

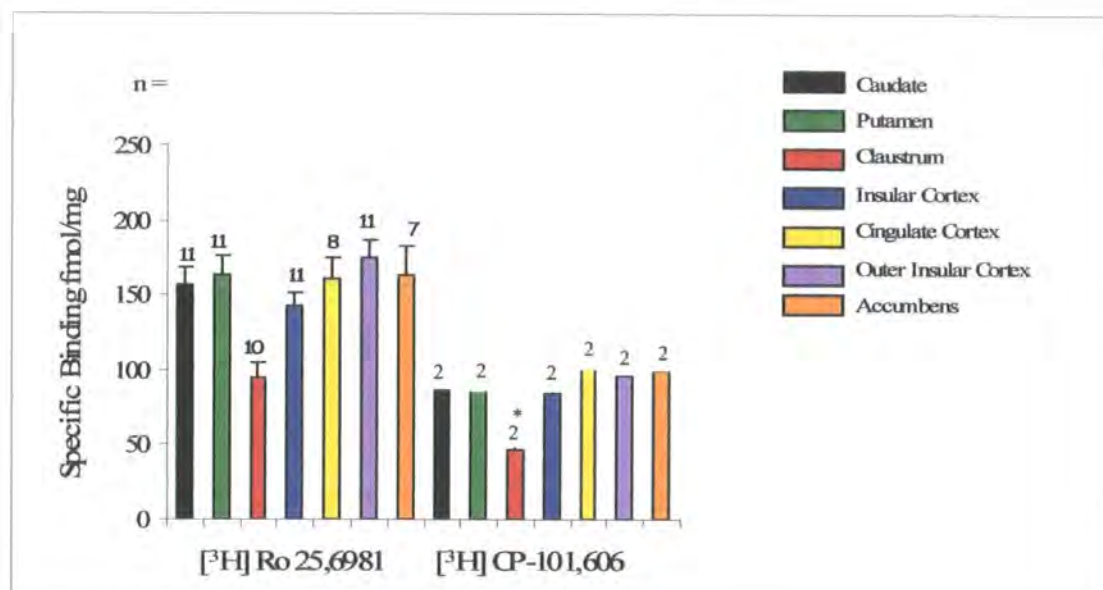


Figure 4.12. Graph showing the significant differences in specific binding (fmol/mg) densities (mean ± SEM for n determinations) between [³H]Ro 25,6981 and [³H]CP-101,606 in pooled male and female AD cases.

Brain tissue samples from the 11 AD cases described in section 4.2.1 and summarised in table 4.1 were assayed for radiolabelled Ro 25,6981 and CP-101,606 binding by autoradiography. As shown in figure 4.12, there were significantly higher levels of binding with [³H]Ro 25,6981 than with [³H]CP-101,606 ($p \leq 0.04$, two-tailed distribution, unpaired t-test) in all brain regions defined except in the claustrum where $p = 0.21$ showing no significance (indicated by *). However, the small n value ($n = 2$) may negate this result. Binding of both radioligands showed differences between the regions analysed, with binding levels in the claustrum consistently lower than all other regions for [³H]Ro 25,6981 and [³H]CP-101,606. A similar pattern of binding levels was observed across the range of brain regions for [³H]Ro 25,6981 and [³H]CP-101,606. Due to low n values in the CP-101,606 male and female cohorts these data were not further analysed for gender differences as results would not be statistically relevant. All cases were statistically valid where ($n \geq 5$).

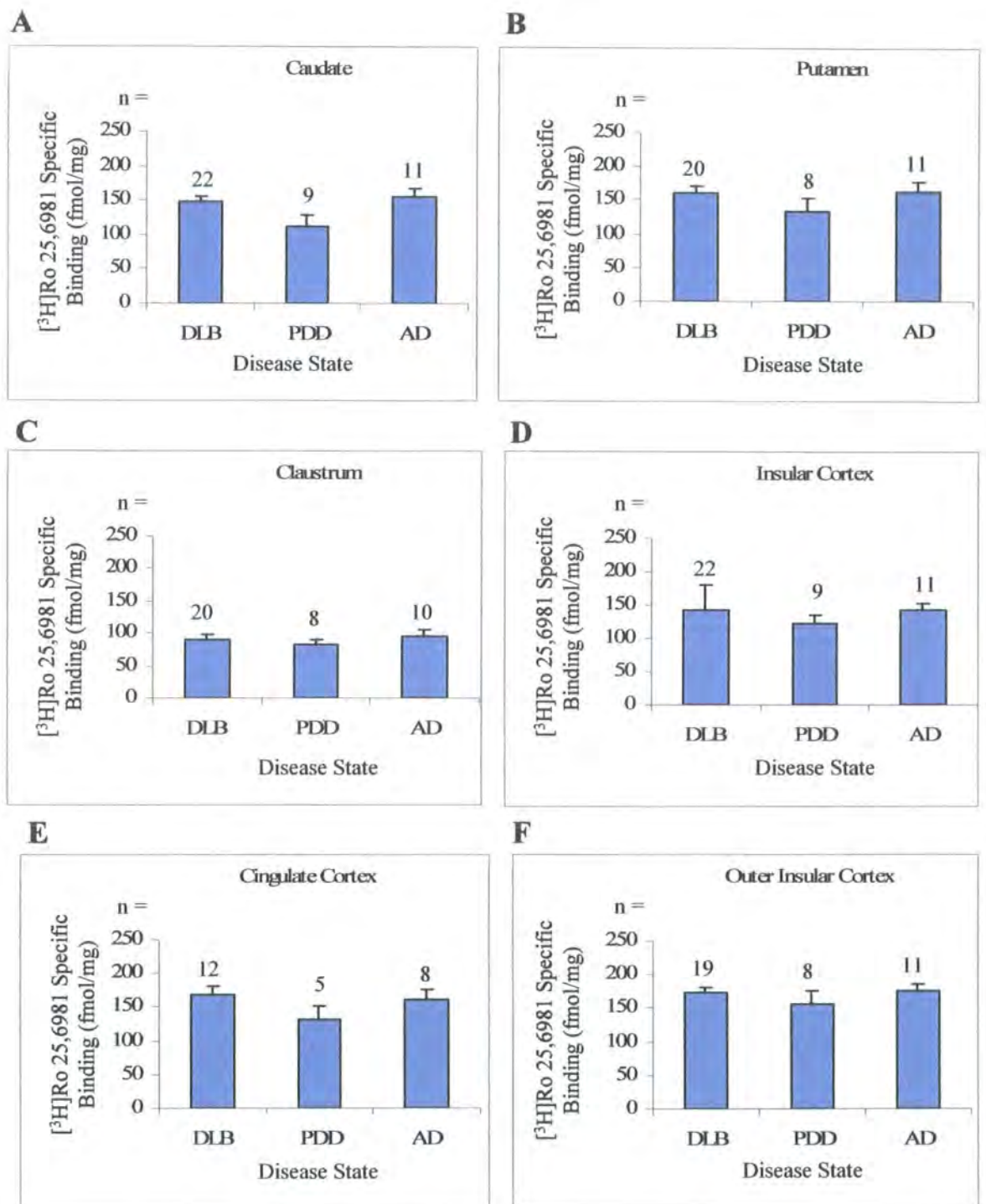


Figure 4.12(a) Graphs showing [³H]Ro 25,6981 specific binding (fmol/mg) densities (mean ± SEM for n determinations) for DLB, PDD and AD cases for (A) Caudate (B) Putamen (C) Claustrum (D) Insular Cortex (E) Cingulate Cortex (F) Outer Insular Cortex and (G) Accumbens.

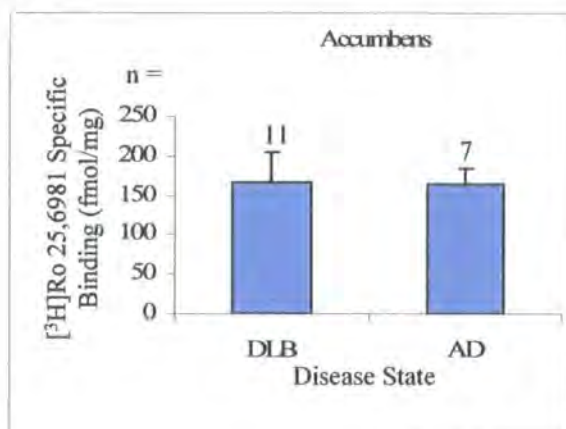
G

Figure 4.12(a) shows there are no significant differences in the binding densities of [³H]Ro 25,6981 in all of the brain areas analysed when comparing between the disease states. On first glance there appears to be a general trend for the binding to be lower in PDD cases in all the regions, although this is not statistically significant. Statistical analysis was performed using a one-way anova test, indicated with the use of GraphPad Prism (version 4) to analyse between disease states in individual regions of the brain. Statistical significance was set at $p < 0.05$ level for the one-way anova analysis.

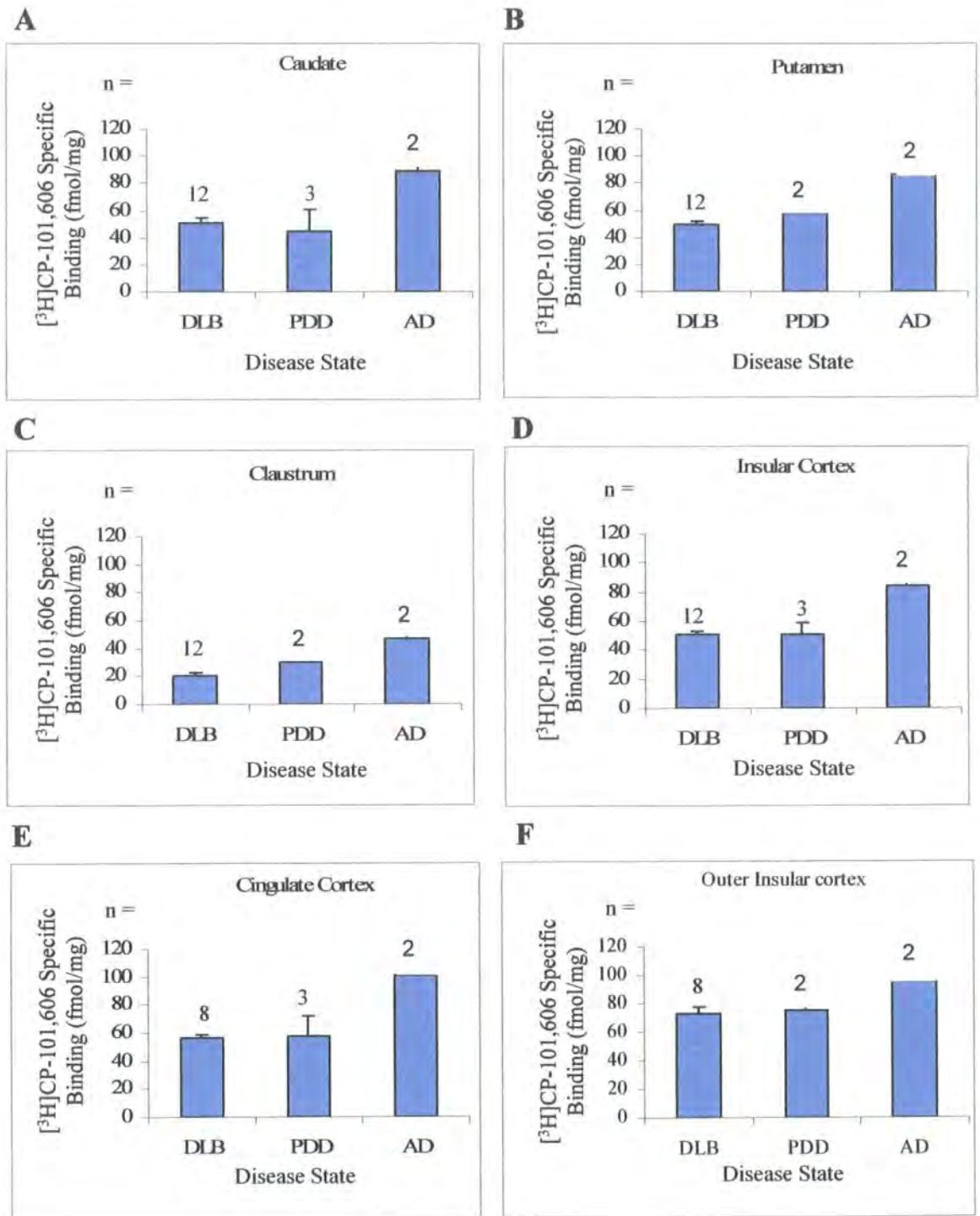


Figure 4.12(b) Graphs showing [³H]CP-101,606 specific binding (fmol/mg) densities (mean ± SEM for n determinations) for DLB, PDD and AD cases for (A) Caudate (B) Putamen (C) Claustrum (D) Insular Cortex (E) Cingulate Cortex (F) Outer Insular Cortex and (G) Accumbens.

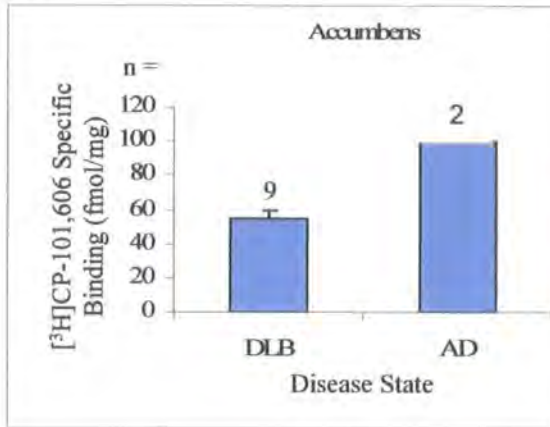
G

Figure 4.12(b) shows that when comparing between the disease states, there are no significant differences in the binding densities of [³H]CP-101,606 in all of the brain areas analysed, with the exception of the cingulate cortex where the AD cases show significantly higher binding than the DLB and PDD cases ($p=0.00$). There would appear to be a general trend for the binding to be higher in AD cases in all the regions, although this was not statistically significant due to the low n numbers. Statistical analysis was initially performed using a one-way anova test (GraphPad Prism) and then a students unpaired t -test, (Microsoft Excel) to analyse individual regions of the brain. Statistical significance was set at $p<0.05$ level for anova and t -test analysis.

(A) Male and Female

	Caudate	Putamen	Clastrum	Insular cx	Cingulate cx	Out ins cx	Ext GP	Int GP	Accumbs	Ro n=	CP n=
Control	38	33	23	35	45	41	8	12		12-29	2-7
DLB	35	31	23	35	34	42			33	11-22	8-12
PDD	41	43	37	42	44	48				5-9	2-3
AD	57	53	49	59	63	55			61	7-11	2

(B) Female

	Caudate	Putamen	Clastrum	Insular cx	Cingulate cx	Out ins cx	Accumbs	Ro n=	CP n=
Control	37	31	24	37	45	42		6-17	3-5
DLB	35	31	30	35	35	50	43	3-7	2-4

(C) Male

	Caudate	Putamen	Clastrum	Insular cx	Cingulate cx	Out ins cx	Accumbs	Ro n=	CP n=
Control	40	38	20	34	47	45		6-12	1-2
DLB	35	31	19	35	33	40	28	7-15	5-8

Table 4.13 (A)-(C)

Percentage Specific Binding of [³H]CP-101,606 relative to [³H]Ro 25,6981 in (A) Male and Female cases, (B) Female cases and (C) Male cases.

4.5.2 Results (Table 4.13 (A-C))

Table 4.13 (A) shows the percentage specific binding of [³H]CP-101,606 relative to [³H]Ro 25,6981 in each of the brain regions analysed for the pooled male and female data in control and disease cases. The main observation from these results is that in all control, DLB and PDD cases and for all brain regions, the percentage binding levels were all less than 50%. Percentages in the control cases ranged from 8% (external globus pallidus) to 45% (cingulate cortex). Percentages in DLB cases ranged from 23% (claustrum) to 42% (outer insular cortex). Percentages in PDD cases ranged from 37% (claustrum) to 48% (outer insular cortex). The AD cases however showed that [³H]CP-101,606 binding levels were proportionately higher than controls, DLB and PDD cases since relative percentages for each region were all greater than 50%, with the exception of the claustrum with 49%. Percentages ranged from 53% (putamen) to 63% (cingulate cortex).

Tables 4.13 (B) and (C) show the same data but divided into female and male cases to see if there is any evidence for gender bias in the relative percentages of [³H]CP-101,606 binding to [³H]Ro 25,6981. Only control and DLB data has been analysed due to low n numbers in the PDD and AD cohorts. In the control cases there was no clear trend, percentages were higher in the female data set in the claustrum and insular cortex, but were higher in the male data set in the caudate, putamen, cingulate cortex and outer insular cortex. In the DLB cases, all relative percentages were either identical in both male and female data sets (caudate, putamen and insular cortex) or there was a bias towards female percentages being higher than the male (claustrum, cingulate cortex, outer insular cortex and accumbens).

A

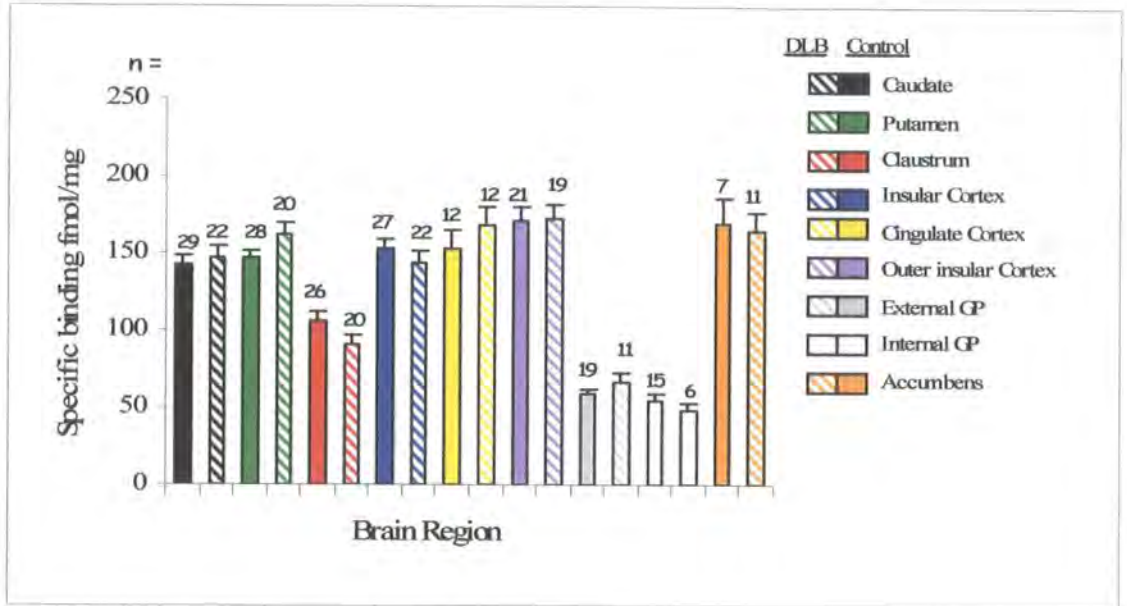


Figure 4.13 (A) Graph showing (mean \pm SEM for n determinations) densities of [3 H]Ro 25,6981 specific binding (fmol/mg) in control and DLB pooled male and female cases in various brain regions.

Brain tissue samples from the 29 control cases and 22 DLB cases described in table 4.1 were assayed for radiolabelled Ro 25,6981 binding by autoradiography. Results of their analysis as previously shown (see graph 4.9 (A-C) and graph 4.10 (A-C)) were combined to assess the potential differences between control and disease state binding levels (fmol/mg) in the brain regions specified. As shown in figure 4.13(A), there were no significant differences in the levels of [3 H]Ro 25,6981 binding between control and DLB cases ($p \geq 0.12$, two-tailed distribution, unpaired t-test) in all 9 brain regions analysed. These data were further analysed for gender differences, see figure 4.13(B,C). A similar pattern of binding was seen across the brain regions for male and female graphs both separately and combined, showing no significant differences between control and DLB cases (females $p \geq 0.47$ with the exception of the cingulate cortex where $p = 0.01$ (indicated by *), and males $p \geq 0.1$, two-tailed distribution, unpaired t-test) in all 9 regions defined. There was no evidence for gender bias except in the cingulate cortex. The claustrum, external and internal globus pallidus binding levels were consistently lower compared to all other regions. All values were statistically valid where $n \geq 5$.

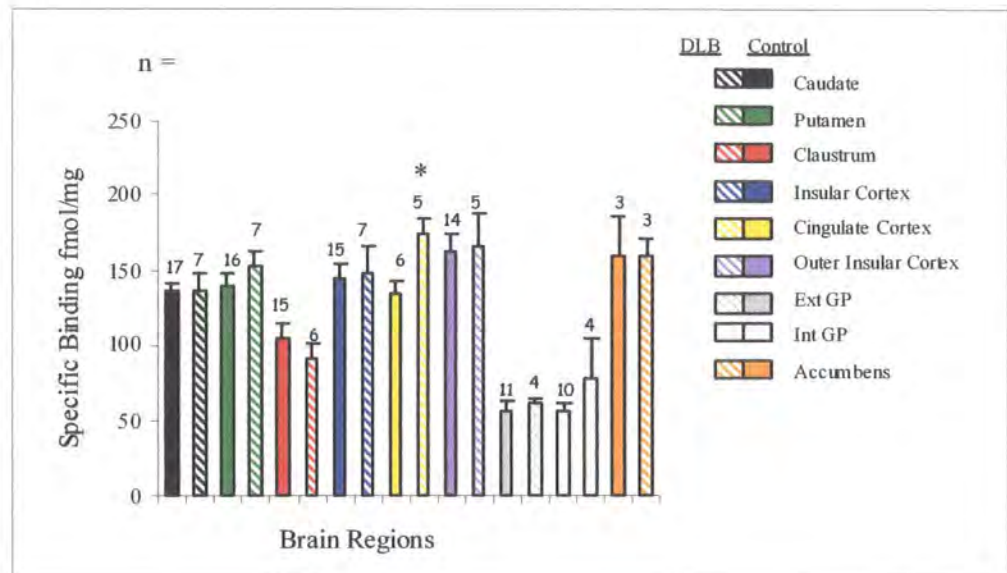
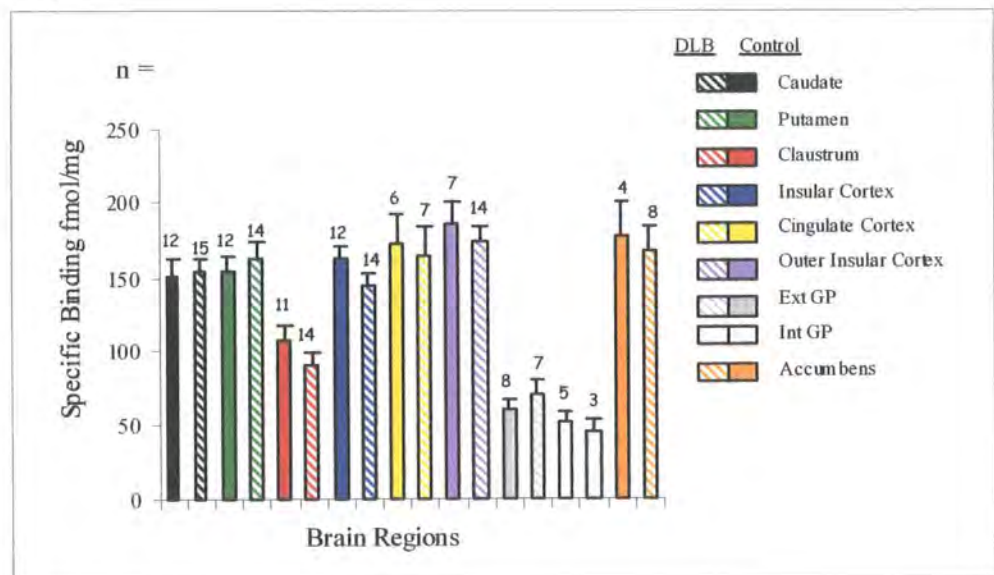
B**C**

Figure 4.13 (B,C) Graphs showing (mean \pm SEM for n determinations) densities of [3 H]Ro 25,6981 specific binding (fmol/mg) in control and DLB in (B) female and (C) male cases in various brain regions.

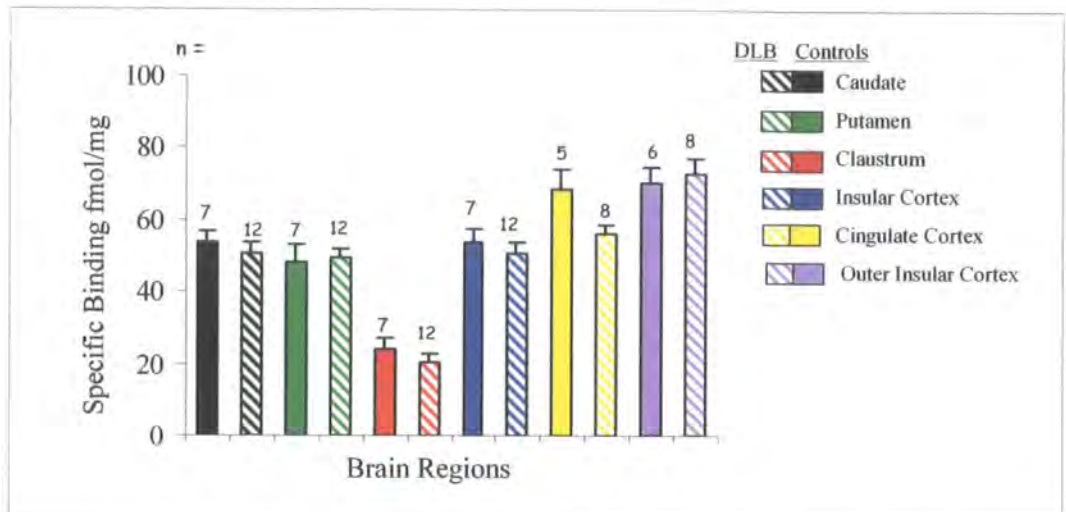


Figure 4.14 Graph showing (mean \pm SEM for n determinations) densities of [^3H]CP-101,606 specific binding (fmol/mg) in control and DLB pooled male and female cases in various brain regions.

Brain tissue samples from the 7 control cases and 12 DLB cases described in table 4.1 were assayed for radiolabelled CP-101,606 binding by autoradiography. Results of their analysis as previously shown (see graph 4.9 (A-C) and graph 4.10 (A-C)) were combined to assess the potential differences between control and disease state binding levels (fmol/mg) in the brain regions specified. As shown in figure 4.14, there were no significant differences in the levels of [^3H]CP-101,606 binding between control and DLB cases ($p \geq 0.11$, two-tailed distribution, unpaired t-test) in all 6 brain regions analysed. Due to low n values in the CP-101,606 male and female cohorts these data were not further analysed for gender differences as results would not be statistically relevant. The claustrum binding levels were consistently lower compared to all other regions. All values were statistically valid where $n \geq 5$.

A

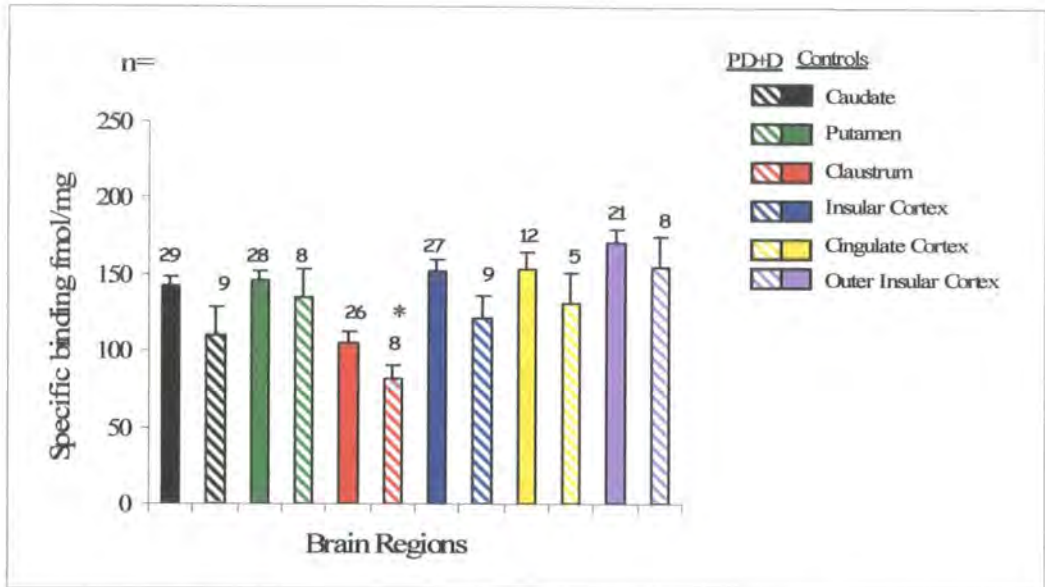


Figure 4.15 (A) Graph showing (mean \pm SEM for n determinations) densities of [3 H]Ro 25,6981 specific binding (fmol/mg) in control and PDD pooled male and female cases in various brain regions.

Brain tissue samples from the 29 control cases and 9 PDD cases described in table 4.1 were assayed for radiolabelled Ro 25,6981 binding by autoradiography. Results of their analysis as previously shown (see graph 4.9 (A-C) and graph 4.11) were combined to assess the potential differences between control and disease state binding levels (fmol/mg) in the brain regions specified. As shown in figure 4.15(A), there were no significant differences in the levels of [3 H]Ro 25,6981 binding between control and PDD cases ($p \geq 0.08$, two-tailed distribution, unpaired t-test) in all brain regions analysed except in the claustrum where $p=0.04$, showing significance (indicated by *). The caudate and insular cortex appear to suggest a higher binding level in the controls compared to PDD cases, although the differences are not statistically significant ($p=0.12$ and $p=0.08$ respectively). This may be due to the considerable difference in n numbers between the two groups.

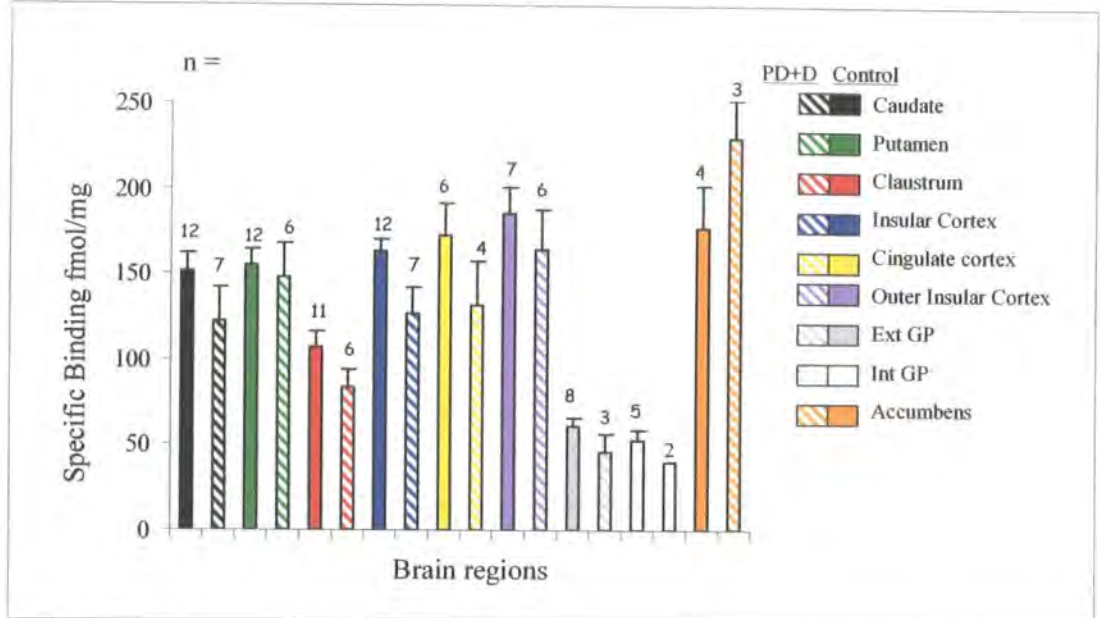
B

Figure 4.15 (B) Graph showing (mean \pm SEM for n determinations) densities of [3 H]Ro 25,6981 specific binding (fmol/mg) in control and PDD male cases in various brain regions.

These data were further analysed for gender differences, see figure 4.15(B). Due to low n values in the Ro 25,6981 PDD female cohort, these data were not further analysed for gender differences as results would not be statistically relevant. A similar pattern of binding was seen across the brain regions for male and combined male and female graphs, showing no significant differences between control and PDD cases (male $p \geq 0.06$, two-tailed distribution, unpaired t-test) in all 9 regions defined. There appears to be a trend for higher binding in the controls in the caudate, claustrum and insular cortex, although this is not statistically significant since $p=0.23$, $p=0.11$ and $p=0.06$ respectively. There was no evidence for gender bias. The claustrum, external and internal globus pallidus binding levels were consistently lower compared to all other regions. All values were statistically valid where $n \geq 5$.

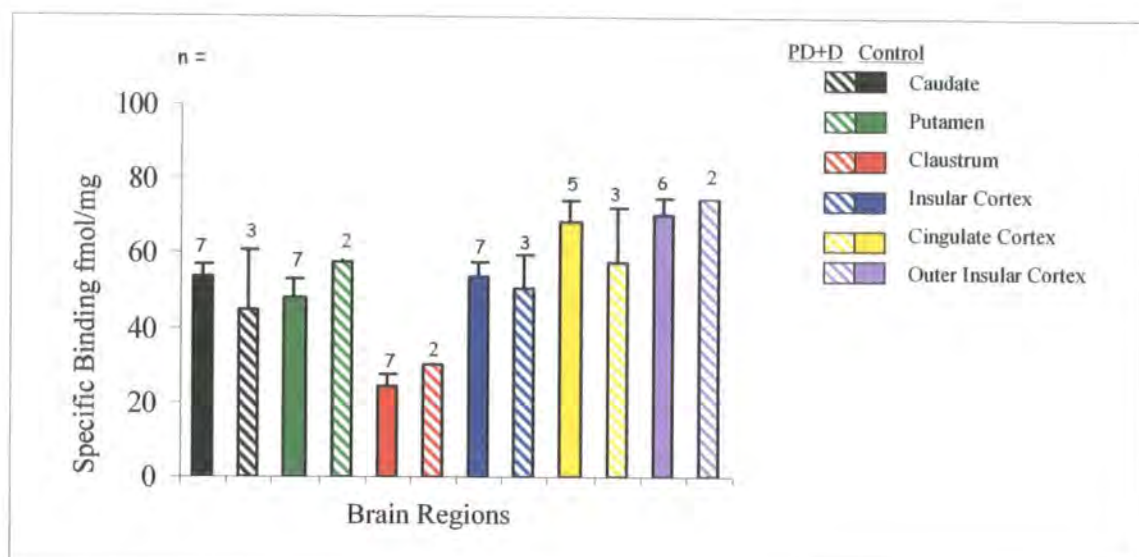


Figure 4.16 Graph showing (mean \pm SEM for n determinations) densities of [3 H]CP-101,606 specific binding (fmol/mg) in control and PDD pooled male and female cases in various brain regions.

Brain tissue samples from the 7 control cases and 3 PDD cases described in table 4.1 were assayed for radiolabelled CP-101,606 binding by autoradiography. Results of their analysis as previously shown (see graph 4.9 (A-C) and graph 4.11) were combined to assess the potential differences between control and disease state binding levels (fmol/mg) in the brain regions specified. As shown in figure 4.16, there were no significant differences in the levels of [3 H]CP-101,606 binding between control and PDD cases ($p > 0.1$, two-tailed distribution, unpaired t-test) in all 6 brain regions analysed. Due to low n values in the CP-101,606 male and female cohorts these data were not further analysed for gender differences as results would not be statistically relevant. The claustrum binding levels were consistently lower compared to all other regions. All values were statistically valid where $n \geq 5$.

A

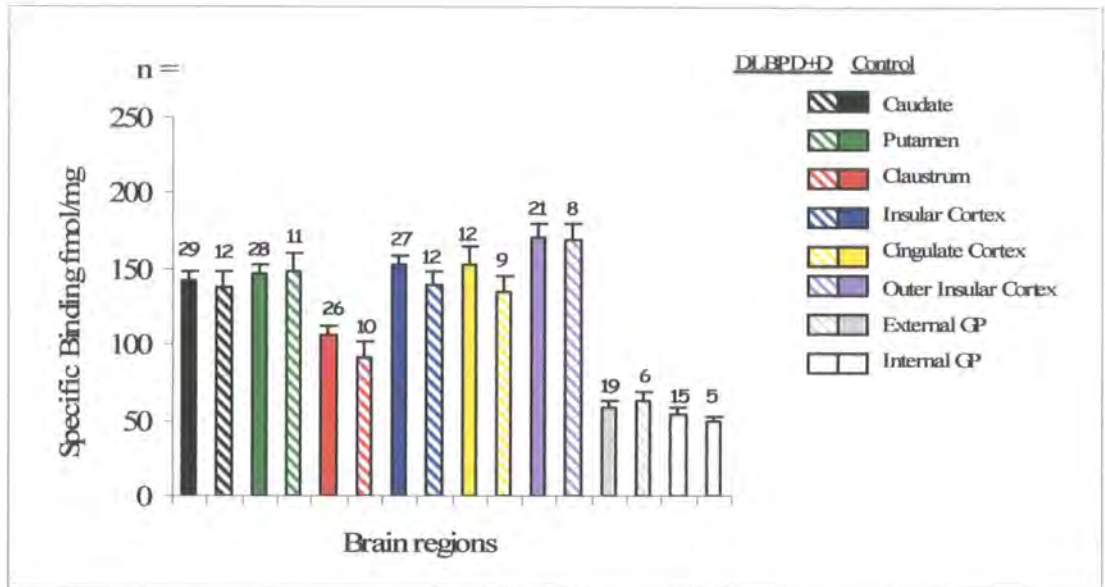


Figure 4.17 (A) Graph showing (mean \pm SEM for n determinations) densities of [3 H]Ro 25,6981 specific binding (fmol/mg) in control and DLBPDD pooled male and female cases in various brain regions.

Brain tissue samples from the 29 control cases and 12 DLBPDD cases described in table 4.1 were assayed for radiolabelled Ro 25,6981 binding by autoradiography. Results of their analysis as previously shown (see graph 4.9 (A-C), DLBPDD data not previously shown) were combined to assess the potential differences between control and disease state binding levels (fmol/mg) in the brain regions specified. As shown in figure 4.17(A), there were no significant differences in the levels of [3 H]Ro 25,6981 binding between control and DLBPDD cases ($p > 0.24$, two-tailed distribution, unpaired t-test) in all 8 brain regions analysed. These data were further analysed for gender differences, see figure 4.17(B,C). A similar pattern of binding was seen across the brain regions for male and female graphs both separately and combined, showing no significant differences between control and DLB cases (females $p \geq 0.08$, males $p \geq 0.06$ with the exception of the caudate where $p = 0.01$, and the Insular Cortex where $p = 0.02$, two-tailed distribution, unpaired t-test, indicated by *) in all 9 regions defined. The claustrum, external and internal globus pallidus binding levels were consistently lower compared to all other regions. All values were statistically valid where $n \geq 5$.

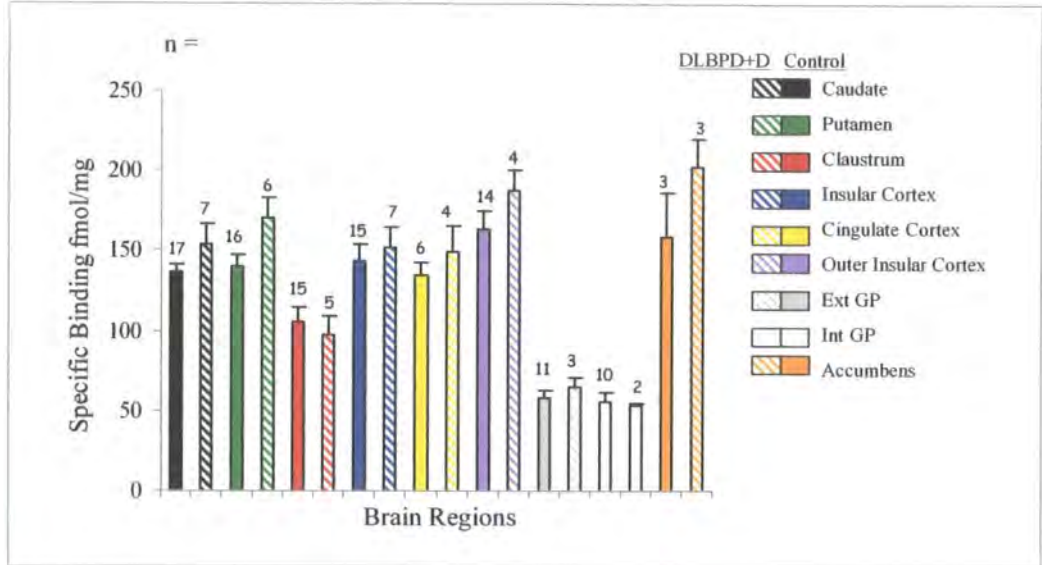
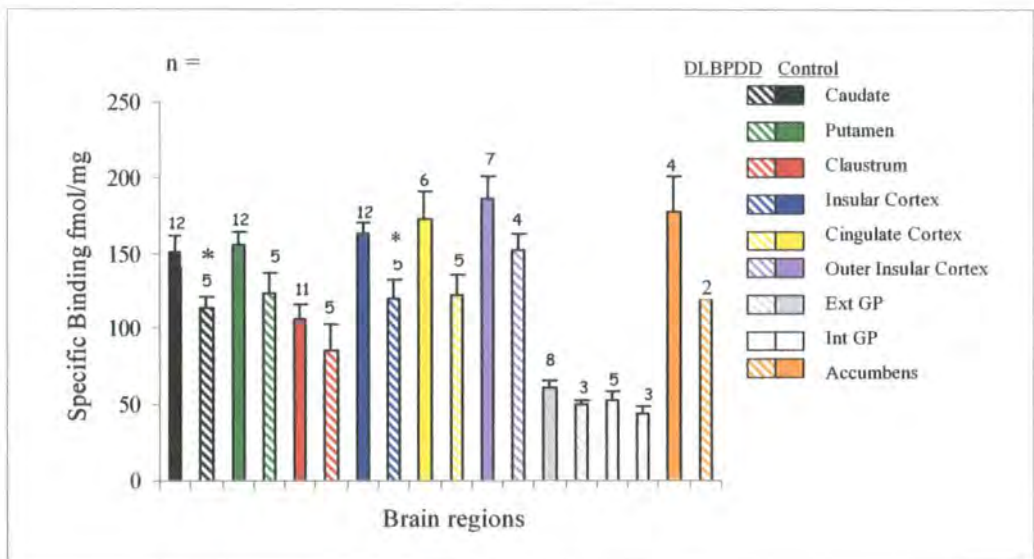
B**C**

Figure 4.17 (B,C) Graph showing (mean \pm SEM for n determinations) densities of [^3H]Ro 25,6981 specific binding (fmol/mg) in control and DLBPDD (B) female and (C) male cases in various brain regions.

A

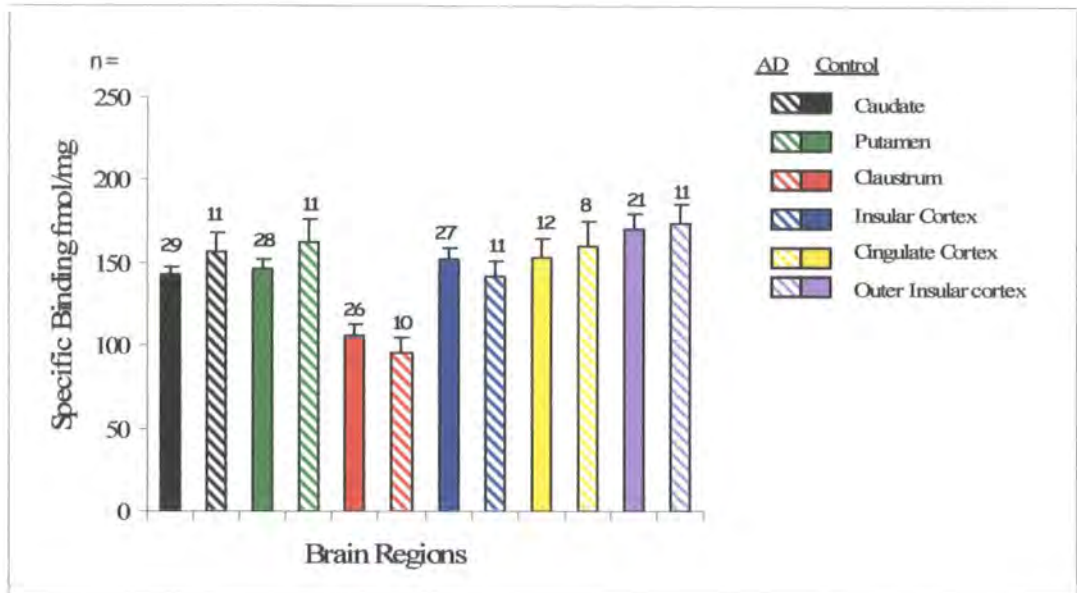


Figure 4.18 (A) Graph showing (mean \pm SEM for n determinations) densities of [3 H]Ro 25,6981 specific binding (fmol/mg) in control and AD pooled male and female cases in various brain regions.

Brain tissue samples from the 29 control cases and 11 AD cases described in table 4.1 were assayed for radiolabelled Ro 25,6981 binding by autoradiography. Results of their analysis as previously shown (see graph 4.9 (A-C) and graph 4.12) were combined to assess the potential differences between control and disease state binding levels (fmol/mg) in the brain regions specified. As shown in figure 4.18(A), there were no significant differences in the levels of [3 H]Ro 25,6981 binding between control and AD cases ($p > 0.1$, two-tailed distribution, unpaired t-test) in all brain regions analysed.

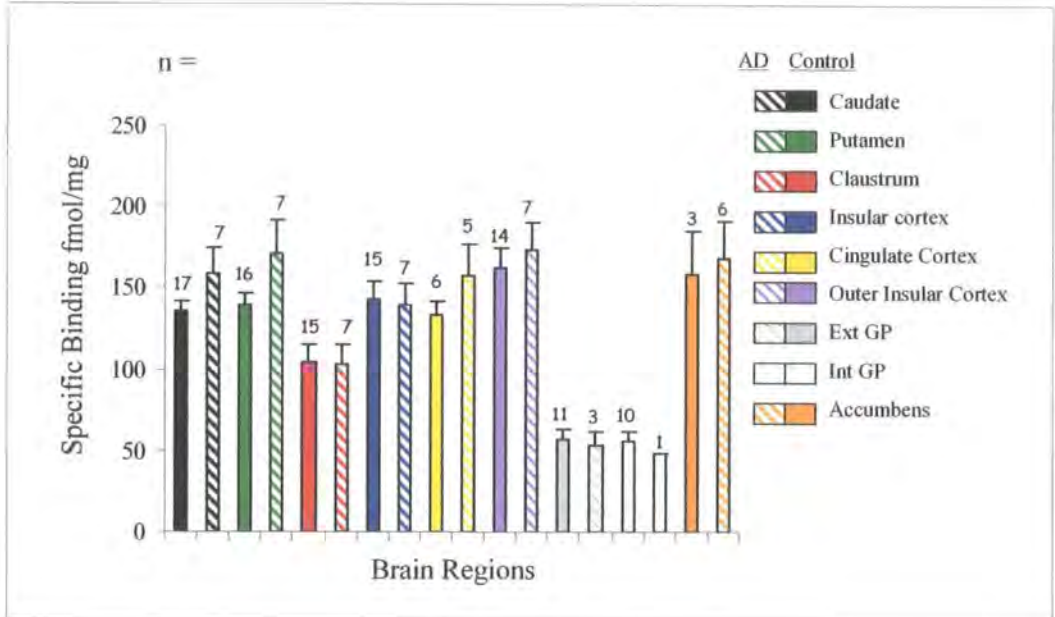
B

Figure 4.18 (B) Graph showing (mean \pm SEM for n determinations) densities of [3 H]Ro 25,6981 specific binding (fmol/mg) in control and AD female cases in various brain regions.

These data were further analysed for gender differences, see figure 4.18(B). Due to low n values in the Ro 25,6981 AD male cohort, these data were not further analysed for gender differences as results would not be statistically relevant. A similar pattern of binding was seen across the brain regions for female and combined male and female graphs, showing no significant differences between control and AD cases (male $p > 0.1$, two-tailed distribution, unpaired t-test) in all 9 regions defined. There was no evidence for gender bias. The claustrum, external and internal globus pallidus binding levels were consistently lower compared to all other regions. All values were statistically valid where $n \geq 5$.

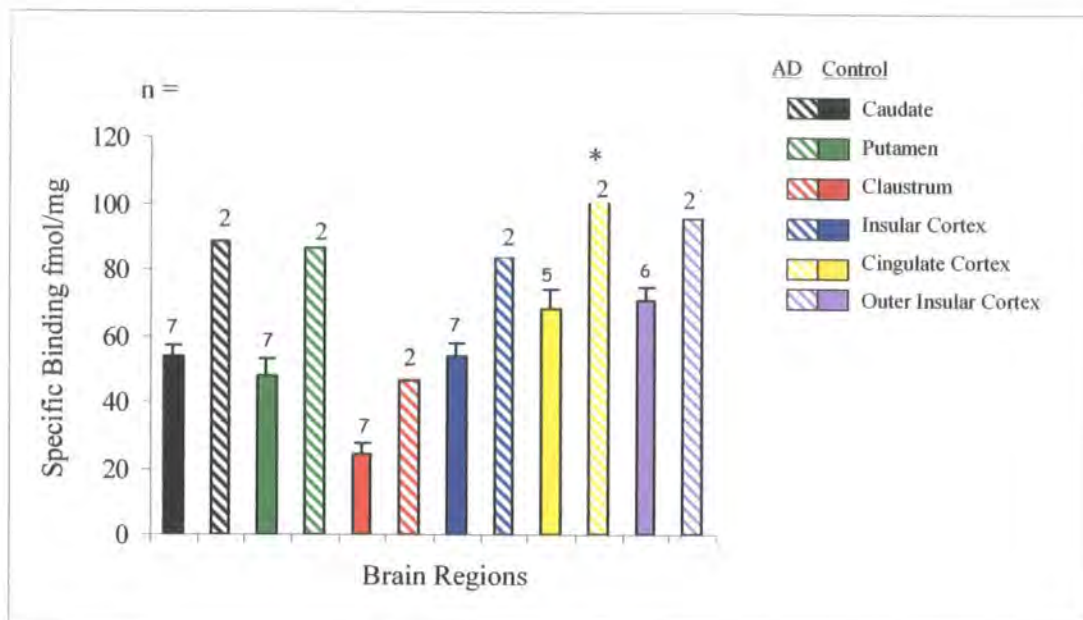


Figure 4.19 Graph showing (mean \pm SEM for n determinations) densities of [3 H]CP-101,606 specific binding (fmol/mg) in control and AD pooled male and female cases in various brain regions.

Brain tissue samples from the 7 control cases and 2 AD cases described in table 4.1 were assayed for radiolabelled CP-101,606 binding by autoradiography. Results of their analysis as previously shown (see graph 4.9 (A-C) and graph 4.12) were combined to assess the potential differences between control and disease state binding levels (fmol/mg) in the brain regions specified. As shown in figure 4.19, there were no significant differences in the levels of [3 H]CP-101,606 binding between control and AD cases ($p \geq 0.09$, two-tailed distribution, unpaired t-test) in all 6 brain regions analysed except in the cingulate cortex where $p=0.004$, showing significance, (indicated by *). This may be due to the low n values in the AD cases, since the graph would appear to show significance between AD and control values. Due to low n values in the CP-101,606 male and female cohorts these data were not further analysed for gender differences as results would not be statistically relevant. The claustrum binding levels were consistently lower compared to all other regions. All values were statistically valid where $n \geq 5$.

4.5.3. Results (Figure 4.20 (A-H) to Figure 4.25 (A-G))

The same data as previously described (see graphs 4.9 (A-C) to graph 4.19) were further analysed to show specific binding levels of both [³H]Ro 25,6981 and [³H]CP-101,606 in various brain regions, correlating fmol/mg binding with age at death of the subject (in years) for each case, and in each brain region defined. Estimated linear regression lines of best fit were produced using GraphPad Prism and are represented on each graph, indicating any age-dependant changes in binding levels in each tissue. The significance of the regression was determined from the generated p value, where $p \leq 0.05$ was considered to show a significant linear relationship between age and binding level. Due to limited availability of the [³H]CP-101,606 ligand a smaller number of cases were analysed, resulting in low n numbers for some of the tissues. In these cases a linear regression line was not shown as it would not have been appropriate where $n = < 3$. The generated correlation coefficient or r value shows how well the data fits to the regression line, where $r = 1$ shows strong correlation and $r = 0$ shows little or none.

Figure 4.20 (A-H) shows the specific binding levels in male and female control cases for [³H]Ro 25,6981 ($n = 29$) and [³H]CP-101,606 ($n = 7$) against age, ranging from 62-91 years in the 8 brain regions defined. There were no significant age-dependant changes in all brain regions analysed ($p \geq 0.17$ in all cases) with the exception of the insular cortex [³H]CP-101,606 data where $p = 0.03$, showing significance. The outer insular cortex [³H]CP-101,606 value showed borderline significance with $p = 0.06$. The [³H]CP-101,606 linear regression line was removed from Figure 4.20(H) due to the low n number, and would not have been statistically valid. The r values ranged from -0.005 ([³H]Ro 25,6981 external globus pallidus) to 0.81 ([³H]CP-101,606 insular cortex), with the [³H]CP-101,606 data

consistently showing better correlation to the linear regression than the [³H]Ro 25,6981 data, possibly due to the lower n numbers. In all cases there were significantly higher levels of [³H]Ro 25,6981 binding than [³H]CP-101,606 binding in each of the tissues analysed.

The data in figure 4.20 (A-H) were further analysed for gender differences. Due to low n values in the [³H]CP-101,606 male cohort, only the female data could be analysed. Figure 4.21 (A-H) shows the specific binding levels in female control cases for [³H]Ro 25,6981 (n = 17) and [³H]CP-101,606 (n = 5) against age, ranging from 62-91 years in the 8 brain regions defined. There were no significant age-dependant changes in all brain regions analysed ($p \geq 0.17$ in all cases) with the exception of the claustrum and insular cortex [³H]CP-101,606 data where $p = 0.08$ in both cases, showing borderline significance, that is $p \leq 0.1$. The [³H]CP-101,606 linear regression line was removed from graphs G and H due to the low n number, and would not have been statistically valid. The r values ranged from 0.03 ([³H]Ro 25,6981 outer insular cortex) to 0.89 ([³H]CP-101,606 cingulate cortex), with the [³H]CP-101,606 data consistently showing better correlation to the linear regression than the [³H]Ro 25,6981 data, possibly due to the lower n numbers. In all cases there were significantly higher levels of [³H]Ro 25,6981 binding than [³H]CP-101,606 binding in each of the tissues analysed.

Figure 4.22 (A-G) shows the specific binding levels in male and female DLB cases for [³H]Ro 25,6981 (n = 22) and [³H]CP-101,606 (n = 12) against age, ranging from 69-92 years in the 7 brain regions defined. There were no significant age-dependant changes in all brain regions analysed ($p \geq 0.23$ in all cases) with the exception of the outer insular cortex [³H]CP-101,606 data where $p = 0.04$, showing significance. The claustrum [³H]Ro 25,6981 value showed borderline significance with $p = 0.07$. The r values ranged from 0.00 ([³H]CP-

101,606 cingulate cortex) to -0.73 ($[^3\text{H}]$ CP-101,606 outer insular cortex). In all cases there were significantly higher levels of $[^3\text{H}]$ Ro 25,6981 binding than $[^3\text{H}]$ CP-101,606 binding in each of the tissues analysed.

The data in figure 4.22 (A-G) were further analysed for gender differences. Due to low n values in the $[^3\text{H}]$ CP-101,606 female cohort, only the male data could be analysed. Figure 4.23 (A-G) shows the specific binding levels in male DLB cases for $[^3\text{H}]$ Ro 25,6981 (n = 15) and $[^3\text{H}]$ CP-101,606 (n = 8) against age, ranging from 69-92 years in the 7 brain regions defined. There were no significant age-dependant changes in all brain regions analysed ($p \geq 0.12$ in all cases). The r values ranged from 0.00 ($[^3\text{H}]$ Ro 25,6981 putamen) to 0.70 ($[^3\text{H}]$ CP-101,606 accumbens), with the $[^3\text{H}]$ CP-101,606 data showing better correlation to the linear regression than the $[^3\text{H}]$ Ro 25,6981 data in each tissue except the claustrum and insular cortex. In all cases there were significantly higher levels of $[^3\text{H}]$ Ro 25,6981 binding than $[^3\text{H}]$ CP-101,606 binding in each of the tissues analysed.

Figure 4.24 (A-F) shows the specific binding levels in male and female PDD cases for $[^3\text{H}]$ Ro 25,6981 (n = 9) and $[^3\text{H}]$ CP-101,606 (n = 3) against age, ranging from 65-86 years in the 6 brain regions defined. There were no significant age-dependant changes in all brain regions analysed ($p \geq 0.15$ in all cases). The $[^3\text{H}]$ CP-101,606 linear regression line was removed from graphs B, C, E and F due to the low n number, and would not have been statistically valid. The r values ranged from 0.27 ($[^3\text{H}]$ Ro 25,6981 insular cortex) to 0.96 ($[^3\text{H}]$ CP-101,606 insular cortex), with the $[^3\text{H}]$ CP-101,606 data consistently showing better correlation to the linear regression than the $[^3\text{H}]$ Ro 25,6981 data. The data could not be further analysed for gender differences due to low n numbers in the $[^3\text{H}]$ CP-101,606 cohort.

In all cases there were significantly higher levels of [³H]Ro 25,6981 binding than [³H]CP-101,606 binding in each of the tissues analysed.

Figure 4.25 (A-G) shows the specific binding levels in male and female AD cases for [³H]Ro 25,6981 (n = 11) and [³H]CP-101,606 (n = 2) against age, ranging from 78-91 years in the 7 brain regions defined. There were significant age-dependant changes in all brain regions analysed ($p \leq 0.01$ in all cases) with the exception of the [³H]Ro 25,6981 claustrum and outer insular cortex data where $p=0.17$ and $p=0.23$ respectively, showing no significance. One observation from these results is a trend for the younger age cases in this AD group to show a higher level of binding than in the same younger age range for other disease states. This may be useful as an indication in the younger age group as a marker for a predisposition for AD. The [³H]CP-101,606 linear regression line was removed from all the graphs due to the low n number, and would not have been statistically valid. The r values ranged from -0.39 ([³H]Ro 25,6981 outer insular cortex) to -0.87 ([³H]Ro 25,6981 accumbens). The data could not be further analysed for gender differences due to low n numbers in the [³H]CP-101,606 cohort. In all cases there were significantly higher levels of [³H]Ro 25,6981 binding than [³H]CP-101,606 binding in each of the tissues analysed.

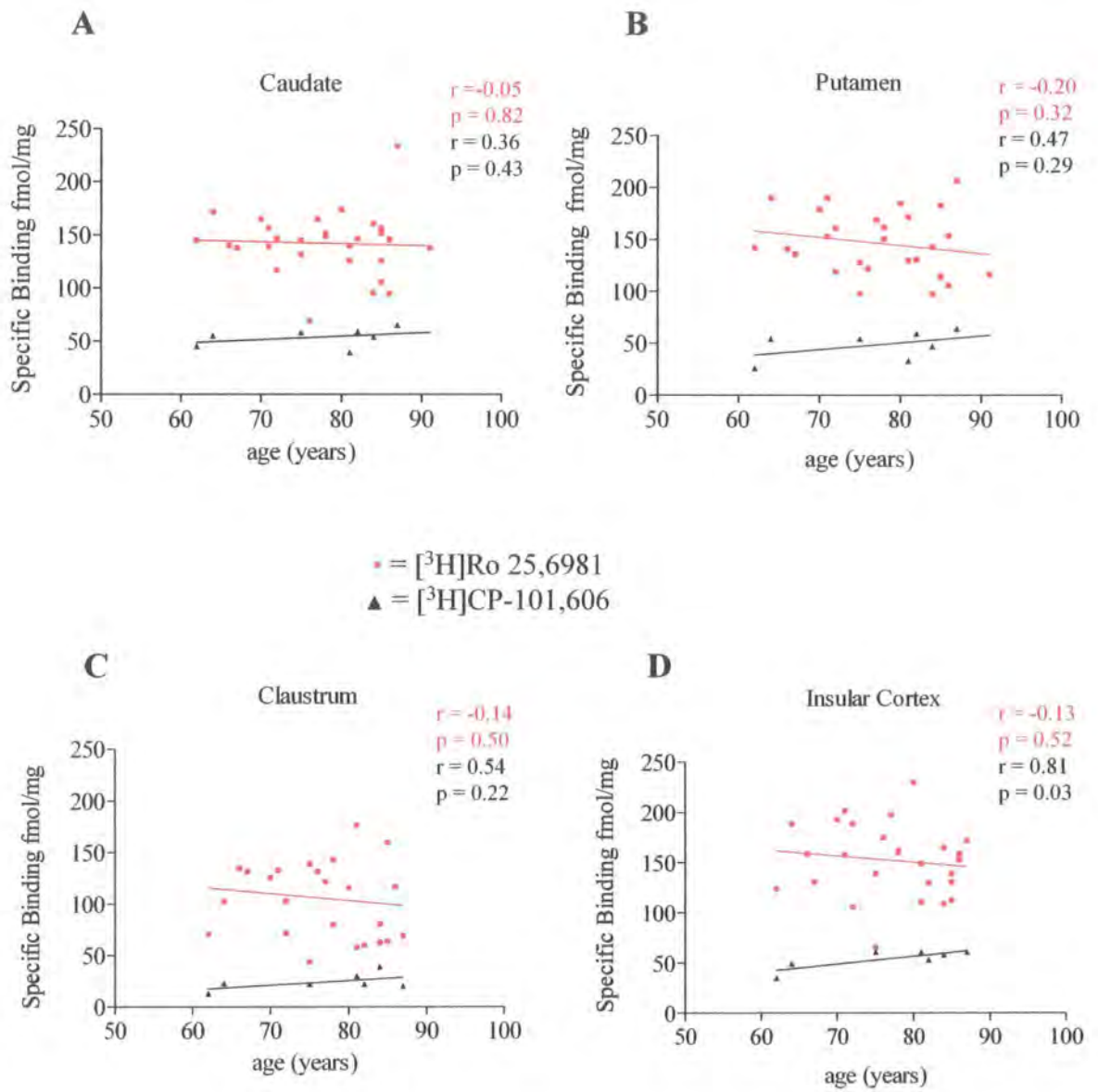


Figure 4.20 (A-D) Age-dependant absolute specific binding of [³H]Ro 25,6981 and [³H]CP-101,606 in male and female control cases in (A) Caudate (B) Putamen (C) Claustrum and (D) Insular cortex.

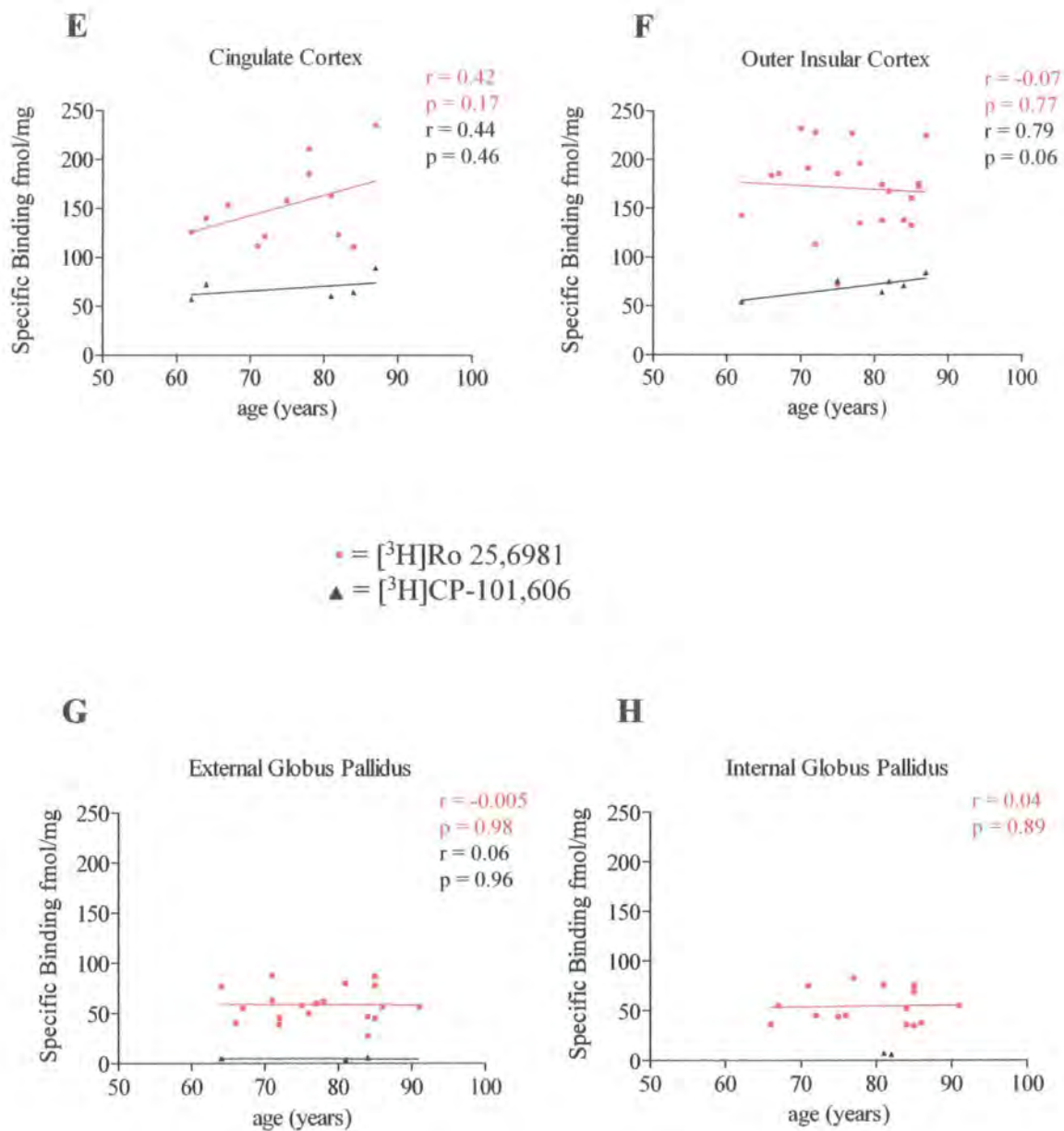


Figure 4.20 (E-H) Age-dependant absolute specific binding of $[^3\text{H}]\text{Ro } 25,6981$ and $[^3\text{H}]\text{CP-101,606}$ in male and female control cases in (E) Cingulate Cortex, (F) Outer Insular Cortex, (G) External Globus Pallidus and (H) Internal Globus Pallidus.

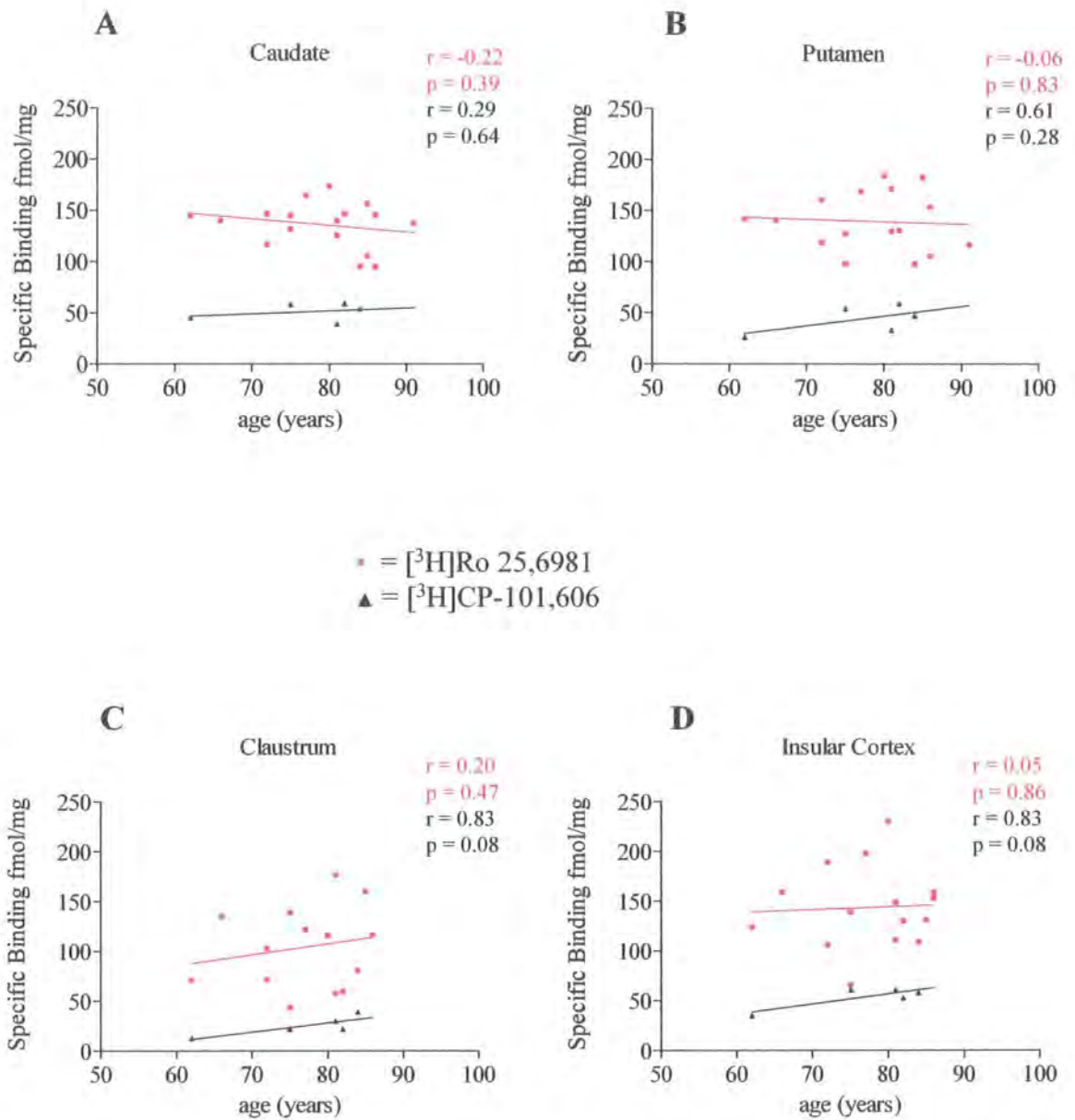


Figure 4.21 (A-D) Age-dependent absolute specific binding of $[^3\text{H}]\text{Ro } 25,6981$ and $[^3\text{H}]\text{CP-101,606}$ in female control cases in (A) Caudate, (B) Putamen, (C) Claustrum and (D) Insular Cortex.

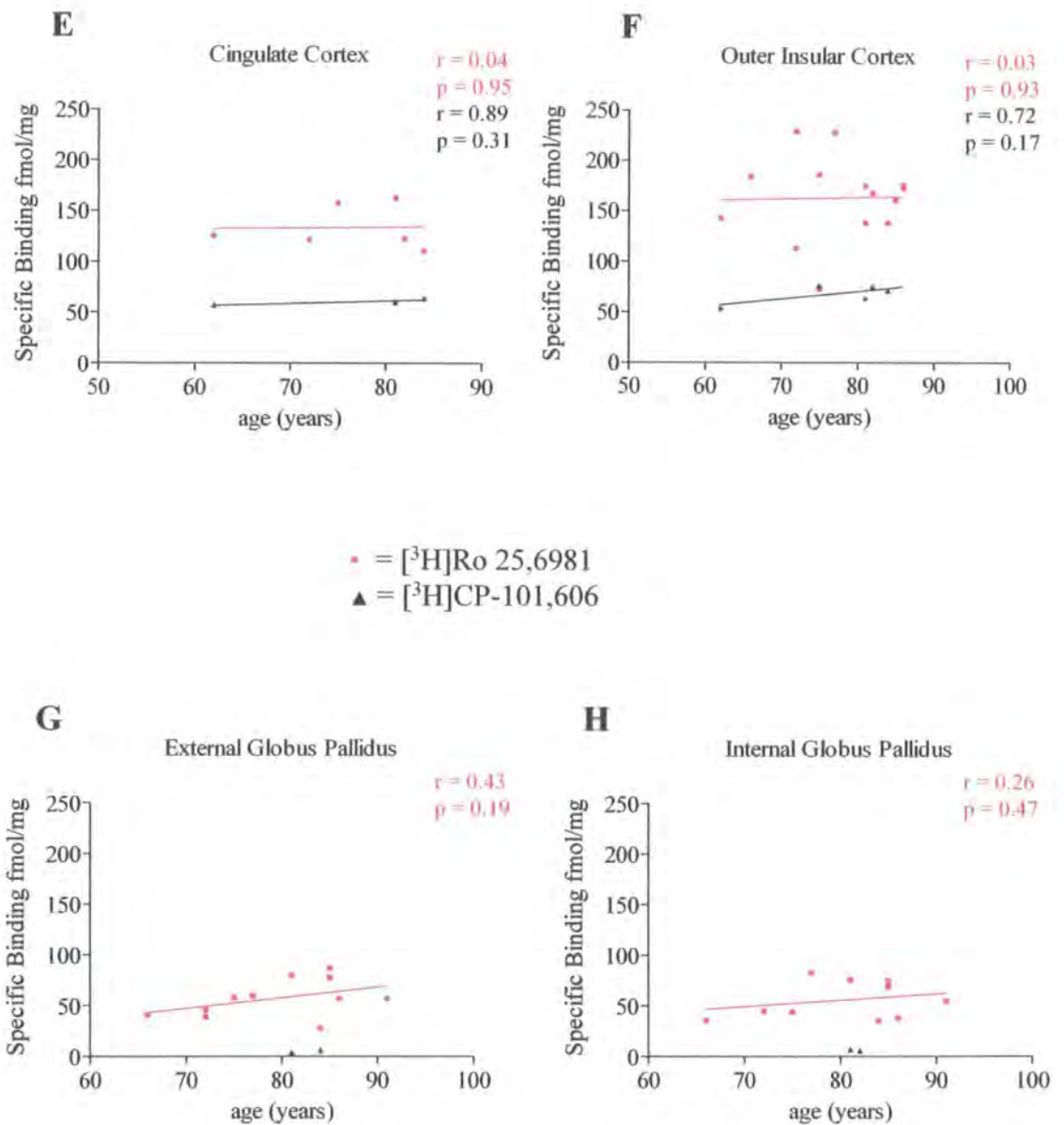


Figure 4.21 (E-H) Age-dependant absolute specific binding of [³H]Ro 25,6981 and [³H]CP-101,606 in female control cases in (E) Cingulate Cortex, (F) Outer Insular Cortex, (G) External Globus Pallidus and (H) Internal Globus Pallidus.

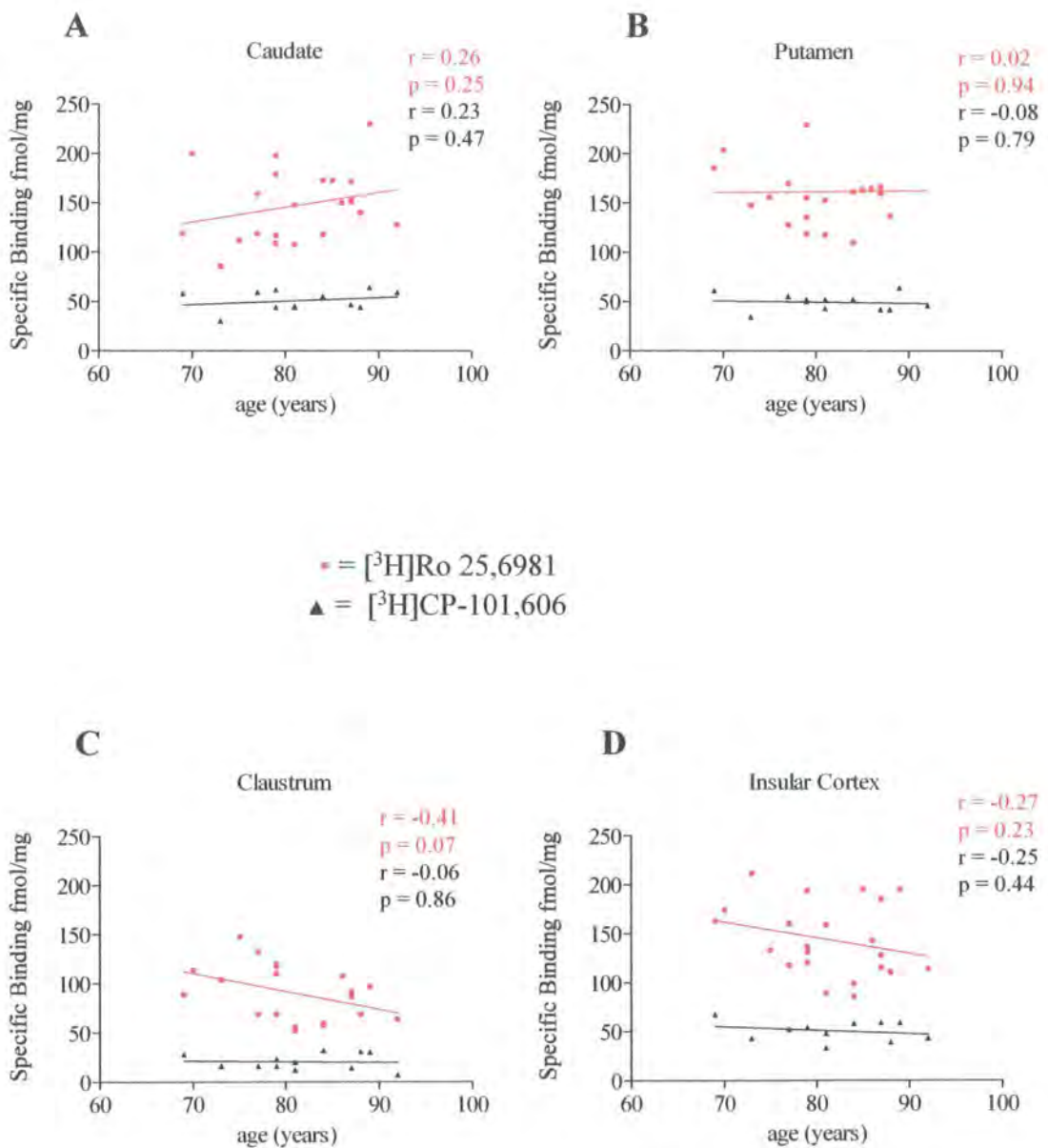


Figure 4.22 (A-D) Age-dependant absolute specific binding of [³H]Ro 25,6981 and [³H]CP-101,606 in male and female DLB cases in (A) Caudate, (B) Putamen, (C) Claustrum and (D) Insular Cortex.

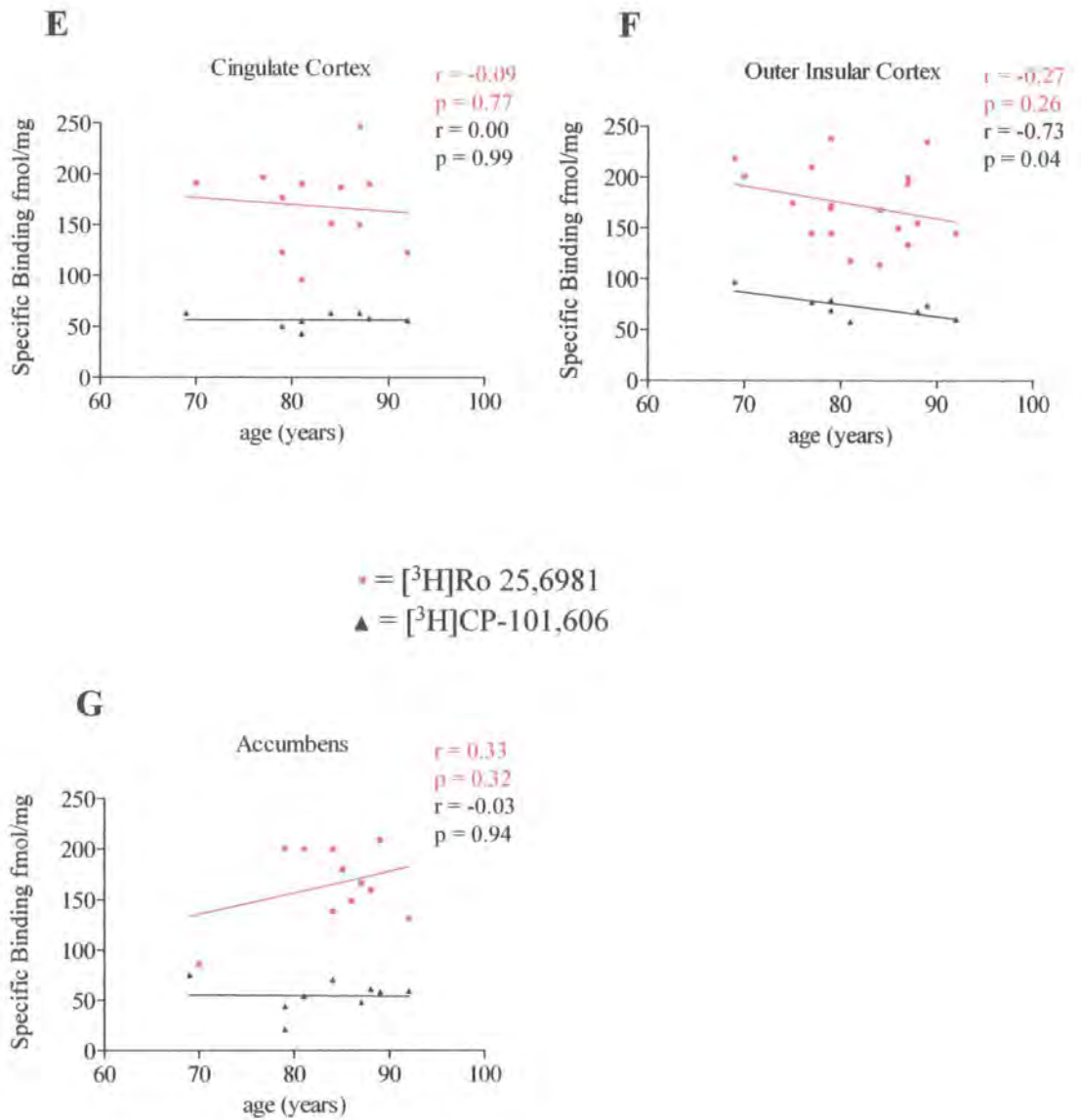


Figure 4.22 (E-G) Age-dependant absolute specific binding of [3H]Ro 25,6981 and [3H]CP-101,606 in male and female DLB cases in (E) Cingulate Cortex, (F) Outer Insular Cortex, (G) Nucleus Accumbens

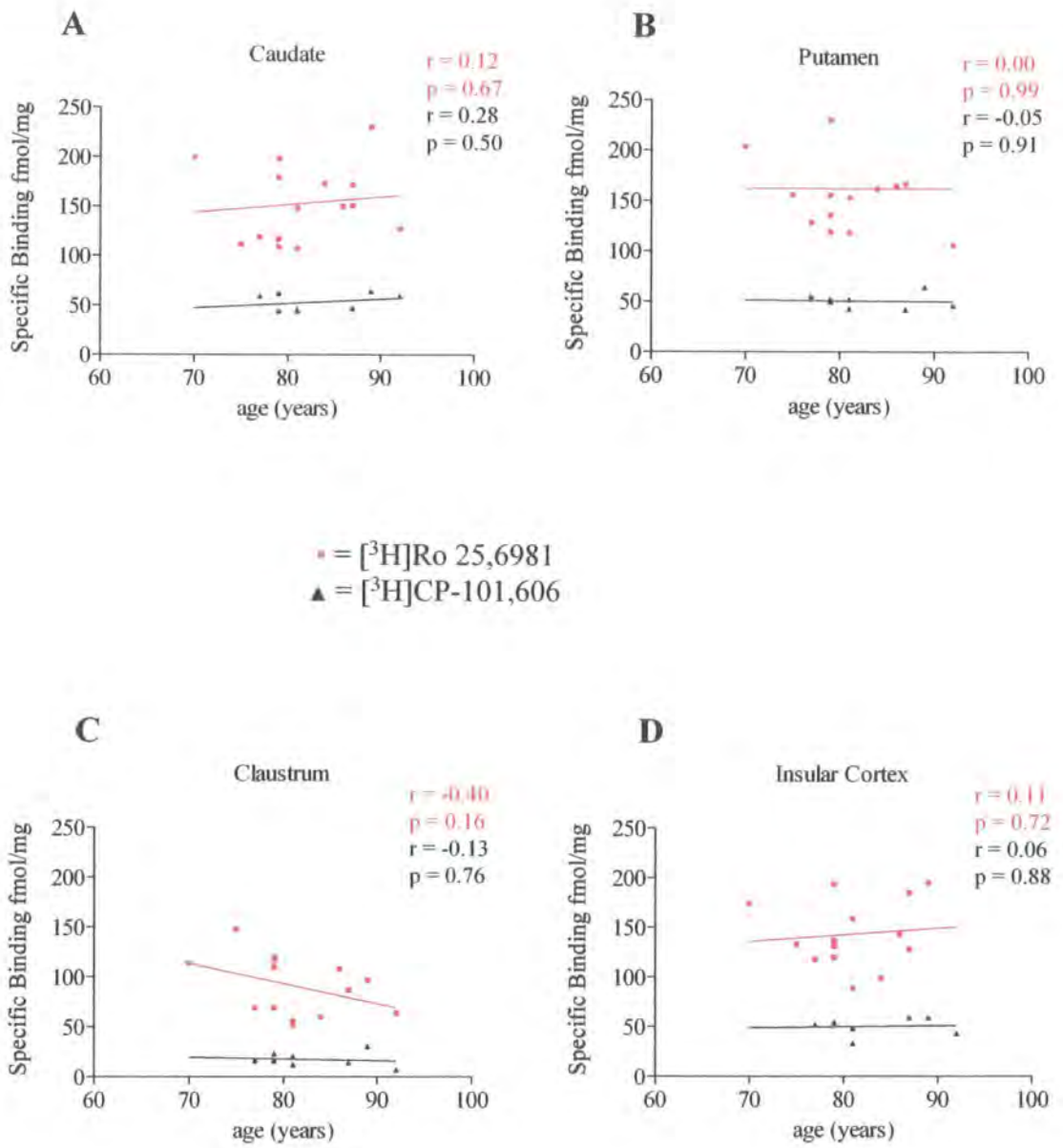


Figure 4.23 (A-D) Age-dependant absolute specific binding of $[^3\text{H}]\text{Ro } 25,6981$ and $[^3\text{H}]\text{CP-101,606}$ in male DLB cases in (A) Caudate, (B) Putamen, (C) Claustrum and (D) Insular Cortex

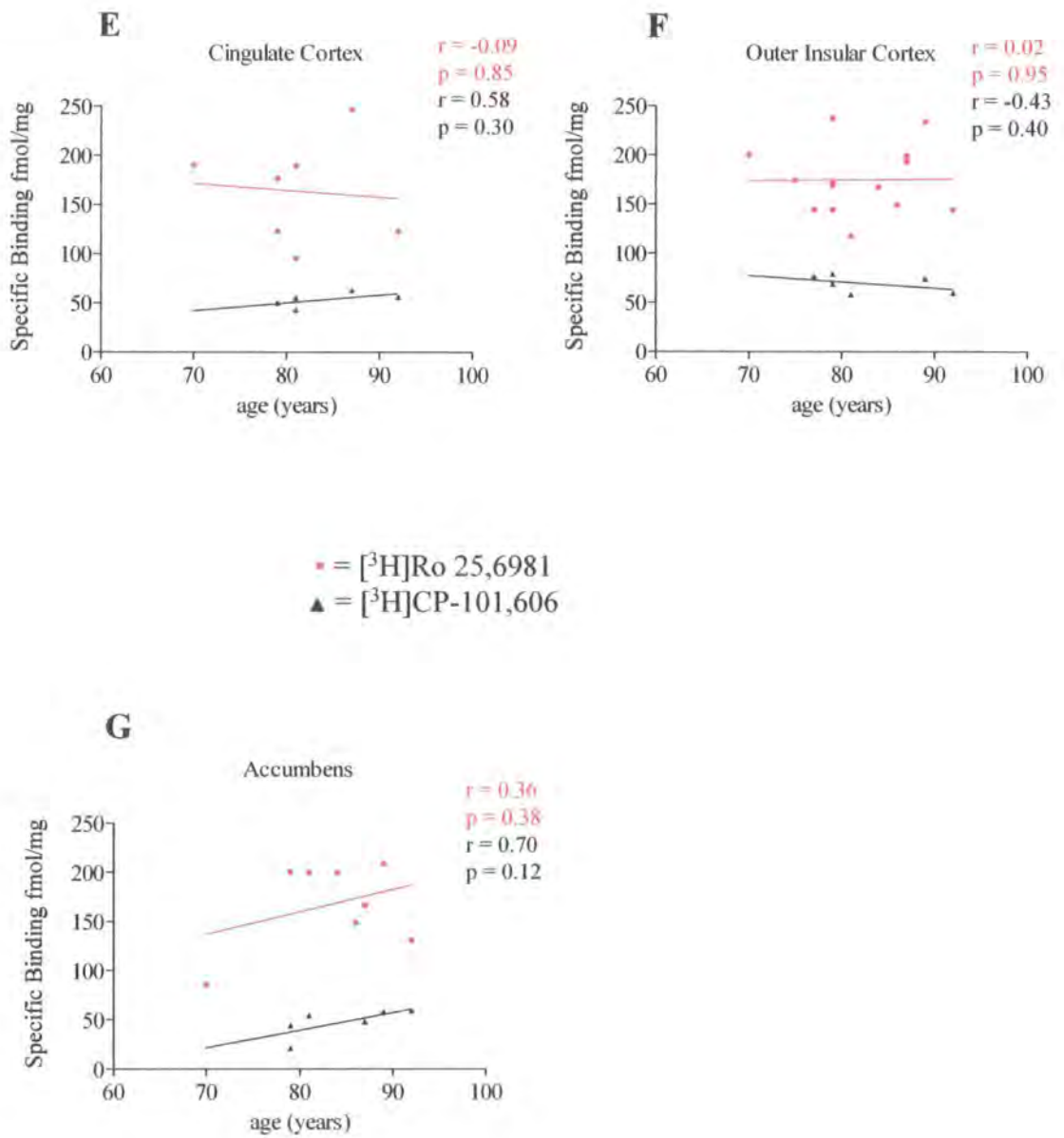


Figure 4.23 (E-G) Age-dependant absolute specific binding of [³H]Ro 25,6981 and [³H]CP-101,606 in male DLB cases in (E) Cingulate Cortex, (F) Outer Insular Cortex, (G) Nucleus Accumbens

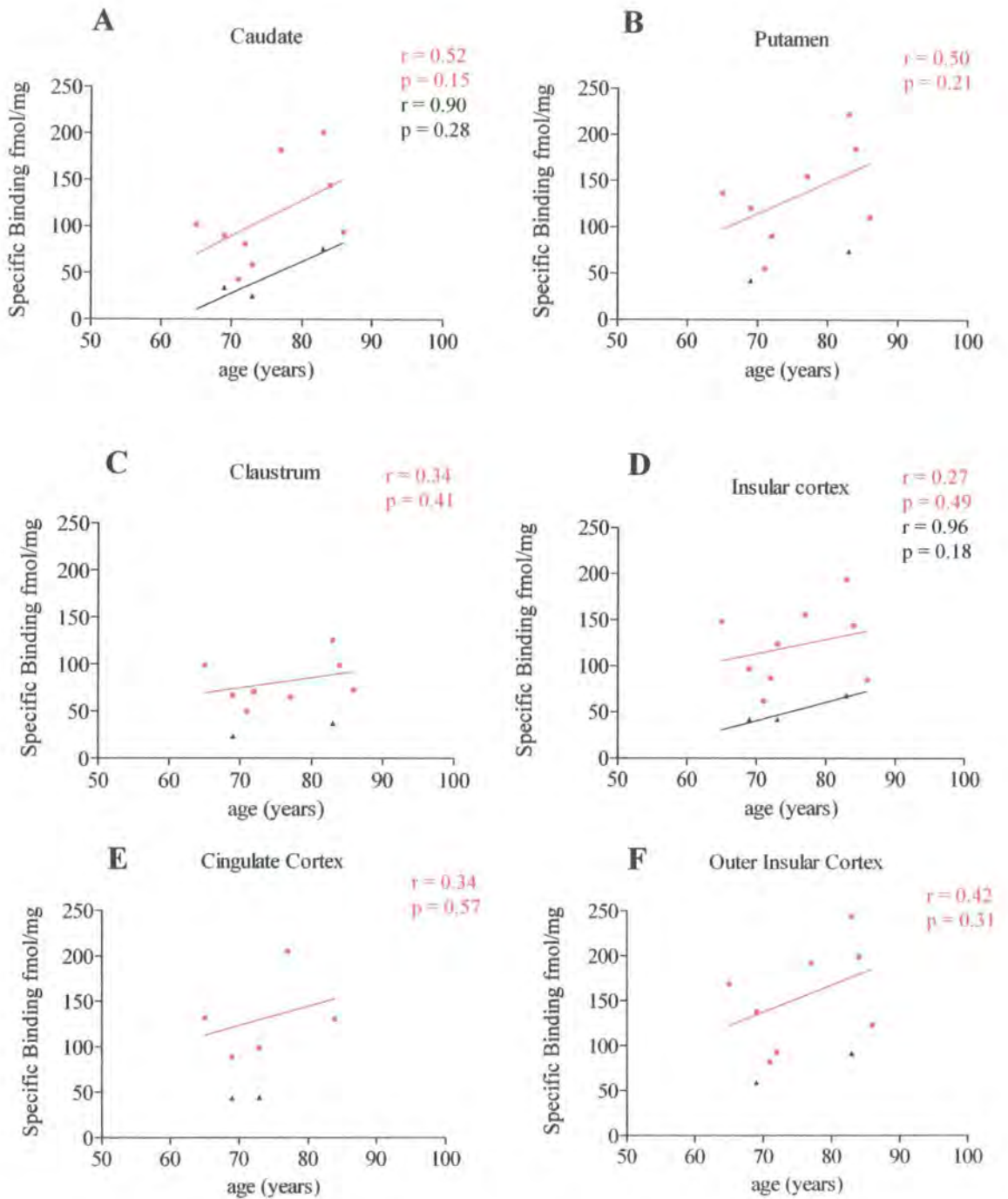


Figure 4.24 (A-F) Age-dependant absolute specific binding of [³H]Ro 25,6981 and [³H]CP-101,606 in male and female PDD cases in (A) Caudate, (B) Putamen, (C) Claustrum, (D) Insular Cortex, (E) Cingulate Cortex and (F) Outer Insular Cortex.

▪ = [³H]Ro 25,6981
 ▲ = [³H]CP-101,606

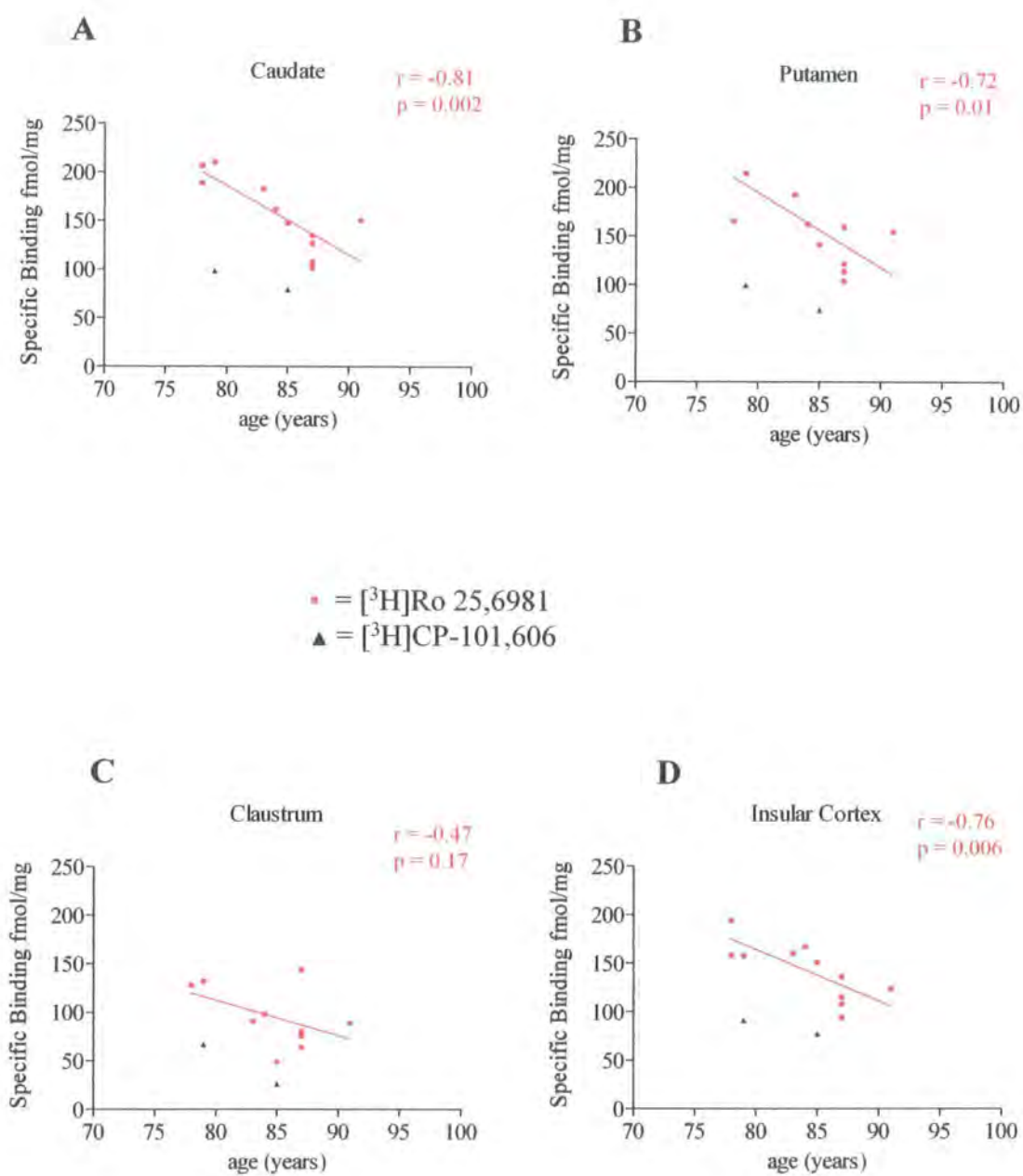


Figure 4.25 (A-D) Age-dependant absolute specific binding of $[^3\text{H}]$ Ro 25,6981 and $[^3\text{H}]$ CP-101,606 in male and female AD cases in (A) Caudate, (B) Putamen, (C) Claustrum and (D) Insular Cortex

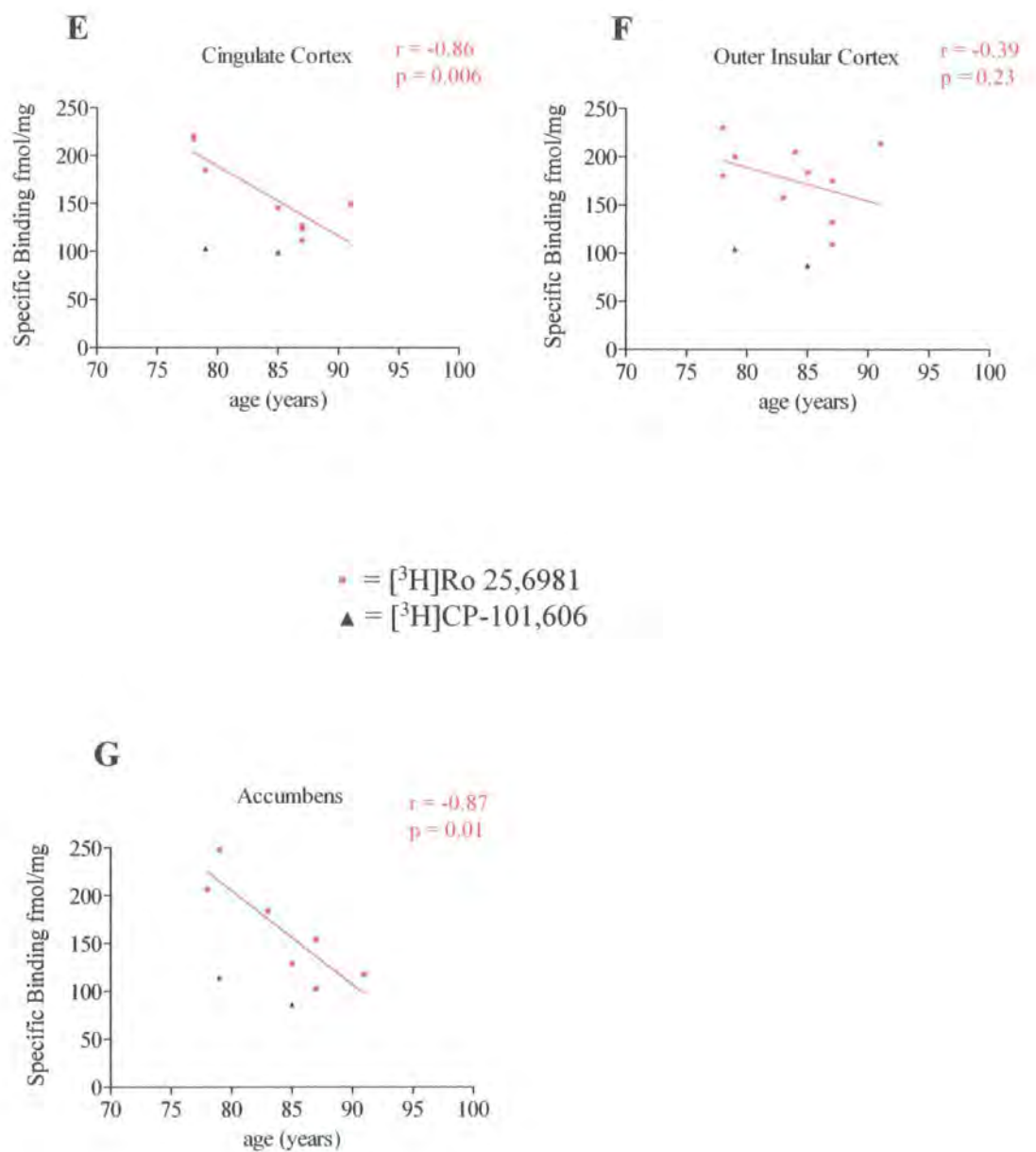


Figure 4.25 (E-G) Age-dependant absolute specific binding of [3H]Ro 25,6981 and [3H]CP-101,606 in male and female AD cases in (E) Cingulate Cortex, (F) Outer Insular Cortex, (G) Nucleus Accumbens

4.5.4 Results (Figure 4.26 (A-I) to Figure 4.29 (A-F))

The same data as previously described (see graphs 4.20 (A-H) to graph 4.25 (A-G)) and summarised in table 4.2, were further analysed to compare age-dependant specific binding levels of [³H]Ro 25,6981 and [³H]CP-101,606 independently between control and disease state cases. The cases were analysed by correlating fmol/mg binding with age at death of the subject (in years) for each case, and in each brain region defined. Estimated linear regression lines of best fit were produced using GraphPad Prism and are represented on each graph, indicating any age-dependant changes in binding levels in each tissue. The significance of the regression was determined from the generated p value, where $p \leq 0.05$ was considered to show a significant linear relationship between age and binding level. Due to limited availability of the [³H]CP-101,606 ligand a smaller number of cases were analysed, resulting in low n numbers for some of the tissues. In these cases a linear regression line was not shown as it would not have been appropriate where $n = < 3$. The generated correlation coefficient or r value shows how well the data fits to the regression line, where $r = 1$ shows strong correlation and $r = 0$ shows little or none.

Figure 4.26 (A-I) shows the specific binding levels in male and female control ($n = 26$) and DLB ($n = 22$) cases (see table 4.2) for [³H]Ro 25,6981 against age, ranging from 67-92 years in the 9 brain regions defined. There were no significant age-dependant changes in all brain regions analysed in control and disease state cases ($p \geq 0.23$ in all cases) with the exception of the claustrum DLB data where $p = 0.07$, showing borderline significance. The regression lines on each graph were very similar for both control and DLB data, showing a slight general decrease in binding levels in each of the tissues. The exception was the cingulate cortex (graph E), where binding levels increased with age in the control data set,

and decreased with age in the DLB data set. The r values ranged from 0.02 (DLB, putamen and control, external globus pallidus) to -0.41 (DLB, claustrum).

The data in figure 4.26 (A-I) were further analysed for gender differences. Figure 4.27 (A-I) shows the specific binding levels in female control ($n = 15$) and DLB ($n = 7$) cases for [^3H]Ro 25,6981 against age, ranging from 62-91 years in the 9 brain regions defined. There were no significant age-dependant changes in all brain regions analysed in control and disease state cases ($p \geq 0.18$ in all cases) with the exception of the outer insular cortex DLB data where $p = 0.08$, showing borderline significance, that is $p \leq 0.1$. The regression lines on each graph varied for both control and DLB data depending on the tissue. Control binding levels decreased as DLB binding levels increased in the caudate, whereas the opposite was true for the putamen, claustrum, insular cortex, cingulate cortex and outer insular cortex. Binding levels were highly similar in the external and internal globus pallidus, and both control and DLB levels increased with age in the nucleus accumbens. The r values ranged from 0.03 (control, outer insular cortex) to -0.84 (DLB, outer insular cortex), with the control data showing better correlation to the linear regression than the DLB data, with the exception of the internal globus pallidus and accumbens.

Figure 4.28 (A-I) shows the specific binding levels in male control ($n = 11$) and DLB ($n = 15$) cases for [^3H]Ro 25,6981 against age, ranging from 62-91 years in the 9 brain regions defined. There were no significant age-dependant changes in all brain regions analysed in control and disease state cases ($p \geq 0.16$ in all cases) with the exception of the claustrum and cingulate cortex control data where $p = 0.02$ and $p = 0.03$ respectively, showing significance. The external globus pallidus control data showed borderline significance with $p = 0.07$. The regression lines on each graph were very similar for both control and DLB data in all the

tissues, with the exception of the cingulate cortex, where control binding levels increased with age as DLB binding levels decreased. The r values ranged from 0.00 (DLB, putamen) to 0.85 (control, cingulate cortex), with the DLB data showing better correlation to the linear regression than the control data, with the exception of the nucleus accumbens.

Figure 4.29 (A-F) shows the specific binding levels in male and female control ($n = 7$) and DLB ($n = 12$) cases for [^3H]CP-101,606 against age, ranging from 62-92 years in the 6 brain regions defined. There were no significant age-dependant changes in the brain regions analysed in control and disease state cases ($p \geq 0.22$ in all cases) with the exception of the insular cortex control data and DLB outer insular cortex data where $p=0.03$ and $p=0.04$ respectively, showing significance. The control outer insular cortex data showed borderline significance with $p=0.06$. The regression lines on each graph were very similar for both control and DLB caudate and cingulate cortex data showing a slight increase with age in both data sets. All other tissues showed a decrease in binding with DLB as control binding increased with age. The r values ranged from 0.00 (DLB, cingulate cortex) to 0.81 (control, insular cortex). The data were not further analysed for gender differences due to the low n numbers in the CP-101,606 cohort.

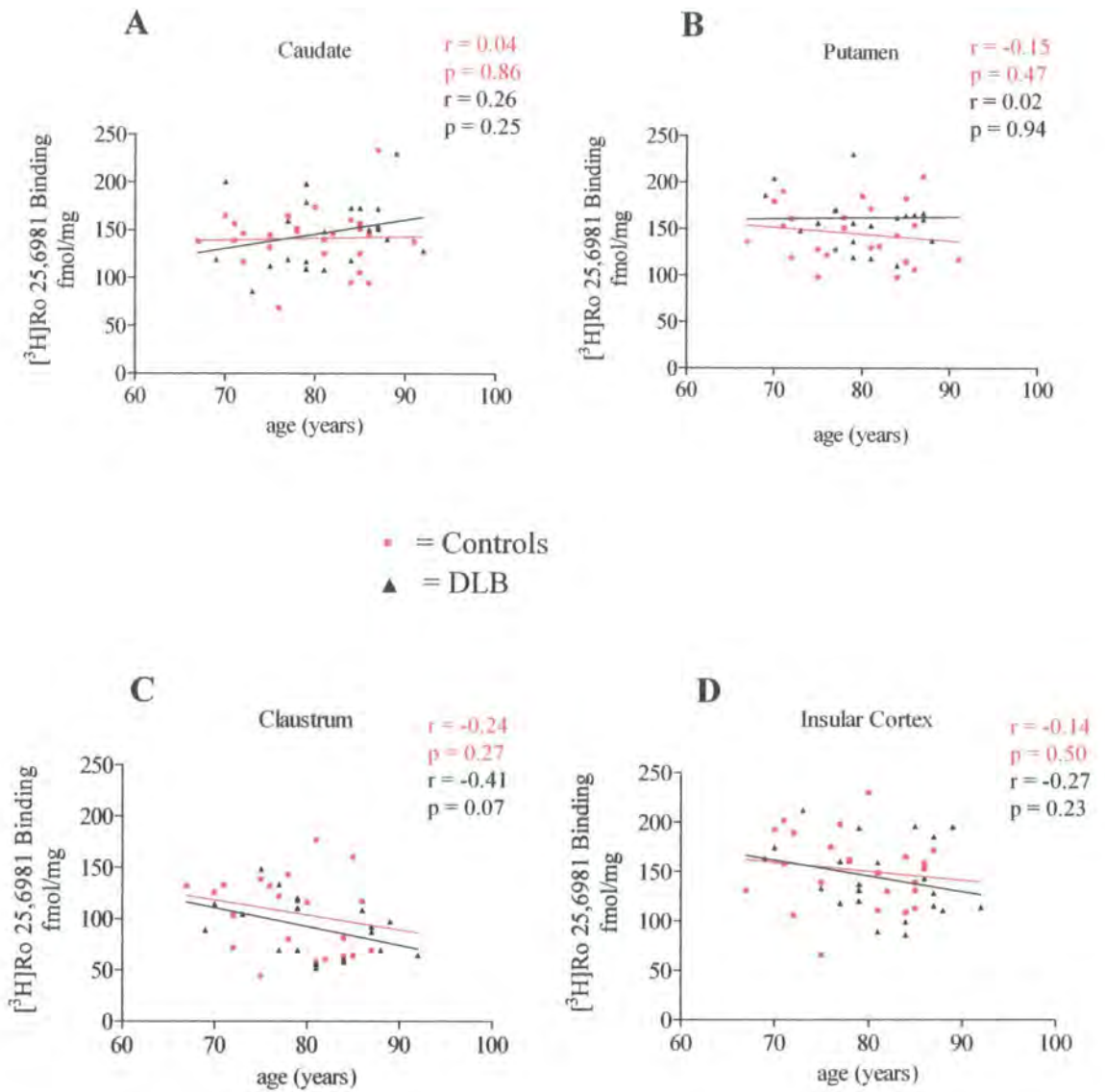


Figure 4.26 (A-D) Age-dependant absolute specific binding of $[^3\text{H}]\text{Ro 25,6981}$ in male and female control and DLB cases in (A) Caudate, (B) Putamen, (C) Claustrum and (D) Insular Cortex

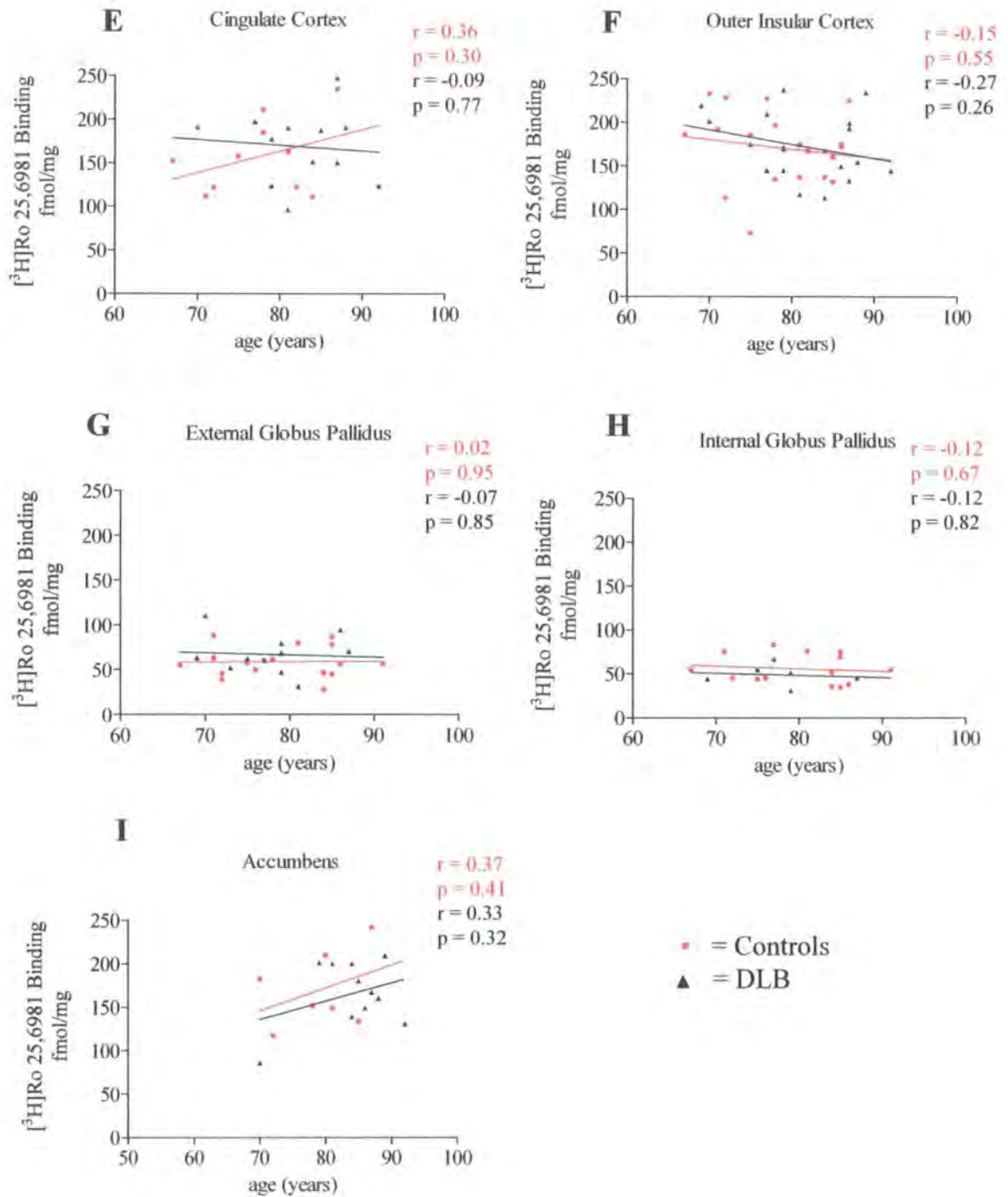


Figure 4.26 (E-I) Age-dependant absolute specific binding of $[^3\text{H}]\text{Ro 25,6981}$ in male and female control and DLB cases in (E) Cingulate Cortex, (F) Outer Insular Cortex, (G) External Globus Pallidus, (H) Internal Globus Pallidus and (I) Nucleus Accumbens

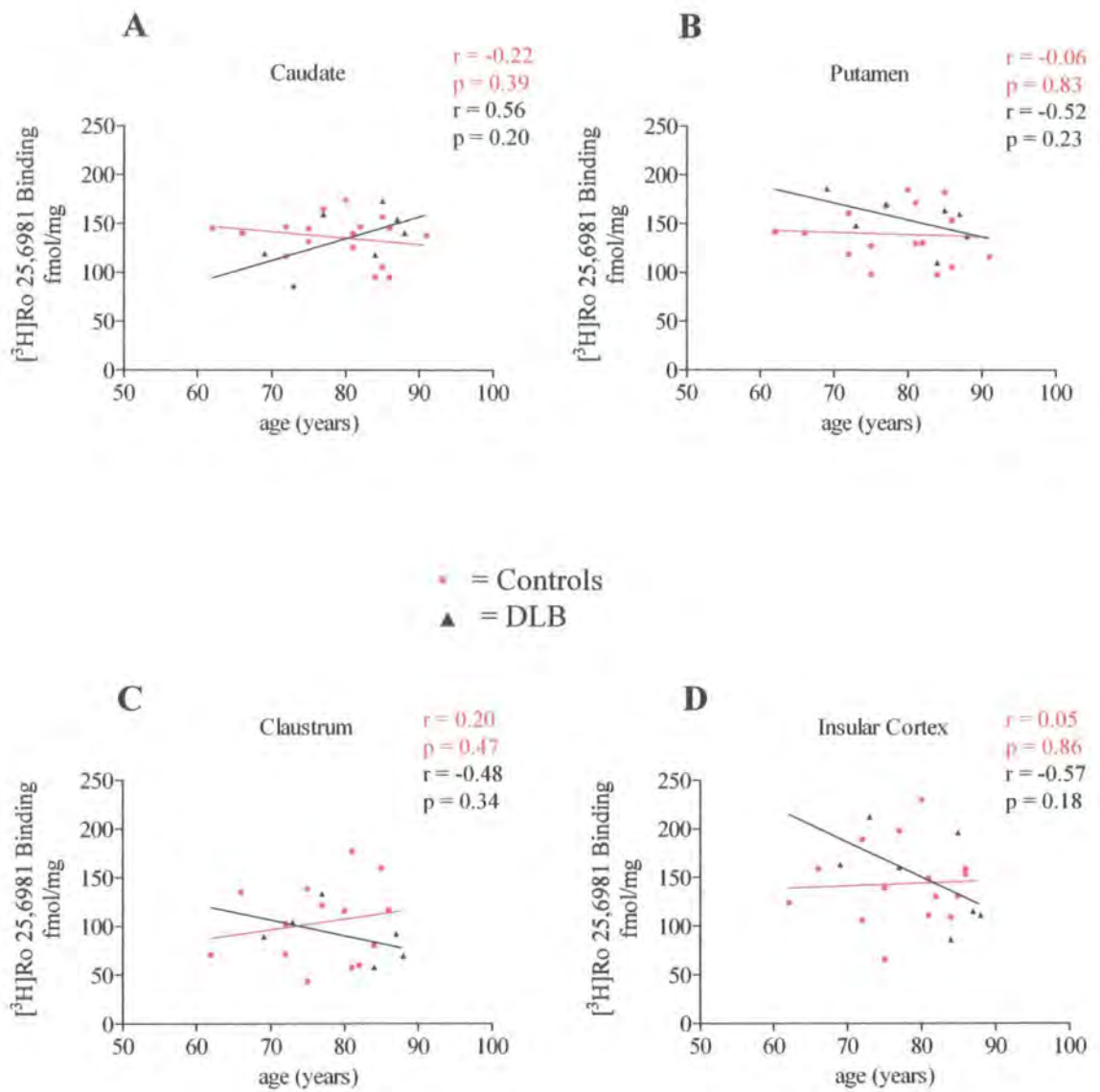


Figure 4.27 (A-D) Age-dependant absolute specific binding of [³H]Ro 25,6981 in female control and DLB cases in (A) Caudate, (B) Putamen, (C) Claustrum and (D) Insular Cortex

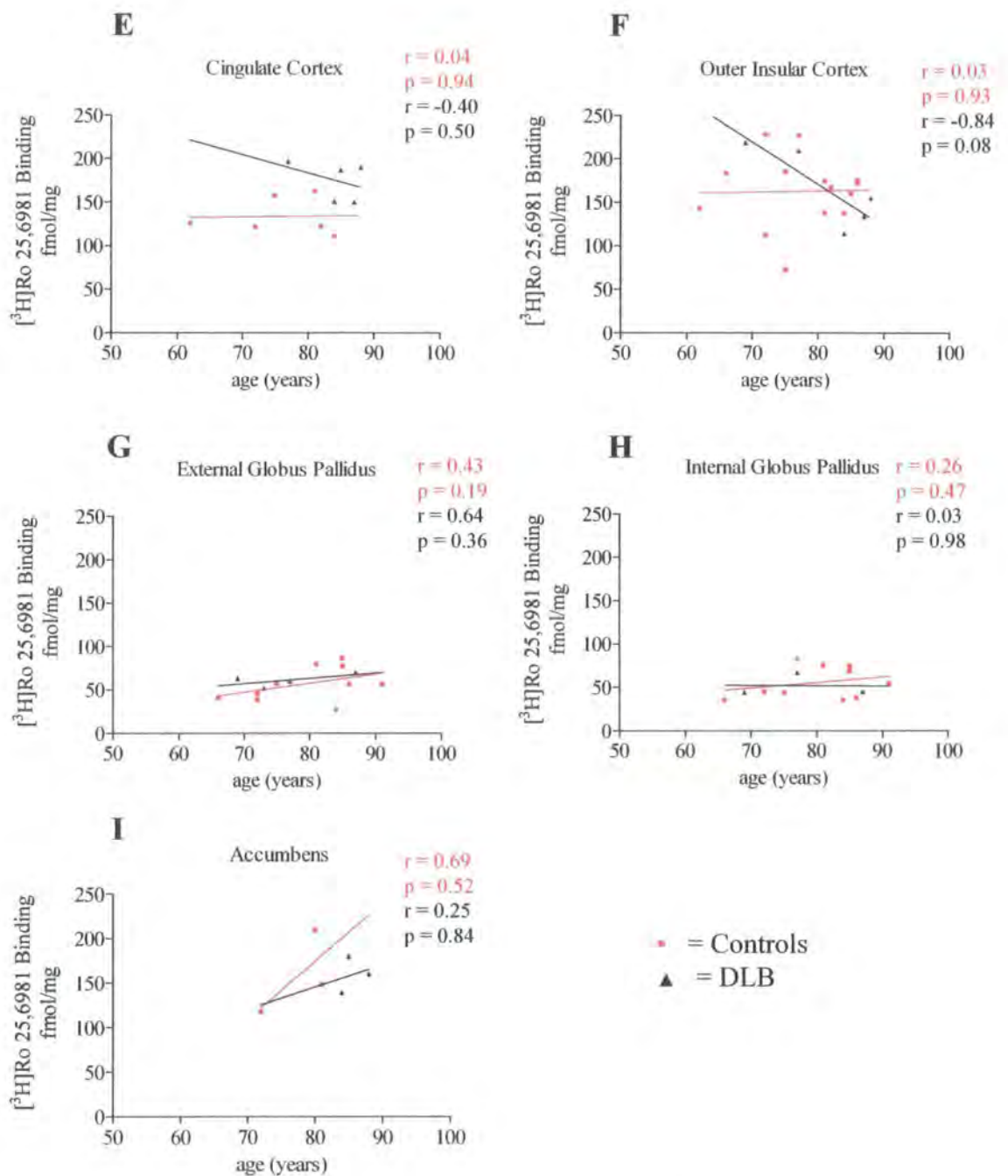


Figure 4.27 (E-I) Age-dependant absolute specific binding of $[^3\text{H}]\text{Ro 25,6981}$ in female control and DLB cases in (E) Cingulate Cortex, (F) Outer Insular Cortex, (G) External Globus Pallidus, (H) Internal Globus Pallidus and (I) Nucleus Accumbens

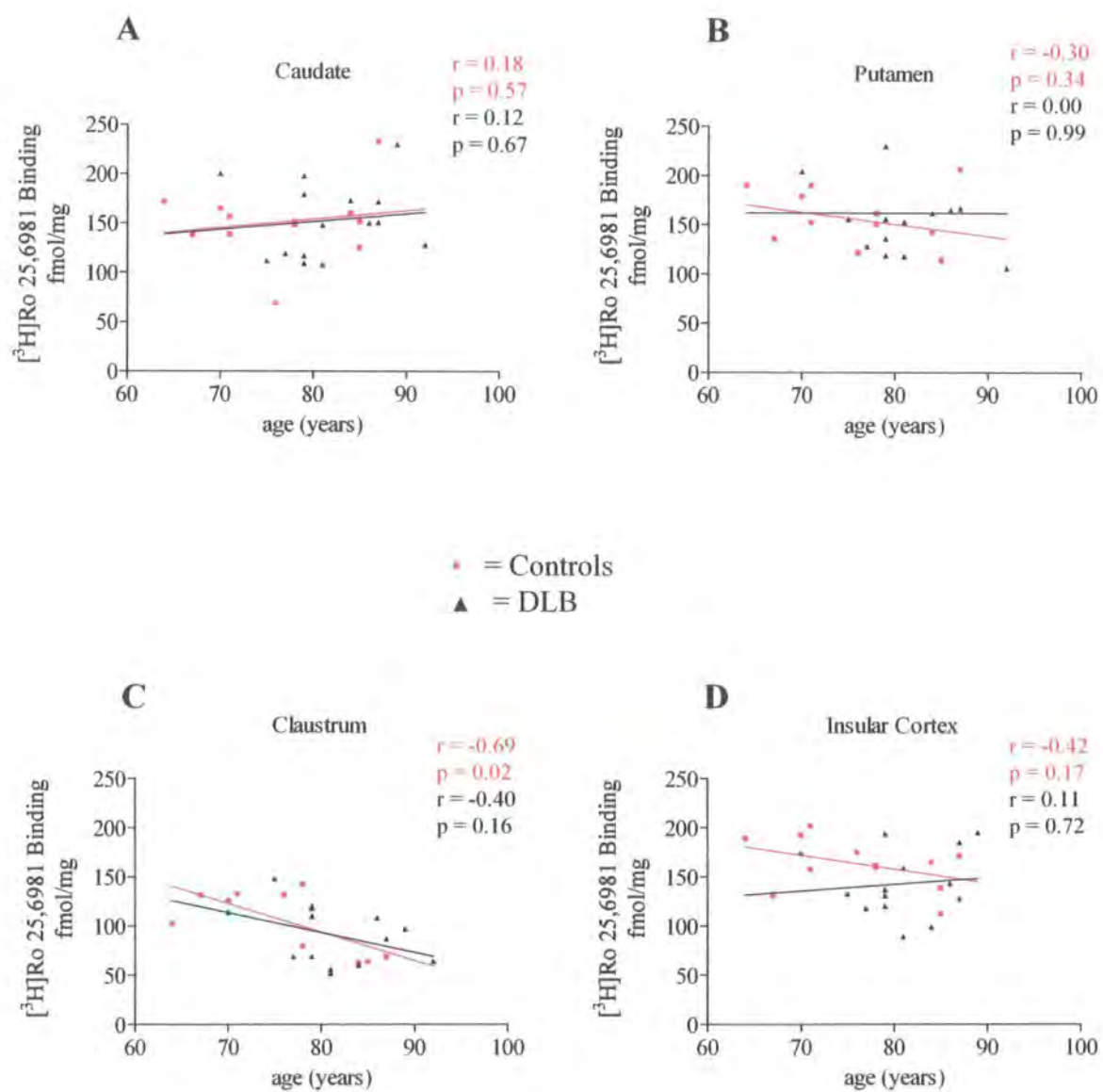


Figure 4.28 (A-D) Age-dependant absolute specific binding of [³H]Ro 25,6981 in male control and DLB cases in (A) Caudate, (B) Putamen, (C) Claustrum and (D) Insular Cortex

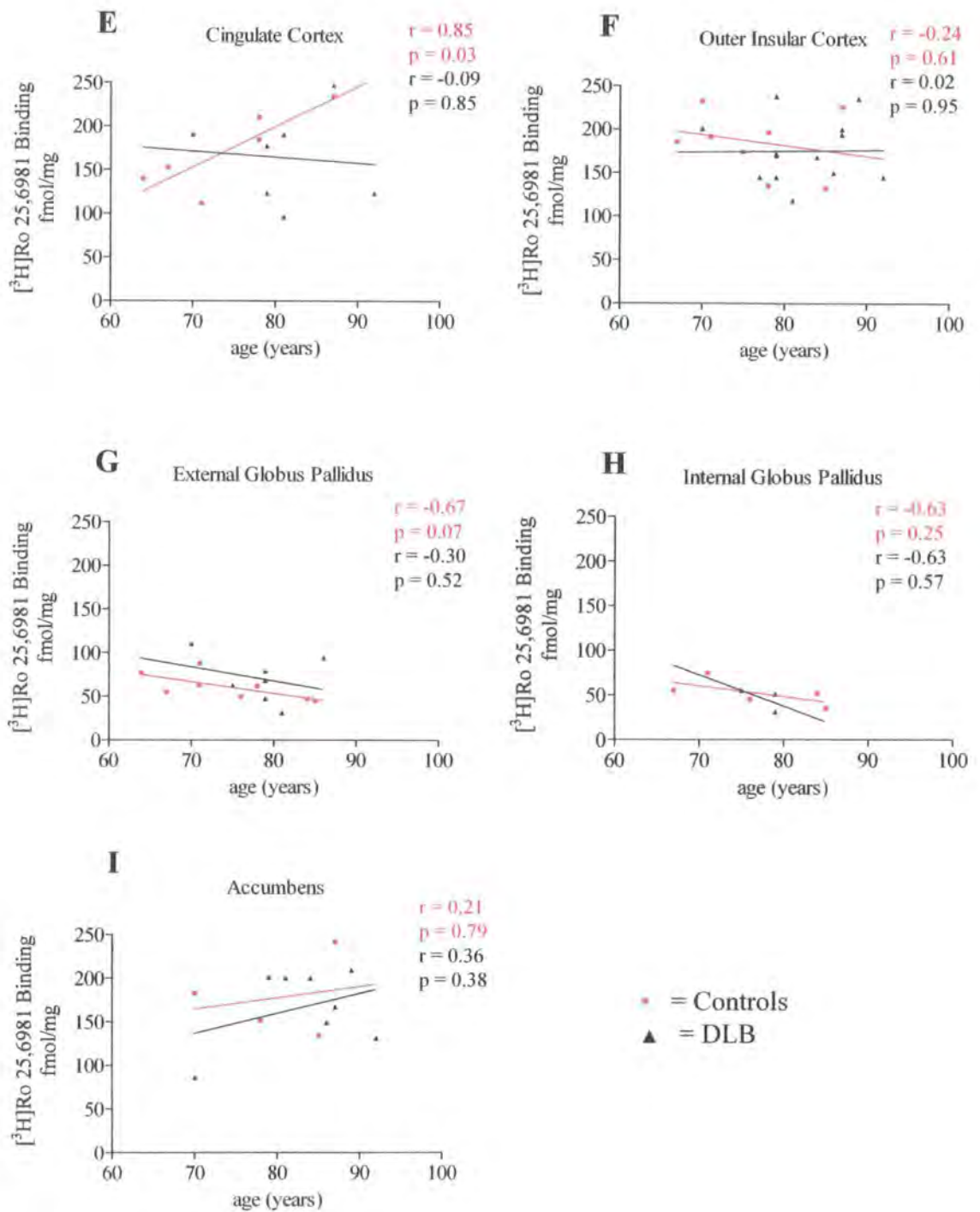


Figure 4.28 (E-I) Age-dependant absolute specific binding of [³H]Ro 25,6981 in male control and DLB cases in (E) Cingulate Cortex, (F) Outer Insular Cortex, (G) External Globus Pallidus, (H) Internal Globus Pallidus and (I) Nucleus Accumbens

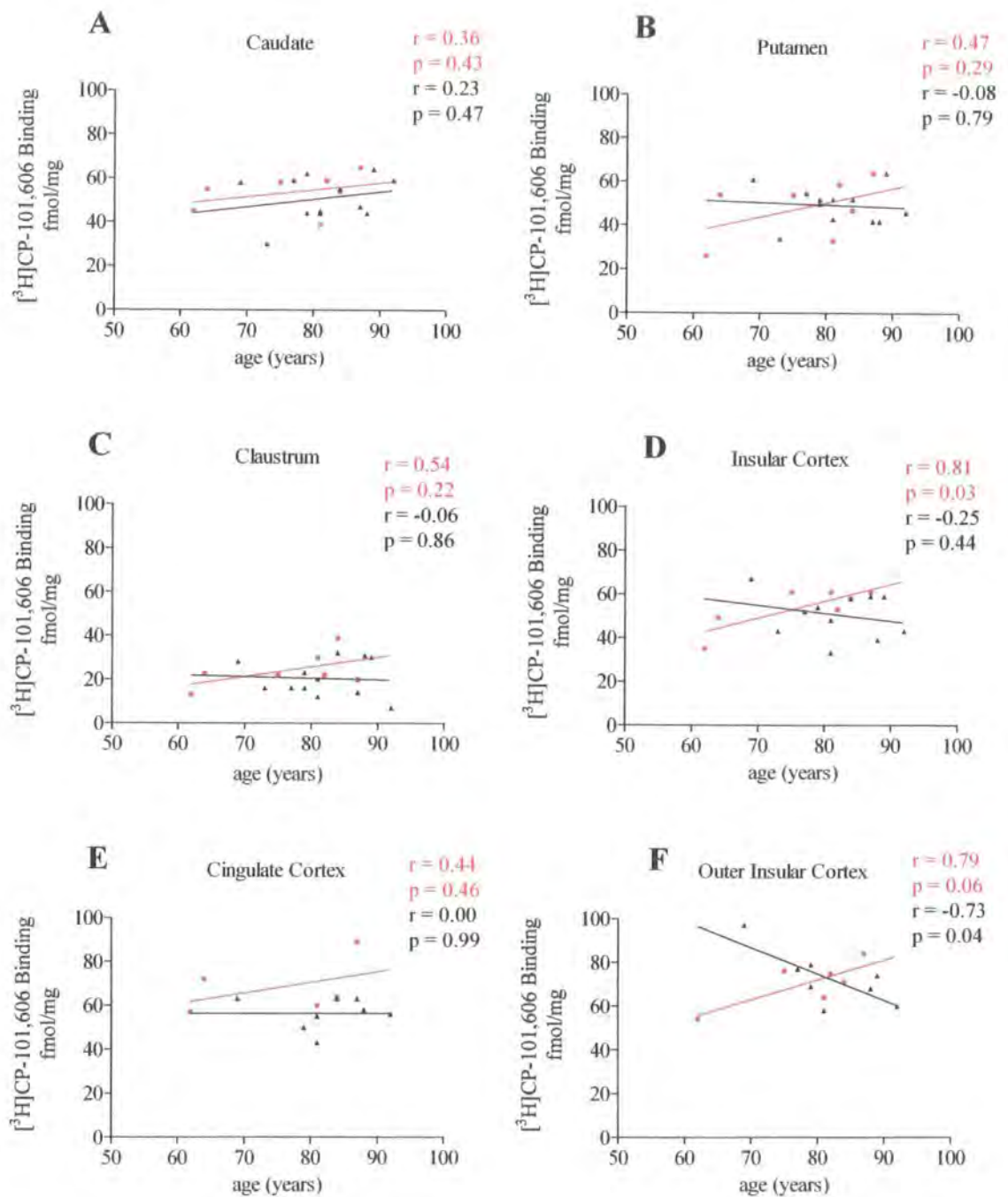


Figure 4.29 (A-F) Age-dependant absolute specific binding of $[^3\text{H}]\text{CP-101,606}$ in male and female control and DLB cases in (A) Caudate, (B) Putamen, (C) Claustrum and (D) Insular Cortex, (E) Cingulate Cortex and (F) Outer Insular Cortex

■ = Controls
 ▲ = DLB

4.5.5 Results (Figure 4.30 (A- I) to 4.32 (A-F)).

Figure 4.30 (A-I) shows the specific binding levels in male and female control (n = 26) and PDD (n = 7) cases (see table 4.2) for [³H]Ro 25,6981 against age, ranging from 67-92 years in the 9 brain regions defined. There were no significant age-dependant changes in all brain regions analysed in control and disease state cases ($p \geq 0.15$ in all cases) with the exception of the external globus pallidus PDD data where $p=0.09$, showing borderline significance. The regression lines on each graph were very similar for both control and DLB data in the cingulate cortex and external globus pallidus, showing a slight increase in binding levels with age. All other tissues showed a sharp increase in PDD binding with age as the control binding levels either slightly decreased, or in the case of the accumbens, slightly increased. The PDD regression line was removed from graph H due to the low n number, as it would not have been statistically valid. The r values ranged from 0.02 (control, external globus pallidus) to 0.98 (PDD, external globus pallidus).

The data in figure 4.30 (A-I) were further analysed for gender differences. Figure 4.31 (A-F) shows the specific binding levels in male control (n = 11) and PDD (n = 6) cases (see table 4.2) for [³H]Ro 25,6981 against age, ranging from 67-91 years in the 6 brain regions defined. There were no significant age-dependant changes in all brain regions analysed in control and disease state cases ($p \geq 0.17$ in all cases) with the exception of the control claustrum and cingulate cortex where $p=0.02$ and $p=0.03$ respectively showing significance. The regression lines on each graph were similar for both control and PDD data in the caudate and cingulate cortex where both showed an increase in binding with age. All other tissues showed an increase in PDD binding with age as the control binding levels decreased. The r values ranged from 0.18 (control, caudate) to 0.85 (control, cingulate cortex). Due to

low n values in the [³H]Ro 25,6981 female PDD cohort, only the male data could be analysed.

Figure 4.32 (A-F) shows the specific binding levels in male and female control (n = 7) and PDD (n = 3) cases (see table 4.2) for [³H]CP-101,606 against age, ranging from 62-87 years in the 6 brain regions defined. There were no significant age-dependant changes in all brain regions analysed in control and disease state cases ($p \geq 0.18$ in all cases) with the exception of the control insular cortex where $p=0.03$ showing significance. The control outer insular cortex showed borderline significance with $p=0.06$. The regression lines on graphs B, C, E and F were removed due to the low n numbers, and would not have been statistically valid. The regression lines were similar for both control and PDD data in the caudate and insular cortex in that both showed an increase in binding with age. The r values ranged from 0.36 (control, caudate) to 0.96 (PDD, insular cortex). The data could not be further analysed for gender differences due to low n numbers in both the control and PDD cohorts.

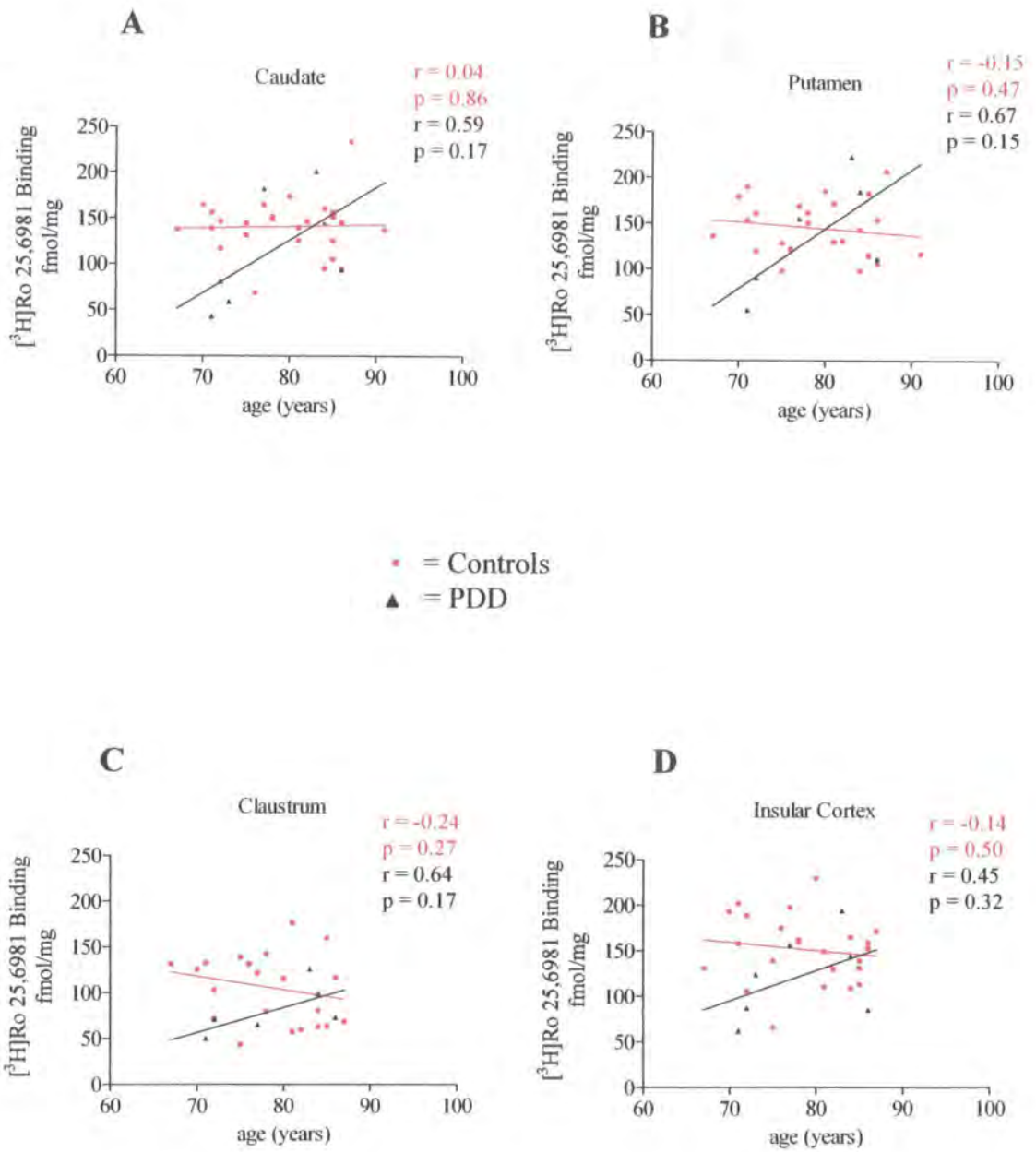


Figure 4.30 (A-D) Age-dependant absolute specific binding of [³H]Ro 25,6981 in male and female control and PDD cases in (A) Caudate, (B) Putamen, (C) Claustrum and (D) Insular Cortex

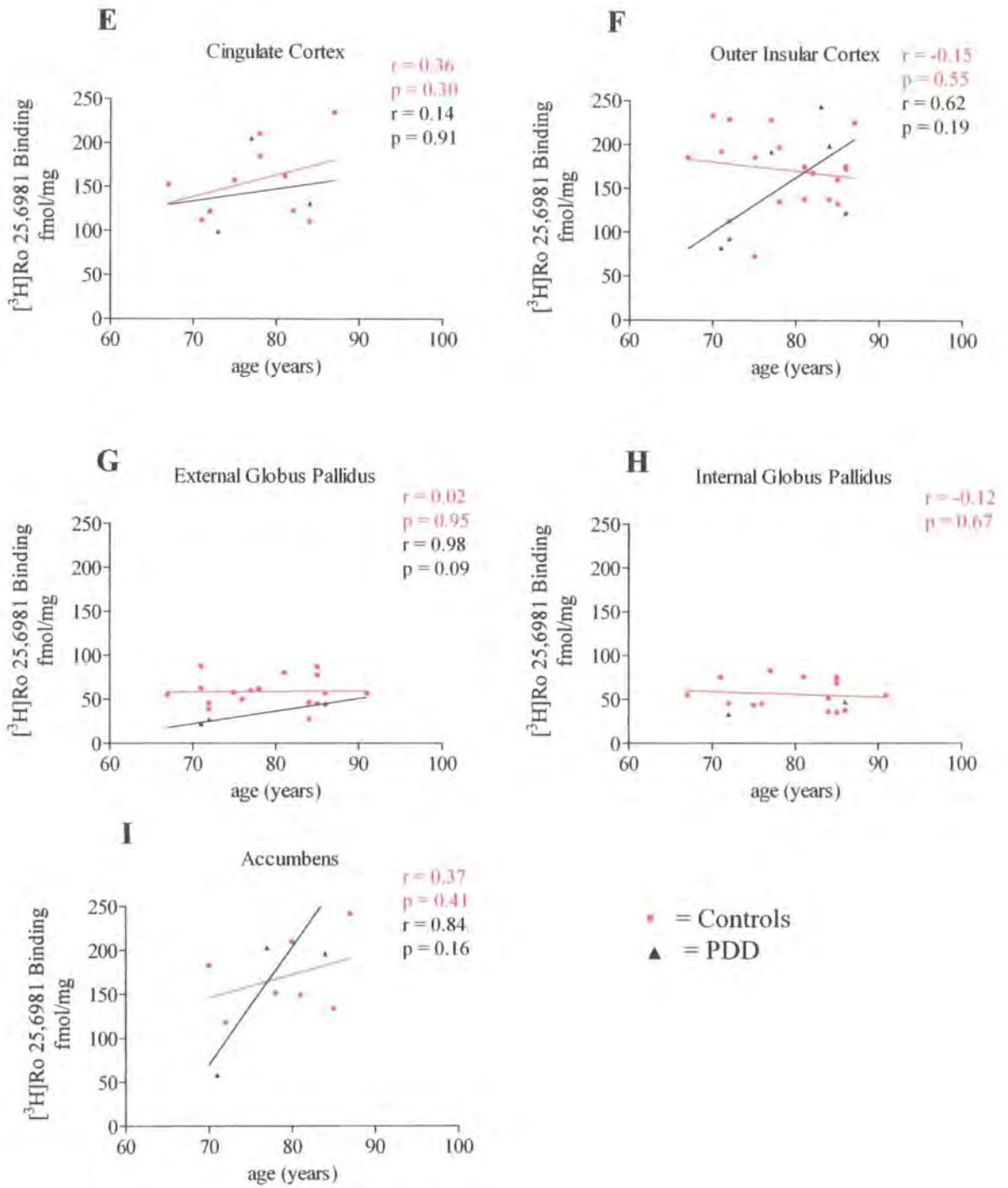


Figure 4.30 (E-I) Age-dependant absolute specific binding of $[^3\text{H}]\text{Ro 25,6981}$ in male and female control and PDD cases in (E) Cingulate Cortex, (F) Outer Insular Cortex, (G) External Globus Pallidus, (H) Internal Globus Pallidus and (I) Nucleus Accumbens

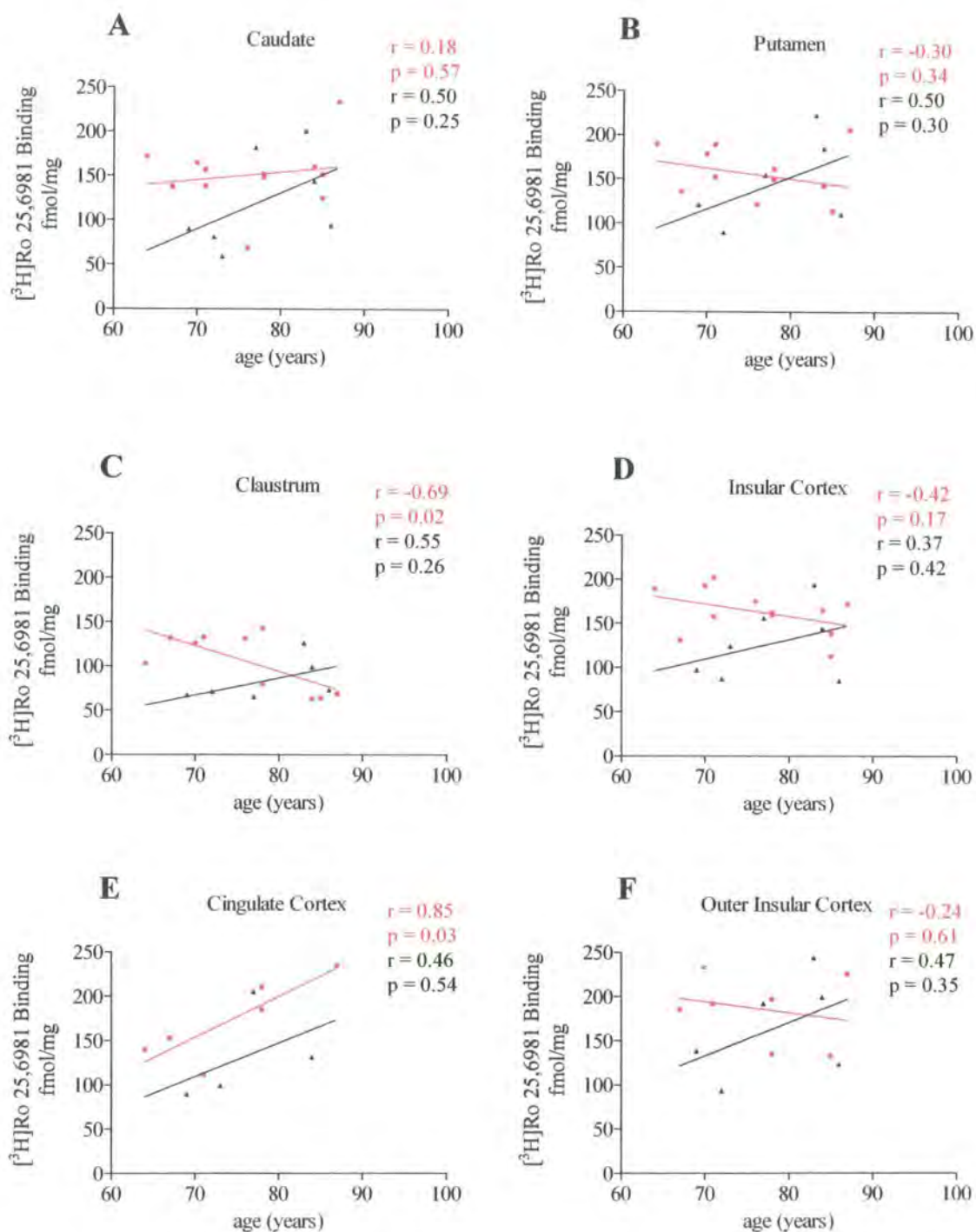


Figure 4.31 (A-F) Age-dependant absolute specific binding of [³H]Ro 25,6981 in male control and PDD cases in (A) Caudate, (B) Putamen, (C) Claustrum, (D) Insular Cortex, (E) Cingulate Cortex and (F) Outer Insular Cortex

▪ = Controls
▲ = PDD
256

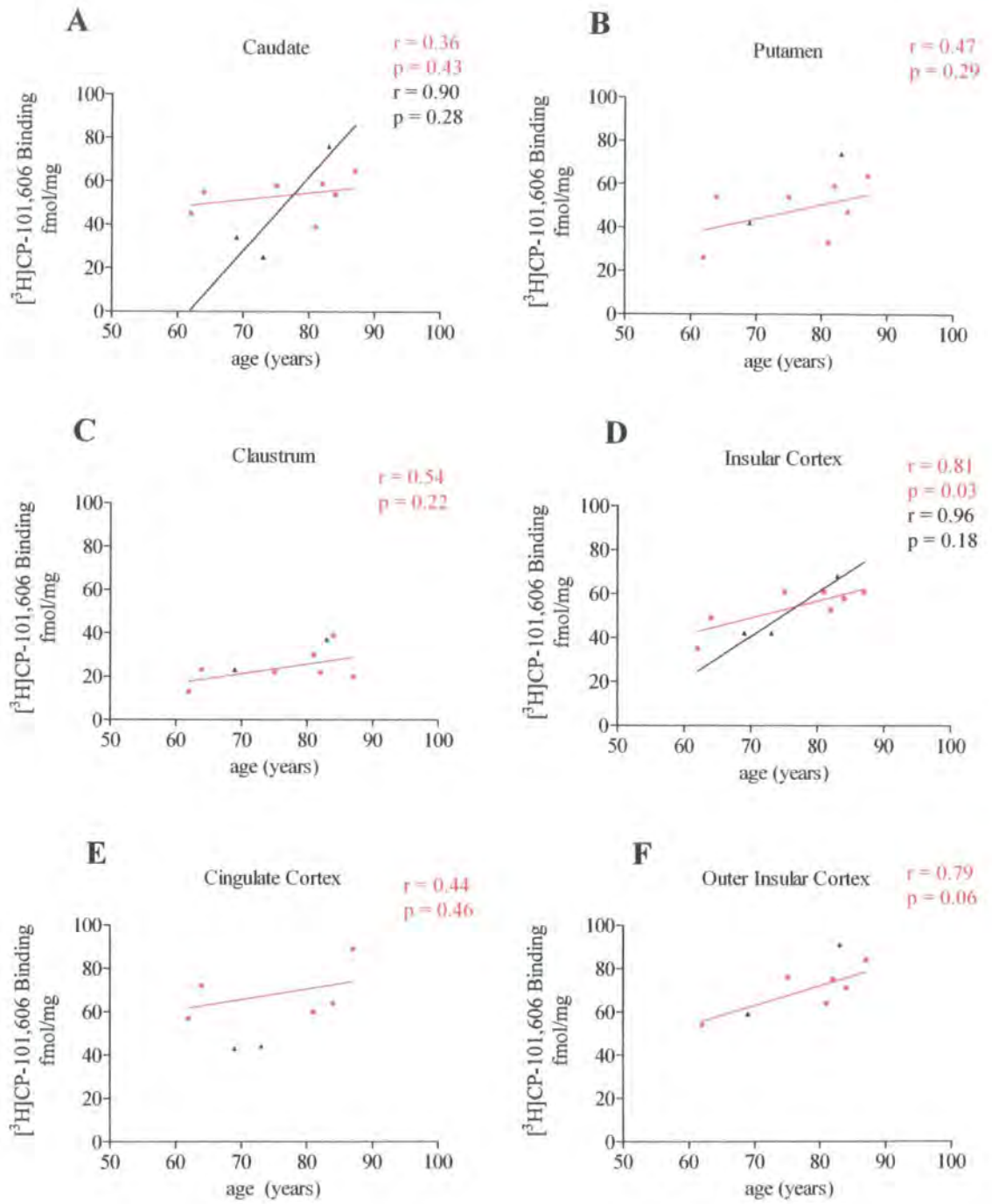


Figure 4.32 (A-F) Age-dependant absolute specific binding of [³H]CP-101,606 in male and female control and PDD cases in (A) Caudate, (B) Putamen, (C) Claustrum, (D) Insular Cortex, (E) Cingulate Cortex and (F) Outer Insular Cortex

▪ = Controls
▲ = PDD

4.5.6 Results (Figure 4.33 (A-I) to 4.35 (A-F)).

Figure 4.33 (A-I) shows the specific binding levels in male and female control (n = 26) and DLBPDD (n = 10) cases (see table 4.2) for [³H]Ro 25,6981 against age, ranging from 67-91 years in the 9 brain regions defined. There were no significant age-dependant changes in all brain regions analysed in control and disease state cases ($p \geq 0.12$ in all cases) with the exception of the insular cortex DLBPDD data where $p = 0.08$, showing borderline significance. The control and DLBPDD regression lines showed a similar pattern on graphs A, B, C, D and F, showing an increase in DLBPDD binding levels as control binding levels decrease with age. Both control and DLBPDD binding levels increased with age in the cingulate cortex and accumbens, while both binding levels decreased with age in the external and internal globus pallidus. The r values ranged from 0.02 (control, external globus pallidus) to 0.74 (DLBPDD, internal globus pallidus), with the control data showing better correlation to the linear regression than the DLBPDD data in all tissues.

The data in figure 4.33 (A-I) were further analysed for gender differences. Figure 4.34 (A-I) shows the specific binding levels in female control (n = 15) and DLBPDD (n = 7) cases for [³H]Ro 25,6981 against age, ranging from 62-91 years in the 9 brain regions defined. There were no significant age-dependant changes in all brain regions analysed in control and disease state cases ($p \geq 0.17$ in all cases) with the exception of the insular cortex DLBPDD data where $p = 0.06$, showing borderline significance. The DLBPDD regression lines showed an increase with age in all the tissues except the external and internal globus pallidus. The control regression lines showed an increase in binding levels with increasing age, with the exception of the caudate and putamen. The r values ranged from 0.03 (control, outer insular cortex) to 0.77 (DLBPDD, accumbens), with the control data showing better

correlation to the linear regression than the DLBPDD data in all tissues except the external globus pallidus.

Figure 4.35 (A-F) shows the specific binding levels in male control (n = 11) and DLBPDD (n = 5) cases for [³H]Ro 25,6981 against age, ranging from 62-87 years in the 6 brain regions defined. There were no significant age-dependant changes in all brain regions analysed in control and disease state cases ($p \geq 0.17$ in all cases) with the exception of the control claustrum and cingulate cortex data where $p=0.02$ and $p=0.03$ respectively, showing significance. The DLBPDD regression lines decreased with age in all the tissues except the putamen, whereas the control regression lines decreased in all but the caudate and cingulate cortex. The r values ranged from 0.18 (control, caudate) to 0.85 (control, cingulate cortex).

Due to low n numbers, the data for [³H]CP-101,606 DLBPDD cases could not be analysed.

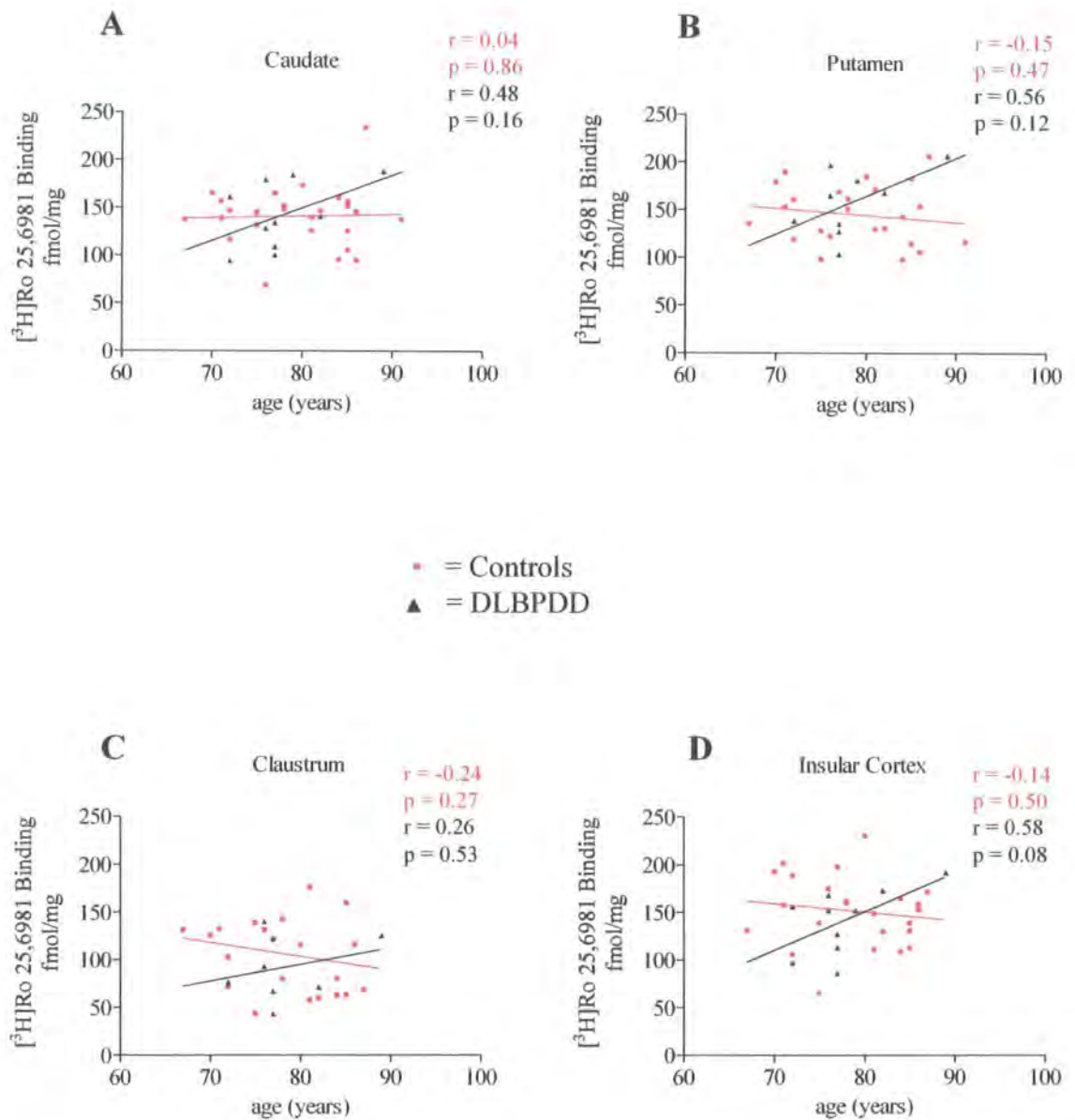


Figure 4.33 (A-D) Age-dependant absolute specific binding of $[^3\text{H}]\text{Ro 25,6981}$ in male and female control and DLBPDD cases in (A) Caudate, (B) Putamen, (C) Claustrum and (D) Insular Cortex

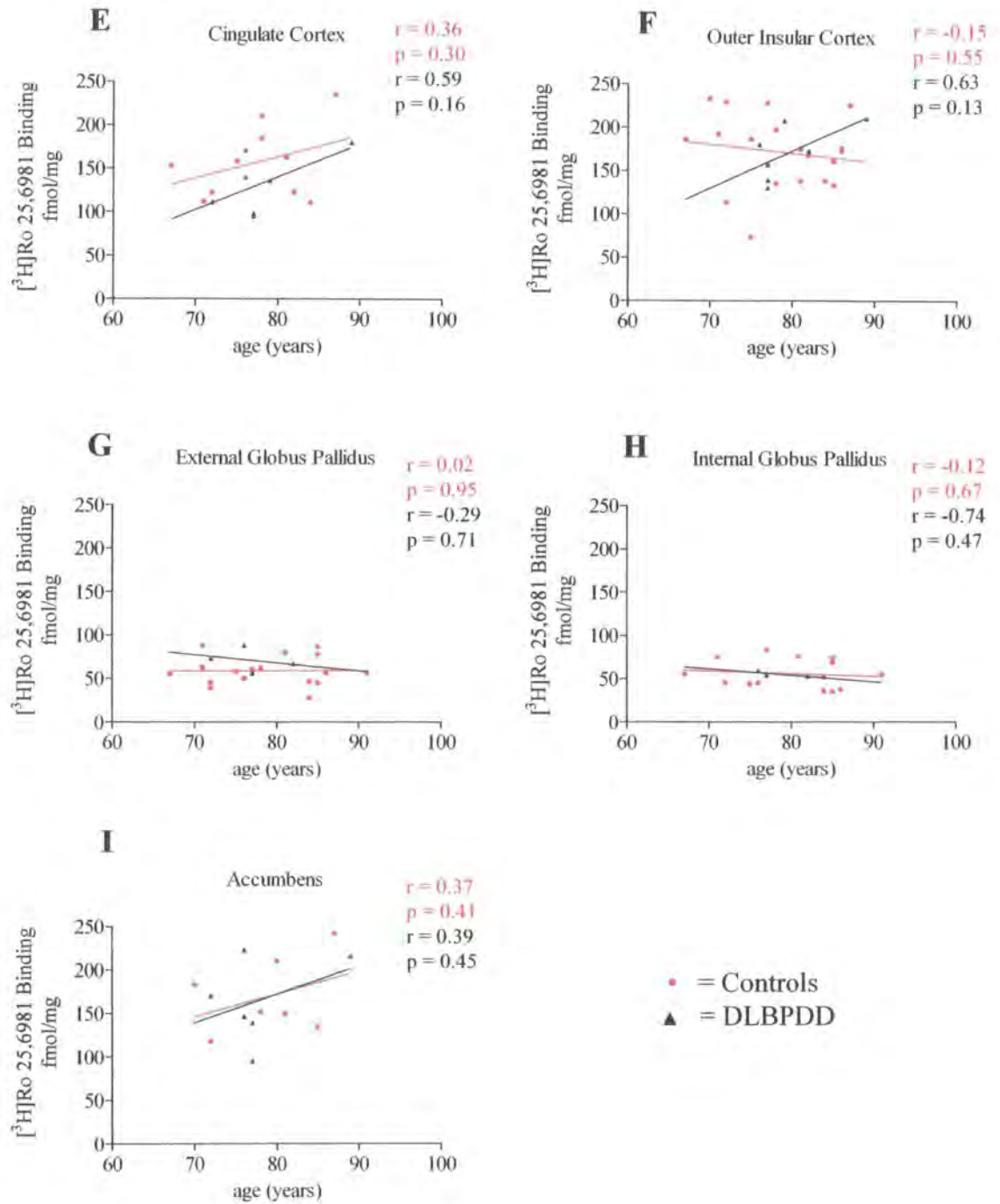


Figure 4.33 (E-I) Age-dependant absolute specific binding of $[^3\text{H}]\text{Ro 25,6981}$ in male and female control and DLBPDD cases in (E) Cingulate Cortex, (F) Outer Insular Cortex, (G) External Globus Pallidus, (H) Internal Globus Pallidus and (I) Nucleus Accumbens

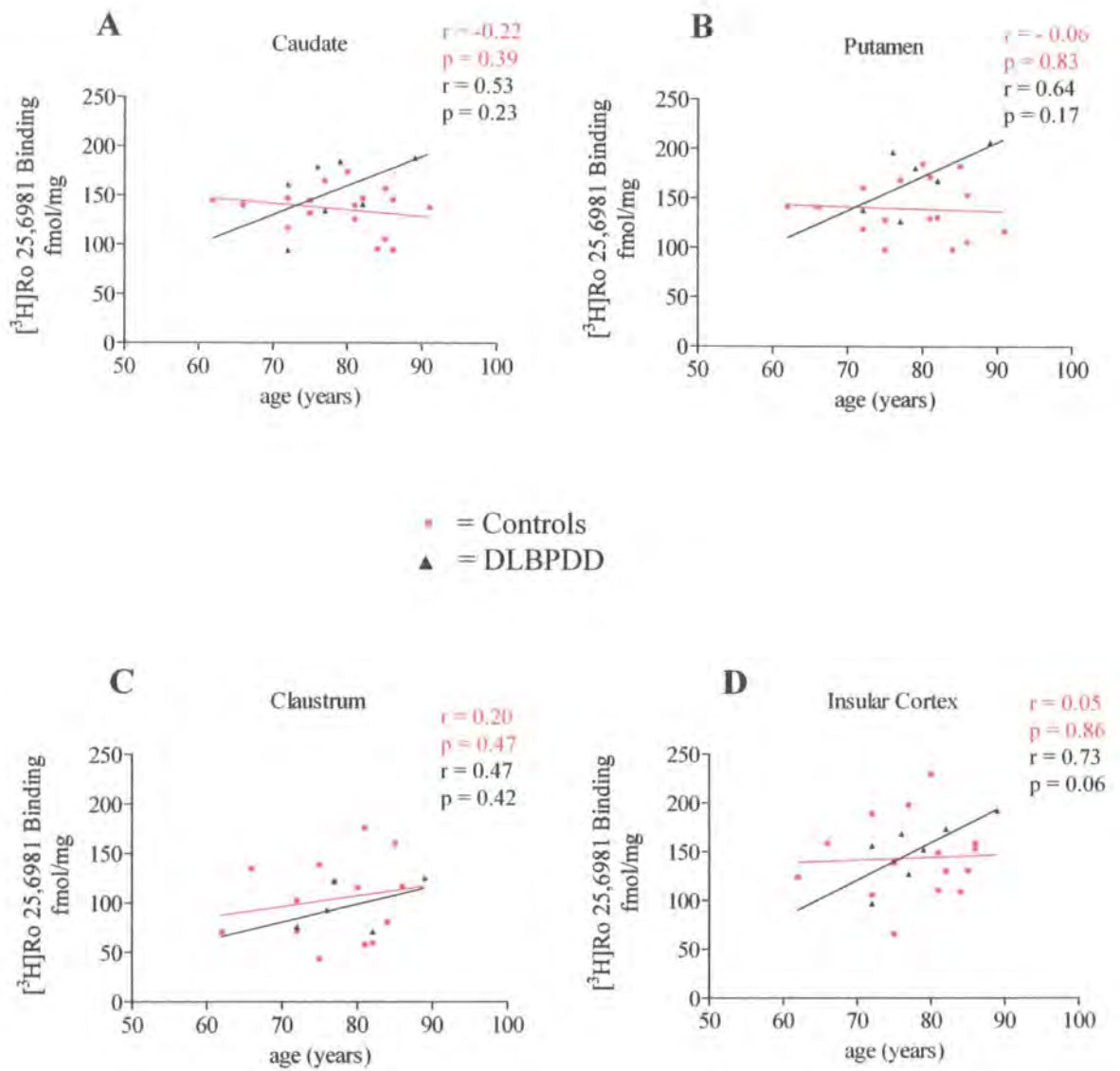


Figure 4.34 (A-D) Age-dependant absolute specific binding of $[^3\text{H}]\text{Ro 25,6981}$ in female control and DLBPDD cases in (A) Caudate, (B) Putamen, (C) Claustrum and (D) Insular Cortex

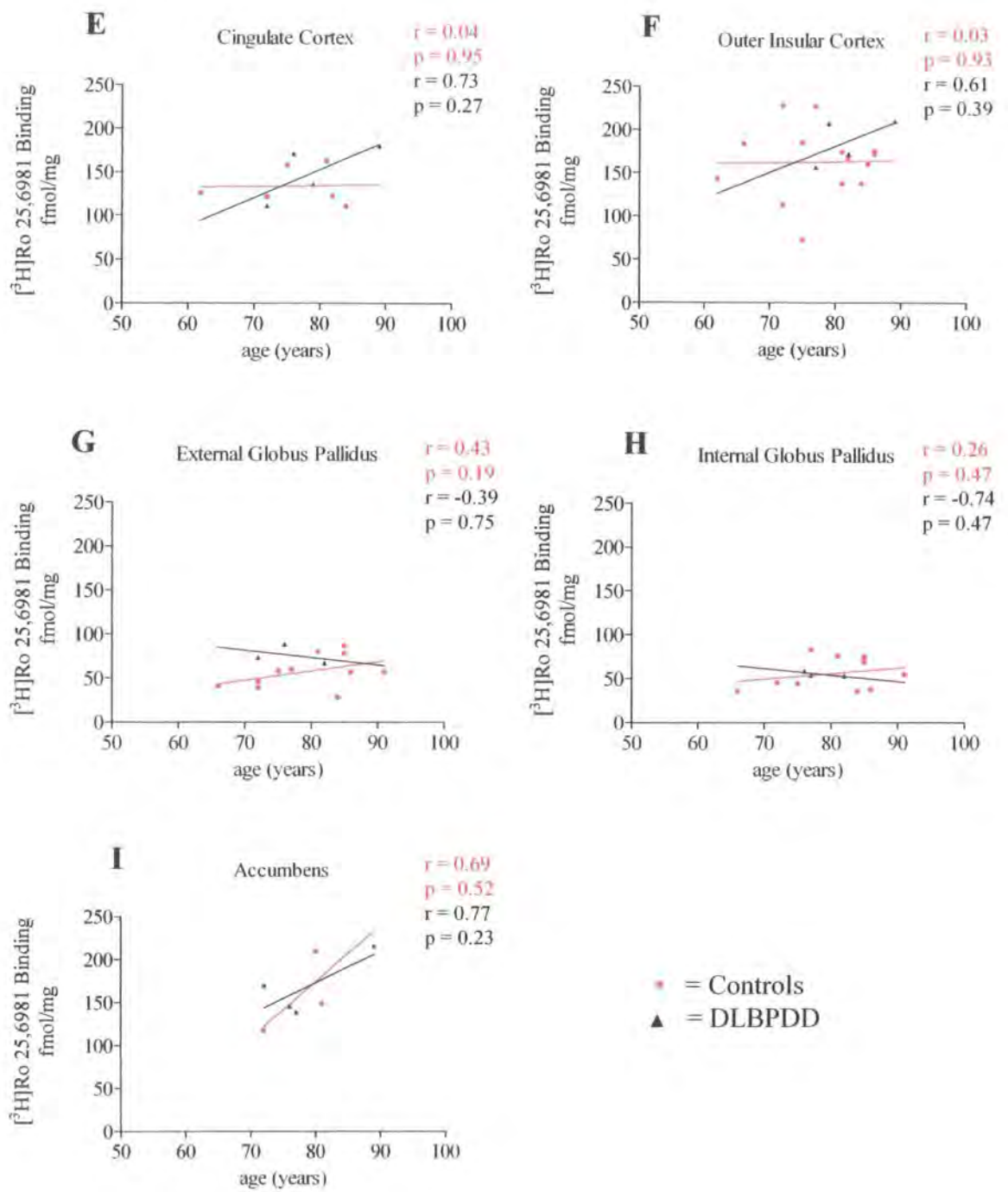


Figure 4.34 (E-I) Age-dependant absolute specific binding of [³H]Ro 25,6981 in female control and DLBPDD cases in (E) Cingulate Cortex, (F) Outer Insular Cortex, (G) External Globus Pallidus, (H) Internal Globus Pallidus and (I) Nucleus Accumbens

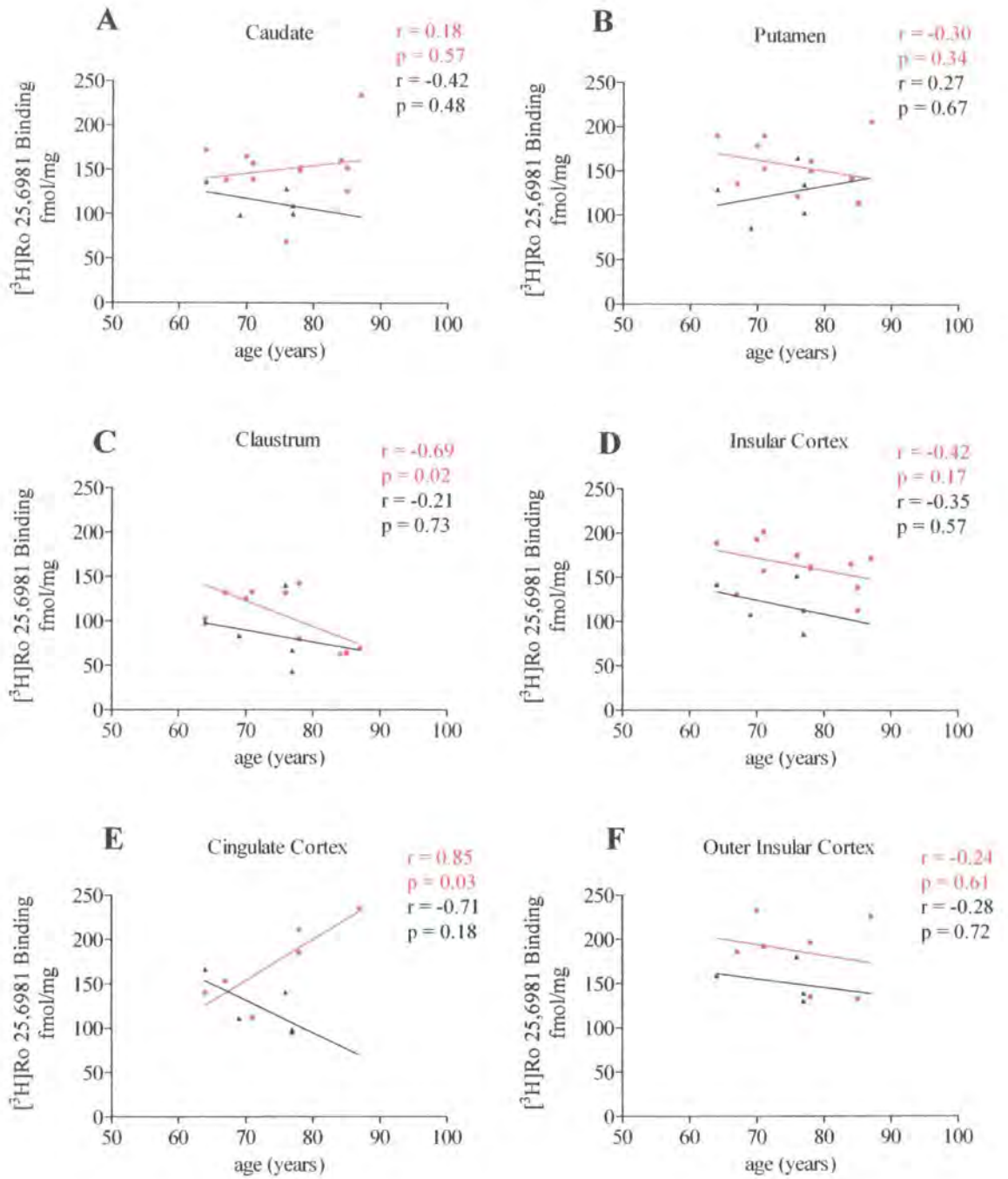


Figure 4.35 (A-F) Age-dependant absolute specific binding of [³H]Ro 25,6981 in male control and DLBPDD cases in (A) Caudate, (B) Putamen, (C) Claustrum and (D) Insular Cortex, (E) Cingulate Cortex and (F) Outer Insular Cortex

• = Controls
 ▲ = DLBPDD

4.5.7 Results (Figure 4.36 (A-I) to Figure 4.38 (A-F))

Figure 4.36 (A-I) shows the specific binding levels in male and female control (n = 26) and AD (n = 10) cases (see table 4.2) for [³H]Ro 25,6981 against age, ranging from 67-91 years in the 9 brain regions defined. There were significant age-dependant changes in all brain regions analysed in the AD cases ($p \leq 0.02$ in all cases) with the exception of the claustrum, external and internal globus pallidus, where $p=0.16$, $p=0.07$ (borderline significance) and $p=0.42$ respectively. There were no significant age-dependant changes in all the regions analysed in the control data. The AD regression lines showed a sharp decrease with age in all the tissues, whereas the control data varied depending on the tissue. The r values ranged from 0.02 (control, external globus pallidus) to 0.98 (AD, cingulate cortex).

The data in figure 4.36 (A-I) were further analysed for gender differences. Figure 4.37 (A-G) shows the specific binding levels in female control (n = 15) and AD (n = 7) cases for [³H]Ro 25,6981 against age, ranging from 62-91 years in the 7 brain regions defined. There were significant age-dependant changes in all brain regions analysed in the AD cases ($p \leq 0.03$ in all cases) with the exception of the claustrum and outer insular cortex data where $p=0.23$ and $p=0.39$ respectively. For the cingulate cortex $p=0.10$, showing borderline significance. As with the male and female graphs combined, the AD regression lines showed a sharp decrease with age in all the tissues, whereas the control data varied depending on the tissue. The r values ranged from 0.03 (control, outer insular cortex) to 0.89 (AD, nucleus accumbens).

Figure 4.38 (A-F) shows the specific binding levels in male and female control (n = 7) and AD (n = 2) cases for [³H]CP-101,606 against age, ranging from 62-87 years in the 6 brain

regions defined. There were no significant age-dependant changes in all brain regions analysed in the control cases ($p \geq 0.22$ in all cases) with the exception of the insular cortex where $p=0.03$, showing significance, and the outer insular cortex where $p=0.06$, showing borderline significance. The AD regression lines could not be shown due to the low n numbers, and would not have been statistically valid. The r values ranged from 0.36 (control, caudate) to 0.81 (control, insular cortex). The data could not be further analysed for gender differences due to the low n numbers.

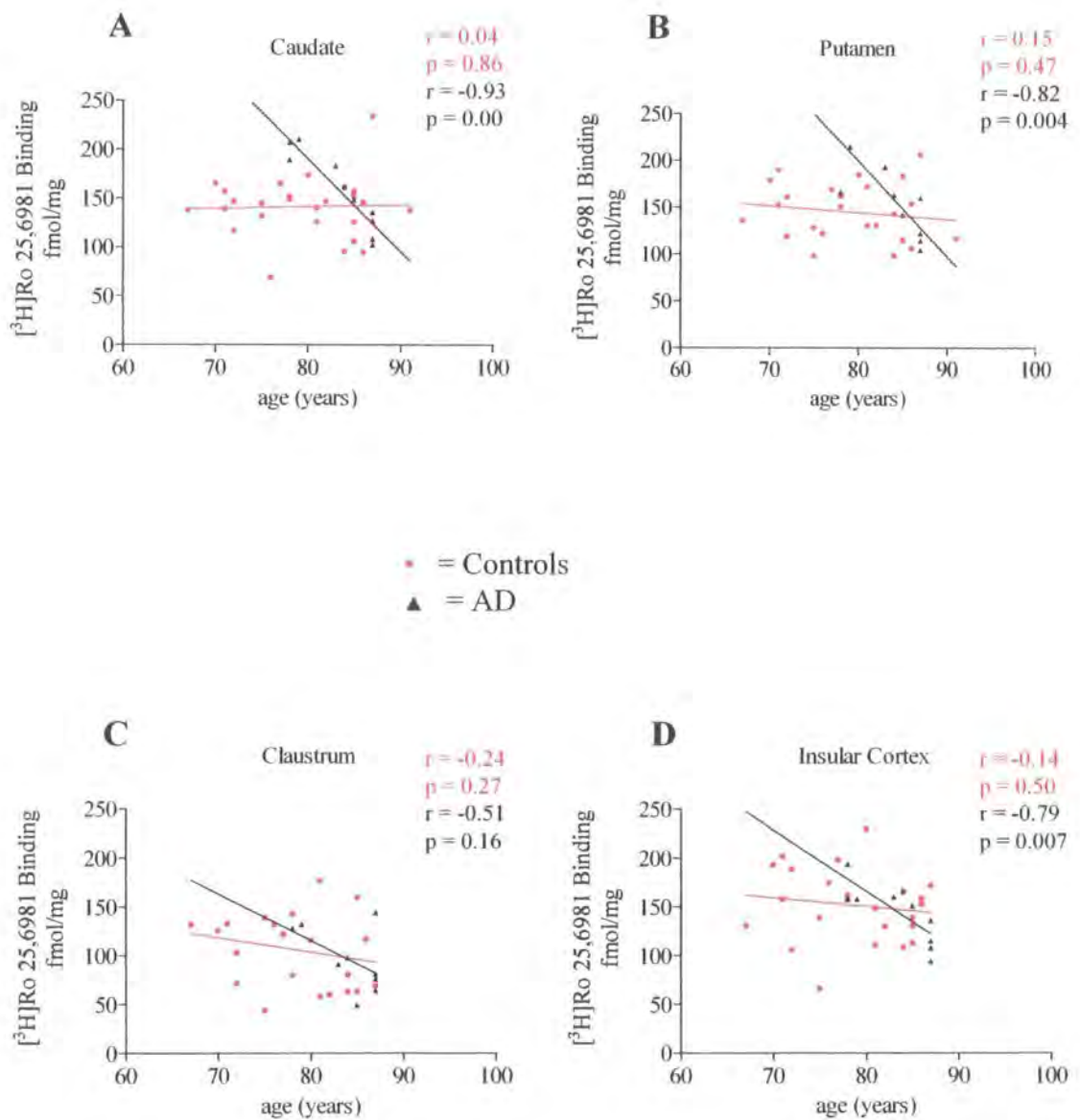


Figure 4.36 (A-D) Age-dependant absolute specific binding of $[^3\text{H}]\text{Ro 25,6981}$ in male and female control and AD cases in (A) Caudate, (B) Putamen, (C) Claustrum and (D) Insular Cortex

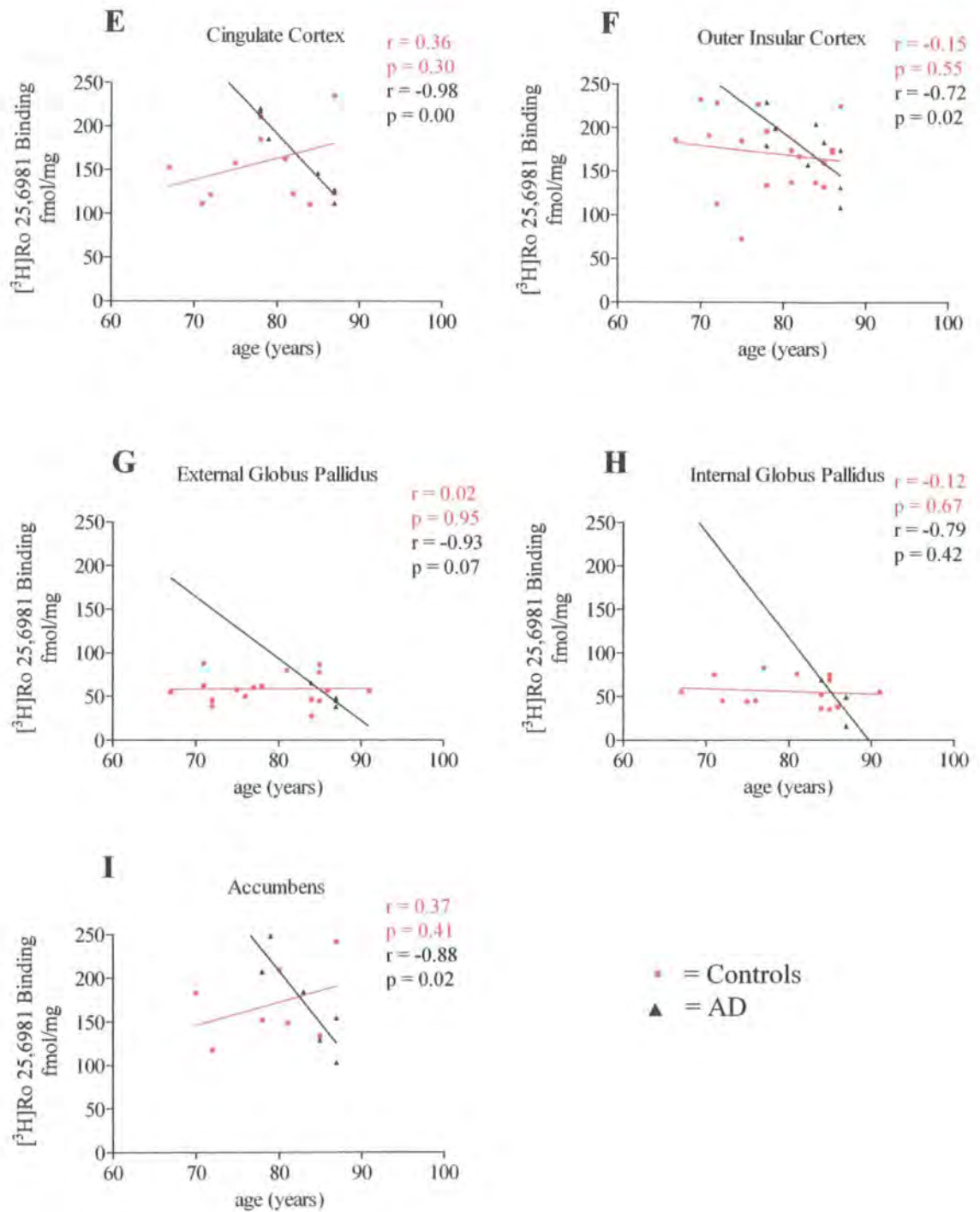


Figure 4.36 (E-I) Age-dependant absolute specific binding of $[^3\text{H}]\text{Ro 25,6981}$ in male and female control and AD cases in (E) Cingulate Cortex, (F) Outer Insular Cortex, (G) External Globus Pallidus, (H) Internal Globus Pallidus and (I) Nucleus Accumbens

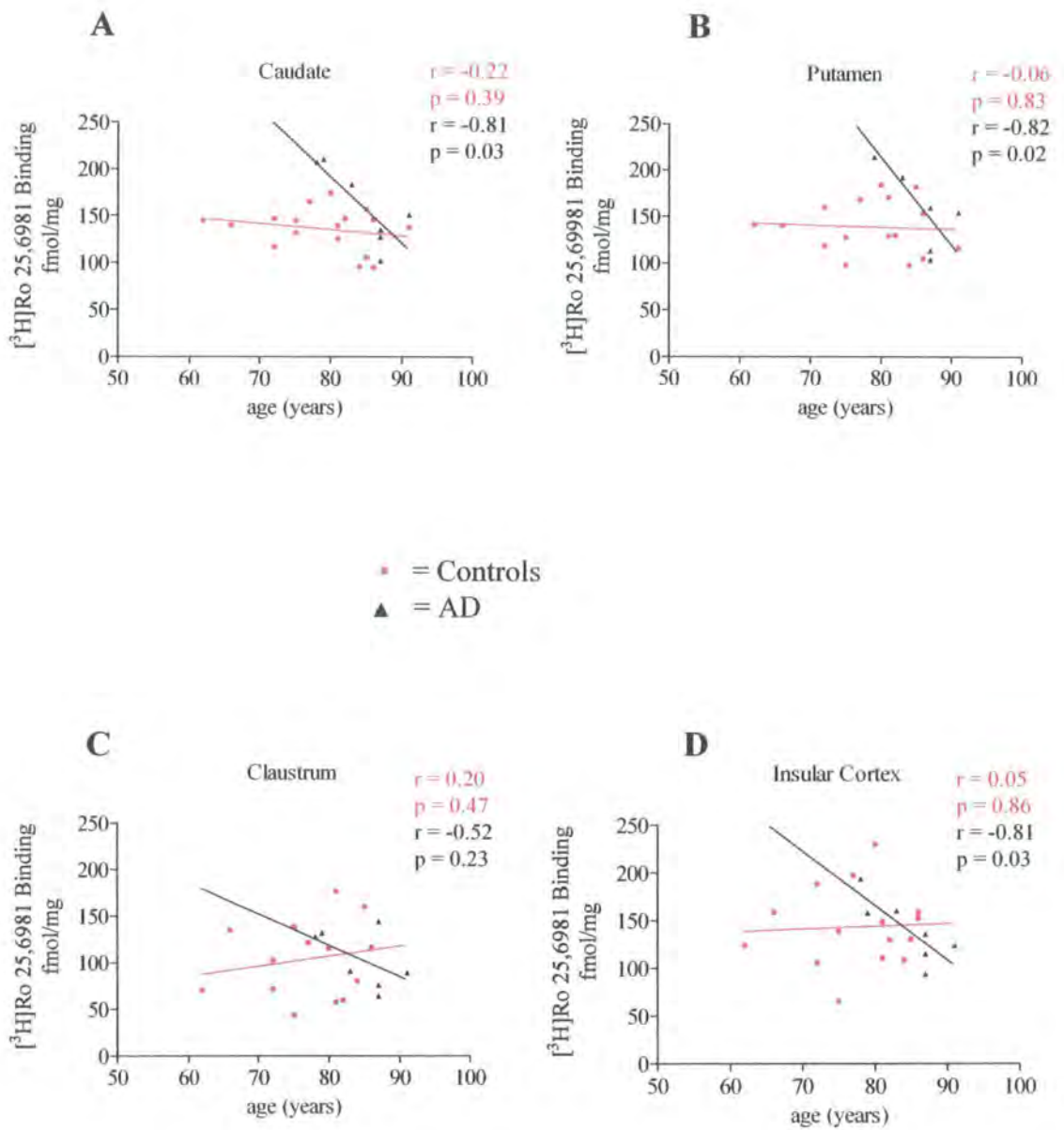


Figure 4.37 (A-D) Age-dependant absolute specific binding of $[^3\text{H}]\text{Ro 25,6981}$ in female control and AD cases in (A) Caudate, (B) Putamen, (C) Claustrum and (D) Insular Cortex

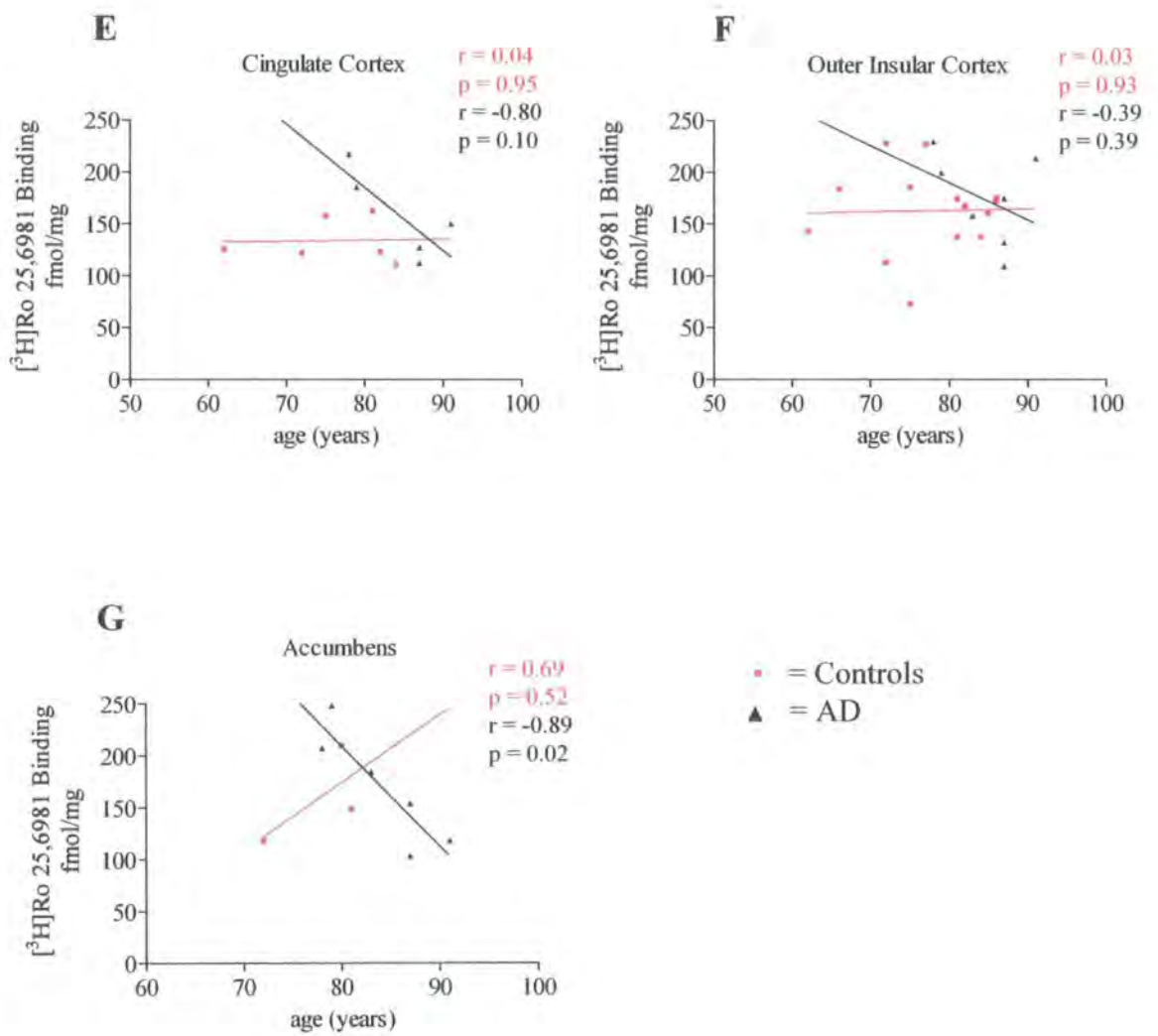


Figure 4.37 (E-G) Age-dependant absolute specific binding of $[^3\text{H}]\text{Ro 25,6981}$ in female control and AD cases in (E) Cingulate Cortex, (F) Outer Insular Cortex and (G) Nucleus Accumbens

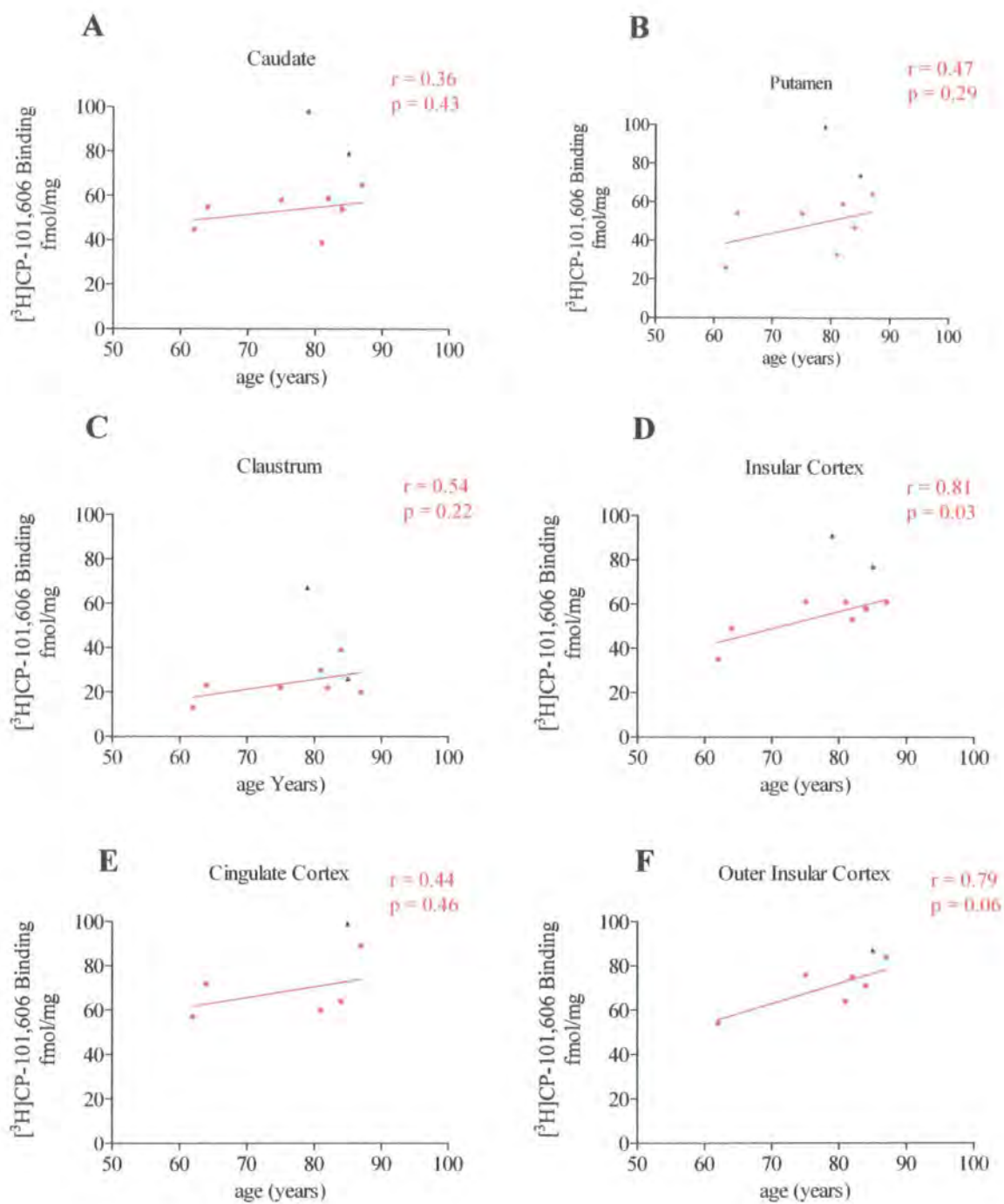


Figure 4.38 (A-F) Age-dependant absolute specific binding of [³H]CP-101,606 in male and female control and AD cases in (A) Caudate, (B) Putamen, (C) Claustrum, (D) Insular Cortex, (E) Cingulate Cortex and (F) Outer Insular Cortex

▪ = Controls
 ▲ = AD

4.5.8 Results (Figure 4.39 (A-I) to Figure 4.44 (A-F))

The data were then further analysed to show specific binding levels of both [³H]Ro 25,6981 and [³H]CP-101,606 individually in various brain regions, analysing all control and disease state groups separately from each other. Radioligand binding levels in fmol/mg were correlated with age at death of the subject (in years) for each case, and in each brain region defined, to look for gender differences in the tissues. Estimated linear regression lines of best fit were produced using GraphPad Prism and are represented on each graph, indicating any age-dependant changes in binding levels in each tissue. The significance of the regression was determined from the generated p value, where $p \leq 0.05$ was considered to show a significant linear relationship between age and binding level. Due to limited availability of the [³H]CP-101,606 ligand a smaller number of cases were analysed, resulting in low n numbers for some of the tissues. In these cases a linear regression line was not shown as it would not have been appropriate where $n = < 3$. The generated correlation coefficient or r value shows how well the data fits to the regression line, where $r = 1$ shows strong correlation and $r = 0$ shows little or none.

Figure 4.39 (A-I) shows the specific binding levels in female ($n = 17$) and male ($n = 12$) control cases (see table 4.1) for [³H]Ro 25,6981 against age, ranging from 62-91 years in the 9 brain regions defined. There were no significant age-dependant changes in all brain regions analysed ($p \geq 0.17$ in all cases) with the exception of the male claustrum and the male cingulate cortex data where $p = 0.02$ and $p = 0.03$ respectively, showing significance. Interestingly, the male claustrum binding level significantly decreased with age, whereas the male cingulate cortex binding level significantly increased with age. The male external globus pallidus data gave $p = 0.07$, showing borderline significance. There did not appear to

be any trends emerging from the data as the regression lines on each graph varied a great deal for male and female cases and depending on which tissue was being analysed. The r values ranged from 0.03 (female, outer insular cortex) to 0.85 (male cingulate cortex).

Figure 4.40 (A-F) shows the specific binding levels in female ($n = 5$) and male ($n = 2$) control cases (see table 4.1) for [^3H]CP-101,606 against age, ranging from 62-87 years in the 6 brain regions defined. Due to the low n numbers for the male data the regression lines could not be drawn, although the female regression lines in each tissue showed an increase in binding level with age, where $p \geq 0.17$ in each case. The claustrum and insular cortex showed borderline significance where $p = 0.08$ in both cases. The r values ranged from 0.29 (female, caudate) to 0.88 (female cingulate cortex).

Figure 4.41 (A-I) shows the specific binding levels in female ($n = 7$) and male ($n = 15$) DLB cases (see table 4.1) for [^3H]Ro 25,6981 against age, ranging from 69-92 years in the 9 brain regions defined. There were no significant age-dependant changes in all brain regions analysed ($p \geq 0.16$ in all cases) with the exception of the female outer insular cortex where $p = 0.08$, showing borderline significance. As with the data in figure 4.39 (A-I), the regression lines on each graph varied a great deal for male and female cases and depending on which tissue was being analysed, and no clear age dependant trends were seen. The r values ranged from 0.00 (male, putamen) to -0.84 (female outer insular cortex).

Figure 4.42 (A-G) shows the specific binding levels in female ($n = 4$) and male ($n = 8$) DLB cases (see table 4.1) for [^3H]CP-101,606 against age, ranging from 69-92 years in the 7 brain regions defined. There were no significant age-dependant changes in all brain regions analysed ($p \geq 0.12$ in all cases). The female outer insular cortex regression line was not shown due to a low n number. Again, the regression lines on each graph varied a great deal for male and female cases and depending on which tissue was being analysed, and no

clear age dependant trends were seen. The accumbens data showed the most distinct difference between female and male data sets, with the female binding level trend decreasing with age, and the male binding level increasing with age. The r values ranged from 0.01 (female, caudate) to -0.88 (female accumbens).

Figure 4.43 (A-F) shows the specific binding levels in female (n = 7) and male (n = 5) DLBPDD cases (see table 4.1) for [³H]Ro 25,6981 against age, ranging from 64-89 years in the 6 brain regions defined. There were no significant age-dependant changes in all brain regions analysed ($p \geq 0.17$ in all cases) with the exception of the female insular cortex where $p=0.06$, showing borderline significance. Unlike the previous data, some clear gender differences with age were seen. The female regression lines for each of the 6 tissues showed an increase in binding levels with age, whereas the male data showed a decrease in binding levels with age in all cases except the putamen. The r values ranged from -0.21 (male, claustrum) to 0.73 (female insular and cingulate cortex).

Figure 4.44 (A-F) shows the specific binding levels in female (n = 7) and male (n = 4) AD cases (see table 4.1) for [³H]Ro 25,6981 against age, ranging from 78-91 years in the 6 brain regions defined. There were significant age-dependant changes in the female caudate, putamen, insular cortex and male cingulate cortex. The male caudate and female cingulate cortex data showed borderline significance with $p=0.09$ and $p=0.1$ respectively. All other tissues showed no significance with $p \geq 0.20$. A clear trend can be seen for both the male and female data, showing a decrease in binding levels for both as age increases. The r values ranged from -0.16 (male, claustrum) to -0.99 (male, cingulate cortex).

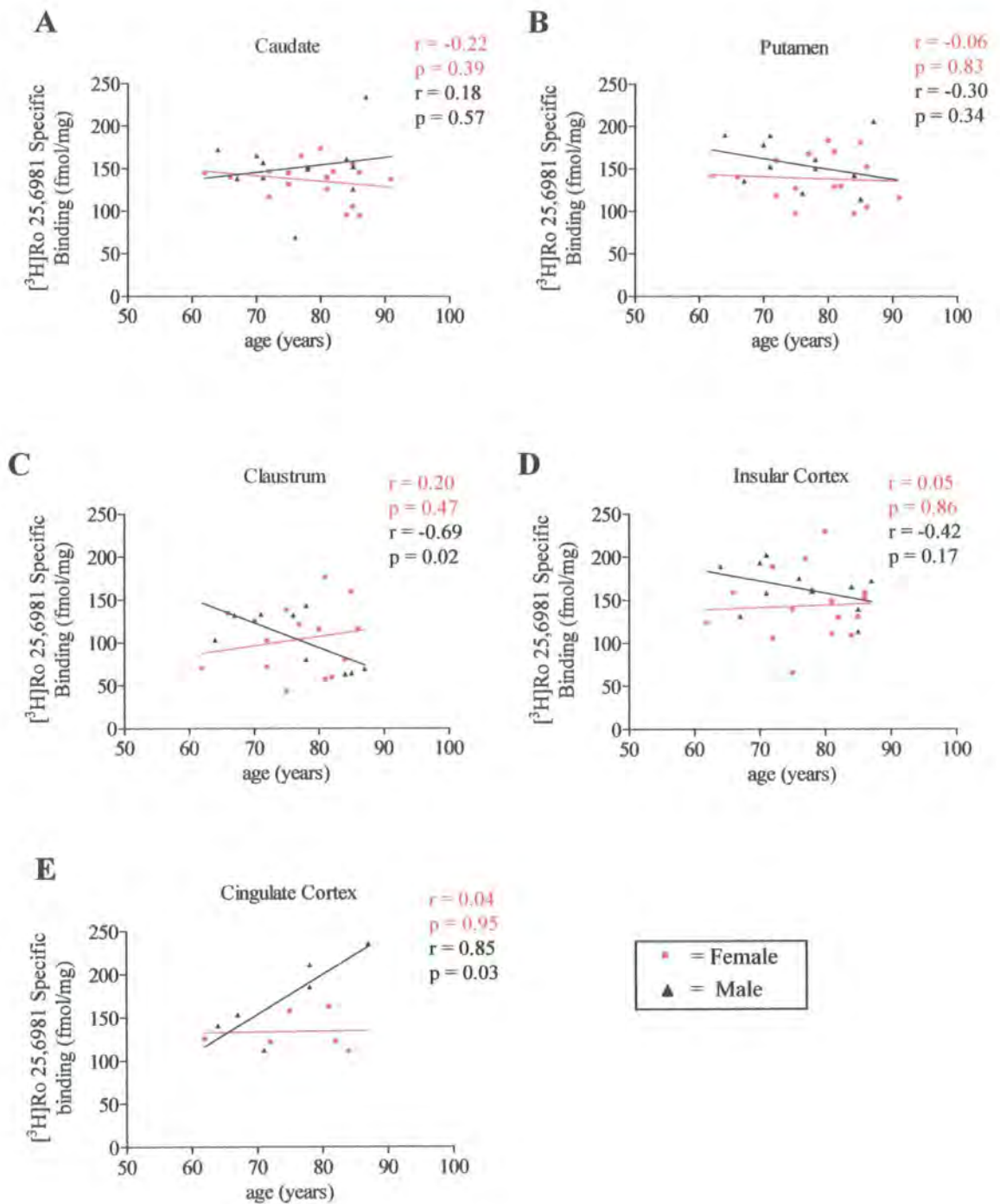


Figure 4.39 (A-E) Age-dependant specific binding of [³H]Ro 25,6981 in Male and Female Control cases in (A) Caudate (B) Putamen (C) Claustrum (D) Insular Cortex and (E) Cingulate Cortex

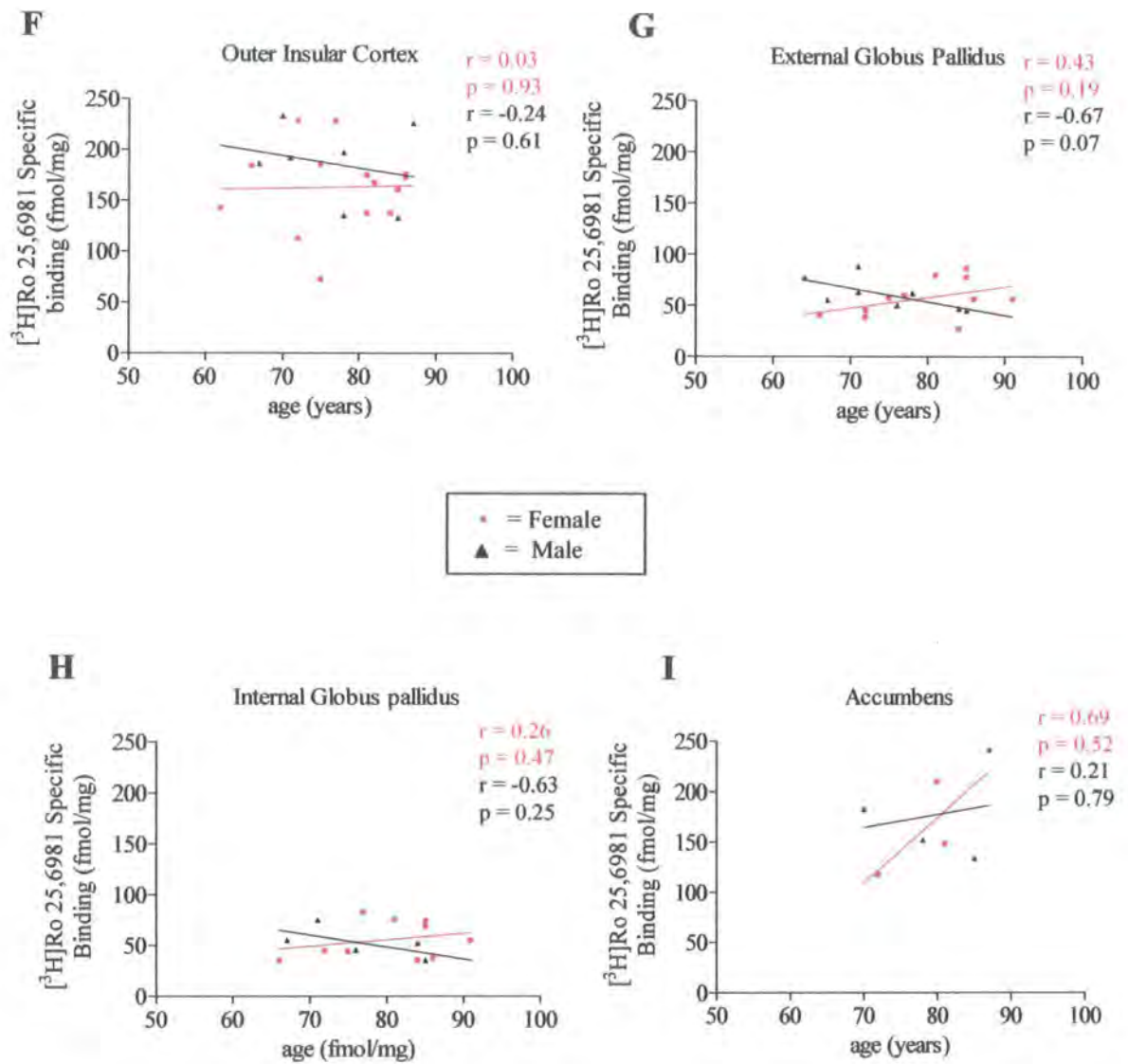


Figure 4.39 (F-I) Age-dependant specific binding of $[^3\text{H}]\text{Ro 25,6981}$ in Male and Female Control cases in (F) Outer Insular Cortex (G) External Globus Pallidus (H) Internal Globus Pallidus and (I) Nucleus Accumbens

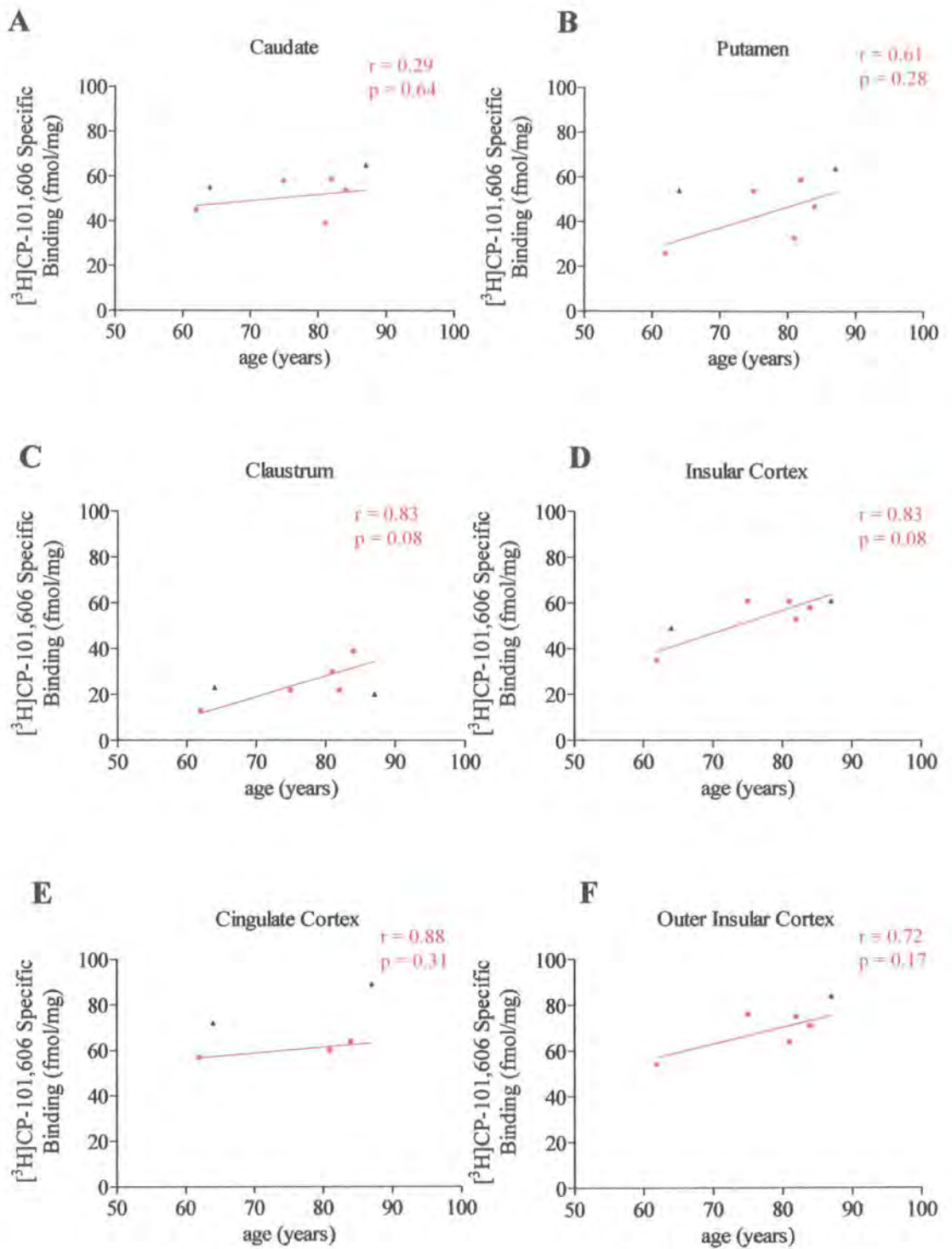


Figure 4.40 (A-F) Age-dependant specific binding of [³H]CP-101,606 in Male and Female Control cases in (A) Caudate (B) Putamen (C) Claustrum (D) Insular Cortex (E) Cingulate Cortex and (F) Outer Insular Cortex

• = Female
▲ = Male

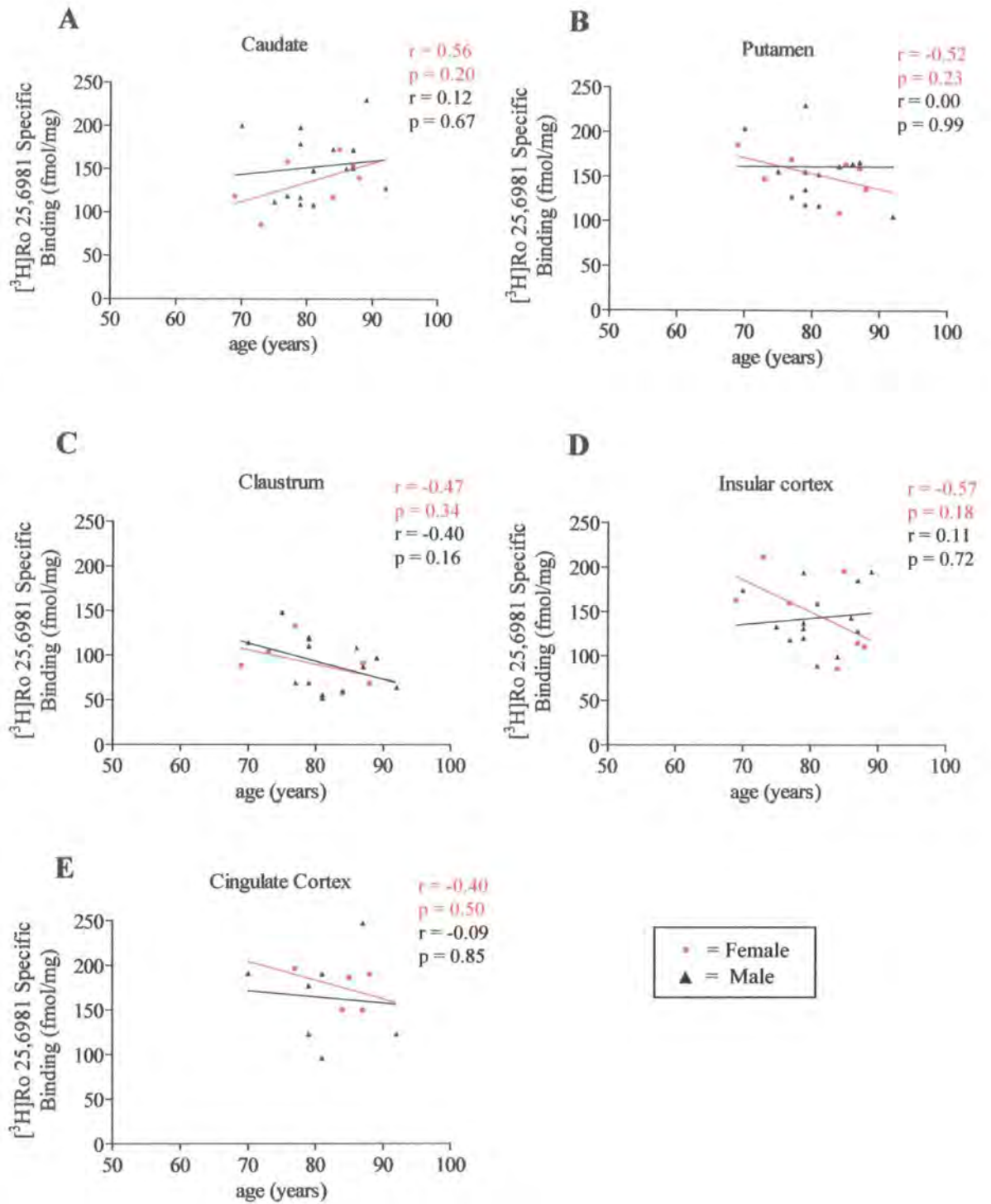


Figure 4.41 (A-E) Age-dependant specific binding of $[^3\text{H}]\text{Ro 25,6981}$ in Male and Female DLB cases in (A) Caudate (B) Putamen (C) Claustrum (D) Insular Cortex and (E) Cingulate Cortex

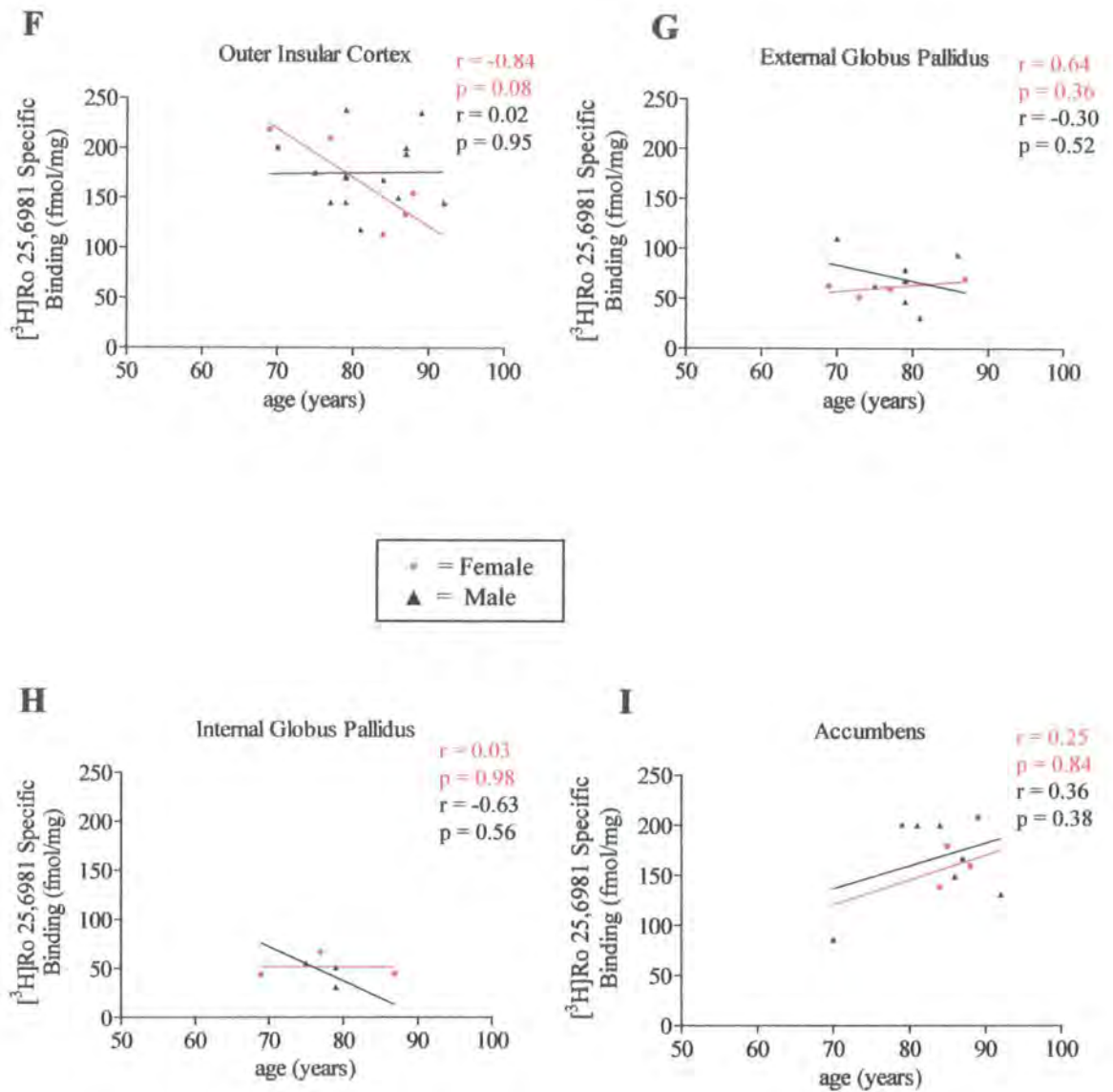


Figure 4.41 (F-I) Age-dependant specific binding of $[^3\text{H}]\text{Ro 25,6981}$ in Male and Female DLB cases in (F) Outer Insular Cortex (G) External Globus Pallidus (H) Internal Globus Pallidus and (I) Nucleus Accumbens

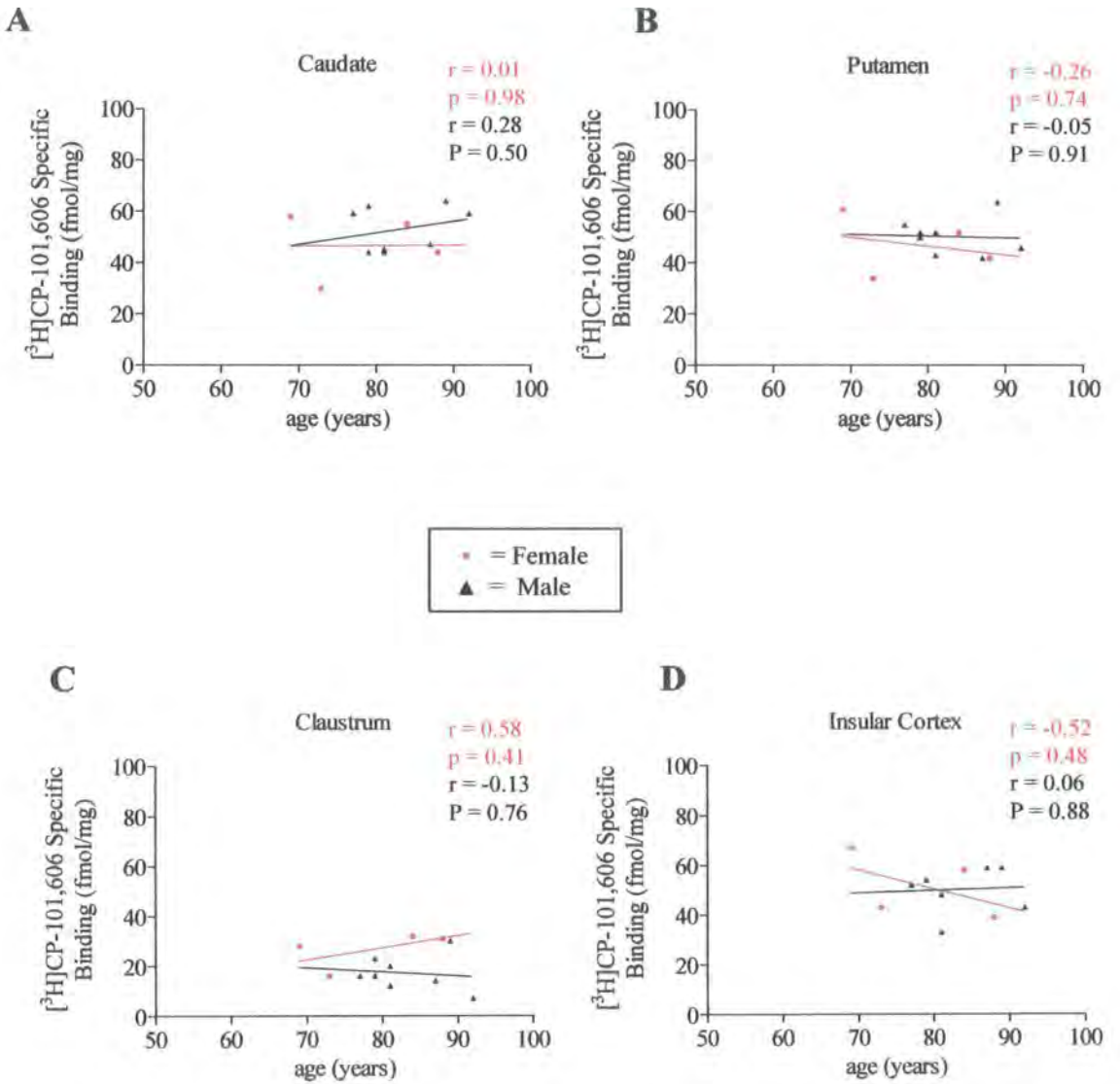


Figure 4.42 (A-D) Age-dependant specific binding of [³H]CP-101,606 in Male and Female DLB cases in (A) Caudate (B) Putamen (C) Claustrum (D) Insular Cortex

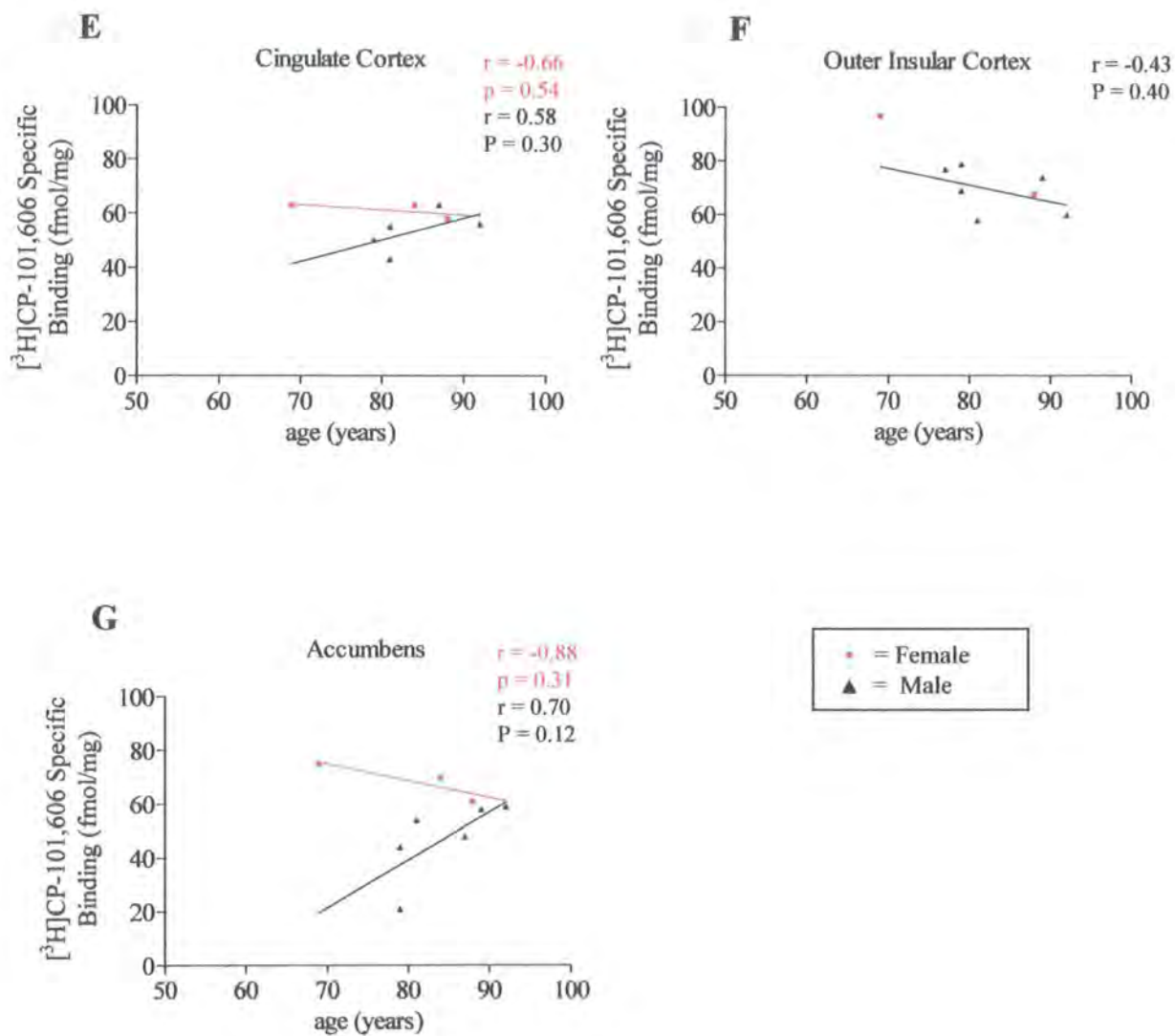


Figure 4.42 (E-G) Age-dependant specific binding of [³H]CP-101,606 in Male and Female DLB cases in (E) Cingulate Cortex (F) Outer Insular Cortex (G) Nucleus Accumbens

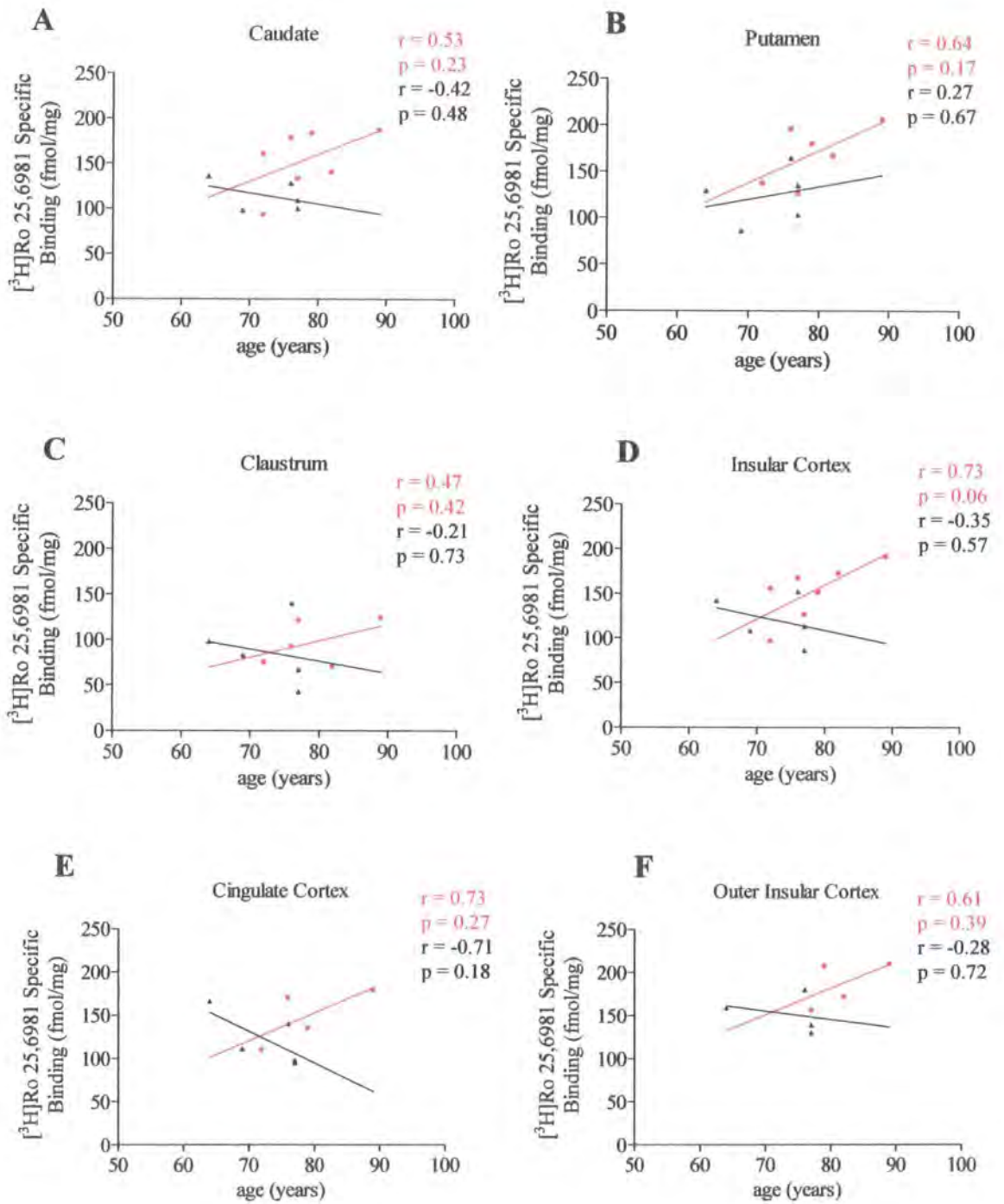


Figure 4.43 (A-F) Age-dependant specific binding of [³H]Ro 25,6981 in Male and Female DLBPDD cases in (A) Caudate (B) Putamen (C) Claustrum (D) Insular Cortex (E) Cingulate Cortex and (F) Outer Insular Cortex

• = Female
 ▲ = Male

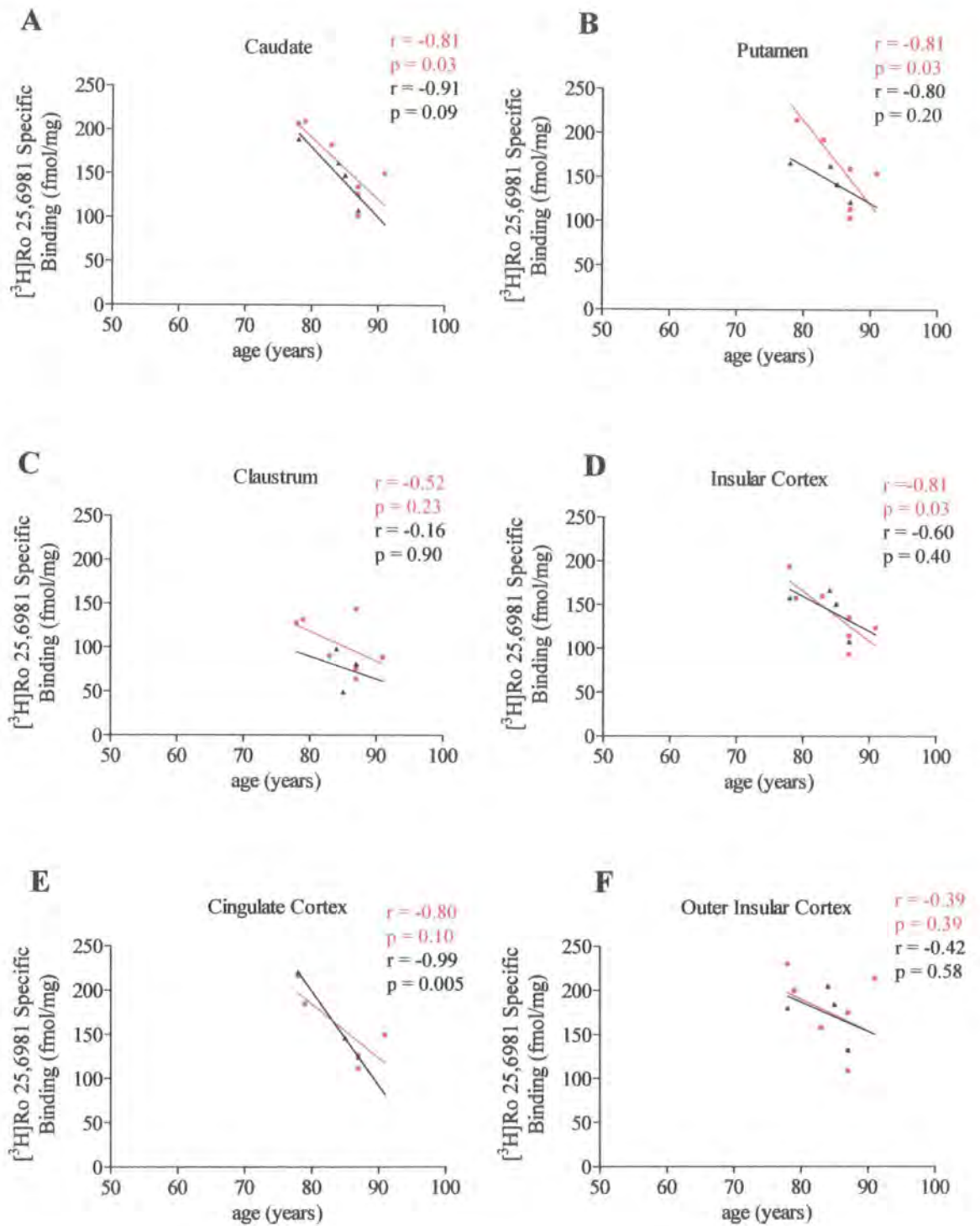


Figure 4.44 (A-F) Age-dependant specific binding of $[^3\text{H}]\text{Ro 25,6981}$ in Male and Female AD cases in (A) Caudate (B) Putamen (C) Claustrum (D) Insular Cortex (E) Cingulate Cortex and (F) Outer Insular Cortex

• = Female
▲ = Male

4.5.9 Results (Figure 4.45 (A-I) to Figure 4.50 (A-F))

The data from figure 4.39 (A-I) were further analysed to show the mean average specific binding (fmol/mg) \pm SD of [³H]Ro 25,6981 in female and male control cases for n determinations in the 9 brain regions defined, shown in figure 4.45 (A-I). In each of the 9 tissues, except the internal globus pallidus, the mean male binding value appeared to be higher than the mean female binding value, although analysis showed this was not statistically significant. The claustrum, internal and external globus pallidus binding levels in both male and female cases were lower than the other tissues, an observation seen in previous graphs.

A similar analysis was performed on the data from figure 4.40 (A-F), showing the mean average specific binding (fmol/mg) \pm SD of [³H]CP-101,606 in female and male control cases for n determinations in the 6 brain regions defined, shown in figure 4.46 (A-F). In each of the tissues, except the claustrum, the mean male binding value appeared to be higher than the mean female binding value, although statistical analysis showed this not to be significant. As for figure 4.45 (A-I), the claustrum binding levels in both male and female cases were lower than the other tissues. The specific binding values for the CP-101,606 ligand were always lower than those seen for the Ro 25,6981 ligand, in all the tissues.

Again, the data from figure 4.41 (A-I) were further analysed to show the mean average specific binding (fmol/mg) \pm SD of [³H]Ro 25,6981 in female and male DLB cases for n determinations in the 9 brain regions defined, shown in figure 4.47 (A-I). In each of the tissues represented on graphs A, B, F, G and I, the mean male binding levels were higher than those of the females, although statistically not significant. However, mean binding levels in the female data were higher in the tissues represented on graphs C, D, E and H,

but again these differences were not statistically significant when analysed by a student's unpaired t-test. As for figure 4.45 (A-I), the claustrum, internal and external globus pallidus binding levels in both male and female cases were lower than the other tissues.

The data from figure 4.42 (A-G) were further analysed to show the mean average specific binding (fmol/mg) \pm SD of [³H]CP-101,606 in female and male DLB cases for n determinations in the 7 brain regions defined, shown in figure 4.48 (A-G). The mean male binding values appeared to be lower than the mean female binding values in all tissues except the caudate and putamen. However, t-test analysis showed that there was no significant difference in levels of binding between male and female data sets in all the tissues except in the accumbens (p=0.02). The claustrum binding levels in both male and female cases were lower than the other tissues.

The data from figure 4.43 (A-F) were analysed to show the mean average specific binding (fmol/mg) \pm SD of [³H]Ro 25,6981 in female and male DLBPDD cases for n determinations in the 6 brain regions defined, shown in figure 4.49 (A-F). The mean male binding values were significantly lower than the mean female binding values in the caudate (p=0.02) and putamen (p=0.04) but were not statistically different in all other tissues. The claustrum binding levels in both male and female cases were lower than the other tissues.

Figure 4.50 (A-F) shows the mean average specific binding (fmol/mg) \pm SD of [³H]Ro 25,6981 in female and male AD cases for n determinations in the 6 brain regions defined. The data was taken from the previous figure 4.44 (A-F). There were no significant differences in the binding levels between male and female data sets in any of the regions analysed. The claustrum binding levels in both male and female cases were lower than the other tissues.

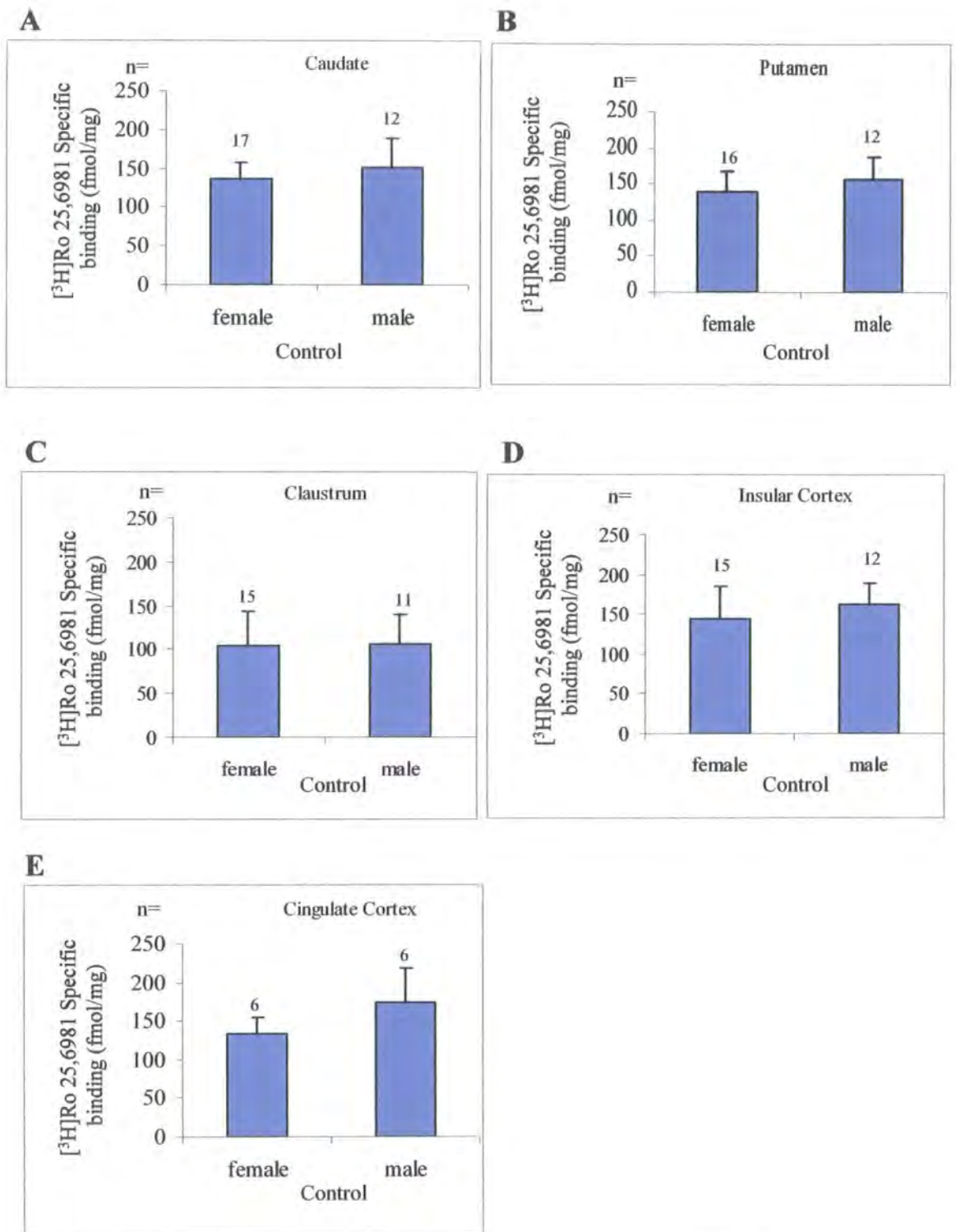


Figure 4.45 (A-E) Mean average specific binding (fmol/mg) \pm SD of $[^3\text{H}]\text{Ro 25,6981}$ in Male and Female Control cases in (A) Caudate (B) Putamen (C) Claustrum (D) Insular Cortex and (E) Cingulate Cortex.

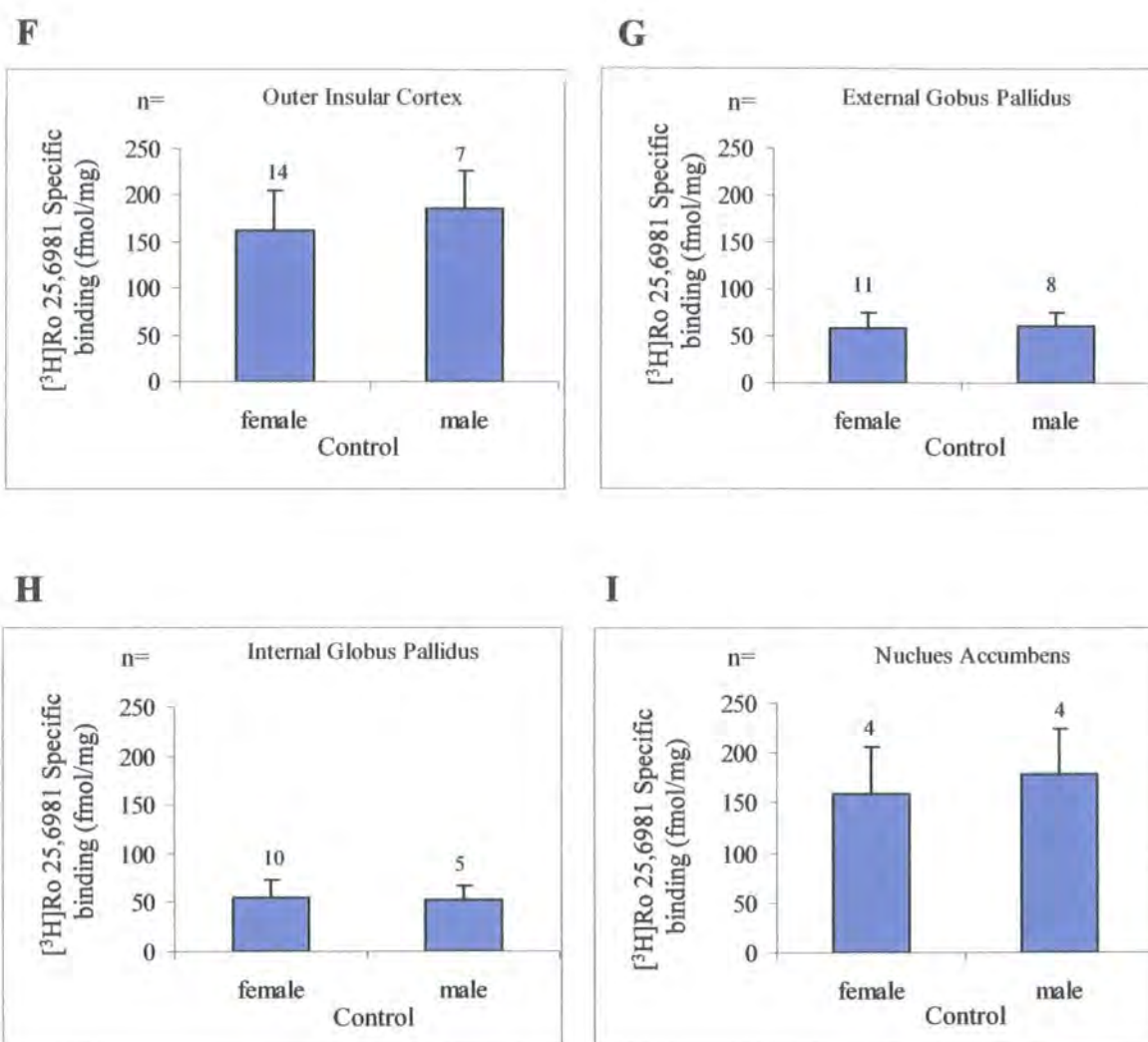


Figure 4.45 (F-I) Mean average specific binding (fmol/mg) \pm SD of $[^3\text{H}]\text{Ro 25,6981}$ in Male and Female Control cases in (F) Outer Insular Cortex (G) External Globus Pallidus (H) Internal Globus Pallidus and (I) Nucleus Accumbens.

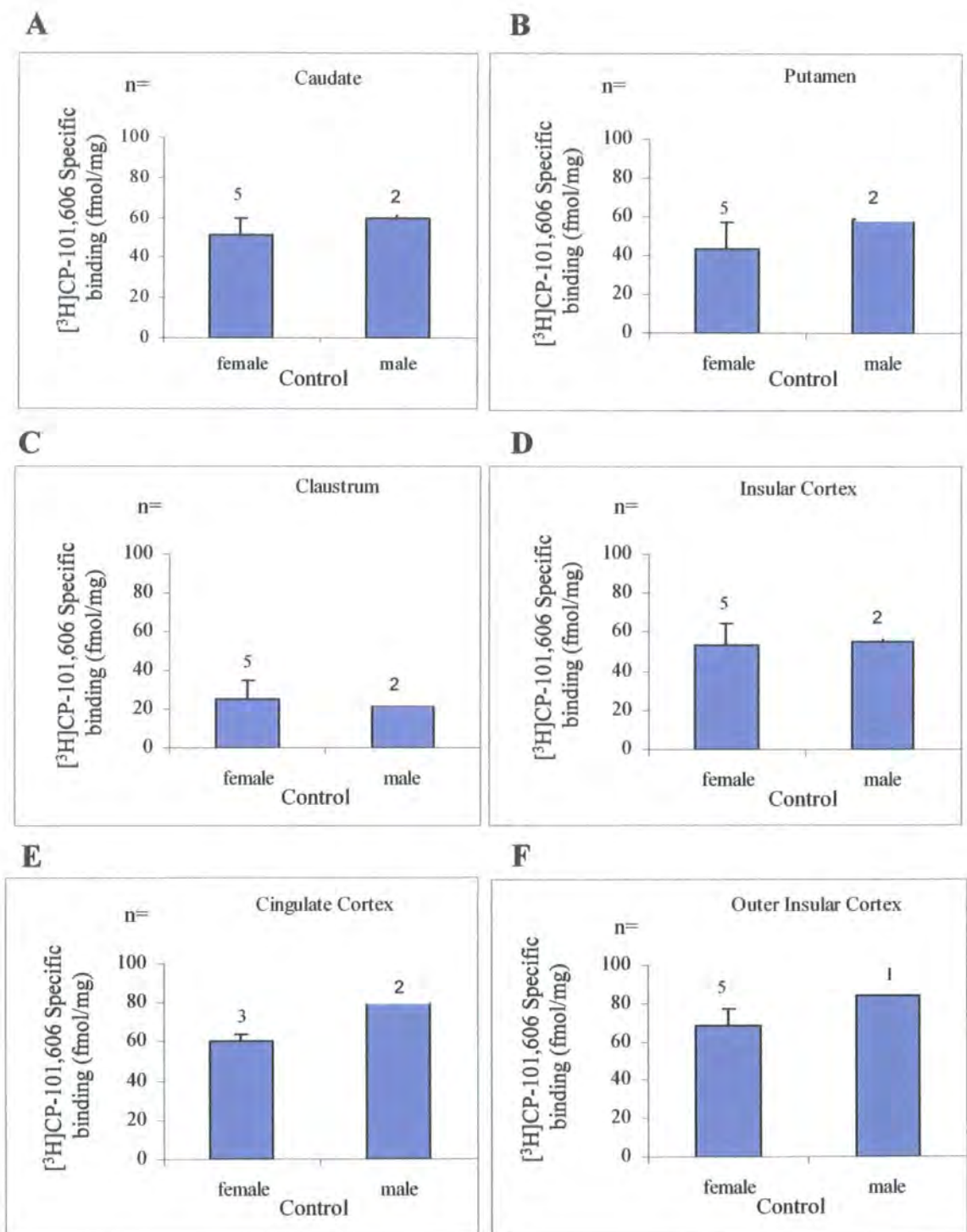


Figure 4.46 (A-F) Mean average specific binding (fmol/mg) \pm SD of [3 H]CP-101,606 in Male and Female Control cases in (A) Caudate (B) Putamen (C) Claustrum (D) Insular Cortex (E) Cingulate Cortex and (F) Outer Insular Cortex.

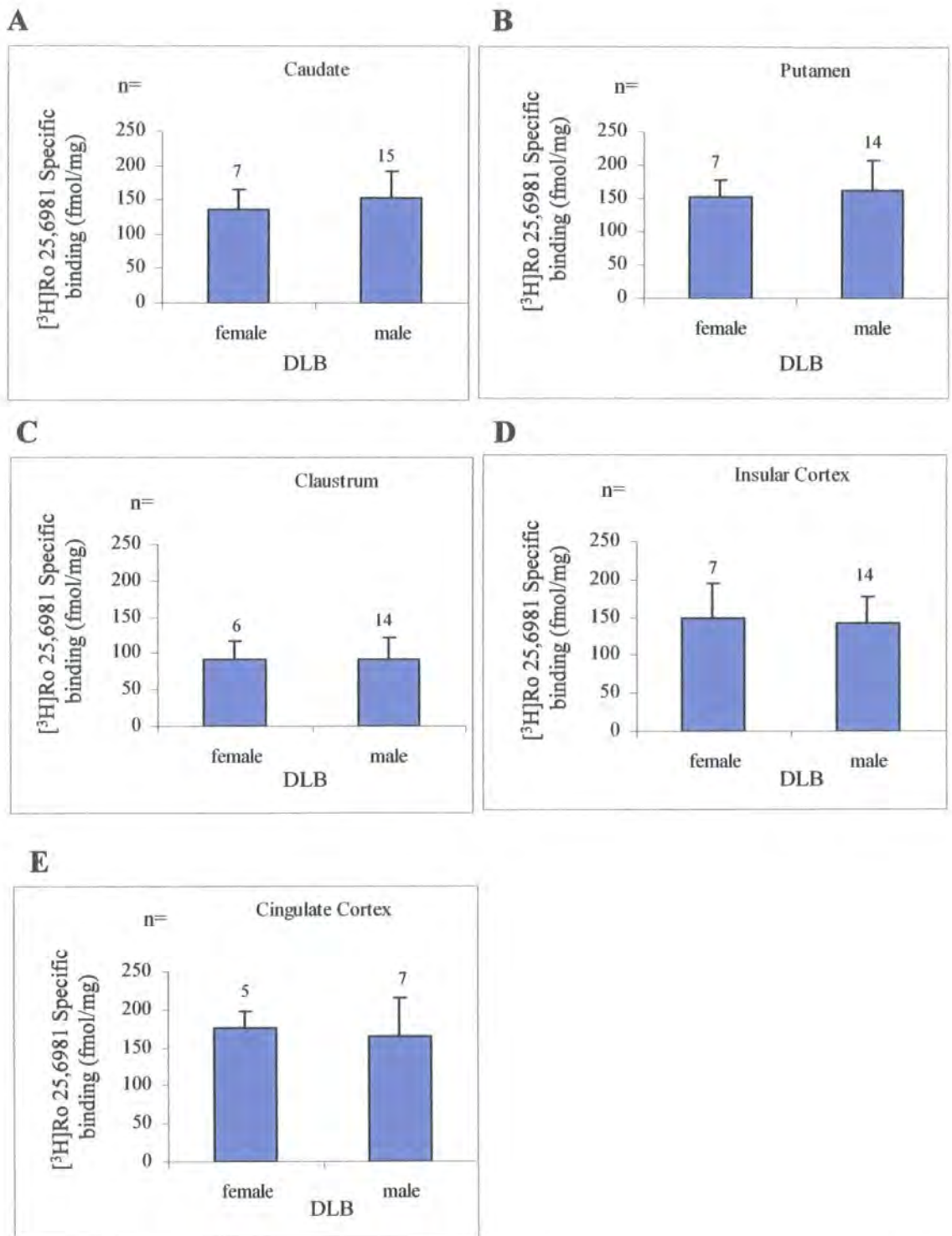


Figure 4.47 (A-E) Mean average specific binding (fmol/mg) \pm SD of [3 H]Ro 25,6981 in Male and Female DLB cases in (A) Caudate (B) Putamen (C) Claustrum (D) Insular Cortex and (E) Cingulate Cortex.

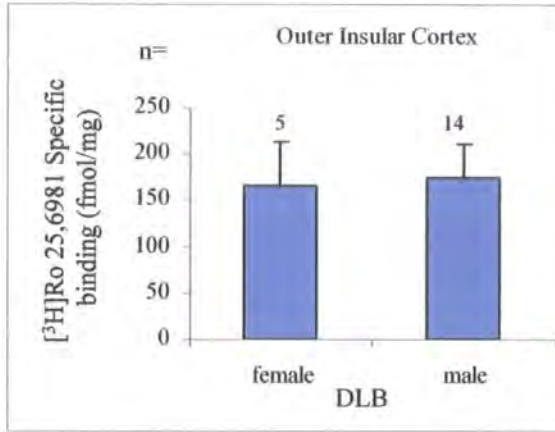
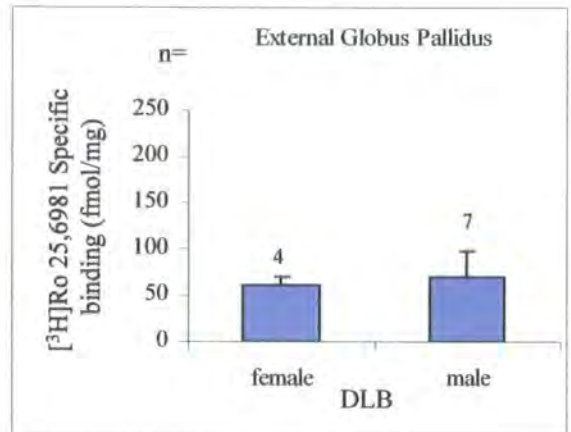
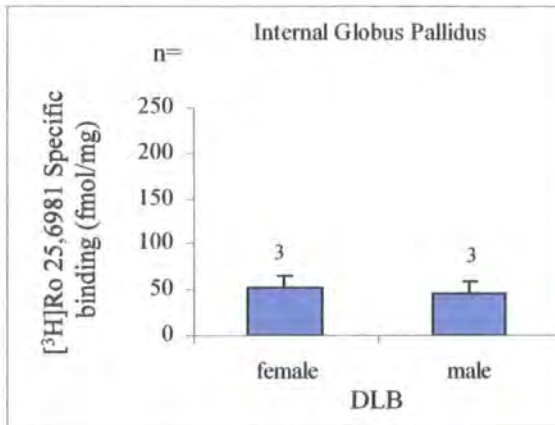
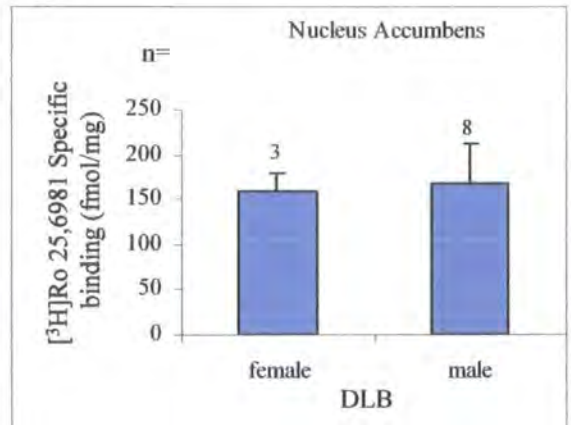
F**G****H****I**

Figure 4.47. (F-I) Mean average specific binding (fmol/mg) \pm SD of $[^3\text{H}]\text{Ro 25,6981}$ in Male and Female DLB cases in (F) Outer Insular Cortex (G) External Globus Pallidus (H) Internal Globus Pallidus and (I) Nucleus Accumbens.

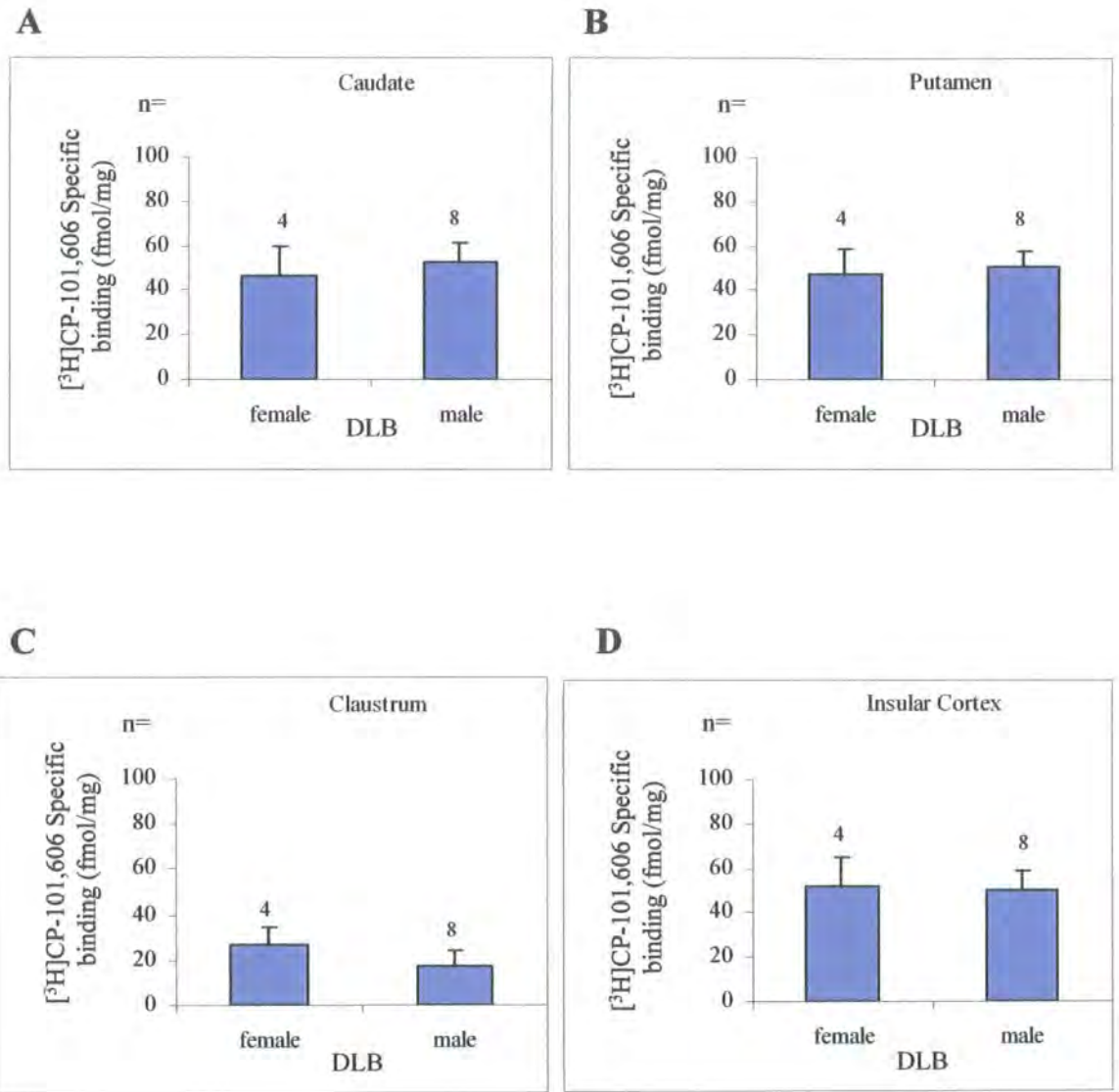


Figure 4.48 (A-D) Mean average specific binding (fmol/mg) \pm SD of $[^3\text{H}]\text{CP-101,606}$ in Male and Female DLB cases in (A) Caudate (B) Putamen (C) Claustrum and (D) Insular Cortex.

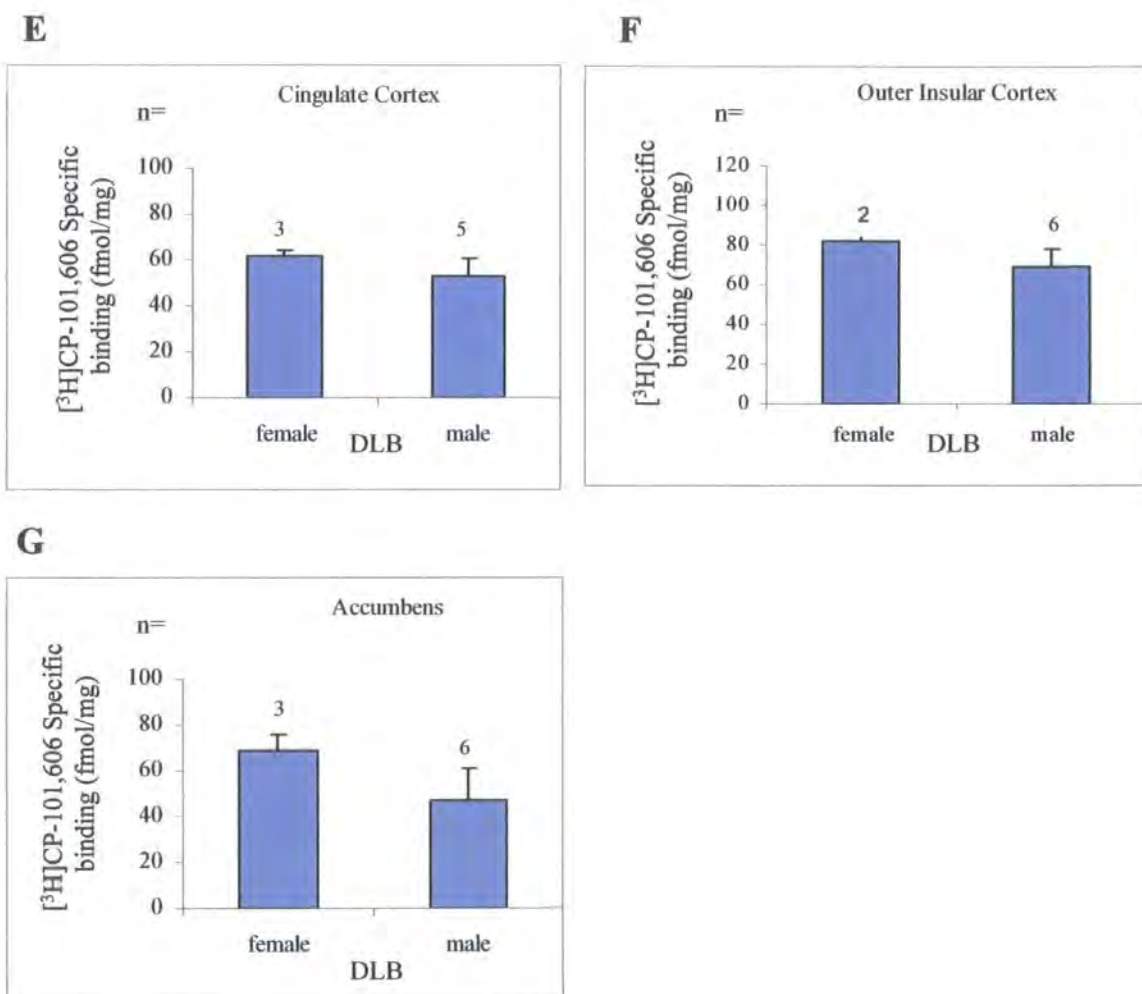


Figure 4.48 (E-G) Mean average specific binding (fmol/mg) \pm SD of $[^3\text{H}]$ CP-101,606 in Male and Female DLB cases in (E) Cingulate Cortex (F) Outer Insular cortex and (G) Nucleus Accumbens.

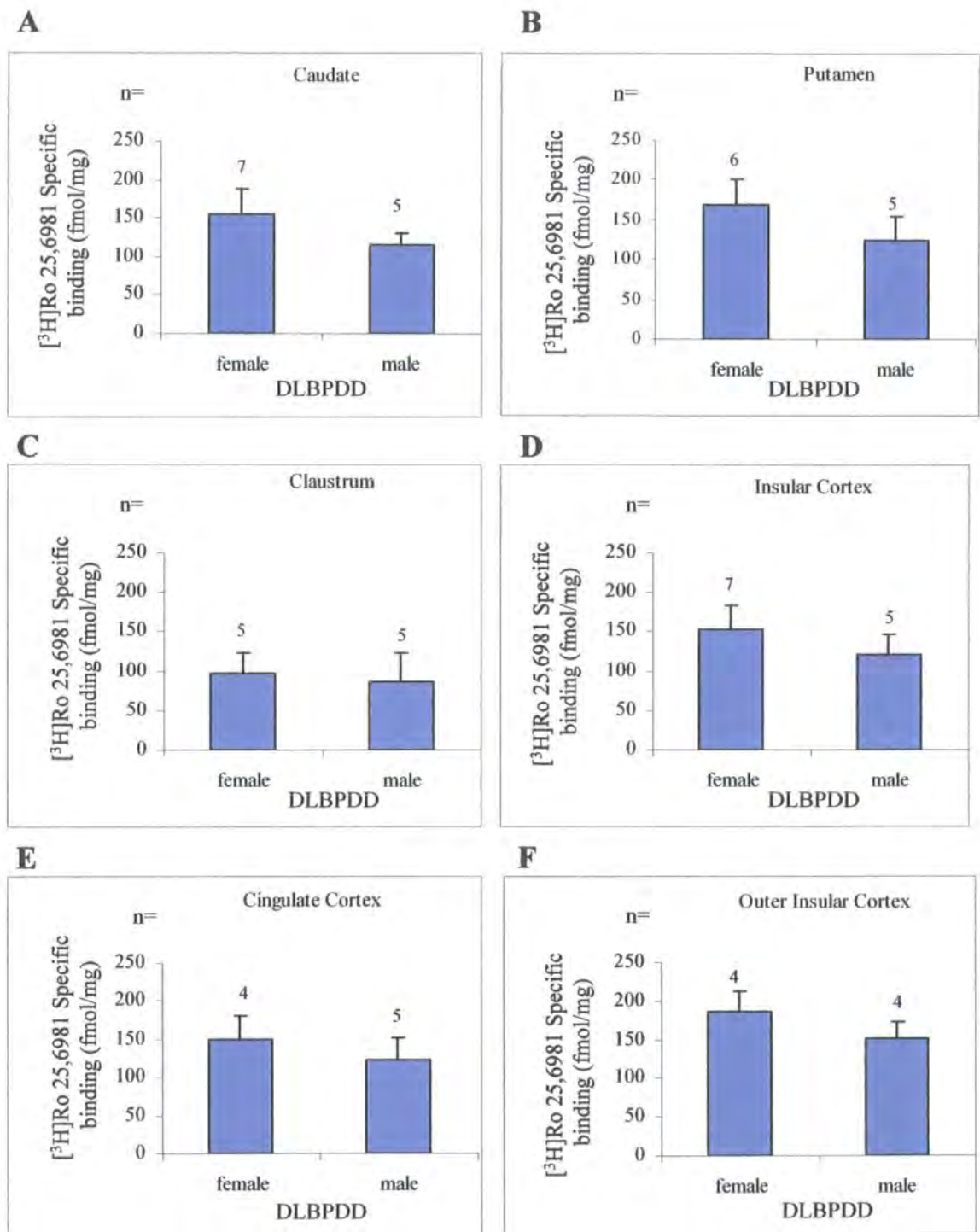


Figure 4.49 (A-F) Mean average specific binding (fmol/mg) \pm SD of [³H]Ro 25,6981 in Male and Female DLBPDD cases in (A) Caudate (B) Putamen (C) Claustrum (D) Insular Cortex (E) Cingulate Cortex and (F) Outer Insular Cortex.

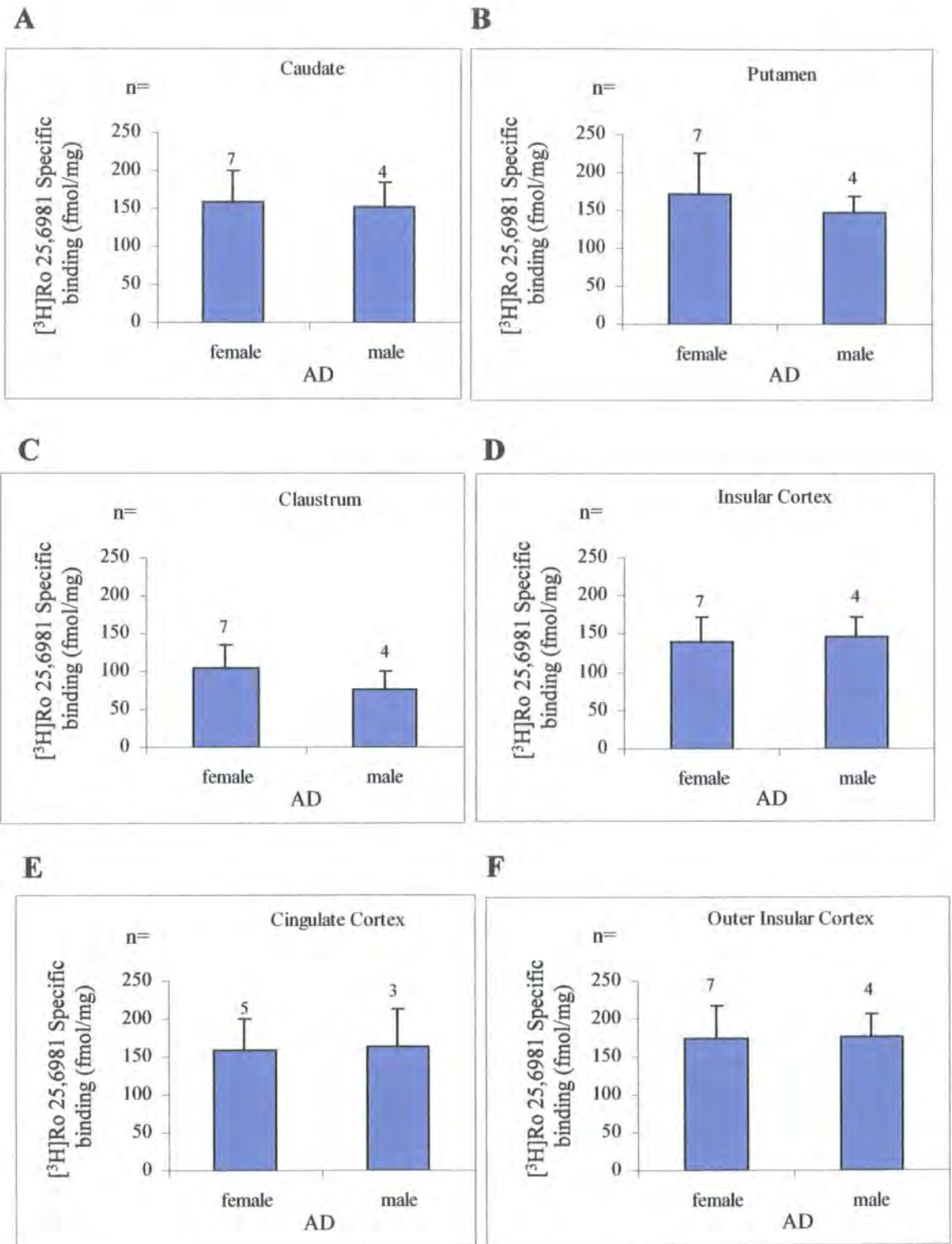


Figure 4.50 (A-F) Mean average specific binding (fmol/mg) \pm SD of [³H]Ro 25,6981 in Male and Female AD cases in (A) Caudate (B) Putamen (C) Claustrum (D) Insular Cortex (E) Cingulate Cortex and (F) Outer Insular Cortex.

4.5.10 Results (Figure 4.51 (A-F) to Figure 4.54 (A-F))

The clinical data corresponding to the cases summarised in tables 4.4 to 4.7 (that is, DLB, PDD, DLBPDD and AD cases respectively) were collated and are summarised in table 4.8 (DLB cases), table 4.9 (PDD cases), table 4.10 (DLBPDD cases) and table 4.11 (AD cases). They show the relevant scores for the MMSE (mini mental state examination, see section 4.3), MTS (mental test score, see section 4.3.1) and UPDRS scores (Unified Parkinson disease rating scale, see section 4.4). Data relating to depression, delusions, dementia and visual hallucinations experienced by each subject were also studied. The severity of the symptoms experienced were measured on the following scale, 0 = none, 1 = mild, 2 = severe, and are indicative of the last assessment before death of the subject. In each case and in each tissue studied, the specific binding levels of [³H]Ro 25,6981 data were shown against the relevant clinical data score. In the case of the MMSE, MTS and UPDRS data, the score could be any value in a given range; therefore each case is represented on the graphs. The depression, delusion, dementia and visual hallucination data has been shown for each of the 0-2 score options, giving the mean score \pm SD against binding levels in fmol/mg. Although in the majority of cases studied clinical data was available, unfortunately not all cases had the relevant data, and therefore only those with the data present are shown. This reduction in n number meant only the [³H]Ro 25,6981 labelled cases were used for the further symptom correlation studies. There were too few cases with the appropriate clinical data in the [³H]CP-101,606 cohort, and so were therefore not used. The Lewy body disease cases represented by DLB, PDD and DLBPDD cases have been put together as they are clinically well defined and show similar results, however the AD cases have been kept separate since they show some interesting trends not seen in the other disease states. Estimated linear regression lines of best fit were produced using GraphPad Prism and are represented on each graph, indicating any changes in binding levels in each

tissue with increasing clinical score. The significance of the regression was determined from the generated p value, where $p \leq 0.05$ was considered to show a significant linear relationship between clinical score and binding level. The generated correlation coefficient or r value shows how well the data fits to the regression line, where $r = 1$ shows strong correlation and $r = 0$ shows little or none.

Figure 4.51 (A-F) shows the specific binding levels in female and male DLB, PDD and DLBPDD ($n = 22$) cases (see tables 4.8- 4.10) for [^3H]Ro 25,6981 against MMSE score, in the 6 brain regions defined. The general trend in all the graphs showed a decrease in binding level with an increase in MMSE score, although there were no significant changes in MMSE score with increasing binding levels in all brain regions analysed ($p \geq 0.06$ in all cases). The insular cortex showed border-line significance with $p = 0.06$ with a decrease in binding with increasing score. The r values ranged from -0.11 (caudate) to -0.41 (insular cortex). Figure 4.51(a) shows the specific binding levels for PDD ($n = 6$) cases (see table 4.9) for [^3H]Ro 25,6981 against MTS score in the 5 brain regions defined. The data appears to show a decrease in binding with increasing MTS score although analysis has shown this not to be statistically significant ($p \geq 0.18$). This may be due to low n numbers. The r values ranged from -0.5 (putamen) to -0.63 (insular cortex). Figure 4.52 (A-F) shows the specific binding levels in female and male AD ($n = 8$) cases (see table 4.11) for [^3H]Ro 25,6981 against MMSE score, in the 6 brain regions defined. The general trend seen in graphs A, B, E and F showed a decrease in binding level with an increase in MMSE score. Graphs C and D showed an increase in binding level with an increase in MMSE score, although there were no significant changes in MMSE score against binding levels in all the brain regions analysed ($p \geq 0.20$ in all cases). The r values ranged from 0.06 (cingulate cortex) to -0.56 (claustrum).

Figure 4.53 (A-F) shows the specific binding levels in female and male DLB, PDD and DLBPDD (n = 26) cases (see tables 4.8- 4.10) for [³H]Ro 25,6981 against UPDRS score, in the 6 brain regions defined. There were no significant changes in UPDRS score with changing binding levels in all brain regions analysed ($p \geq 0.14$ in all cases). The cingulate cortex data showed a decrease in binding level as UPDRS score increased, although all the other tissues showed an increase in binding level with increasing UPDRS score. The r values ranged from -0.30 (cingulate cortex) to 0.34 (claustrum). Figure 4.54 (A-F) shows the specific binding levels in female and male AD (n = 8) cases (see table 4.11) for [³H]Ro 25,6981 against UPDRS score, in the 6 brain regions defined. The general trend seen in all the graphs A-F showed a decrease in binding level with an increase in UPDRS score, with the caudate ($p=0.05$) and putamen ($p=0.04$) regression lines showing significance. The insular cortex, cingulate cortex and outer insular cortex showed borderline significance with $p=0.07$, $p=0.06$ and $p=0.06$ respectively. The r values ranged from -0.61 (claustrum) to -0.78 (cingulate cortex).

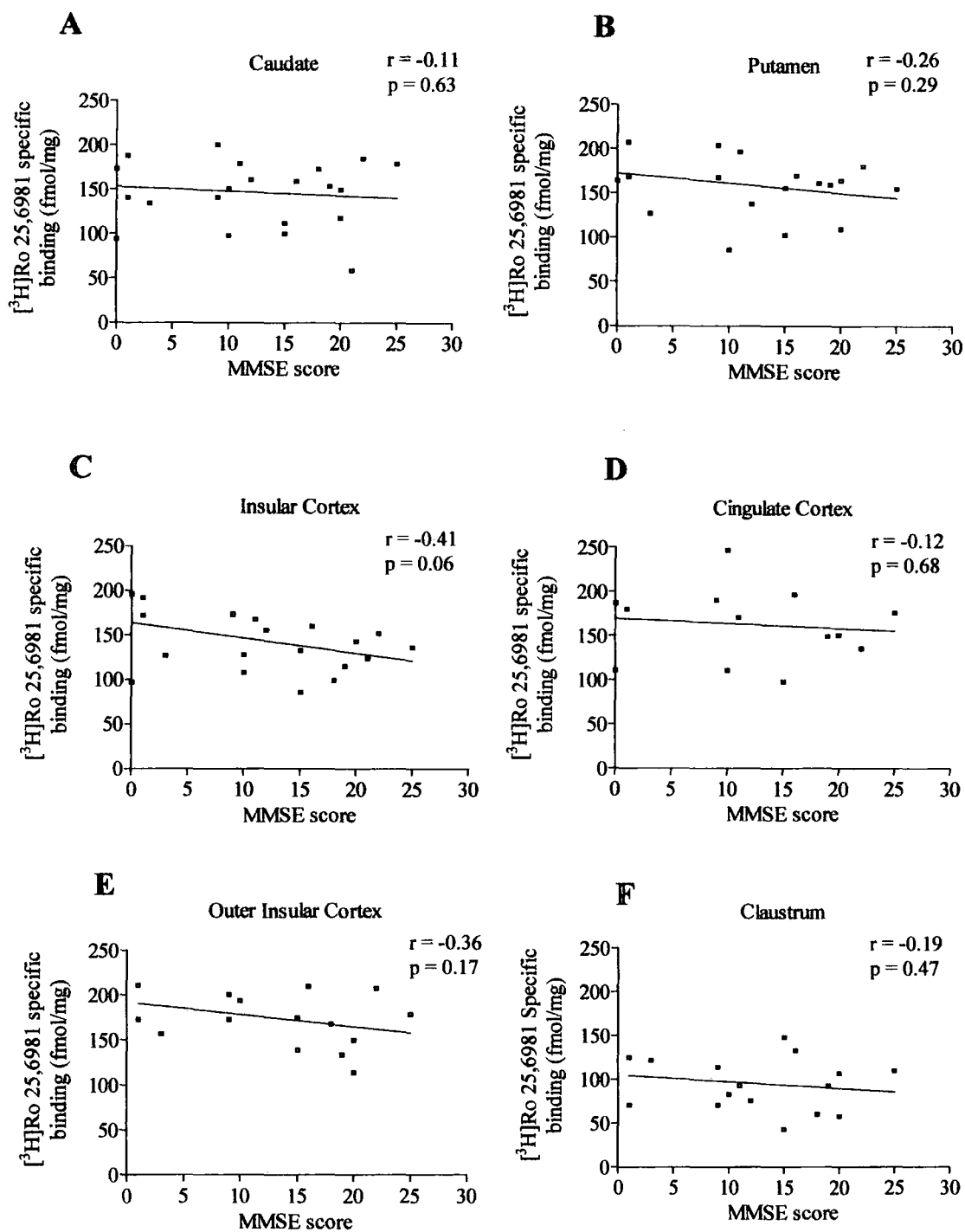


Figure 4.51 Mini mental state examination score against specific binding of $[^3\text{H}]\text{Ro 25,6981}$ in DLB, PDD and DLBPDD cases in (A) caudate (B) Putamen (C) Insular cortex (D) Cingulate cortex (E) Outer insular cortex and (F) Claustrum.

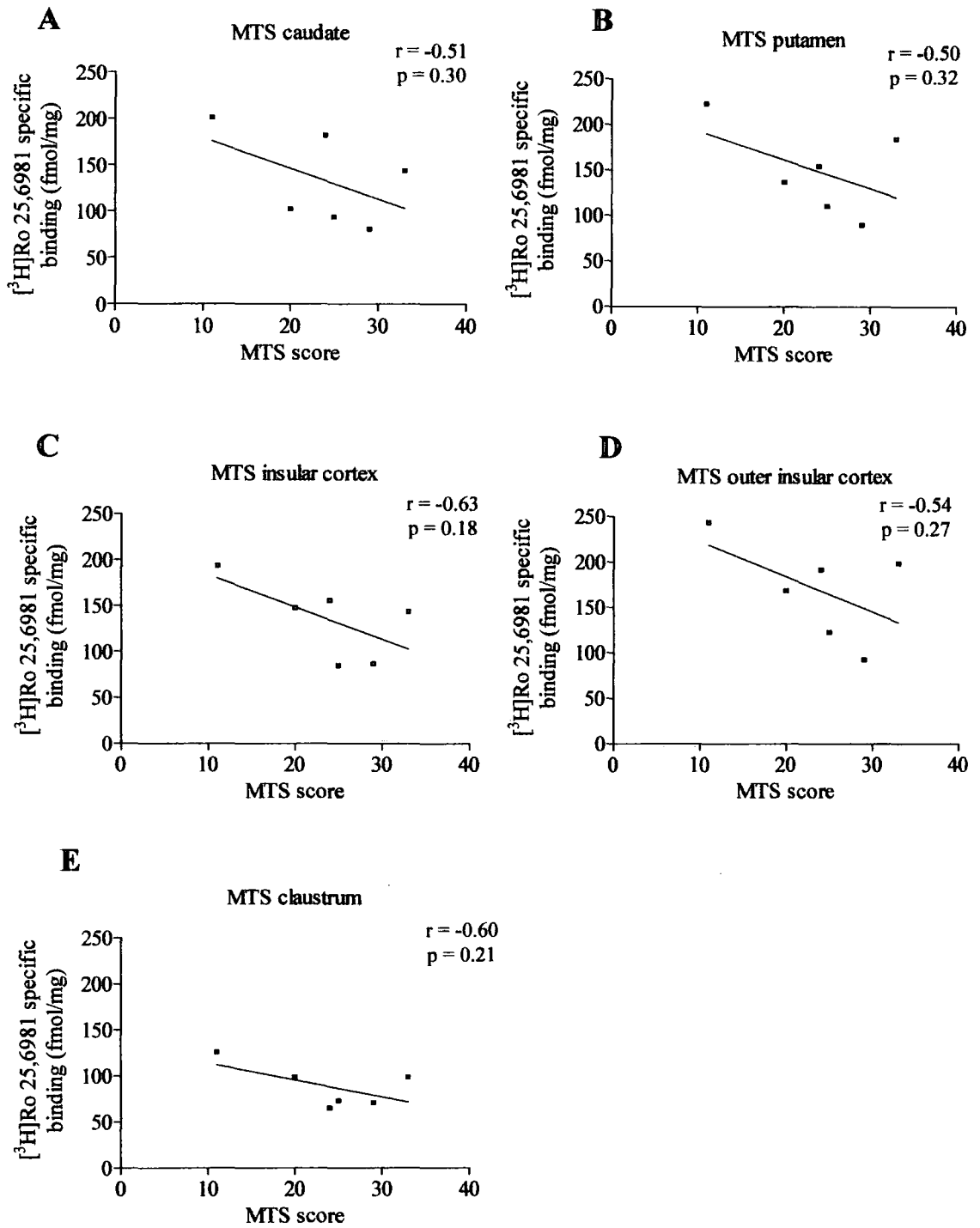


Figure 4.51(a) Mental Test Score against specific binding of $[^3\text{H}]\text{Ro 25,6981}$ in PDD cases in (A) caudate (B) Putamen (C) Insular cortex (D) Outer insular cortex and (E) Claustrum.

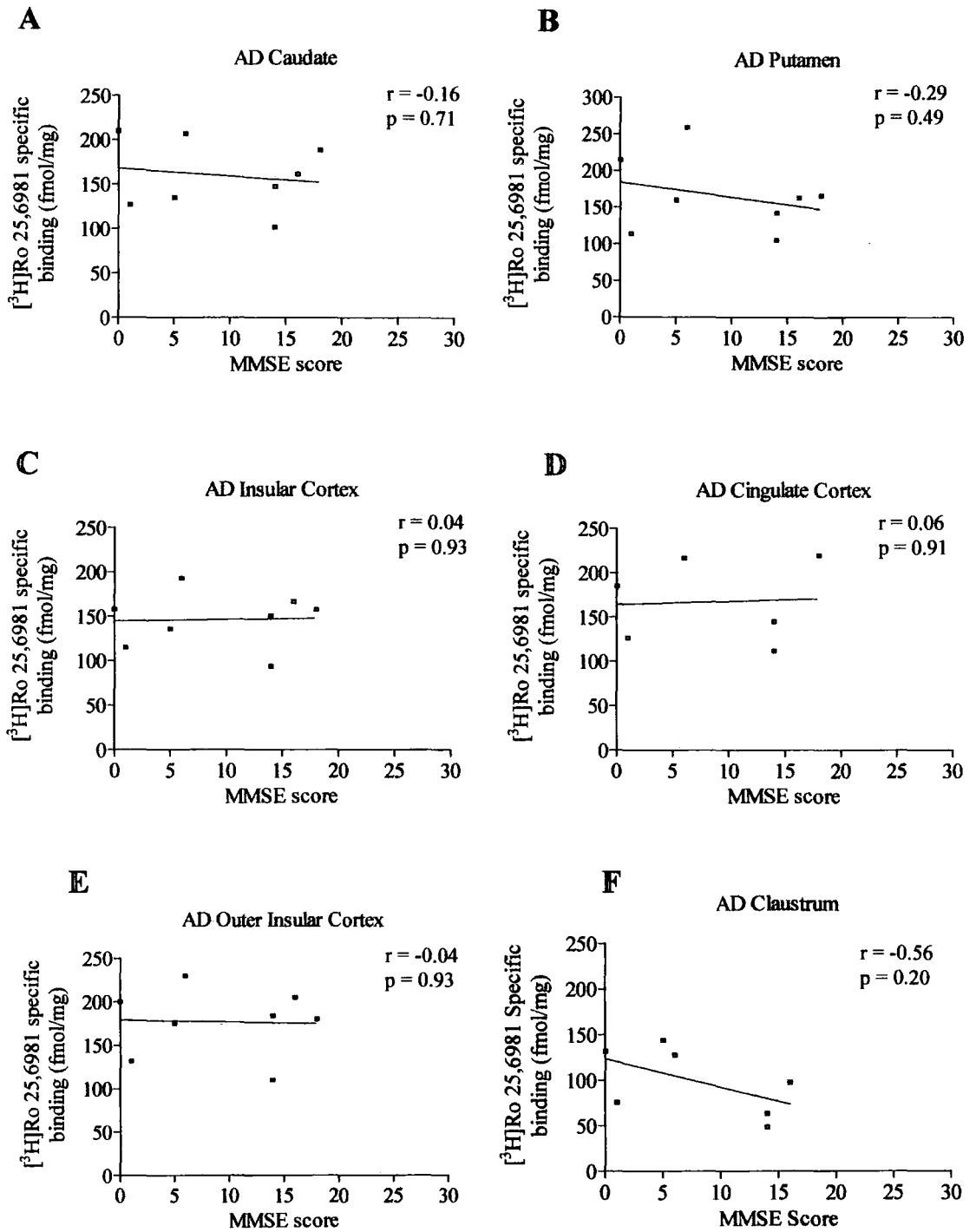


Figure 4.52 Mini mental state examination score against specific binding of $[^3\text{H}]\text{Ro 25,6981}$ in AD cases in (A) caudate (B) Putamen (C) Insular cortex (D) Cingulate cortex (E) Outer insular cortex and (F) Claustrum.

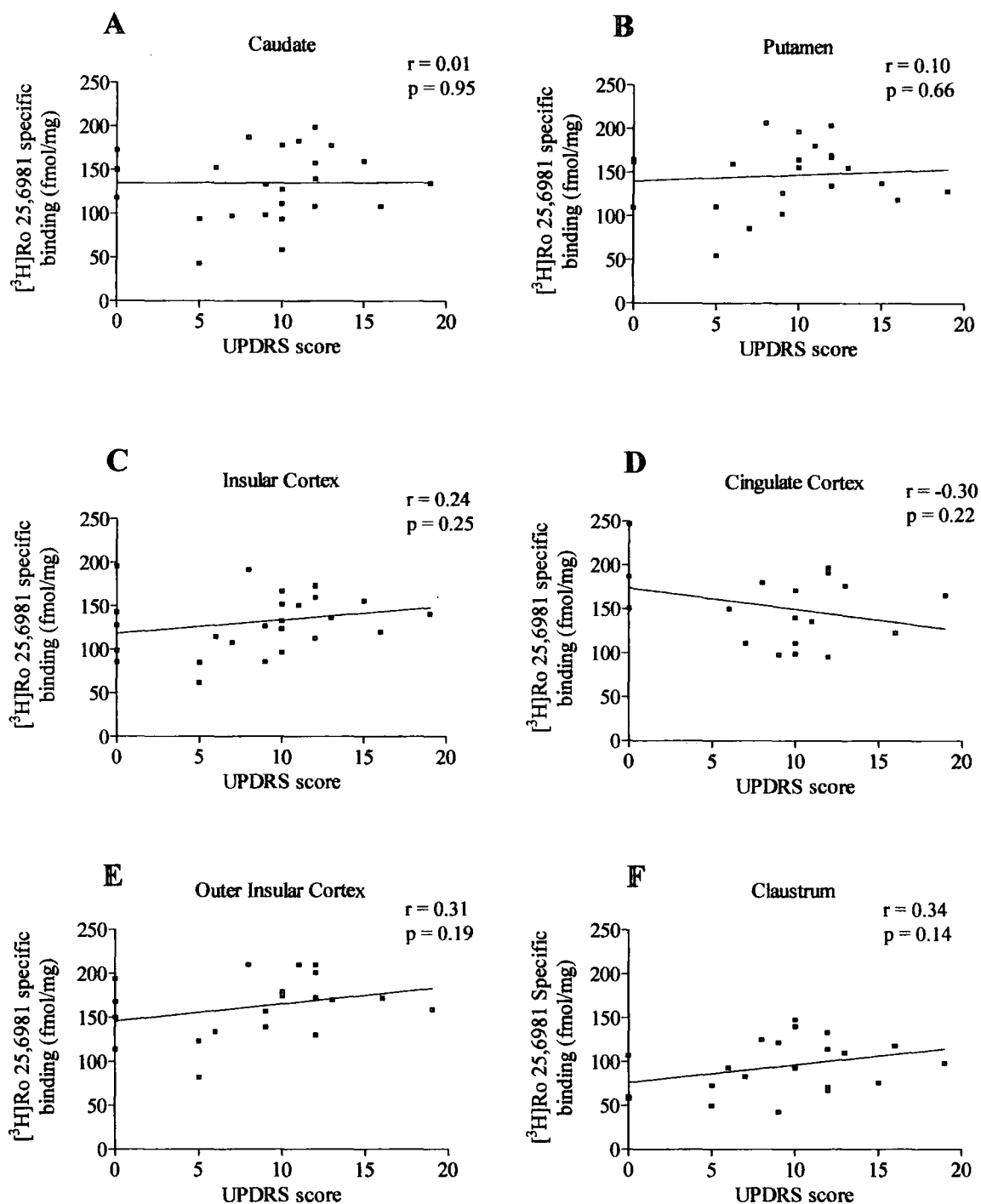


Figure 4.53 Unified Parkinson Disease Rating Scale data against $[^3\text{H}]\text{Ro 25,6981}$ specific binding (fmol/mg) in DLB, PDD and DLBPDD cases in (A) Caudate (B) Putamen (C) Insular Cortex (D) Cingulate Cortex (E) Outer Insular Cortex (F) Claustrum

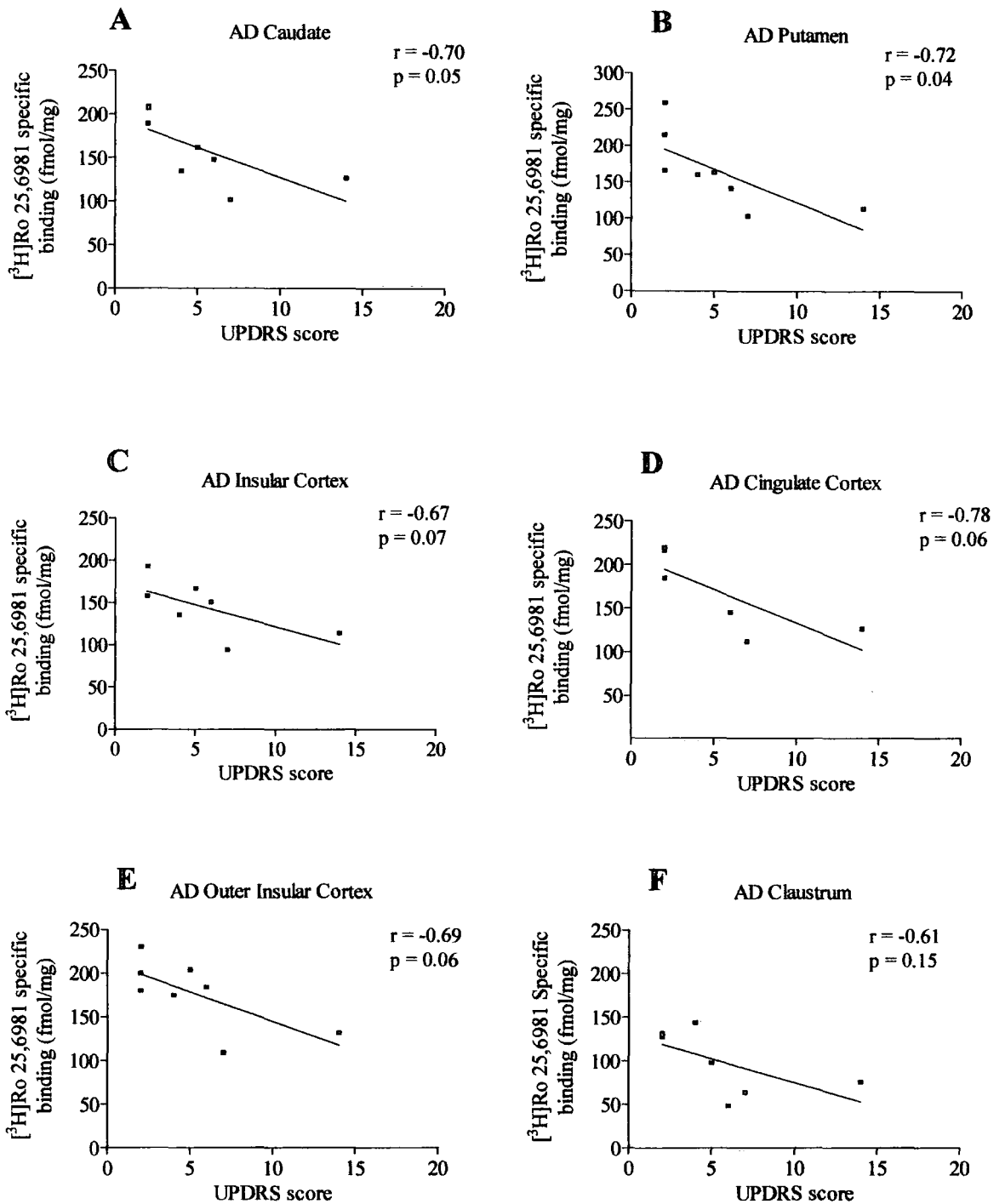


Figure 4.54 Unified Parkinson Disease Rating Scale data against [³H]Ro 25,6981 specific binding (fmol/mg) in AD cases in (A) Caudate (B) Putamen (C) Insular Cortex (D) Cingulate Cortex (E) Outer Insular Cortex (F) Claustrum.

4.5.11 Results (Figure 4.55 (A-F) to Figure 4.62 (A-F))

Figure 4.55 (A-F) shows the mean specific binding levels \pm SD (fmol/mg) in female and male DLB, PDD and DLBPDD (n = 19) cases (see tables 4.7- 4.10) for [³H]Ro 25,6981 against depression score, in the 6 brain regions defined. There were no significant differences between binding levels in any of the brain regions shown, or between the depression scores in the tissues individually. The claustrum binding levels for all scores were slightly lower than in other tissues. The binding levels tended to be slightly lower for the score of 2 compared to 0 or 1 score, but was not always the case. The same analysis was carried out for the AD cases, see figure 4.56 (A-F), showing the mean specific binding levels \pm SD (fmol/mg) in female and male AD (n = 8) cases (see table 4.11) for [³H]Ro 25,6981 against depression score, in the 6 brain regions defined. There were no significant differences in levels of binding for depression score 2 compared to 0 in all the tissues studied, although the mean binding value for score 2 was always slightly higher than for score 0. The claustrum binding levels for all scores were slightly lower than in other tissues. Figure 4.57 (A-F) shows the mean specific binding levels \pm SD (fmol/mg) in female and male DLB, PDD and DLBPDD (n = 25) cases (see tables 4.7- 4.10) for [³H]Ro 25,6981 against delusion score, in the 6 brain regions defined. The mean binding levels tended to be slightly higher for the score of 1 compared to 0 or 2 score in each tissue, although these differences were not significant. Binding levels were very similar in the brain regions shown and between the depression scores in the tissues individually. The claustrum binding levels for all scores were lower than in other tissues. The same analysis was carried out for the AD cases, see figure 4.58 (A-F), showing the mean specific binding levels \pm SD (fmol/mg) in female and male AD (n = 9) cases (see table 4.11) for [³H]Ro 25,6981 against delusion score, in the 6 brain regions defined. There were no significant differences in

levels of binding for depression score 0, 1 or 2 in all the tissues studied. The claustrum binding levels for all scores were lower than in other tissues.

The dementia data for the female and male DLB, PDD and DLBPDD cases (n = 40) is shown in figure 4.59 (A-F) against mean specific binding levels \pm SD (fmol/mg) for each of the 6 brain regions defined. As with the previous graphs, no significant differences have emerged between binding levels for each score, or between the different regions analysed. The same is true for the female and male AD cases (n = 9), see figure 4.60 (A-F). Low n numbers make the comparisons statistically invalid.

Figure 4.61 (A-F) shows the mean specific binding levels \pm SD (fmol/mg) in female and male DLB, PDD and DLBPDD (n = 29) cases (see tables 4.7- 4.10) for [³H]Ro 25,6981 against visual hallucination score, in the 6 brain regions defined. There were no significant differences between binding levels in any of the brain regions shown with the exception of the Outer insular cortex where $p=0.001$ between scores 0 and 1. The claustrum binding levels for all scores were lower than in other tissues. The female and male AD cases (n = 10), shown in figure 4.62 (A-F) shows no significant differences in binding level as the clinical score increases.

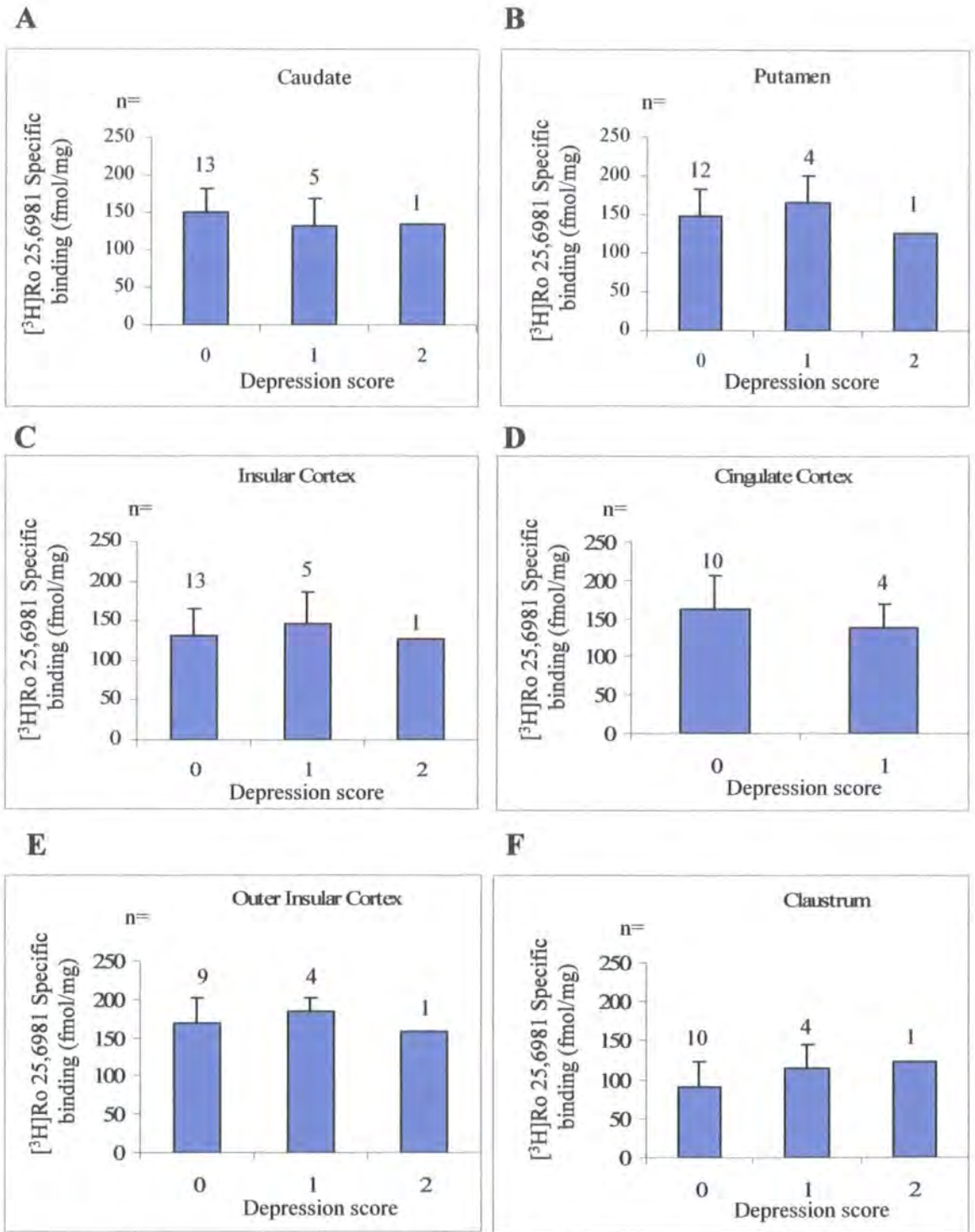


Figure 4.55 Depression score against [³H]Ro 25,6981 specific binding (fmol/mg) for DLB, PDD and DLBPDD cases in (A) Caudate (B) Putamen (C) Insular Cortex (D) Cingulate Cortex (E) Outer Insular Cortex and (F) Claustrum.

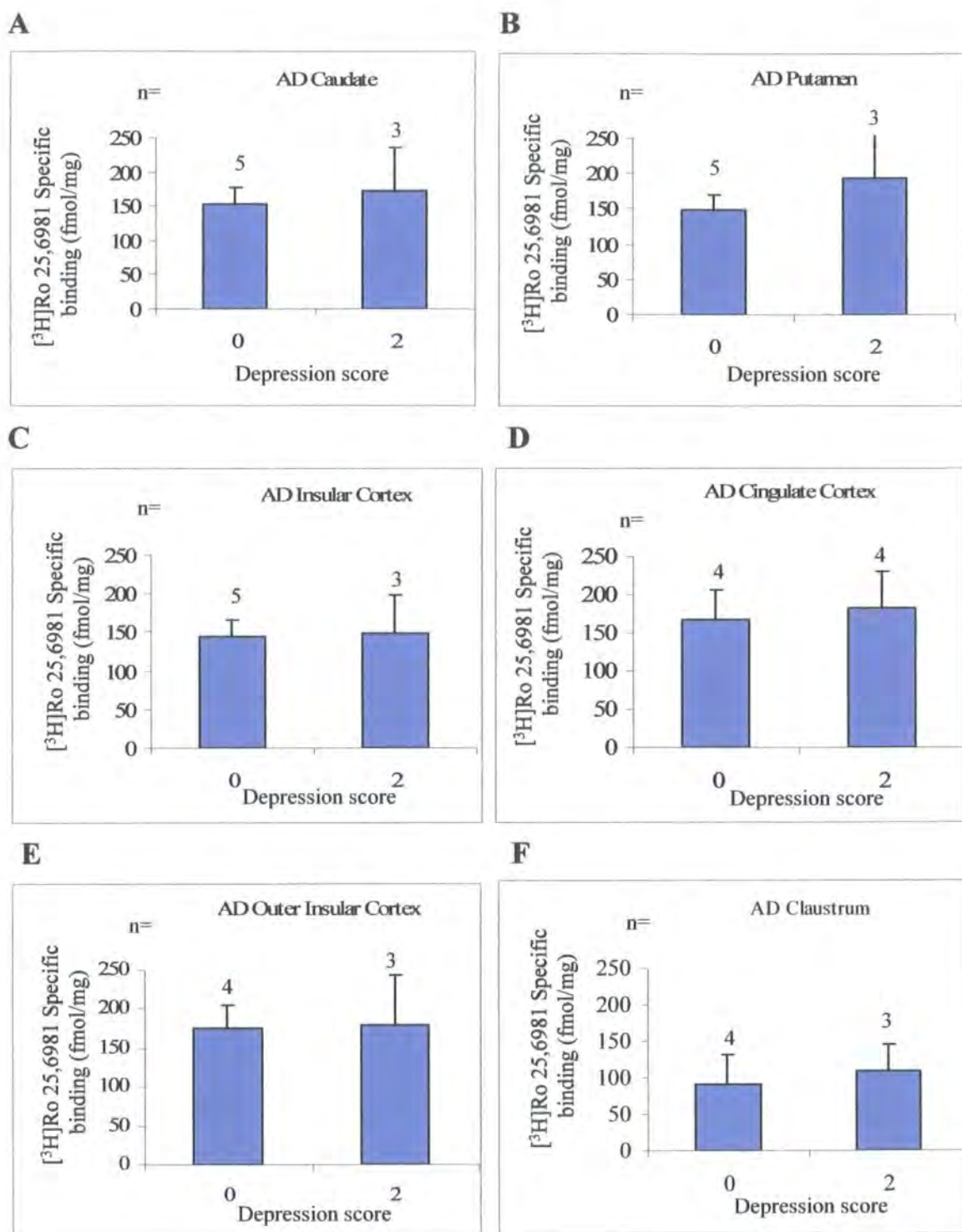


Figure 4.56 Depression score against [³H]Ro 25,6981 specific binding (fmol/mg) for AD cases in (A) Caudate (B) Putamen (C) Insular Cortex (D) Cingulate Cortex (E) Outer Insular Cortex and (F) Claustrum.

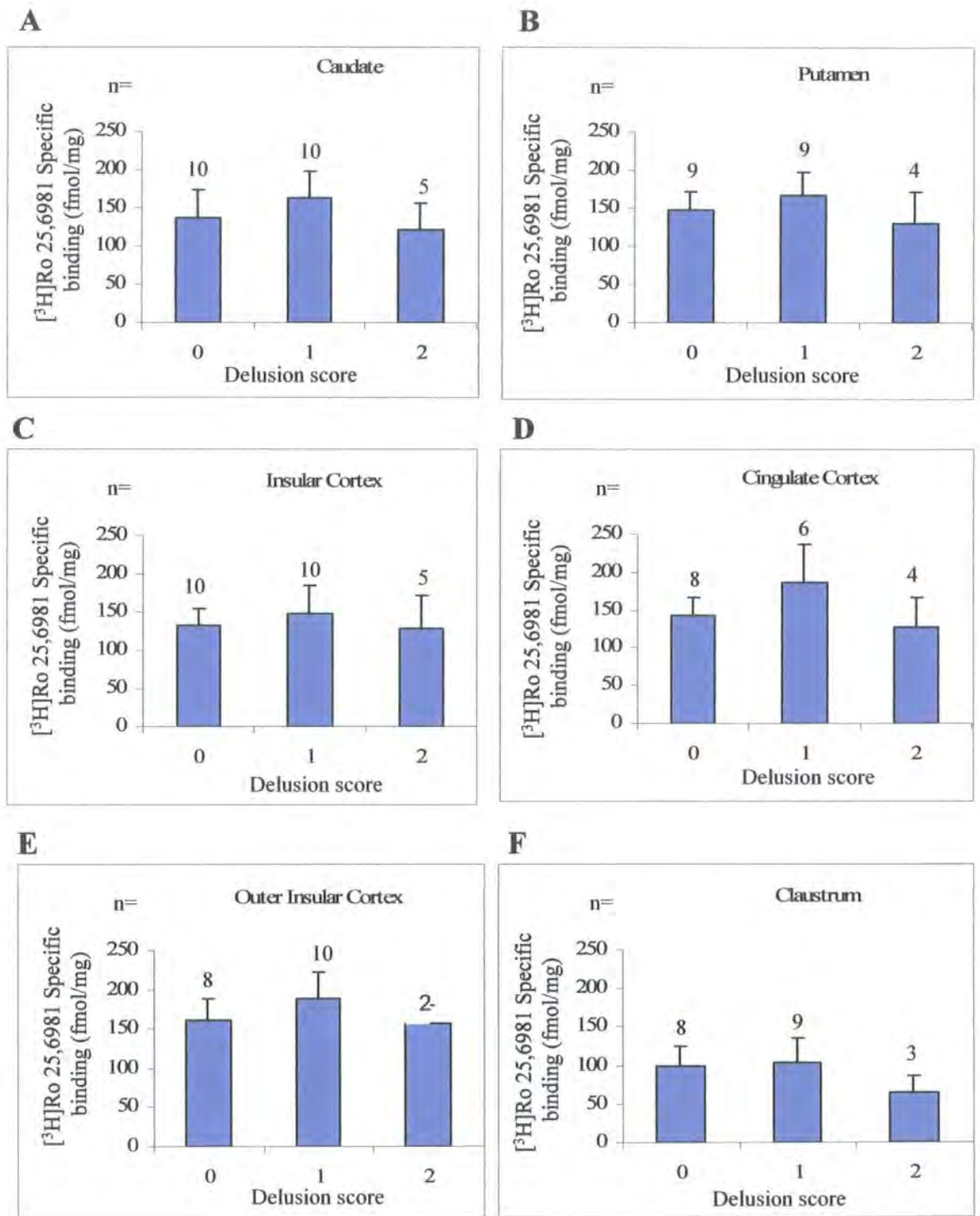


Figure 4.57 Delusion score against [³H]Ro 25,6981 specific binding (fmol/mg) for DLB, PDD and DLBPDD cases in (A) Caudate (B) Putamen (C) Insular Cortex (D) Cingulate Cortex (E) Outer Insular Cortex and (F) Claustrum.

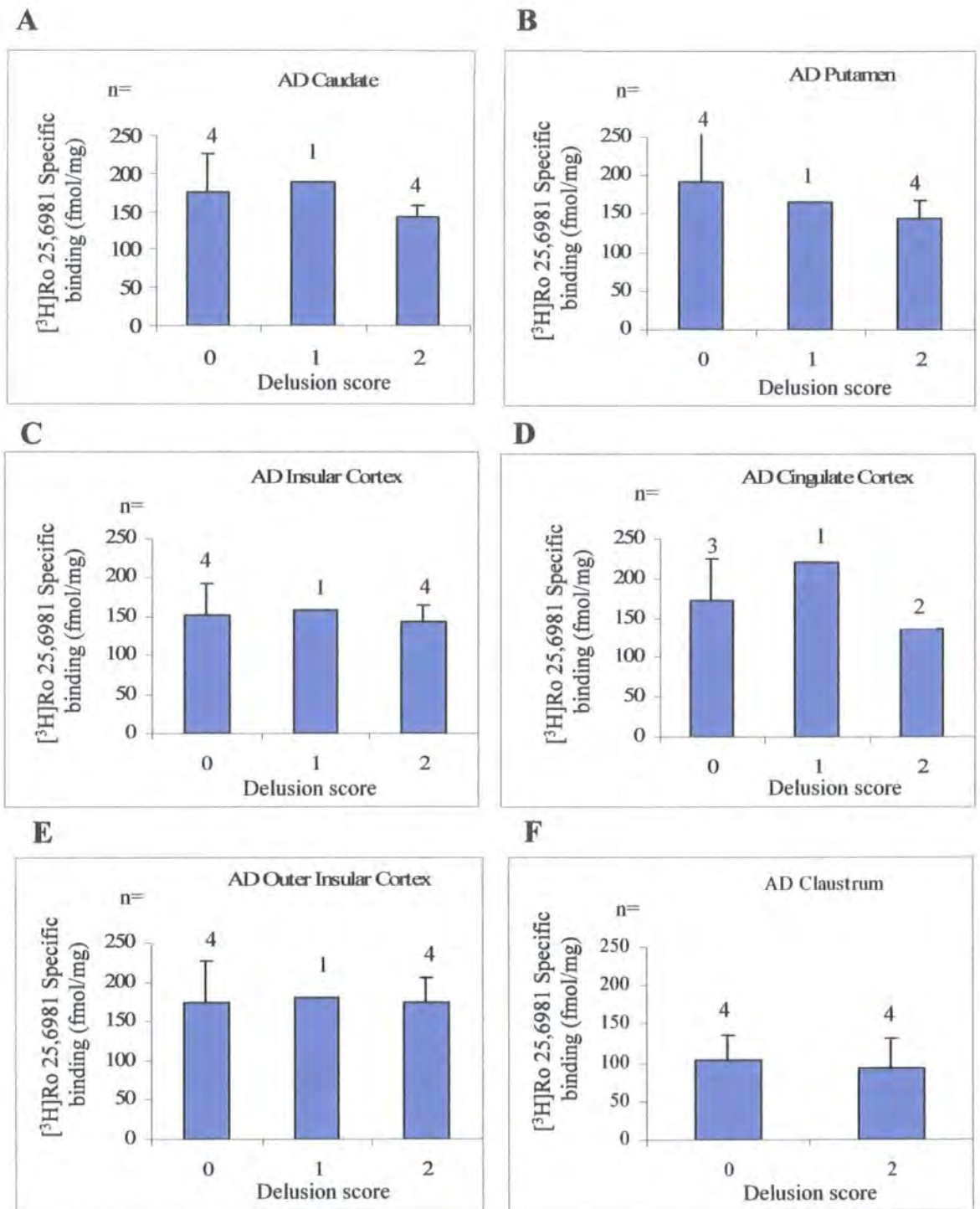


Figure 4.58 Delusion score against [³H]Ro 25,6981 specific binding (fmol/mg) for AD cases in (A) Caudate (B) Putamen (C) Insular Cortex (D) Cingulate Cortex (E) Outer Insular Cortex and (F) Claustrum.

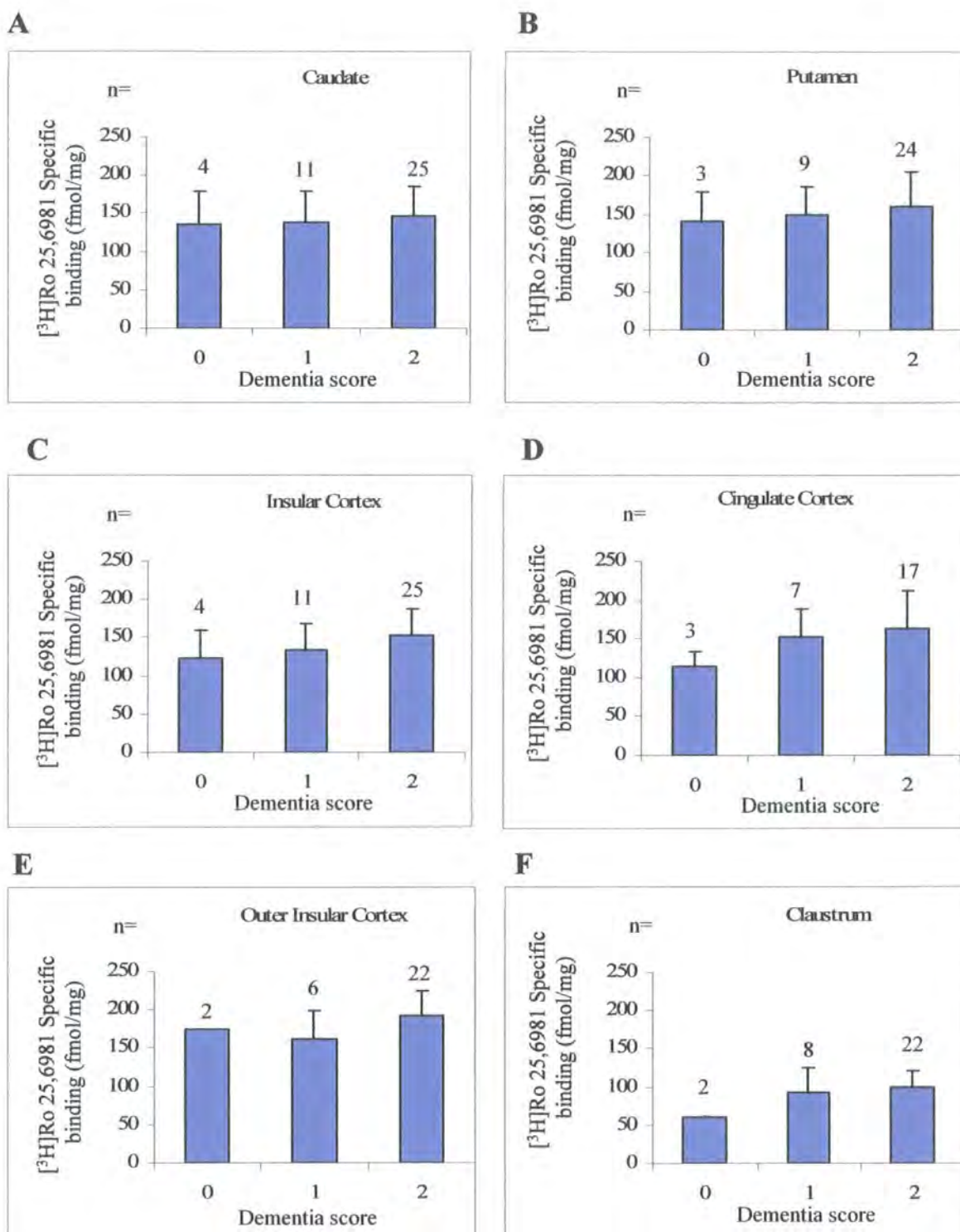


Figure 4.59 Dementia score against [³H]Ro 25,6981 specific binding (fmol/mg) for DLB, PDD and DLBPDD cases in (A) Caudate (B) Putamen (C) Insular Cortex (D) Cingulate Cortex (E) Outer Insular Cortex and (F) Claustrum.

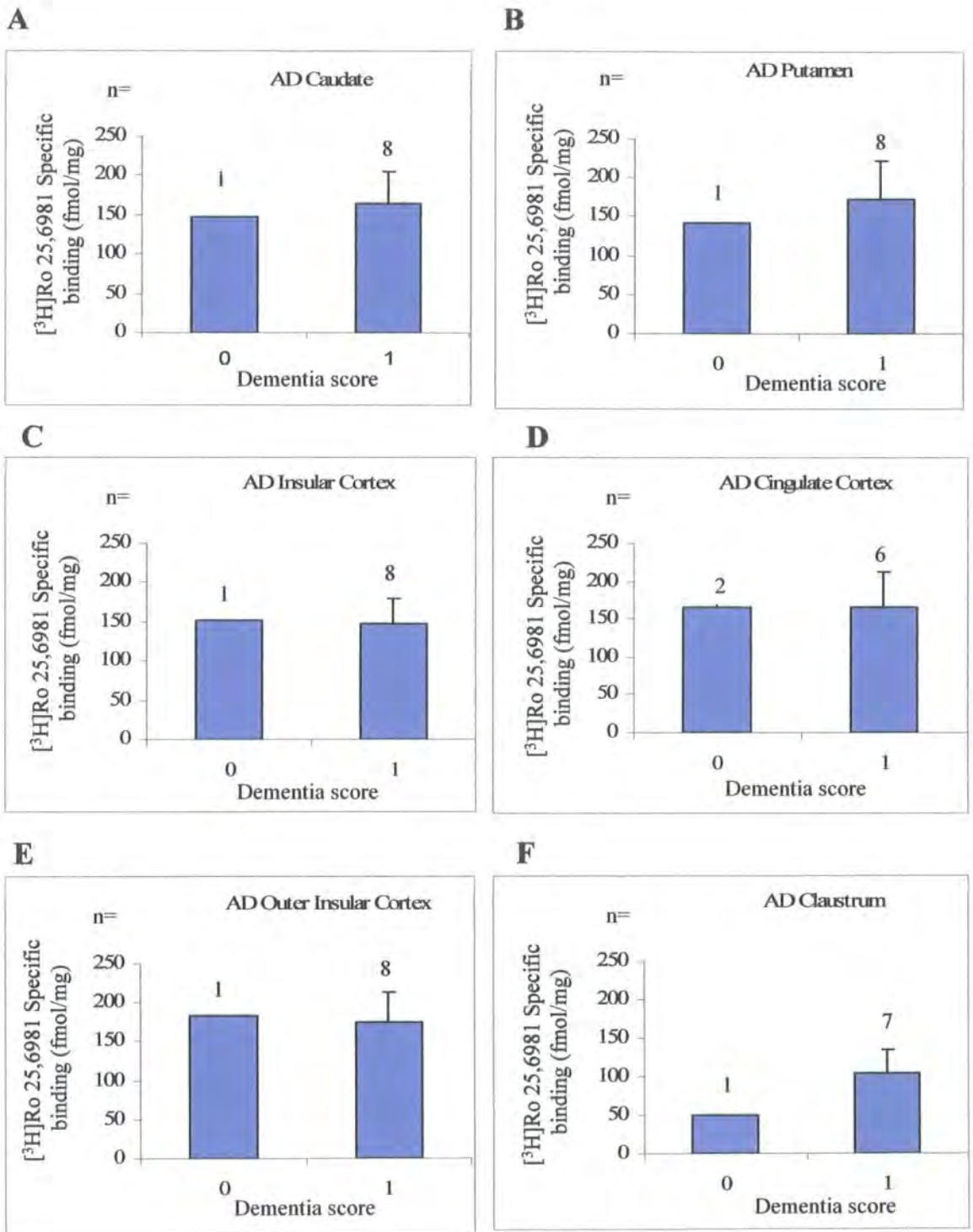


Figure 4.60 Dementia score against [³H]Ro 25,6981 specific binding (fmol/mg) for AD cases in (A) Caudate (B) Putamen (C) Insular Cortex (D) Cingulate Cortex (E) Outer Insular Cortex and (F) Claustrum.

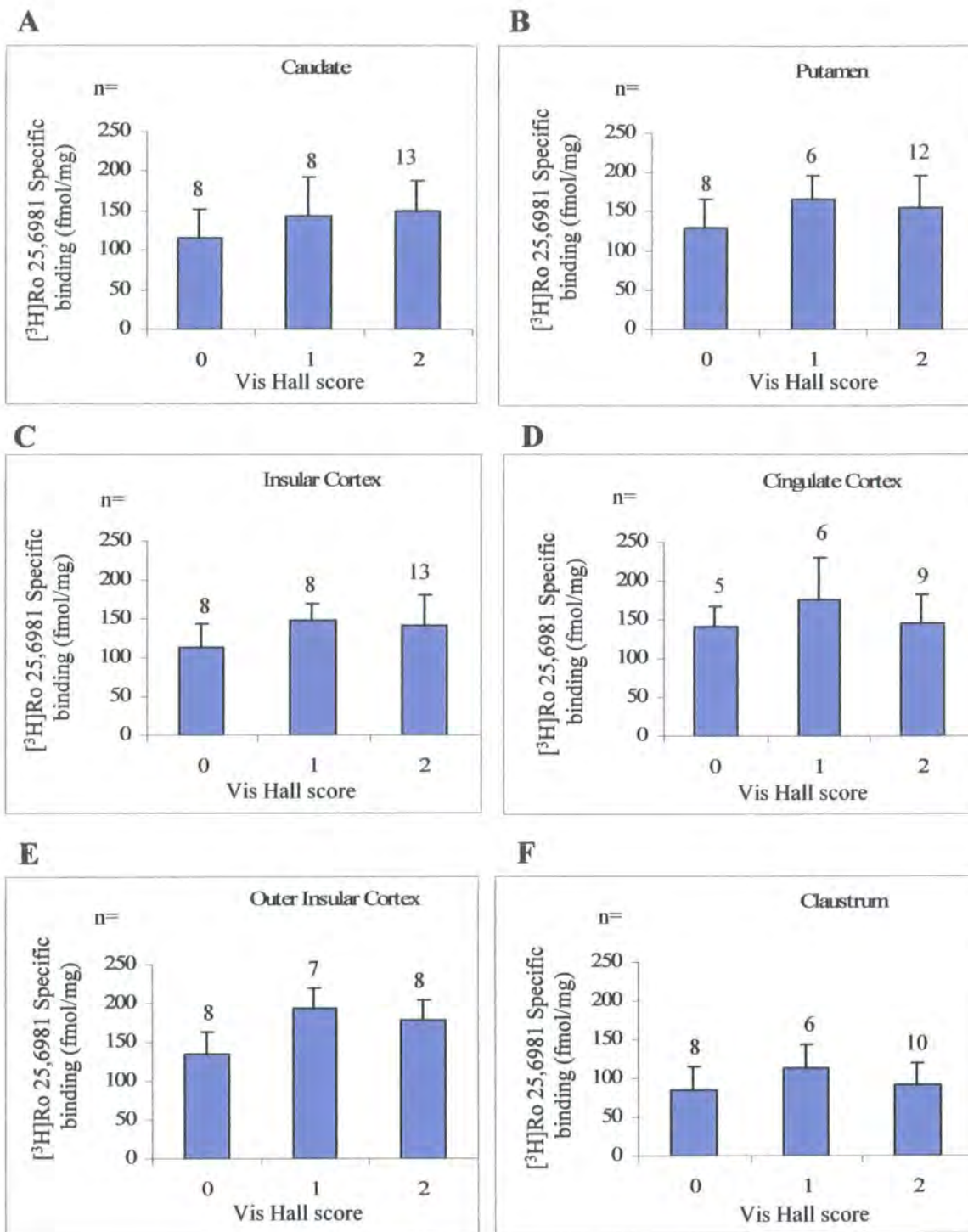


Figure 4.61 Visual Hallucination score against [³H]Ro 25,6981 specific binding (fmol/mg) for DLB, PDD and DLBPDD cases in (A) Caudate (B) Putamen (C) Insular Cortex (D) Cingulate Cortex (E) Outer Insular Cortex and (F) Claustrum.

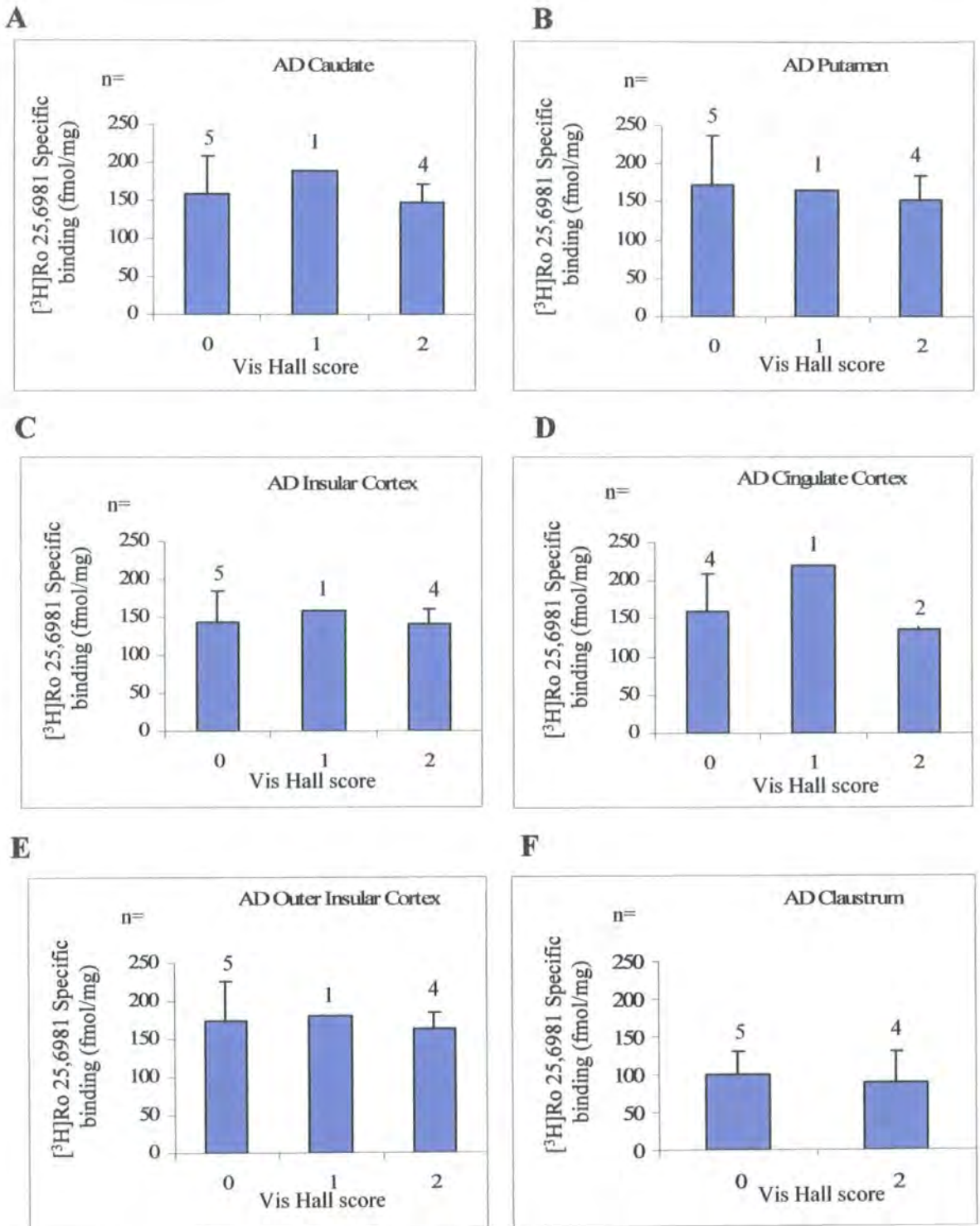


Figure 4.62 Visual Hallucination score against [³H]Ro 25,6981 specific binding (fmol/mg) for AD cases in (A) Caudate (B) Putamen (C) Insular Cortex (D) Cingulate Cortex (E) Outer Insular Cortex and (F) Claustrum.

4.6 Discussion

The autoradiographical assays performed in this study have been to distinguish and quantify different populations of NMDAR2B subunit-containing NMDA receptors, visualised using [³H]Ro 25,6981 and [³H]CP-101,606, NR2B-selective ligands. A range of brain structures implicated in the characteristic symptoms of DLB, PDD and AD were investigated. For example, the striatum (consisting of the caudate nucleus and putamen) is known for its role in the planning and modulation of movement pathways, but is also involved in a variety of other cognitive processes involving executive function. This area may be affected in neurological disorders where movement is impaired, such as PD. The cerebral cortex is involved in many complex brain functions including memory, attention, perceptual awareness, language and consciousness. More specifically, the cingulate cortex is thought to be associated with mood and emotions, and the insular cortex is believed to process convergent information to produce an emotionally relevant context for sensory experience, such as anxiety and pain. These are brain areas whose functions are affected by dementia and chronic neurodegenerative diseases where cognition steadily declines. The main focus has been to determine any changes in the NR2B receptor subtypes in relation to age and gender in control, DLB, PDD, DLBPDD and AD cases.

Over the last several years, an increasing number of reports have demonstrated the importance of the NR2B subunit in a variety of functions such as learning, memory processing and synaptic plasticity, as well as being involved in a number of human disorders (Loftis & Janowsky, 2003). Perturbations in glutamate neurotransmission and glutamate receptor activation may be fundamental to a variety of neurological disorders. Excessive release of glutamate contributing to excitotoxic neuronal death has been implicated as an etiologic mechanism in anoxic-ischemic injury, epilepsy and chronic neurodegenerative disorders such as Alzheimer's disease (Sze *et al.*, 2001). Most

researchers agree that NMDARs produce neurotoxicity via rapid Ca^{2+} influx leading to cellular Ca^{2+} overload (Zhou & Baudry, 2006). Abnormal function of NMDA receptors has been suggested to be correlated with the pathogenesis of Parkinson's disease (PD) as well as with the development of L-DOPA induced dyskinesia (Gardoni *et al.*, 2006). NMDA receptor antagonists exert a beneficial effect in experimental models of PD (Nash *et al.*, 2000; Loschmann *et al.*, 2004) and they are also effective in blocking the development of L-DOPA-induced dyskinesias (Wessell *et al.*, 2004). NMDA receptors have several important functions in the motor circuits of the basal ganglia, and are viewed as important targets for the development of new drugs to prevent or treat Parkinson's disease (PD). NMDA receptors present in the striatum are crucial for dopamine-glutamate interactions. The abundance, structure, and function of striatal receptors are altered by the dopamine depletion and further modified by the pharmacological treatments used in PD. In animal models, NMDA receptor antagonists are effective antiparkinsonian agents and can reduce the complications of chronic dopaminergic therapy. Use of these agents in humans has been limited because of the adverse effects associated with non-selective blockade of NMDA receptor function, but the development of more potent and selective pharmaceuticals holds the promise of an important new therapeutic approach for PD (Hallett & Standaert 2004). Dementia with Lewy bodies (DLB) is the second commonest cause of neurodegenerative dementia in older people and is a primary, neurodegenerative dementia sharing clinical and pathological characteristics with both Parkinson's disease (PD) and Alzheimer's disease (AD). NMDA receptors are known to play a pivotal role in synaptic mechanisms of learning and memory and NR2B ligands were chosen for this study since the NR2B subunit is a potential drug target for the treatment of such neurological disorders.

Ro 25,6981, a Roche compound, is an NR2B-selective antagonist, which binds to the ifenprodil binding site (Grimwood *et al.*, 2000; Mutel *et al.*, 1998, Lynch *et al.*, 2001).

Fischer *et al.* (1997) studied the characteristics of the interaction between Ro 25,6981 and NMDA receptors in a variety of different tests in vitro. They demonstrated that Ro 25,6981 is a highly selective, activity dependant blocker of NMDA receptors that contain the NR2B subunit, with potent neuroprotective effects in vitro. CP-101,606, a Pfizer compound, acts to inhibit NMDA receptor channel activity (Mott *et al.*, 1998), has been shown to be a potent neuroprotectant selective for forebrain neurons. Autoradiography indicates the CP-101,606 binding site is located in forebrain, most notably in hippocampus and the outer layers of cortex (Menniti *et al.*, 1997). Work carried out by Chazot *et al.* (2002) has provided evidence that CP-101,606 may represent a class of NR2B-directed NMDA receptor antagonist whose binding is affected significantly by the presence of another NR2 subunit type within the receptor complex.

4.6.1 Control Data

The first aim of this study was to determine the distribution pattern of ligand binding in the normal human brain and whether there were any differences in binding levels between the two NMDAR2B receptor ligands. 29 control cases were used representing normal ageing ranging from 62 -91 years. Figure 4.1(a) shows the agonal state score against [³H]Ro 25,6981 specific binding in the control data set for the putamen and insular cortex. There was no significant difference seen in the binding densities between agonal state scores, suggesting rapid or prolonged death does not significantly affect NR2B-containing NMDA receptor density in post-mortem tissue. Figure 4.3 and 4.4 show radioligand binding in control cases, labelling NR2B-containing receptors in distinct brain regions. These data agree with and support similar findings in previous experiments. For example, autoradiographical studies have shown high density NR2B binding in the rat cerebral cortex, hippocampus, dentate gyrus, caudate, putamen, globus pallidus and thalamus, with low

binding levels in the cerebellum (Mutel *et al.*, 1998). NMDA receptor high-affinity [³H]ifenprodil binding sites were found in the cortex, hippocampus, striatum and thalamus of the rat brain, with little or no labelling in the cerebellar region (Nicolas & Carter, 1994). Menniti *et al* (1997) used autoradiography to indicate the CP-101,606 binding site is localized in forebrain, particularly in hippocampus and the outer layers of cortex. Chapter 3, section 3.1 describes the regions where NR2B binding was high in the mouse brain. High ligand binding levels were seen in the CA1, CA3, granule layer of the dentate gyrus, entorhinal cortex and outer layers of the frontal cortex. Chapter 3, section 3.2.3 also shows that in the rat brain, the higher binding levels of [³H]Ro 25,6981 and [³H]CP-101,606 were found in the CA1, CA3, granule layer of the dentate gyrus, entorhinal cortex and outer layer of the frontal cortex. Figure 4.3 and 4.4 also show clear differences in the levels of binding between the two ligands in control tissues, with the [³H]Ro 25,6981 sections visibly darker than the [³H]CP-101,606, indicating higher binding levels, and therefore a higher presence of NR2B-containing receptor. These binding differences can be clearly seen in figure 4.9 (A-C) showing that in all the tissues, the levels of binding were significantly greater for [³H]Ro 25,6981 than for [³H]CP-101,606 when control male and female data were presented both together and individually. Table 4.13 shows that CP-101,606 binding relative to Ro 25,6981 was always less than 50% in pooled and separate male and female data sets, showing limited evidence for gender bias in the data. The percentage of CP-101,606 binding relative to Ro 25,6981 was variable between the regions (8-45% pooled male and female, 24-45% female only data and 20-47% male only data), suggesting a different proportion of the NR2B subtype population is present in each of the different tissues. These findings provide evidence that [³H]CP-101,606 labels a discrete population of NR2B-containing NMDA receptors in all the brain regions studied, consistent with previous studies by Chazot *et al* (2002).

The control data were further analysed for age-related changes, a phenomenon already observed in animal models, and to see whether there were any gender differences in the receptor level in normal ageing. Wenk *et al* (1991) demonstrated a significant decrease in NMDA receptor binding in the brains of aged rats and rhesus monkeys. A significant decrease in the mRNA expression of the NR2B subunit was also seen in the prefrontal cortex and caudate nucleus between young and old macaque monkeys, results similar to those previously seen in C57BL/6 mice during ageing (Bai *et al.*, 2004). Declines in spatial memory abilities are seen in humans, monkeys and rodents, and are thought to be related to changes in NR2B subunit expression. Peters *et al.* (2000) reported age-related alterations in primary visual cortex myelin in monkeys. A significant correlation was seen between the breakdown of the myelin and the impairments in cognition exhibited by individual monkeys. Age-related decreases of the NMDA receptor complex in the rat cerebral cortex and hippocampus have also been described by Tamaru *et al.* (1991). The evidence suggests age does effect NMDA receptor expression in animal models of normal ageing; therefore the purpose of this part of the study was to investigate potential NR2B subunit expression changes in normal human ageing. Figure 4.20 shows no significant changes in level of [³H]Ro 25,6981 or [³H]CP-101,606 binding in any region over the age range studied, with the exception of the [³H]CP-101,606 insular and outer insular cortex data, showing p=0.03 (significance) and p=0.06 (border-line significance) respectively. The data for these two regions shows an increase in binding as age increases, suggesting an increase in NR2B-subunit containing receptor population with age. This is interesting since the published literature suggests overall NR2B expression decreases with age in normal ageing animal models. A similar observation is seen in Figure 4.21 where the female control [³H]Ro 25,6981 and [³H]CP-101,606 binding data is shown against age. There were again no significant changes in binding levels with age for either of the two ligands, with the

exception of the [³H]CP-101,606 claustrum and insular cortex data, where $p=0.08$ (border-line significance) in both cases. As with the pooled insular and outer insular cortex male and female data in Figure 4.21, there is again an increase in binding level in these two regions with increasing age. If the overall NR2B subtype population (NR1/2B/2A, or 2B/2C and 2B/2D) is said to decrease with age (Wenk *et al.* 1991, Bai *et al.* 2004) and the NR2B subtype population (NR1/2B) is shown in this study to increase with age (shown by the CP-101,606 binding), then a possible switch in a class of NR2B subtype population with age may be occurring to compensate for these changes. An early age dependant switch was also detected in the rat, see Figure 3.2.3.10 in Section 3.2.3, Chapter 3. Figure 4.20-4.21 also clearly show the absolute binding levels of [³H]Ro 25,6981 were significantly higher than the [³H]CP-101,606 binding levels in pooled male and female, and female only data sets.

The data were analysed for gender differences over the age range. Figure 4.39 shows the separate control male and female binding levels for [³H]Ro 25,6981 against age. There were no significant age-related differences in the regions analysed except in the male claustrum and external globus pallidus ($p=0.02$ and $p=0.07$ respectively, where binding decreased with age) and male cingulate cortex ($p=0.03$ binding increased with age). The function of the claustrum is not completely known although it may be one of the most probable key components of consciousness (Crick & Koch 2005), and the cerebral cortex is known to be related to memory, attention, perceptual awareness and consciousness. Changes in NR2B receptors in these areas with age may be important in cognitive changes seen with increasing age. Figure 4.40 shows the separate control male and female binding levels for [³H]CP-101,606 versus age. There were no significant changes seen in binding with increasing age. The female data showed only border-line significance ($p=0.08$) in the claustrum and insular cortex. The same data in Figure 4.39 and 4.40 is represented as a

mean average specific binding value (\pm SD) for female and male data sets in Figure 4.45 and 4.46. There were no differences seen between the male and female data in all brain regions and for both ligands. The general trend in the majority of brain regions in the control data set is that there is no evidence for gender bias in overall binding levels within the age range of the two ligands. Sex differences in normal cognitive functioning in ageing remain largely unexplored (Finkel *et al.* (2006). Studies of genetic and environmental contributions to sex differences in level of cognitive performance and rate of decline were carried out by Finkel *et al.* (2006). Results indicated sex differences in mean performance for five cognitive measures, although despite differential longevity and susceptibility to disease, there were no consistent indications that men and women show different patterns of cognitive ageing. Wahlin *et al.* (2006) examined how health and biological age influence age and sex differences in cognitive ageing. A complex pattern emerged for the mediation of sex differences. Although biological age accounted for sex-related variation in cognitive performance, health operated to suppress these differences. Overall, both health and biological age predicted cognitive variation independently of chronological age. Read *et al.* (2006) investigated sex differences in genetic and environmental effects on cognitive abilities among older adult twins. Lower performance in all cognitive measures was related to increasing age. A Sex x Age interaction was observed, with greater deficits in the performance of women compared with those of men at higher ages, however, no sex-specific genetic influences were seen. The same genetic effects were operating for men and women.

Having looked at the control group separately, the next stage was to determine whether there were any changes in NR2B receptor binding levels in DLB, PDD, DLBPDD and AD cases when compared to the age-matched controls, and to determine if there are gender

differences between disease groups compared to age-matched controls. This is covered in the following section.

4.6.2 Disease State data (DLB, PDD, DLBPDD and AD)

Images of DLB, PDD and AD brain sections in Figures 4.5- 4.8 show a visible difference between binding levels of the two ligands in each disease state, with the [³H]CP-101,606 levels reduced when compared with [³H]Ro 25,6981, indicated by the reduced intensity of the image. The brain regions labelled by both ligands were similar to those labelled in the control sections, and again agree with published literature. The caudate, putamen, insular cortex, cingulate cortex and claustrum all show NR2B labelling. The difference in binding level between the two ligands was reflected well when statistically analysed, figures 4.10 to 4.12 show that binding of [³H]CP-101,606 in all the tissues (except the claustrum for the AD data) was significantly lower than with [³H]Ro 25,6981 in all the disease states. This again would support the hypothesis that CP-101,606 labels a subtype of NR2B containing NMDA receptor. The data were further analysed to see if there were differences in the level of NR2B binding between the disease states, and these data are shown in Figure 4.12(a) and 4.12(b). Binding levels of [³H]Ro 25,6981 showed no significant differences between the disease states in any of the brain regions. This is interesting since it suggests that there is no significant change in NR2B receptor population in any one form of neurodegenerative disease compared to another. DLB, PDD and AD all have cognitive decline as a major symptom of the disease progression. In rodents, cognitive decline has correlated to decreases in NR2B subtype populations in the brain. Bai *et al* (2004) studied the changes in the expression of the NR2B subunit during ageing in macaque monkeys. They demonstrated that humans, non-human primates and rodents show decline in spatial memory abilities with increased age. They put forward that some of these decline in mice

are related to changes in the expression of the NR2B subunit of the NMDA receptor. More specifically, they showed a significant decrease in the mRNA expression of the NR2B subunit overall in the prefrontal cortex and in the caudate nucleus between young (6-12 years) and old (24-26 years) monkeys. There were no significant changes in NR2B mRNA expression in the hippocampus or the parahippocampal gyrus. Previous studies in C57BL/6 mice showed similar results to those in the prefrontal cortex, caudate and hippocampus during ageing, suggesting that mice could be more useful models for primates to further examine the age-related changes in NR2B subunit expression in several important regions of the brain. There is no direct quantifiable correlation between abundance of the NR2B subunit and severity of dementia. Previous studies by Hynd *et al* (2004) showed that there was significantly lower expression of individual NR2A and NR2B transcripts in susceptible regions of the AD brain, whereas expression of NR2C and NR2D transcripts did not differ from that in controls. Also the expression of the NR1 subunit mRNA splice variants in Alzheimer's disease brain varied according to regional susceptibility to pathological damage. NMDA receptor dysfunction might give rise to the regionally selective pattern of neuronal loss that is characteristic of AD. Binding levels of [³H]CP-101,606 between the disease states again showed no significant differences except in the AD data, where the cingulate cortex was higher than the DLB and PDD data. This result may be a reflection of the low n numbers, and a larger study would need to be carried out to confirm the significance of this finding. Table 4.13(a) showed the DLB and PDD [³H]CP-101,606 binding levels in all brain regions were less than 50% of the [³H]Ro 25,6981 levels. The AD data showed a greater than 50% binding level compared to [³H]Ro 25,6981, except in the claustrum. It is known from Figure 4.12 however, that there is a significant difference between the binding levels except in the claustrum. Alzheimer's disease is characterized by loss of specific cell populations within selective subregions of the hippocampus. Mishizen-

Eberz *et al* (2004) demonstrated that with increasing AD neuropathology, protein levels and mRNA expression for NR1 and NR2B subunits were significantly reduced, while the NR2A subunit mRNA expression and protein levels were unchanged. Their work supports the hypothesis that alterations occur in the expression of specific NMDA receptor subunits with increasing AD pathologic severity, which is hypothesized to contribute to the vulnerability of these neurons. Data from Bi *et al.*(2002) also suggest that alterations in NMDA receptor subunits, particularly NR2A and NR2B, may be important in AD, especially in neuronal populations that underlie impaired learning and memory. When the data were divided by gender, there were no trends seen between the binding of the two ligands.

When the binding data for each ligand was correlated with age in each of the DLB and PDD disease cases, there were no significant changes occurring (with the exception of the DLB CP-101,606 outer insular cortex $p=0.04$) see figures 4.22 to 4.24. This was surprising at first since previous evidence points to a decrease in the NR2B subunit with age and a corresponding decrease in cognitive performance in animal models (Clayton *et al.*, 2002). However, in the AD group, see Figure 4.25, a significant age-dependant reduction in [³H]Ro 25,6981 binding density was evident in the striatum, nucleus accumbens, cingulate and insular cortex. The AD cases were used to compare changes in a disease group of equivalent age which have dementia but do not show signs of motor complications associated with a reduced dopaminergic function, such as seen in PD. As previously stated, the DLB and PDD cases did not demonstrate this decline with age, with the exception of the DLB [³H]CP-101,606 insular cortex, showing a significant decline. Possibly a wider age range is necessary to show any age-dependant changes in the control data, however, the results so far indicate age-dependant differences in the NR2B subtype populations between

the three dementia groups (DLB, PDD and AD) and normal ageing. Age is therefore a factor to take into consideration when carrying out further analysis.

Having studied the effects of age on the binding levels of the two ligands, the data was then divided by gender to see if there were gender differences in binding across the age-range. Figure 4.41 and 4.42 show the male and female DLB data for [³H]Ro 25,6981 and [³H]CP-101,606 respectively. In both cases there were no significant differences. This was the same for the DLBPDD [³H]Ro 25,6981 data shown in Figure 4.43. These results provide evidence that the ligand binding does not vary between male and female cases, and that age is not an influencing factor in the binding level in either gender group across the age-range. However, this is not the case when analysing the AD data. There were significant age-dependant reductions in [³H]Ro 25,6981 binding in the female caudate, putamen and insular cortex and male cingulate cortex. All other tissues showed a trend for decreased binding as age increased, although were not statistically significant. There is increasing evidence for the involvement of glutamate-mediated neurotoxicity in the pathogenesis of AD. The NMDA receptor antagonist memantine is used as a symptomatological and neuroprotective treatment for Alzheimer's disease (Danysz & Parsons 2003). Continuous mild activation of the receptors may lead to neuronal damage and impairment of synaptic plasticity (learning). Inflammatory processes in the central nervous system are also thought to contribute to AD. Chronic administration of nonsteroidal anti-inflammatory drugs (NSAIDs) decreases the incidence of Alzheimer's disease. There are very few studies, however, on the cognitive impact of chronic NSAID administration. The NMDA receptor is implicated in learning and memory, and age-related decreases in the NMDA NR2B subunit correlate with memory deficits. Mesches *et al* (2004) administered Sulindac, an NSAID that is a nonselective cyclooxygenase (COX) inhibitor, to aged Fischer 344 rats for 2 months. Sulindac, but not its non-COX active metabolite, attenuated age-related deficits in

learning and memory as assessed in the radial arm water maze and contextual fear conditioning tasks. Sulindac treatment also attenuated an age-related decrease in the NR1 and NR2B NMDA receptor subunits and prevented an age-related increase in the pro-inflammatory cytokine, interleukin 1beta (IL-1beta), in the hippocampus. These findings support the inflammation hypothesis of ageing and have important implications for potential cognitive enhancing effects of NSAIDs in the elderly (Mesches *et al.* 2004). Magnusson 1998 reported that the effects of aging on NMDA receptors may be associated with age-related declines in spatial learning. C57B1/6 mice aged 3, 10, and 26 months were tested for spatial learning in the Morris water maze. Ten and 26 month old mice were ad libitum-fed or diet restricted (60% of ad libitum-fed calories). Diet restriction significantly improved memory performance among the 10 and 26 month olds. Diet restricted 26 month olds did not differ significantly from 3 month olds or any other groups. There was a significant correlation in memory test score with [³H]glutamate binding densities for the NMDA receptors in the frontal cortex and CA1 region of the hippocampus. These results suggest that there is a sparing of spatial memory with diet restriction in aging C57B1/6 mice. There are however several flaws in the water maze technique which must be considered. These include factors such as movement disorders of the animal and anxiety levels due to emersion in water. A human study is necessary due to these flaws making the water maze not an ideal model. Braak & Braak (1998) studied neuronal changes in the course of Alzheimer's disease. Many neuronal systems are involved in the degradation of a few types of nerve cells in AD. Brody (1980) reported that as the nervous system ages, an area-, time- and rate-specific neuronal cell loss is observed in human and animal species. The same data are also presented in Figure 4.47 to 4.50 showing the mean average specific binding data (\pm SD) for male and female cases for each disease state. Figure 4.47 (Ro 25,6981 DLB) and Figure 4.50 (Ro 25,6981 AD) showed no significant differences

between male and female data. Figure 4.48 (CP-101,606 DLB) showed the accumbens binding level was higher in the female than the male, but all other regions showed no significant differences. Figure 4.49 (Ro 25,6981 DLBPDD) also had higher female binding in the caudate and putamen, with all other regions showing no differences. Apart from the three regions mentioned above, the overall result is that there is no gender bias with regards to the binding of the two NR2B-selective ligands in the regions analysed in DLB, DLBPDD and AD cases. There is little known about the effects of gender on the NMDA population in the brain, and the literature does not provide evidence for there being a bias in NR2B subtype binding. The data in this section would suggest that gender has very little or no influence on NR2B binding and therefore does not in turn influence decline in cognitive ability that may be associated with a decrease in NMDAR2B receptors.

The control and disease state data so far have been analysed separately for differences in ligand binding levels, and age-related changes in binding as a whole data set and for male and female data individually. The next section looks at the disease data compared to the age-matched control case data to analyse for similar changes.

4.6.3 Control v Disease State data

The control and disease state data have been compared in Figure 4.13 to 4.19. Control against DLB data is shown for Ro 25,6981 and CP-101,606 binding on Figure 4.13 and 4.14 respectively. In both cases there were no significant differences seen between the two groups of data in all the brain regions analysed. The only significant difference to emerge was a higher female binding level in DLB cingulate cortex compared to control. This may be due to the female control binding being lower than the male, suggesting a higher expression of NR2B receptor subtype in the DLB female region compared to the others. It would be surprising to see an increase in NR2B receptor in the disease state compared to

control, since it was expected that DLB cases may have shown a decrease in NR2B receptor expression corresponding to a decline in cognitive ability and increased dementia compared to normal. Control versus PDD data are shown for Ro 25,6981 and CP-101,606 binding in Figure 4.15 and 4.16. The binding levels for both ligands did not significantly vary between the two groups and the only difference in the data set was a lower Ro 25,6981 binding level in PDD caudate compared to control. The PDD cohort used in this study lacked dyskinesias since the UPDRS scores were all below 30, indicating mild movement disorders. The data could therefore not be related to movement correlation. Calon *et al* (2003) studied NMDA receptors in the brains of controls and Parkinson's disease (PD) patients, of which 10 of 14 developed motor complications (dyskinesias and/or wearing-off) following levodopa therapy. [³H] Ro 25-6981 binding to the NR1/NR2B NMDA receptor was increased in the putamen of PD patients experiencing motor complications compared to those who did not (+53%) and compared to controls (+18%) whereas binding remained unchanged in the caudate nucleus. The results from this section showed no difference in PDD putamen [³H]Ro 25,6981 binding levels compared with controls and a decrease in caudate binding rather than an increase as described by the literature above. In human postmortem tissue, unchanged (Calon *et al.*, 2003) or increased (Lange *et al.*, 1997) NR2A binding and increased NR2B binding (Calon *et al.*, 2003) has been reported. It is clear that the literature on NMDA receptor binding in PD in both experimental models and human tissue is inconclusive. The different ligands utilized to study NMDA receptor binding sites, extent of dopamine depletion, and severity of motor complications associated with dopaminergic therapy, may in part explain the differences in results between these studies. Another important aspect, however, is the complexity of the NMDA receptor system itself, and variety of different mechanisms that regulate these channels. In human postmortem brain, only NR1 expression has been examined closely, and in two studies was shown not

to be substantially altered in PD (Meoni *et al.*, 1999 and Calon *et al.*, 2003). NMDA receptors present in the striatum are crucial for dopamine-glutamate interactions. The abundance, structure, and function of striatal receptors are altered by the dopamine depletion and further modified by the pharmacological treatments used in PD (Hallet & Standaert, 2004).

Figure 4.17 shows [³H]Ro 25,6981 control versus DLBPDD data, with no significant differences seen between the two groups except when the data are divided into male and female. The male DLBPDD caudate and insular cortex data show a lower binding level than the control. This may suggest that the male DLBPDD caudate and insular cortex are more susceptible to NR2B receptor changes than controls. Control versus AD data are shown for Ro 25,6981 and CP-101,606 binding on Figure 4.18 and 4.19 respectively. There were no significant differences in binding level of both ligands between the two groups, and no gender bias was observed. Only the CP-101,606 AD cingulate cortex showed a significantly higher binding level than the control. The n numbers were low for the AD data set therefore a larger study would need to be carried out to see statistical significance between AD and control data. The exact cause of memory loss that leads to dementia in AD is not known. The amyloid precursor protein + presenilin-1 (APP+PS1) transgenic mouse is a model for amyloid deposition, and like AD, the mice develop memory deficits as amyloid deposits accumulate. At the age when these animals developed cognitive dysfunction, they had reduced mRNA expression of several genes essential for LTP and memory formation (Arc, Zif268, NR2B, GluR1, Homer-1a, Nur77/TR3). These changes appeared to be related to amyloid deposition, because mRNA expression was unchanged in the regions that did not accumulate amyloid (Dickey *et al.*, 2003).

The control versus disease state data were then further analysed for age-dependant changes. The hypothesis is that both control and disease state binding levels will decrease with age,

since NR2B receptor populations in the brain are thought to decrease with age and increasing cognitive deficits. The disease state binding levels however would be expected to decrease more dramatically than the normal level of decline seen in control cases. The NR2B subunit is implicated in neurological disease where impairment of memory may occur, and has been shown to decrease with age in previous studies in rodents (Clayton *et al.* 2002).

Control versus DLB [³H]Ro 25,6981 binding is shown in Figure 4.26 to 4.28. For the pooled male and female data and separate female data, there were no significant differences in binding level with increasing age in either control or DLB data sets. The male data set however showed a significant increase in binding in the control cingulate cortex (p=0.03), and decrease in binding in the control claustrum (p=0.02). Control against [³H]CP-101,606 binding, shown in Figure 4.29, shows no significant differences, except in the control insular cortex (p=0.03) and DLB outer insular cortex (p=0.04). There is border-line significance decrease in the control outer insular cortex (p=0.06). These results do not provide evidence for a clear trend in changes of the NR2B subtype populations with age in DLB compared with control cases.

Control versus PDD [³H]Ro 25,6981 and [³H]CP-101,606 data are shown in Figure 4.30 to 4.32, and control versus DLBPDD data are shown in Figure 4.33 to 4.35. There were no significant differences between control and PDD or control and DLBPDD binding levels in any of the region except those which have already been described for the [³H]Ro 25,6981 male control data above (that is, control claustrum, cingulate cortex and insular cortex) and the [³H]CP-101,606 control pooled data insular cortex also already described. The main finding in this section is again relating to the AD data. Figure 4.36 to 4.38 shows the control and AD binding levels against age for both ligands. The [³H]Ro 25,6981 control pooled male and female data is as previously described, however the AD data shows

significant age-dependant decreases in binding for all brain regions with the exception of the claustrum and internal and external globus pallidus. The separate female data set also shows significant decreases in binding with age in all brain areas except the claustrum, outer insular cortex and cingulate cortex. The findings from this study of AD cases show that with increasing age, the population of NR2B-containing NMDA receptors is decreasing. These data support studies which have been outlined previously in this section. An interesting observation however, is that the binding levels in AD cases at the early ages studied, showed higher binding levels than the age-matched control cases, which with increasing age, dropped to levels similar to those seen in the age-matched controls. This data would suggest that elevated NR2B levels might be an early marker for a predisposition for AD progression later in life.

Haug & Eggers (1991) studied ageing of the human cortex cerebri and corpus striatum. They found that there was not a loss of the neurones themselves with age, but the size of the neurons and the number of synapses decrease with age. Various regions of the brain age differently and there is a genetically determined decreased brain function during ageing which can only be inhibited, not permanently preserved. Perhaps there is a decrease in NR2B receptor subtype with age as the size rather than abundance of NR2B expressing neurons decreases with age. Huttenlocher (1979) studied developmental changes and effects of normal human ageing (ranging from newborn to 90 years) by focusing on synaptic density in the human frontal cortex. The human cerebral cortex showed a loss of neurons and synapses at late developmental stage.

The next section focuses on the disease state symptom and cognitive ability data collated from clinical records of the cases used in this study.

4.6.4 Disease State Symptom Correlation Studies

In this section the [³H]Ro 25,6981 and [³H]CP-101,606 binding levels have been correlated with scores from various clinical tests carried out at the last examination before death of each subject in the study. Figure 4.51, 4.51(a) and 4.52 show the [³H]Ro 25,6981 specific binding levels against MMSE (see section 4.3) and MTS (see section 4.3.1) scores. For all the pooled DLB, PDD, DLBPDD (Lewy Body dementias) and AD cases and in all the brain regions analysed there were no significant changes in binding level with increasing score. Only the Lewy Body dementias insular cortex showed a border-line decrease in binding with increasing MMSE score. There was however an overall trend for binding levels to decrease as MMSE and most notably MTS score increased in all the regions analysed. An MMSE score of $\leq 23/30$ and an MTS score of $\leq 30/37$ indicates cognitive impairment. The data would suggest an increase in binding with a decrease in score and a parallel decrease in cognitive performance. This does not support the theory that the NR2B subtype of NMDA receptor may decrease with age and cognitive decline. Sze *et al* (2001) report that phosphorylated NR2B (56%, $P < 0.01$) were selectively reduced in entorhinal cortex in AD when compared to controls, and that both phosphorylated and non-phosphorylated NMDA receptor protein levels in entorhinal cortex correlated (increased as score increased) with Mini-Mental Status Examination (MMSE) and Blessed (BIMC) scores. MMSE scores in this study ranged from 13-30, indicating all cases studied had cognitive impairment within a similar range to the present study. Analysis of all cases, showed the levels of P-NR2B and NR2B in entorhinal cortex correlated with MMSE scores ($r = 0.675$, $P < 0.005$; $r = 0.620$, $P < 0.01$) and Blessed (BIMC) scores ($r = -0.655$, $P < 0.005$; $r = -0.556$, $P < 0.025$). The loss of NR1 protein correlated with the severity of cognitive impairment, as measured by the MMSE, BIMC (Blessed Information, Memory and Concentration Test), and Free Recall (memory recall test) scores ($r = 0.692$, $P < 0.01$; $r = -0.641$, $P < 0.01$; $r = 0.586$,

$P < 0.025$) in the hippocampus. NR2B protein levels in the hippocampus correlated with MMSE and BIMC scores ($r = 0.588$, $P < 0.025$; $r = 0.565$, $P < 0.025$). The binding data versus UPDRS score (see section 4.4) are shown in Figure 4.53 and 4.54 for DLB, DLBPDD, PDD and AD respectively. Figure 4.53 shows no correlation between binding level and UPDRS score in any of the brain regions. This suggests that the severity of PD symptoms experienced by the patient does not affect the expression of NR2B receptors in the brain regions studied here, or vice-versa. The most significant and interesting observation from all the symptom studies in this section is shown in Figure 4.54. Here the binding level against UPDRS score for AD cases is shown. There is a significant decrease in binding with increasing score in the caudate and putamen, as well as border-line significant decreases in binding in the insular cortex, cingulate cortex and outer insular cortex. Studies show that a continuous mild activation of NMDA receptors may lead to neuronal damage and impairment of synaptic plasticity and learning (Danysz & Parsons, 2003). These results show that as UPDRS score increases, showing behavioural and motor deficits, NR2B receptor populations are decreasing, shown by decreases in binding level. Conversely, and in support of this data, Tang *et al* (1999) reported that transgenic mice over-expressing the NR2B subunit exhibit superior ability in learning and memory in various behavioural tasks, showing that NR2B is critical in gating the age-dependent threshold for plasticity and memory formation. The disease cases in this study had low motor impairment, with UPDRS scores less than 30, indicating mild movement deficits in the cohort. Therefore expression of NR2B may not be affected significantly by this factor. The changes in NR2B expression seen in the AD cases may be due to the behavioural side of the UPDRS assessment rather than the cognitive, even though UPDRS score is low.

The scoring system for each of the depression, delusion, dementia and visual hallucination data is the same, ranging from 0-2, where the severity of the symptoms experienced were

given a score of either 0 = none, 1 = mild and 2 = severe. The data for these are shown in Figure 4.55 to 4.62. There were no significant differences between [³H]Ro 25,6981 binding levels between any of the scores, and in any of the brain regions analysed, this applied to both DLB and AD data alike. The only significant difference seen was in the DLB outer insular cortex visual hallucination data, where the binding for score 1 was higher than score 0. The data does not provide evidence for a change in NR2B binding with an increase in severity of psychiatric symptoms. The previous literature suggests a decline in NR2B receptor subtype with increasing age (Bai *et al.* 2004) which may be associated with decline in cognitive function, although the dementia results from this study do not show a significant change in binding with increasing severity of the symptoms. The dementia score defines a qualitative analysis and cannot be considered to be accurate as the MMSE and MTS data which is quantitative. Mesches *et al* (2004) used Sulindac and showed improved memory and increased NMDA receptor subunits in aged Fischer 344 rats. The results from this study do not however appear to suggest that a decreased ability in learning and memory (represented by increased severity of symptom) shows a decrease in NMDARB receptor subunits. The psychotic symptom data in the study, that is, the delusion and visual hallucination data, did not show any significant differences between binding levels and score with the exception in the DLB outer insular cortex visual hallucination data. Several lines of investigation support a hypothesis of glutamatergic dysfunction in schizophrenia, including reports of altered NMDA receptor subunit and associated intracellular protein transcripts in the thalamus of elderly patients with schizophrenia (Clinton & Meador-Woodruff, 2004).

Akbarian *et al.* (1996) reported no significant changes in the expression of NR2A, NR2B, NR2C, or NR2D mRNA in prefrontal, parieto-temporal, and cerebellar cortices of postmortem brains from schizophrenic patients compared with control subjects. However,

using different methodology, Grimwood *et al.* (1999) found somewhat conflicting results. As measured by radioligand binding with [³H]ifenprodil, NR2B-containing receptors are selectively up-regulated in the superior temporal cortex in schizophrenia, but not in the pre-motor cortex. Although changes in transcript levels are not always indicative of corresponding alterations in protein expression (and *visa versa*), these findings suggested that further investigation of the role of NR2B in schizophrenia is needed. Gao *et al.* (2000) analyzed postmortem hippocampal tissue from people with schizophrenia and from control subjects. Glutamate receptor autoradiography of various subfields in the hippocampus provided no evidence of ligand-binding differences between the groups. Interestingly, *in situ* hybridization experiments were also performed and the level of mRNA for the NR2B subunit in CA2 of the hippocampus was found to be 40% higher in schizophrenia tissue than in control tissue.

4.6.5 Overall Summary.

Some key findings have come out of the work done in this chapter. The first observation is the general overall preservation of NR2B-containing receptors in the control and disease state cases over age. Published literature states that NMDA receptors are involved in memory, learning and synaptic plasticity (Loftis & Janowsky, 2003; Tang *et al.*, 1999) and that with advancing age there is a decrease in the expression of the NR2B subunit in rodents (Clayton *et al.* 2001; Bi *et al.* 2002; Hynd *et al.* 2004; Mishizen-Eberz *et al.* 2004). This decline could be associated with a decline in cognitive ability, both in normal ageing and with pathological progression. The data from this study shows that in general there is no decline in NR2B-containing receptor expression with age in the human cases studied, and therefore does not fully agree with the previous published rodent data. This means that functional NR2B receptors are still present in several brain regions of normal and disease

state aged cases. Functional receptors are therefore available as therapeutic targets for NMDA antagonist compounds, which could potentially be used to alleviate symptoms of cognitive decline associated with AD, DLB and PD as seen in the cases used in this study. High levels of NR2B expression were seen in the earlier age cases of AD. NR2B levels were higher than those seen in the control and other disease state cases in that age range, and showed a marked decline with increasing age. The decrease however brought the level of NR2B expression down to similar levels seen in the other cohorts and did not decrease beyond the other older age range levels. The higher NR2B expression seen in the AD cases could act as an early marker for the disease, showing an alteration in NR2B expression to be indicative of later AD progression. There is a limited correlation overall of NR2B expression to dementia and psychiatric scores in the tissues studied. A general trend for increased binding levels with decreasing MMSE and MTS score was seen in the Lewy Body and AD cases. The AD cases also showed a general increased binding level with decreasing UPDRS score. The psychotic symptom data in the study (delusion and visual hallucination data) did not show any significant differences between binding levels and score with the exception of the DLB outer insular cortex visual hallucination data. In selective brain regions of those studied, there were some gender differences seen in the control cohort. The control male cingulate cortex binding level significantly increased with age ($p=0.03$), and the control male claustrum binding level significantly decreased with age ($p=0.02$).

This study clearly demonstrates that CP-101,606 and Ro 25,6981 label distinct NMDA NR2B sub-type populations in the human brain, and that NR2B expression does not significantly decrease with age in the control and disease state cases used. Additional experiments are required to assess any further NR2B expression alterations that may exist in a wider age range than used here, and using a larger cohort.

Chapter 5

Overall discussion and future direction

The overall aim of this project was to carry out a comparative study of rodent and human brain in ageing and disease using novel NMDAR-2B selective probes. The rodent brain study covered the age range from postnatal day 21 (3 weeks) to adult (3 months). The human study covered control and pathological (DLB, PDD and AD) cases, across the age range 62 to 92 years. The study involved a variety of experimental techniques to analyse the abundance, distribution and temporal changes of both the NR2B subunit protein and NR2B containing receptor complexes. These included ligand autoradiography, radioligand binding and immunohistochemistry.

Previous studies have revealed the subtype selectivities and affinities of Ro 25,6981 and CP-101,606 for binding to recombinant mouse NR2B receptors as well as native NR2B rodent receptors (Chazot et al. 2002b; Menniti et al. 1997; Mutel et al, 1998). Previous evidence from the laboratory suggested that Ro 25,6981 and CP-101,606 label distinct populations of mouse NR2B-containing receptors (Chazot et al. 2002b). Therefore, the first part of this study involved ligand autoradiography of the adult mouse brain. [³H]Ro 25,6981 and [³H]CP-101,606 NR2B-selective ligands were used to map the distribution pattern of NR2B NMDA receptors and the difference between the binding levels of the two ligands in mouse brain sections. Both Ro 25,6981 and CP-101,606 showed high binding levels in the CA1, CA3 hippocampal subfields, granule layer of the dentate gyrus, entorhinal cortex and outer layers of the frontal cortex, with the

lowest binding levels seen in the thalamus, inner layers of the frontal cortex, pyramidal cell layer of the hippocampus and cerebellum. There were significantly higher levels of [³H]Ro 25,6981 binding in all the regions analysed, with the exception of the pyramidal cells, the frontal cortex inner layer and the cerebellum. The NR2B distribution and abundance shown by these results supports the published literature and provides further evidence for two distinct classes of NMDA-R2B antagonists, represented by Ro 25,6981 (all NR2B receptors) and CP-101,606 (NR1/NR2B subtype only) (Chazot et al. 2002b).

A HEK 293 clonal cell model system was employed to analyse the inhibition of [³H]CP-101,606 binding by Ro 25,6981 to NR1/NR2B receptors. Transfection of HEK 293 cells have been successfully used in previous studies, and were therefore chosen for this study (Chazot et al, 1999). Radioligand binding studies revealed displacement of [³H]CP-101,606 binding by Ro 25,6981, which demonstrates that CP-101,606 and Ro 25, 6981 can bind to overlapping binding sites on the NMDA receptor.

The main focus of this thesis was to study the native NR2B subtype receptor population in the rodent and human brain in two stages of ageing. Pharmacological characterisation of NR2B ligands binding to native receptors in 3-week old and adult 3-month rat forebrain membranes was performed using [³H]Ro 25,6981 and [³H]MK-801. Firstly, the stimulation of [³H]MK-801 by spermidine and histamine (NR2B positive modulators) was more pronounced in the P21 rat brain than the adult. This is consistent with the hypothesis that the level of NR2B expression is higher in P21 than the adult rat brain (Dumas 2005). The saturation binding data for [³H]Ro 25,6981 binding shows that there were 3-fold higher levels of NR2B-containing receptors in the P21 rat brain than the

adult, although the affinities were very similar, with K_D values at 9.5 and 11.9nM, respectively. The inhibition of [3 H]Ro 25,6981 binding by ifenprodil, haloperidol, Ro 25,6981 and CP-101,606 was analysed and revealed that each ligand bound to variable percentages of high- and low-affinity binding sites in P21 and adult rat forebrain membranes. The results provide further evidence for heterogeneity in NR2B subunit containing receptors, and that the composition of the receptor can affect the pharmacological properties, shown here by the differences in binding between the NR2B-selective ligands.

Having studied the pharmacological properties of the native NR2B-containing receptors in the rat brain membranes, the distribution pattern and abundance of these receptors was further studied in the rat brain for both P21 and adult age groups, using ligand autoradiography. Firstly, there were higher levels of [3 H]Ro 25,6981 binding in P21 rat brain tissue than in adult tissue, confirming again a higher expression of NR2B-containing NMDA receptors in the P21 tissue. The exceptions to this were seen in the CA3 SO, thalamus and striatum where binding levels were very similar between the two ages. In contrast, there were similar binding levels of [3 H]CP-101,606 in the P21 and adult rat brain sections with the exceptions being the CA1, outer regions of the frontal cortex and the striatum, which showed significantly higher binding levels of [3 H]CP-101,606 in the adult than in the P21 tissue. Therefore, these data show that Ro 25,6981 binding decreases with age, and CP-101,606 binding remains constant or in certain areas increases. No significant differences in binding levels of the two ligands were seen in the adult tissue, and interestingly, higher binding levels of Ro 25,6981 than CP-101, 606 were seen in the P21 tissue. Therefore, if the NR1/NR2B subunit subpopulation remains constant or is increasing with age (suggested by the CP-101,606 results) yet the overall NR2B-containing receptor population is

decreasing with age (suggested by the Ro 25,6981 results), then perhaps another NR2 subunit population is decreasing in compensation. This further supports the theory that these two ligands are labelling distinct populations of NR2B receptors. Furthermore, there is an age-dependant decline in overall NR2B subtypes between 3 weeks and 3 months of age in rats. Clear evidence for a switch in NR2B subtypes during the earlier period of ageing is presented in this thesis.

A preliminary immunohistochemical study was carried out using in-house produced and purified anti-NR2B receptor antibodies (Chazot et al, 1992). These were used as immunological probes to study the cellular distribution and abundance of native NR2B subunit protein in P21 and adult rat brain. This study builds on previous results using NMDAR subunit-specific antibodies in the rat brain (Thompson et al, 2002). Results showed that there was a greater expression of NR2B protein in the P21 rat brain than the adult, which agrees with the autoradiography results from this project. The main areas of NR2B expression labelling were the outer layers of the frontal and entorhinal cortex, thalamus, striatum and stratum oriens and radiatum of the CA1, CA2 and dentate gyrus of the hippocampal formation, again consistent with the ligand autoradiographical data.

Future studies to analyse rodent brain sections from a wider age range would build on existing data that suggest plastic changes in early adulthood. For instance, analysis of rodent brain from birth to 12 months in set time increments, would give a detailed overview of exactly how the expression of NR2B receptors are altering at each stage of development. This earlier period of ageing covers changes in NR2B expression possibly related to changes in synaptic plasticity and development.

The second part of this thesis investigated the NR2B receptor in the human brain, in both control and a range of common dementia cases over late adulthood (age 62-92). The NMDA receptor is implicated in normal neuronal development, normal ageing and neurological diseases where changes in learning and memory may occur (Piggott et al., 1994). Autoradiographical studies using [³H]Ro 25,6981 and [³H]CP-101,606 showed that NR2B-containing receptors were present in the striatum, claustrum, insular cortex, cingulate cortex, and internal and external globus pallidus. Contrary to our initial prediction, this study revealed a general overall preservation of NR2B-containing receptors in the control and disease state cases over age, which is distinct from the published rodent literature (Magnusson, 2000; Tamaru et al, 1991; Wenk et al, 1991; Kito et al, 1990) where a decline in NR2B expression with age, corresponding to a decline in cognitive ability with age has been reported. This indicates that there are functional NR2B-containing receptors present in various brain regions of normal and disease state aged cases, which could be used as therapeutic targets, to manage some of the symptoms associated with neurological degeneration. The study demonstrated that Ro 25,6981 and CP-101,606 label distinct NMDA NR2B subtype populations in the human brain (as seen in the mouse and rat), and that there is no significant decrease in NR2B receptor expression with age (in contrast to the rodent reports) in control, DLB and PDD cases used in this study. Interestingly, higher levels of NR1/NR2B containing receptors were seen in the earlier age cases of AD when compared to controls and other disease state cases. The reduction in binding levels with age however, reached similar levels seen in the other cohorts and did not decrease beyond the controls. The higher NR2B expression seen in the younger AD cases may act as an early marker for the disease, indicating that an alteration in NR2B expression to be indicative of later AD progression. The study also

showed a modest limited correlation between NR2B expression and dementia and psychiatric test scores, where binding level increased as scores decreased, indicating a higher NR2B expression correlating to less severe cognitive decline. In selective brain regions, there were some gender differences seen in the control cohort. The control male cingulate cortex binding level significantly increased with age ($p=0.03$), and the control male claustrum binding level significantly decreased with age ($p=0.02$). Notably, NR2B-containing receptors are significantly lower in control female cases than male counterparts, and all DLB cases. Further studies to assess the effects of age on NR2B receptor expression over a wider age range in control and disease state cases will prove extremely useful, in order to reveal if the trends seen in this data set are indeed a general principle. A larger cohort of control as well as disease state cases, especially those labelled with [^3H]CP-101,606 would provide a statistically larger and therefore more complete data set. Further research will involve autoradiographical analysis of PD cases, which can be compared to the present data for differences in receptor expression and dyskinesia symptom correlation. The overall preservation of NR2B receptors with increasing age opens up the possibility for potential changes in other NMDAR subtype populations. Other receptor subtypes may show an alteration in expression over age, and further autoradiographical studies would provide this information, painting a clearer picture of the changes which are occurring in the composition of the NMDA receptor, not only in normal ageing, but in the progression of pathological conditions.

In summary, the main findings from this research project were:

1. Reduction and changes in the overall NR2B subtype populations between 3 week-old and adult rat brain.

2. Ro 25,6981 and CP-101,606 label distinct NMDA NR2B subtype populations in the human brain (as seen in the mouse and rat), demonstrating that distinct ifenprodil-like compounds distinguish between NR2B subtype populations.
3. NR2B subtype preservation in human ageing and major human dementias, and limited correlation to MMSE scores in human dementias.
4. First evidence that the NR2B subtype plays no or only a limited role in neuronal loss and learning deficits in human dementias

This present study builds on the work from previous experiments which have provided a wealth of information. The research has enabled a greater understanding of the pharmacology of a variety of NR2B-selective ligands, and has shown clearly distinct binding properties of the Ro 25,6981 and CP-101,606 NR2B antagonists. The rodent brain analysis has confirmed previous findings in terms of brain regions showing NR2B expression, but has also provided further data on NR2B subtype population changes occurring during the early adult developmental period. This project presents the first data on the distribution and abundance of NR2B-containing receptors, labelled by Ro 25,6981 and CP-101,606, in aged human control and disease cases, and increases understanding not only of NMDAR changes occurring with normal ageing, but also those occurring in pathological states over age. This work in turn has provided a platform from which many future studies will arise, since there are many unanswered questions about the pharmacological properties of native NMDA receptors, and their composite alterations in a variety of developmental and pathological stages.

References

- Adams, I. and D. G. Jones (1982). "Quantitative ultrastructural changes in rat cortical synapses during early-, mid- and late-adulthood." Brain Res **239**(2): 349-63.
- Akbarian, S., Sucher N. J, Bradley, D., Tafazzoli, A., Trinh, D., Hetrick, W. P., Potkin, S. G., Sandman, C. A., Bunney, W.E.Jr., Jones, E.G. (1996). "Selective alterations in gene expression for NMDA receptor subunits in prefrontal cortex of schizophrenics." J Neurosci **16**(1): 19-30.
- Albensi, B. C., Igoechi, C., Janigro, D., Ilkanich, E. (2004a). "Why do many NMDA antagonists fail, while others are safe and effective at blocking excitotoxicity associated with dementia and acute injury?" Am J Alzheimers Dis Other Demen **19**(5): 269-74.
- Albensi, B. C. and E. Ilkanich (2004b). "Open-channel blockers of the NMDA receptor complex." Drug News Perspect **17**(9): 557-62.
- Andersen, P., Eccles J. C., Loynning, Y. (1963). "Recurrent inhibition in the hippocampus with identification of the inhibitory cell and its synapses." Nature **198**: 540-2.
- Anis, N. A., Berry S. C., Burton, N.R., Lodge, D. (1983). "The dissociative anaesthetics, ketamine and phencyclidine, selectively reduce excitation of central mammalian neurones by N-methyl-aspartate." Br J Pharmacol **79**(2): 565-75.
- Babb, T., Mikuni, N., Najm, I., Wylie, C., Olive, M., Dollar, C., MacLennan, H. (2005). 'Pre- and postnatal expressions of NMDA receptors 1 and 2B subunit proteins in the normal rat cortex.' Epilepsy Research **64**: 23-30.
- Bai, L., Hof, P.R., Standaert, D.G., Xing, Y., Nelson, S.E., Young, A.B., Magnusson, K.R. (2004). "Changes in the expression of the NR2B subunit during aging in macaque monkeys." Neurobiol Aging **25**(2): 201-8.

- Barber, R., Panikkar, A., McKeith, I.G. (2001). "Dementia with Lewy bodies: diagnosis and management." Int J Geriatr Psychiatry **16 Suppl 1**: S12-8.
- Barnes, C. A. (1979). "Memory deficits associated with senescence: a neurophysiological and behavioral study in the rat." J Comp Physiol Psychol **93**(1): 74-104.
- Behe, P., Stern, P., Wyllie, D.J., Nassar, M., Schoepfer, R., Colquhoun, D. (1995). "Determination of NMDA NR1 subunit copy number in recombinant NMDA receptors." Proc Biol Sci **262**(1364): 205-13.
- Bennett, M. R. (2000). "The concept of long term potentiation of transmission at synapses." Prog Neurobiol **60**(2): 109-37.
- Benveniste, M. and M. L. Mayer (1991). "Kinetic analysis of antagonist action at N-methyl-D-aspartic acid receptors. Two binding sites each for glutamate and glycine." Biophys J **59**(3): 560-73.
- Bi, H. and C. I. Sze (2002). "N-methyl-D-aspartate receptor subunit NR2A and NR2B messenger RNA levels are altered in the hippocampus and entorhinal cortex in Alzheimer's disease." J Neurol Sci **200**(1-2): 11-8.
- Blahos, J., 2nd and R. J. Wenthold (1996). "Relationship between N-methyl-D-aspartate receptor NR1 splice variants and NR2 subunits." J Biol Chem **271**(26): 15669-74.
- Blanchet, P. J., Konitsiotis, S., Whittemore, E.R., Zhou, Z.L., Woodward, R.M., Chase, T.N. (1999). "Differing effects of N-methyl-D-aspartate receptor subtype selective antagonists on dyskinesias in levodopa-treated 1-methyl-4-phenyl-tetrahydropyridine monkeys." J Pharmacol Exp Ther **290**(3): 1034-40.
- Bliss, T. V. and A. R. Gardner-Medwin (1973). "Long-lasting potentiation of synaptic transmission in the dentate area of the unanaesthetized rabbit following stimulation of the perforant path." J Physiol **232**(2): 357-74.

- Bliss, T. V. and T. Lomo (1973). "Long-lasting potentiation of synaptic transmission in the dentate area of the anaesthetized rabbit following stimulation of the perforant path." J Physiol **232**(2): 331-56.
- Bliss, T. V. P. and M. A. Lynch (1988). "Long-term potentiation of synaptic transmission in the hippocampus: properties and mechanisms." Long-term potentiation: From Biophysics to Behaviour: 3-72.
- Braak, H. and E. Braak (1998). "Evolution of neuronal changes in the course of Alzheimer's disease." J Neural Transm Suppl **53**: 127-40.
- Brickley, S. G., Misra, C., Mok, M.H., Mishina, M., Cull-Candy, S.G. (2003). "NR2B and NR2D subunits coassemble in cerebellar Golgi cells to form a distinct NMDA receptor subtype restricted to extrasynaptic sites." J Neurosci **23**(12): 4958-66.
- Brimecombe, J. C., Boeckman, F.A., Aizenman, E. (1997). "Functional consequences of NR2 subunit composition in single recombinant N-methyl-D-aspartate receptors." Proc Natl Acad Sci U S A **94**(20): 11019-24.
- Brody, H. (1955). "Organization of the cerebral cortex. III. A study of aging in the human cerebral cortex." J Comp Neurol **102**(2): 511-6.
- Brody, H. (1980). "The nervous system and aging." Adv Pathobiol **7**: 200-9.
- Brose, N., Gasic, G.P., Vetter, D.E., Sullivan, J.M., Heinemann, S.F. (1993). "Protein chemical characterization and immunocytochemical localization of the NMDA receptor subunit NMDA R1." J Biol Chem **268**(30): 22663-71.
- Calabresi, P., Mercuri, N.B., Sancesario, G., Bernardi, G. (1993). "Electrophysiology of dopamine-denervated striatal neurons. Implications for Parkinson's disease." Brain **116** (Pt 2): 433-52.

- Calon, F., Rajput, A.H., Hornykiewicz, O., Bedard, P.J., Di Paolo, T. (2003). "Levodopa-induced motor complications are associated with alterations of glutamate receptors in Parkinson's disease." Neurobiol Dis **14**(3): 404-16.
- Carpenter, M. K., Parker, I., Miledi, R. (1992). "Messenger RNAs coding for receptors and channels in the cerebral cortex of adult and aged rats." Brain Res Mol Brain Res **13**(1-2): 1-5.
- Carter, C., Benavides, J., Legendre, P., Vincent, J.D., Noel, F., Thuret, F., Lloyd, K.G., Arbilla, S., Zivkovic, B., Mackenzie, E.T., et al. (1988). "Ifenprodil and SL 82.0715 as cerebral anti-ischemic agents. II. Evidence for N-methyl-D-aspartate receptor antagonist properties." J Pharmacol Exp Ther **247**(3): 1222-32.
- Castellano, C., Cestari, V., Ciamei, A. (2001). "NMDA receptors and learning and memory processes." Curr Drug Targets **2**(3): 273-83.
- Chazot, P. L., Cik, M., Stephenson, F.A. (1992). "Immunological detection of the NMDAR1 glutamate receptor subunit expressed in embryonic kidney 293 cells and in rat brain." J Neurochem **59**(3): 1176-8.
- Chazot, P. L., Fotherby, A., Stephenson, F.A. (1993). "Evidence for the involvement of a carboxyl group in the vicinity of the MK801 and magnesium ion binding site of the N-methyl-D-aspartate receptor." Biochem Pharmacol **45**(3): 605-10.
- Chazot, P. L., Coleman, S.K., Cik, M., Stephenson, F.A. (1994). "Molecular characterization of N-methyl-D-aspartate receptors expressed in mammalian cells yields evidence for the coexistence of three subunit types within a discrete receptor molecule." J Biol Chem **269**(39): 24403-9.
- Chazot, P. L. and F. A. Stephenson (1997a). "Biochemical evidence for the existence of a pool of unassembled C2 exon-containing NR1 subunits of the mammalian forebrain NMDA receptor." J Neurochem **68**(2): 507-16.

- Chazot, P. L. and F. A. Stephenson (1997b). "Molecular dissection of native mammalian forebrain NMDA receptors containing the NR1 C2 exon: direct demonstration of NMDA receptors comprising NR1, NR2A, and NR2B subunits within the same complex." J Neurochem **69**(5): 2138-44.
- Chazot, P. L., Cik, M., Stephenson, F.A. (1999). "Transient expression of functional NMDA receptors in mammalian cells." Methods Mol Biol **128**: 33-42.
- Chazot, P. L. (2000). "CP-101606 Pfizer Inc." Curr Opin Investig Drugs **1**(3): 370-4.
- Chazot, P. L., Lawrence, S., Thompson, C.L. (2002a). "Studies on the subtype selectivity of CP-101,606: evidence for two classes of NR2B-selective NMDA receptor antagonists." Neuropharmacology **42**(3): 319-24.
- Chazot, P. L., Godukhin, O.V., McDonald, A., Obrenovitch, T.P. (2002b). "Spreading depression-induced preconditioning in the mouse cortex: differential changes in the protein expression of ionotropic nicotinic acetylcholine and glutamate receptors." J Neurochem **83**(5): 1235-8.
- Chazot, P. (2003). "British Neuroscience Association--17th National Meeting: 13-16 April 2003, Harrogate, UK." IDrugs **6**(6): 536-8.
- Chazot, P. L. (2004). "The NMDA receptor NR2B subunit: a valid therapeutic target for multiple CNS pathologies." Curr Med Chem **11**(3): 389-96.
- Chenard, B. L. and F. S. Menniti (1999). "Antagonists selective for NMDA receptors containing the NR2B subunit." Curr Pharm Des **5**(5): 381-404.
- Cheng, Y. and W. H. Prusoff (1973). "Relationship between the inhibition constant (K₁) and the concentration of inhibitor which causes 50 per cent inhibition (I₅₀) of an enzymatic reaction." Biochem Pharmacol **22**(23): 3099-108.

- Ciabarra, A. M., Sullivan, J.M., Gahn, L.G., Pecht, G., Heinemann, S., Sevarino, K.A. (1995). "Cloning and characterization of chi-1: a developmentally regulated member of a novel class of the ionotropic glutamate receptor family." J Neurosci **15**(10): 6498-508.
- Clark, A. S., Magnusson, K.R., Cotman, C.W. (1992). "In vitro autoradiography of hippocampal excitatory amino acid binding in aged Fischer 344 rats: relationship to performance on the Morris water maze." Behav Neurosci **106**(2): 324-35.
- Clayton, D. A. and M. D. Browning (2001). "Deficits in the expression of the NR2B subunit in the hippocampus of aged Fisher 344 rats." Neurobiol Aging **22**(1): 165-8.
- Clayton, D. A., Mesches, M.H., Alvarez, E., Bickford, P.C., Browning, M.D. (2002). "A hippocampal NR2B deficit can mimic age-related changes in long-term potentiation and spatial learning in the Fischer 344 rat." J Neurosci **22**(9): 3628-37.
- Clements, J. D. and G. L. Westbrook (1991). "Activation kinetics reveal the number of glutamate and glycine binding sites on the N-methyl-D-aspartate receptor." Neuron **7**(4): 605-13.
- Clinton, S. M. and J. H. Meador-Woodruff (2004). "Abnormalities of the NMDA Receptor and Associated Intracellular Molecules in the Thalamus in Schizophrenia and Bipolar Disorder." Neuropsychopharmacology **29**(7): 1353-62.
- Collingridge, G. L., Kehl, S.J., McLennan, H. (1983). "Excitatory amino acids in synaptic transmission in the Schaffer collateral-commissural pathway of the rat hippocampus." J Physiol **334**: 33-46.
- Coughenour, L. L. and B. M. Barr (2001). "Use of trifluoroperazine isolates a [(3)H]ifenprodil binding site in rat brain membranes with the pharmacology of the voltage-independent ifenprodil site on N-methyl-D-aspartate receptors containing NR2B subunits." J Pharmacol Exp Ther **296**(1): 150-9.

- Crick, F. C. and C. Koch (2005). "What is the function of the claustrum?" Philos Trans R Soc Lond B Biol Sci **360**(1458): 1271-9.
- Cull-Candy, S. G., Brickley, S.G., Misra, C., Feldmeyer, D., Momiyama, A., Farrant, M. (1998). "NMDA receptor diversity in the cerebellum: identification of subunits contributing to functional receptors." Neuropharmacology **37**(10-11): 1369-80.
- Cull-Candy, S., Brickley, S., Farrant, M. (2001). "NMDA receptor subunits: diversity, development and disease." Curr Opin Neurobiol **11**(3): 327-35.
- Curtis, D. R., Phillis, J.W., Watkins, J.C. (1959). "Chemical excitation of spinal neurones." Nature **183**(4661): 611-2.
- Dagert, M. and S. D. Ehrlich (1979). "Prolonged incubation in calcium chloride improves the competence of Escherichia coli cells." Gene **6**(1): 23-8.
- Danysz, W. and C. G. Parsons (2003). "The NMDA receptor antagonist memantine as a symptomatological and neuroprotective treatment for Alzheimer's disease: preclinical evidence." Int J Geriatr Psychiatry **18**(Suppl 1): S23-32.
- Das, S., Sasaki, Y.F., Rothe, T., Premkumar, L.S., Takasu, M., Crandall, S.E., Dikkes, P., Conner, D.A., Rayudu, P.V., Cheung, W., Chen, H.S., Lipton, S.A., Nakanishi, N. (1998). "Increased NMDA current and spine density in mice lacking the NMDA receptor subunit NR3A." Nature **393**(6683): 377-81.
- Davies, J., Francis, A., Jones, A.W., Watkins, J.C. (1981). "2-Amino-5-phosphonovalerate (2APV), a potent and selective antagonist of amino acid-induced and synaptic excitation." Neurosci Lett **21**(1): 77-81.
- Dekaban, A. S. (1978). "Changes in brain weights during the span of human life: relation of brain weights to body heights and body weights." Ann Neurol **4**(4): 345-56.

- DeLong, M. R. (1990). "Primate models of movement disorders of basal ganglia origin." Trends Neurosci **13**(7): 281-5.
- Dickey, C. A., Loring, J.F., Montgomery, J., Gordan, M., Eastman, P., Morgan, D. (2003). "Selectively reduced expression of synaptic plasticity-related genes in amyloid precursor protein + presenilin-1 transgenic mice." J Neurosci **23**(12): 5219-26.
- Dingledine, R. (1983). "N-methyl aspartate activates voltage-dependent calcium conductance in rat hippocampal pyramidal cells." J Physiol **343**: 385-405.
- Dingledine, R., Borges, K., Bowie, D., Traynelis, S. (1999). "The glutamate receptor ion channels." Pharmacol Rev **51**(1): 7-61.
- Dolphin, A. C. (1982). "Neuronal Plasticity and Memory Formation." International Brain Research Organisation. TINS **9**.
- Douglas, R. M. and G. V. Goddard (1975). "Long-term potentiation of the perforant path-granule cell synapse in the rat hippocampus." Brain Res **86**(2): 205-15.
- Duffy, C., Teyler, T., Shashoua, V. (1981). "Long-term potentiation in the hippocampal slice: evidence for stimulated secretion of newly synthesized proteins." Science **212**(4499): 1148-51.
- Duggan, M. J., Pollard, S., Stephenson, F.A. (1991). "Immunoaffinity purification of GABAA receptor alpha-subunit iso-oligomers. Demonstration of receptor populations containing alpha 1 alpha 2, alpha 1 alpha 3, and alpha 2 alpha 3 subunit pairs." J Biol Chem **266**(36): 24778-84.
- Duggan, M. J. and F. A. Stephenson (1989). "Bovine gamma-aminobutyric acidA receptor sequence-specific antibodies: identification of two epitopes which are recognised in both native and denatured gamma-aminobutyric acidA receptors." J Neurochem **53**(1): 132-9.

- Dumas, T. C. (2005). "Developmental regulation of cognitive abilities: modified composition of a molecular switch turns on associative learning." Prog Neurobiol **76**(3): 189-211.
- Dunah, A. W., Luo, J., Wang, Y., Yasuda, R., Wolfe, B. (1998). "Subunit composition of N-methyl-D-aspartate receptors in the central nervous system that contain the NR2D subunit." Mol Pharmacol **53**(3): 429-37.
- Durand, G. M., Gregor, P., Zheng, X., Bennett, M., Uhl, G., Zukin, R. (1992). "Cloning of an apparent splice variant of the rat N-methyl-D-aspartate receptor NMDAR1 with altered sensitivity to polyamines and activators of protein kinase C." Proc Natl Acad Sci U S A **89**(19): 9359-63.
- Ebraldize, A. K., Rossi, D., Tonegawa, S., Slater, N. (1996). "Modification of NMDA receptor channels and synaptic transmission by targeted disruption of the NR2C gene." J Neurosci **16**(16): 5014-25.
- Fifkova, E. and A. Van Harreveld (1977). "Long-lasting morphological changes in dendritic spines of dentate granular cells following stimulation of the entorhinal area." J Neurocytol **6**(2): 211-30.
- Finkel, D., Reynolds, C., Berg, S., Pedersen, N. (2006). "Surprising lack of sex differences in normal cognitive aging in twins." Int J Aging Hum Dev **62**(4): 335-57.
- Fischer, G., Mutel, V., Trube, G., Malherbe, P., Kew, J., Mohacsi, E., Heitz, M., Kemp, J. (1997). "Ro 25-6981, a highly potent and selective blocker of N-methyl-D-aspartate receptors containing the NR2B subunit. Characterization in vitro." J Pharmacol Exp Ther **283**(3): 1285-92.
- Folstein, M. F., Folstein, S., McHugh, P. (1975). "'Mini-mental state'. A practical method for grading the cognitive state of patients for the clinician." J Psychiatr Res **12**(3): 189-98.

- Forrest, D., Yuzaki, M., Soares, H., Ng, L., Luk, D., Sheng, M., Stewart, C., Morgan, J., Conner, J., Curran, T. (1994). "Targeted disruption of NMDA receptor 1 gene abolishes NMDA response and results in neonatal death." Neuron **13**(2): 325-38.
- Fujisawa, S. and C. Aoki (2003). "In vivo blockade of N-methyl-D-aspartate receptors induces rapid trafficking of NR2B subunits away from synapses and out of spines and terminals in adult cortex." Neuroscience **121**(1): 51-63.
- Gallagher, M. J., Huang, H., Lynch, D. (1998). "Modulation of the N-methyl-D-aspartate receptor by haloperidol: NR2B-specific interactions." J Neurochem **70**(5): 2120-8.
- Gardoni, F., Picconi, B., Ghiglieri, V., Polli, F., Bagetta, V., Bernardi, G., Cattabeni, F., Di Luca, M., Calabresi, P. (2006). "A critical interaction between NR2B and MAGUK in L-DOPA induced dyskinesia." J Neurosci **26**(11): 2914-22.
- Gelb, A. W. (1999). "Mechanisms of brain injury and potential therapies." Acta Anaesthesiol Belg **50**(4): 193-7.
- Goebel, D. J. and M. S. Poosch (1999). "NMDA receptor subunit gene expression in the rat brain: a quantitative analysis of endogenous mRNA levels of NR1Com, NR2A, NR2B, NR2C, NR2D and NR3A." Brain Res Mol Brain Res **69**(2): 164-70.
- Gorman, C. M., Gies, D., McCray, G. (1990). "Transient Production of Proteins using an adenovirus Transformed Cell Line." DNA Protein Eng Technol **52**: 470-478.
- Grimwood, S., Slater, P., Deakin, J., Hutson, P. (1999). "NR2B-containing NMDA receptors are up-regulated in temporal cortex in schizophrenia." Neuroreport **10**(3): 461-5.
- Grimwood, S., Richards, P., Murray, F., Harrison, N., Wingrove, P., Hutson, P. (2000). "Characterisation of N-methyl-D-aspartate receptor-specific [(3)H]Ifenprodil binding to recombinant human NR1a/NR2B receptors compared with native receptors in rodent brain membranes." J Neurochem **75**(6): 2455-63.

- Guttman, C. R., Jolesz, F., Kikinis, R., Killiany, R., Moss, M., Sandor, T., Albert, M. (1998). "White matter changes with normal aging." Neurology **50**(4): 972-8.
- Hallett, P. J. and D. G. Standaert (2004). "Rationale for and use of NMDA receptor antagonists in Parkinson's disease." Pharmacol Ther **102**(2): 155-74.
- Harris, E. W., Ganong, A., Cotman, C. (1984). "Long-term potentiation in the hippocampus involves activation of N-methyl-D-aspartate receptors." Brain Res **323**(1): 132-7.
- Hashimoto, A., Nishikawa, T., Oka, T., Takahashi, K. (1993). "Endogenous D-serine in rat brain: N-methyl-D-aspartate receptor-related distribution and aging." Journal of Neurochemistry **60**(2): 783-6.
- Haug, H., Barmwater, U., Eggers, R., Fischer, D., Kuhel, S., Sass, N. (1983). "Anatomical changes in aging brain: morphometric analysis of the human presencephalon." Cervos-Navarro J, Sarkander H.I. Aging. New York: 1-12.
- Haug, H. and R. Eggers (1991). "Morphometry of the human cortex cerebri and corpus striatum during aging." Neurobiol Aging **12**(4): 336-8; discussion 352-5.
- Hawkins, L. M., Chazot, P.L., Stephenson, F.A. (1999). "Biochemical evidence for the co-association of three N-methyl-D-aspartate (NMDA) R2 subunits in recombinant NMDA receptors." J Biol Chem **274**(38): 27211-8.
- Hebb, D. O. (1949). "The Organization of Behaviour." Wiley, New York.
- Higgins, G. A., Ballard, T., Enderlin, M., Haman, M., Kemp, J. (2005). "Evidence for improved performance in cognitive tasks following selective NR2B NMDA receptor antagonist pre-treatment in the rat." Psychopharmacology (Berl) **179**(1): 85-98.

- Hirai, H., Kirsch, J., Laube, B., Betz, H., Kuhse, J. (1996). "The glycine binding site of the N-methyl-D-aspartate receptor subunit NR1: identification of novel determinants of co-agonist potentiation in the extracellular M3-M4 loop region." Proc Natl Acad Sci U S A **93**(12): 6031-6.
- Hollmann, M. and S. Heinemann (1994). "Cloned glutamate receptors." Annu Rev Neurosci **17**: 31-108.
- Hoyer, S. and C. Krier (1986). "Ischemia and aging brain. Studies on glucose and energy metabolism in rat cerebral cortex." Neurobiol Aging **7**(1): 23-9.
- Hrabetova, S., Serrano, P., Blace, N., Tse, H., Skifter, D., Jane, D., Monaghan, D., Sacktor, T. (2000). "Distinct NMDA receptor subpopulations contribute to long-term potentiation and long-term depression induction." J Neurosci **20**(12): RC81.
- Huttenlocher, P. R. (1979). "Synaptic density in human frontal cortex - developmental changes and effects of aging." Brain Res **163**(2): 195-205.
- Hynd, M. R., Scott, H., Dodd, P. (2004). "Differential expression of N-methyl-D-aspartate receptor NR2 isoforms in Alzheimer's disease." J Neurochem **90**(4): 913-9.
- Ikeda, K., Nagasawa, M., Mori, H., Araki, K., Sakimura, K., Watanabe, M., Inoue, Y., Mishina, M. (1992). "Cloning and expression of the epsilon 4 subunit of the NMDA receptor channel." FEBS Lett **313**(1): 34-8.
- Jacobs, B. and A. B. Scheibel (1993). "A quantitative dendritic analysis of Wernicke's area in humans. I. Lifespan changes." J Comp Neurol **327**(1): 83-96.
- Janssen, W. G., Vissavajhala, P., Andrews, G., Moran, T., Hof, P., Morrison, J. (2005). "Cellular and synaptic distribution of NR2A and NR2B in macaque monkey and rat hippocampus as visualized with subunit-specific monoclonal antibodies." Exp Neurol **191 Suppl 1**: S28-44.

- Jarrard, L. E. (1978). "Selective hippocampal lesions: differential effects on performance by rats of a spatial task with preoperative versus postoperative training." J Comp Physiol Psychol **92**(6): 1119-27.
- Johnson, J. W. and P. Ascher (1987). "Glycine potentiates the NMDA response in cultured mouse brain neurons." Nature **325**(6104): 529-31.
- Kandel, E. R., Spencer, W., Brinley, F. Jr. (1961). "Electrophysiology of hippocampal neurons. I. Sequential invasion and synaptic organization." J Neurophysiol **24**: 225-42.
- Kew, J. N. and J. A. Kemp (2005). "Ionotropic and metabotropic glutamate receptor structure and pharmacology." Psychopharmacology (Berl).
- Kito, S., Miyoshi, R., Nomato, T. (1990). "Influence of age on NMDA receptor complex in rat brain studied by in vitro autoradiography." J Histochem Cytochem **38**(12): 1725-31.
- Kleckner, N. W. and R. Dingledine (1988). "Requirement for glycine in activation of NMDA-receptors expressed in *Xenopus* oocytes." Science **241**(4867): 835-7.
- Krebs, C., Fernandes, H., Sheldon, C., Raymond, L., Baimbridge, K. (2003). "Functional NMDA receptor subtype 2B is expressed in astrocytes after ischemia in vivo and anoxia in vitro." J Neurosci **23**(8): 3364-72.
- Kuehl-Kovarik, M. C., Partin, K., Magnusson, K. (2003). "Acute dissociation for analyses of NMDA receptor function in cortical neurons during aging." J Neurosci Methods **129**(1): 11-7.
- Kuryatov, A., Laube, B., Betz, H., Kuhse, J. (1994). "Mutational analysis of the glycine-binding site of the NMDA receptor: structural similarity with bacterial amino acid-binding proteins." Neuron **12**(6): 1291-300.

- Kutsuwada, T., Kashiwabuchi, N., Mori, H., Sakimura, K., Kushiya, E., Araki, K., Meguso, H., Masaki, H., Kumanishi, T., Arakawa, M. (1992). "Molecular diversity of the NMDA receptor channel." Nature **358**(6381): 36-41.
- Kutsuwada, T., Sakimura, K., Manabe, T., Takayama, C., Katakura, N., Kushiya, E., Natsume, R., Watanabe, M., Inoue, Y., Yagi, T., et al. (1996). "Impairment of suckling response, trigeminal neuronal pattern formation, and hippocampal LTD in NMDA receptor epsilon 2 subunit mutant mice." Neuron **16**(2): 333-44.
- Lange, K. W., Kornhuber, J., Riederer, P. (1997). "Dopamine/glutamate interactions in Parkinson's disease." Neurosci Biobehav Rev **21**(4): 393-400.
- Lau, W. K., Lui, P., Wong, C., Chan, Y., Yung, K. (2003). "Differential expression of N-methyl-D-aspartate receptor subunit messenger ribonucleic acids and immunoreactivity in the rat neostriatum during postnatal development." Neurochem Int **43**(1): 47-65.
- Laube, B., Kuhse, J., Betz, H. (1998). "Evidence for a tetrameric structure of recombinant NMDA receptors." J Neurosci **18**(8): 2954-61.
- Laurie, D. J., Bartke, I., Schoepfer, R., Naujoks, K., Seeburg, P. (1997). "Regional, developmental and interspecies expression of the four NMDAR2 subunits, examined using monoclonal antibodies." Brain Res Mol Brain Res **51**(1-2): 23-32.
- Laurie, D. J. and P. H. Seeburg (1994a). "Regional and developmental heterogeneity in splicing of the rat brain NMDAR1 mRNA." J Neurosci **14**(5 Pt 2): 3180-94.
- Laurie, D. J. and P. H. Seeburg (1994b). "Ligand affinities at recombinant N-methyl-D-aspartate receptors depend on subunit composition." Eur J Pharmacol **268**(3): 335-45.

- Law, A. J., Weickert, C., Webster, M., Herman, M., Kleinman, J., Harrison, P. (2003). "Expression of NMDA receptor NR1, NR2A and NR2B subunit mRNAs during development of the human hippocampal formation." Eur J Neurosci **18**(5): 1197-205.
- Lee, J. and N. Rajakumar (2003). "Role of NR2B-containing N-methyl-D-aspartate receptors in haloperidol-induced c-Fos expression in the striatum and nucleus accumbens." Neuroscience **122**(3): 739-45.
- Li, Y., Erzurumlu, R., Chen, C., Jhaveri, S., Tonegawa, S. (1994). "Whisker-related neuronal patterns fail to develop in the trigeminal brainstem nuclei of NMDAR1 knockout mice." Cell **76**(3): 427-37.
- Linden, D. J. and J. A. Connor (1993). "Cellular mechanisms of long-term depression in the cerebellum." Curr Opin Neurobiol **3**(3): 401-6.
- Linden, D. J., Dickinson, M., Smeyne, M., Connor J. (1991). "A long-term depression of AMPA currents in cultured cerebellar Purkinje neurons." Neuron **7**(1): 81-9.
- Liu, L., Wong, T., Pozza, M., Lingenhoehl, K., Wang, Y., Sheng, M., Auberson, Y., Wang, Y. (2004a). "Role of NMDA receptor subtypes in governing the direction of hippocampal synaptic plasticity." Science **304**(5673): 1021-4.
- Liu, X. B., Murray, K., Jones, E. (2004b). "Switching of NMDA receptor 2A and 2B subunits at thalamic and cortical synapses during early postnatal development." J Neurosci **24**(40): 8885-95.
- Loftis, J. M. and A. Janowsky (2003). "The N-methyl-D-aspartate receptor subunit NR2B: localization, functional properties, regulation, and clinical implications." Pharmacol Ther **97**(1): 55-85.
- Lomo, T. (1966). "Frequency potentiation of excitatory synaptic activity in the dentate area of the hippocampal formation." Acta Physiol Scand **68** (suppl. 277): 128.

- Loschmann, P. A., De Groote, C., Smith, L., Wullner, U., Fischer, G., Kemp, J., Jenner, P., Klockgether, T. (2004). "Antiparkinsonian activity of Ro 25-6981, a NR2B subunit specific NMDA receptor antagonist, in animal models of Parkinson's disease." Exp Neurol **187**(1): 86-93.
- Lowry, O. H., Rosebrough, N., Farr, A., Randall, R. (1951). "Protein measurement with the Folin phenol reagent." J Biol Chem **193**(1): 265-75.
- Lowy, M. T., Wittenberg, L., Yamamoto, B. (1995). "Effect of acute stress on hippocampal glutamate levels and spectrin proteolysis in young and aged rats." J Neurochem **65**(1): 268-74.
- Lu, J., Goula, D., Sousa, N., Almeida, O. (2003). "Ionotropic and metabotropic glutamate receptor mediation of glucocorticoid-induced apoptosis in hippocampal cells and the neuroprotective role of synaptic N-methyl-D-aspartate receptors." Neuroscience **121**(1): 123-31.
- Luo, J., Wang, Y., Yasuda, R., Dunah, A., Wolfe, B. (1997). "The majority of N-methyl-D-aspartate receptor complexes in adult rat cerebral cortex contain at least three different subunits (NR1/NR2A/NR2B)." Mol Pharmacol **51**(1): 79-86.
- Lynch, D. R., Shim, S., Siefert, K., Kuraparthi, S., Mutel, V., Gallagher, M., Guttmann, R. (2001). "Pharmacological characterization of interactions of RO 25-6981 with the NR2B (epsilon2) subunit." Eur J Pharmacol **416**(3): 185-95.
- Lynch, G., Halpain, S., Baudry, M. (1982). "Effects of high-frequency synaptic stimulation on glutamate receptor binding studied with a modified in vitro hippocampal slice preparation." Brain Res **244**(1): 101-11.
- Lynch, G., Larson, J., Kelso, S., Barrionuevo, G., Schottler, F. (1983). "Intracellular injections of EGTA block induction of hippocampal long-term potentiation." Nature **305**(5936): 719-21.

- MacKinnon, R. (1995). "Pore loops: an emerging theme in ion channel structure." Neuron **14**(5): 889-92.
- Madden, D. R. (2002a). "The structure and function of glutamate receptor ion channels." Nat Rev Neurosci **3**(2): 91-101.
- Madden, K. (2002). "NMDA receptor antagonists and glycine site NMDA antagonists." Curr Med Res Opin **18** Suppl 2: s27-31.
- Magnusson, K. R. and C. W. Cotman (1993a). "Age-related changes in excitatory amino acid receptors in two mouse strains." Neurobiol Aging **14**(3): 197-206.
- Magnusson, K. R. and C. W. Cotman (1993). "Effects of aging on NMDA and MK801 binding sites in mice." Brain Res **604**(1-2): 334-7.
- Magnusson, K. R. (1998). "Aging of glutamate receptors: correlations between binding and spatial memory performance in mice." Mech Ageing Dev **104**(3): 227-48.
- Magnusson, K. R. (2000). "Declines in mRNA expression of different subunits may account for differential effects of aging on agonist and antagonist binding to the NMDA receptor." J Neurosci **20**(5): 1666-74.
- Magnusson, K. R., Nelson, S., Young, A. (2002). "Age-related changes in the protein expression of subunits of the NMDA receptor." Brain Res Mol Brain Res **99**(1): 40-5.
- Magnusson, K. R., Kresge, D., Supon, J. (2006). "Differential effects of aging on NMDA receptors in the intermediate versus the dorsal hippocampus." Neurobiol Aging **27**(2): 324-33.
- Mai, J. K., Assheuer, J., Paxinos, G. (1997). "Atlas of the Human Brain." San Diego and London.
- Malenka, R. C. (1993). "Long-term depression: not so depressing after all." Proc Natl Acad Sci U S A **90**(8): 3121-3.

- Malenka, R. C. and R. A. Nicoll (1993). "NMDA-receptor-dependent synaptic plasticity: multiple forms and mechanisms." Trends Neurosci **16**(12): 521-7.
- Masliah, E. (1998). "Mechanisms of synaptic pathology in Alzheimer's disease." J Neural Transm Suppl **53**: 147-58.
- Massey, P. V., Johnson, B., Moulton, P., Auberson, Y., Brown, M., Molnar, E., Collingridge, G., Bashir, Z. (2004). "Differential roles of NR2A and NR2B-containing NMDA receptors in cortical long-term potentiation and long-term depression." J Neurosci **24**(36): 7821-8.
- Matsumae, M., Kikinis, R., Morocz, I., Lorenzo, A., Sandor, T., Albert, M., Black, P., Jolesz, F. (1996). "Age-related changes in intracranial compartment volumes in normal adults assessed by magnetic resonance imaging." J Neurosurg **84**(6): 982-91.
- Mayer, M. L., Westbrook, G., Guthrie, P. (1984). "Voltage-dependent block by Mg²⁺ of NMDA responses in spinal cord neurones." Nature **309**(5965): 261-3.
- McBain, C. J. and M. L. Mayer (1994). "N-methyl-D-aspartic acid receptor structure and function." Physiol Rev **74**(3): 723-60.
- McKeith, I. G., Galasko, D., Kosaka, K., Perry, E., Dickson, D., Hansen, L., Salmon, D., Lowe, J., Mirra, S., Byrne, E., Lennox, G., Quinn, N, et al. (1996). "Consensus guidelines for the clinical and pathologic diagnosis of dementia with Lewy bodies (DLB): report of the consortium on DLB international workshop." Neurology **47**(5): 1113-24.
- McKeith, I. G. (2002). "Dementia with Lewy bodies." Br J Psychiatry **180**: 144-7.
- McKeith, I. G., Burn, D., Ballard, C., Collerton, D., Jaros, E., Morris, C., McLaren, A., Perry, E., Perry, R., Piggott, M., O'Brien, J. (2003). "Dementia with Lewy bodies." Semin Clin Neuropsychiatry **8**(1): 46-57.

- McNaughton, B. L., Douglas, R., Goddard, G. (1978). "Synaptic enhancement in fascia dentata: cooperativity among coactive afferents." Brain Res **157**(2): 277-93.
- McNaughton, B. L., Barnes, C., Meltzer, J., Sutherland, R. (1989). "Hippocampal granule cells are necessary for normal spatial learning but not for spatially-selective pyramidal cell discharge." Exp Brain Res **76**(3): 485-96.
- Meier-Ruge, W., Hunziker, O., Iwangoff, P., Reichlmleiter, K., Sandoz, P. (1978). "Alteration of Morphological and neurochemical parameters of the brain due to normal aging." Senile dementia: Biochemical Approach. New York: 33-44.
- Menniti, F., Chenard, B., Collins, M., Ducat, M., Shalaby, I., White, F. (1997). "CP-101,606, a potent neuroprotectant selective for forebrain neurons." Eur J Pharmacol **331**(2-3): 117-26.
- Menniti, F., S., Shah, A., Williams, S., Wilner, K., Frostwhite, W., Chenard, B. (1998). "CP-101,606: An NR2B-Selective NMDA Receptor Antagonist." CNS Drug Reviews **4**(4): 307-322.
- Meoni, P., Bunnemann, B., Kingsbury, A., Trist, D., Bowery, N. (1999). "NMDA NR1 subunit mRNA and glutamate NMDA-sensitive binding are differentially affected in the striatum and pre-frontal cortex of Parkinson's disease patients." Neuropharmacology **38**(5): 625-33.
- Mesches, M. H., Gemma, C., Veng, L., Allgeier, C., Young, D., Browning, M., Bickford, P. (2004). "Sulindac improves memory and increases NMDA receptor subunits in aged Fischer 344 rats." Neurobiol Aging **25**(3): 315-24.
- Mishizen-Eberz, A. J., Rissman, R., Carter, T., Ikonovic, M., Wolfe, B., Armstrong, D. (2004). "Biochemical and molecular studies of NMDA receptor subunits NR1/2A/2B in hippocampal subregions throughout progression of Alzheimer's disease pathology." Neurobiol Dis **15**(1): 80-92.

- Monyer, H., Sprengel, R., Schoepfer, R., Herb, A., Higuchi, M., Lomeli, M., Burnashev, N., Sakmann, B., Seeburg, P. (1992). "Heteromeric NMDA receptors: molecular and functional distinction of subtypes." Science **256**(5060): 1217-21.
- Monyer, H., Burnashev, N., Laurie, D., Sakmann, B., Seeburg, P. (1994). "Developmental and regional expression in the rat brain and functional properties of four NMDA receptors." Neuron **12**(3): 529-40.
- Mori, H., Masaki, H., Yamakura, T., Mishina, M. (1992). "Identification by mutagenesis of a Mg(2+)-block site of the NMDA receptor channel." Nature **358**(6388): 673-5.
- Mori, H. and M. Mishina (1995). "Structure and function of the NMDA receptor channel." Neuropharmacology **34**(10): 1219-37.
- Moriyoshi, K., Masu, M., Ishii, T., Shigemoto, R., Mizuno, N., Nakanishi, S. (1991). "Molecular cloning and characterization of the rat NMDA receptor." Nature **354**(6348): 31-7.
- Morris, R. G., Garrud, P., Rawlins, J., O'Keefe, J. (1982). "Place navigation impaired in rats with hippocampal lesions." Nature **297**(5868): 681-3.
- Morris, R. G., Anderson, E., Lynch, G., Baudry, M. (1986). "Selective impairment of learning and blockade of long-term potentiation by an N-methyl-D-aspartate receptor antagonist, AP5." Nature **319**(6056): 774-6.
- Morris, R. G. (2003). "Long-term potentiation and memory." Philos Trans R Soc Lond B Biol Sci **358**(1432): 643-7.
- Mott, D. D., Doherty, J., Zhang, S., Washburn, M., Fendley, M., Lyuboslavsky, P., Traynelis, S., Dingledine, R. (1998). "Phenylethanolamines inhibit NMDA receptors by enhancing proton inhibition." Nat Neurosci **1**(8): 659-67.
- Mountjoy, C. Q. (1986). "Correlations between neuropathological and neurochemical changes." Br Med Bull **42**(1): 81-5.

- Mutel, V., Buchy, D., Klingelschmidt, A., Messer, J., Bleuel, Z., Kemp, J., Richards, J. (1998). "In vitro binding properties in rat brain of [3H]Ro 25-6981, a potent and selective antagonist of NMDA receptors containing NR2B subunits." J Neurochem **70**(5): 2147-55.
- Myers, S. J., Dingledine, R., Borges, K. (1999). "Genetic regulation of glutamate receptor ion channels." Annu Rev Pharmacol Toxicol **39**: 221-41.
- Nakane, P. K. and G. B. Pierce, Jr. (1967). "Enzyme-labeled antibodies for the light and electron microscopic localization of tissue antigens." J Cell Biol **33**(2): 307-18.
- Nakanishi, N., Axel, R., Schneider, N. (1992). "Alternative splicing generates functionally distinct N-methyl-D-aspartate receptors." Proc Natl Acad Sci U S A **89**(18): 8552-6.
- Nakazawa, T., Komai, S., Tezuka, T., Hisatsune, C., Ilmemori, H., Semba, K., Mishina, M., Manabe, T., Yamamoto, T. (2001). "Characterization of Fyn-mediated tyrosine phosphorylation sites on GluR epsilon 2 (NR2B) subunit of the N-methyl-D-aspartate receptor." J Biol Chem **276**(1): 693-9.
- Nash, J. E. and J. M. Brotchie (2000). "A common signaling pathway for striatal NMDA and adenosine A2a receptors: implications for the treatment of Parkinson's disease." J Neurosci **20**(20): 7782-9.
- Nicholl, D. (2003). "Tutorials in Neurology: Parkinson's Disease." Department of Clinical Neurosciences. <http://medweb.bham.ac.uk>.
- Nicolas, C. and C. Carter (1994). "Autoradiographic distribution and characteristics of high- and low-affinity polyamine-sensitive [3H]ifenprodil sites in the rat brain: possible relationship to NMDAR2B receptors and calmodulin." J Neurochem **63**(6): 2248-58.
- Nikam, S. S. and L. T. Meltzer (2002). "NR2B selective NMDA receptor antagonists." Curr Pharm Des **8**(10): 845-55.

- Nishi, M., Hinds, H., Lu, H., Kawata, M., Hayashi, Y. (2001). "Motoneuron-specific expression of NR3B, a novel NMDA-type glutamate receptor subunit that works in a dominant-negative manner." J Neurosci **21**(23): RC185.
- Nowak, L., Bregestovski, P., Ascher, P., Herbet, A., Prochiantz, A. (1984). "Magnesium gates glutamate-activated channels in mouse central neurones." Nature **307**(5950): 462-5.
- O'Keefe, J. and D. H. Conway (1978). "Hippocampal place units in the freely moving rat: why they fire where they fire." Exp Brain Res **31**(4): 573-90.
- Pabel, J., Hofner, G., Wanner, K. (2000). "Synthesis and resolution of racemic eliprodil and evaluation of the enantiomers of eliprodil as NMDA receptor antagonists." Bioorg Med Chem Lett **10**(12): 1377-80.
- Parkinson, J. (2002). "An essay on the shaking palsy. 1817." J Neuropsychiatry Clin Neurosci **14**(2): 223-36; discussion 222.
- Parsons, C. G., Danysz, W., Hesselink, M., Hartmann, S., Lorenz, B., Wollenburg, C, Quack, G. (1998a). "Modulation of NMDA receptors by glycine--introduction to some basic aspects and recent developments." Amino Acids **14**(1-3): 207-16.
- Parsons, C. G., Danysz, W., Quack, G. (1998). "Glutamate in CNS disorders as a target for drug development: an update." Drug News Perspect **11**(9): 523-79.
- Perry, E. K., Piggott, M., Court, J., Johnson, M., Perry, R. (1993). "Transmitters in the developing and senescent human brain." Ann N Y Acad Sci **695**: 69-72.
- Perry, R. H. (1993). "A guide to the cortical regions." Neuropsychiatric Disorders: pp. 1.1-1.10.
- Peters, A., Moss, M., Sethares, C. (2000). "Effects of aging on myelinated nerve fibers in monkey primary visual cortex." J Comp Neurol **419**(3): 364-76.

- Philpot, B. D., Weisberg, M., Ramos, M., Sawtell, N., Tang, Y., Tsien, J., Bear, M. (2001). "Effect of transgenic overexpression of NR2B on NMDA receptor function and synaptic plasticity in visual cortex." Neuropharmacology **41**(6): 762-70.
- Piggott, M. A., Perry, E., Perry, R., Court, J. (1992). "[3H]MK-801 binding to the NMDA receptor complex, and its modulation in human frontal cortex during development and aging." Brain Res **588**(2): 277-86.
- Piggott, M. A., Perry, E., Court, J., Perry, R. (1994). "Modulation of [3H]MK-801 binding by polyamines in human development and aging." Neuroscience Research communications **15**: 49-58.
- Premkumar, L. S. and A. Auerbach (1997). "Stoichiometry of recombinant N-methyl-D-aspartate receptor channels inferred from single-channel current patterns." J Gen Physiol **110**(5): 485-502.
- Racine, R. J., Milgram, N., Hafner, S. (1983). "Long-term potentiation phenomena in the rat limbic forebrain." Brain Res **260**(2): 217-31.
- Read, S., Pedersen, N., Gatz, M., Berg, S., Vuoksimaa, E., Malmberg, B., Johansson, B., McClearn, G. (2006). "Sex differences after all those years? Heritability of cognitive abilities in old age." J Gerontol B Psychol Sci Soc Sci **61**(3): P137-43.
- Reymann, K. G., Matthies, H., Schulzeck, K., Matthies, H. (1989). "N-methyl-D-aspartate receptor activation is required for the induction of both early and late phases of long-term potentiation in rat hippocampal slices." Neurosci Lett **96**(1): 96-101.
- Reynolds, I. J. and R. J. Miller (1989). "Ifenprodil is a novel type of N-methyl-D-aspartate receptor antagonist: interaction with polyamines." Mol Pharmacol **36**(5): 758-65.
- Richter, A. (2003). "The NMDA receptor NR2B subtype selective antagonist Ro 25-6981 aggravates paroxysmal dyskinesia in the dt(sz) mutant." Eur J Pharmacol **458**(1-2): 107-10.

- Rypma, B. and M. D'Esposito (2000). "Isolating the neural mechanisms of age-related changes in human working memory." Nat Neurosci **3**(5): 509-15.
- Sakimura, K., Kutsuwada, T., Ito, I., Manabe, T., Takayama, C., Kushiya, E., Yagi, T., Aizawa, S., Inoue, Y., Sugiyama, H., et al. (1995). "Reduced hippocampal LTP and spatial learning in mice lacking NMDA receptor epsilon 1 subunit." Nature **373**(6510): 151-5.
- Sambrook, J., Fritsch, E., Maniatis, T. (1989). "Molecular Cloning. A Laboratory Manual." Cold Spring Harbor, Laboratory Press, NY 2nd Edition.
- Scheibel, M. E., Lindsay, R., Tomiyasu, U., Scheibel, A. (1975). "Progressive dendritic changes in aging human cortex." Exp Neurol **47**(3): 392-403.
- Schwartzkroin, P. A. and K. Wester (1975). "Long-lasting facilitation of a synaptic potential following tetanization in the in vitro hippocampal slice." Brain Res **89**(1): 107-19.
- Scoville, W. B. and B. Milner (1957). "Loss of recent memory after bilateral hippocampal lesions." J Neurol Neurosurg Psychiatry **20**(1): 11-21.
- Sharma, T. A. and I. J. Reynolds (1999). "Characterization of the effects of polyamines on [125I]MK-801 binding to recombinant N-methyl-D-aspartate receptors." J Pharmacol Exp Ther **289**(2): 1041-7.
- Sheng, M., Cummings, J., Roldan, L., Jan, Y., Jan, L. (1994). "Changing subunit composition of heteromeric NMDA receptors during development of rat cortex." Nature **368**(6467): 144-7.
- Shi, S. R., Key, M., Kalra, K. (1991). "Antigen retrieval in formalin-fixed, paraffin-embedded tissues: an enhancement method for immunohistochemical staining based on microwave oven heating of tissue sections." J Histochem Cytochem **39**(6): 741-8.

- Standaert, D. G., Testa, C., Young, A., Penney, J. (1994). "Organization of N-methyl-D-aspartate glutamate receptor gene expression in the basal ganglia of the rat." J Comp Neurol **343**(1): 1-16.
- Steece-Collier, K., Chambers, L., Jaw-Tsai, S., Menniti, F., Greenamyre, J. (2000). "Antiparkinsonian actions of CP-101,606, an antagonist of NR2B subunit-containing N-methyl-d-aspartate receptors." Exp Neurol **163**(1): 239-43.
- Sucher, N. J., Akbarian, S., Chi, C., Leclarc, C., Awobuluyi, M., Deitcher, D., Wu, M., Yuan, J., Jones, E., Lipton, S. (1995). "Developmental and regional expression pattern of a novel NMDA receptor-like subunit (NMDAR-L) in the rodent brain." J Neurosci **15**(10): 6509-20.
- Sugihara, H., Moriyoshi, K., Ishii, T., Masu, M., Nakanishi, S. (1992). "Structures and properties of seven isoforms of the NMDA receptor generated by alternative splicing." Biochem Biophys Res Commun **185**(3): 826-32.
- Sun, L., Shipley, M., Lidow, M. (2000). "Expression of NR1, NR2A-D, and NR3 subunits of the NMDA receptor in the cerebral cortex and olfactory bulb of adult rat." Synapse **35**(3): 212-21.
- Sze, C., Bi, H., Kleinschmidt-De Masters, B., Filley, C., Martin, L. (2001). "N-Methyl-D-aspartate receptor subunit proteins and their phosphorylation status are altered selectively in Alzheimer's disease." J Neurol Sci **182**(2): 151-9.
- Takai, H., Katayama, K., Yasoshima, A., Uetsuka, K., Nakayama, H., Doi, K. (2003a). "NMDA-induced apoptosis in the developing rat brain." Exp Toxicol Pathol **55**(1): 33-7.
- Takai, H., Katayama, K., Uetsuka, K., Nakayama, H., Doi, K. (2003b). "Distribution of N-methyl-D-aspartate receptors (NMDARs) in the developing rat brain." Exp Mol Pathol **75**(1): 89-94.

- Tamaru, M., Yoneda, Y., Ogita, K., Shimizu, J., Nagata, Y. (1991). "Age-related decreases of the N-methyl-D-aspartate receptor complex in the rat cerebral cortex and hippocampus." Brain Res **542**(1): 83-90.
- Tang, Y. P., Shimizu, E., Dube, G., Rampon, C., Kerchner, G., Zhou, M., Liu, G., Tsien, J. (1999). "Genetic enhancement of learning and memory in mice." Nature **401**(6748): 63-9.
- Tang, Y. P., Wang, H., Feng, R., Kyin, M., Tsien, J. (2001). "Differential effects of enrichment on learning and memory function in NR2B transgenic mice." Neuropharmacology **41**(6): 779-90.
- Thompson, C. L., Drewery, D., Atkins, H., Stephenson, F.A., Chazot, P. (2000). "Immunohistochemical localization of N-methyl-D-aspartate receptor NR1, NR2A, NR2B and NR2C/D subunits in the adult mammalian cerebellum." Neurosci Lett **283**(2): 85-8.
- Thompson, C. L., Drewery, D., Atkins, H., Stephenson, F.A., Chazot, P. (2002). "Immunohistochemical localization of N-methyl-D-aspartate receptor subunits in the adult murine hippocampal formation: evidence for a unique role of the NR2D subunit." Brain Res Mol Brain Res **102**(1-2): 55-61.
- Timiras, P. S., Hudson, D., Oklund, S. (1973). "Changes in central nervous system free amino acids with development and aging." Prog Brain Res **40**(0): 267-75.
- Tossman, U., Segovia, J., Ungerstedt, U. (1986). "Extracellular levels of amino acids in striatum and globus pallidus of 6-hydroxydopamine-lesioned rats measured with microdialysis." Acta Physiol Scand **127**(4): 547-51.
- Wafford, K. A., Bain, C., Le Bourdelles, B., Whiting, P., Kemp, J. (1993). "Preferential co-assembly of recombinant NMDA receptors composed of three different subunits." Neuroreport **4**(12): 1347-9.

- Wahlin, A., Macdonald, S., De Frias, C., Nilsson, L., Dixon, R. (2006). "How do health and biological age influence chronological age and sex differences in cognitive aging: moderating, mediating, or both?" Psychol Aging **21**(2): 318-32.
- Wang, Y. H., Bosy, T., Yasuda, R., Grayson, D., Vicini, S., Pizzorusso, T., Wolfe, B. (1995). "Characterization of NMDA receptor subunit-specific antibodies: distribution of NR2A and NR2B receptor subunits in rat brain and ontogenic profile in the cerebellum." J Neurochem **65**(1): 176-83.
- Wang, C. X. and A. Shuaib (2005). "NMDA/NR2B selective antagonists in the treatment of ischemic brain injury." Curr Drug Targets CNS Neurol Disord **4**(2): 143-51.
- Watanabe, M., Inoue, Y., Sakimura, K., Mishina, M. (1992). "Developmental changes in distribution of NMDA receptor channel subunit mRNAs." Neuroreport **3**(12): 1138-40.
- Watanabe, M., Inoue, Y., Sakimura, K., Mishina, M. (1993). "Distinct distributions of five N-methyl-D-aspartate receptor channel subunit mRNAs in the forebrain." J Comp Neurol **338**(3): 377-90.
- Watkins, J. C. (1962). "The Synthesis Of Some Acidic Amino Acids Possessing Neuropharmacological Activity." J Med Pharm Chem **91**: 1187-99.
- Watkins, J. C., Krogsgaard-Larsen, P., Honore, T. (1990). "Structure-activity relationships in the development of excitatory amino acid receptor agonists and competitive antagonists." Trends Pharmacol Sci **11**(1): 25-33.
- Wenk, G. L., Walker, L., Price, D., Cork, L. (1991). "Loss of NMDA, but not GABA-A, binding in the brains of aged rats and monkeys." Neurobiol Aging **12**(2): 93-8.
- Wenzel, A., Scheurer, L., Kunzi, R., Fritschy, J., Mohler, H., Benke, D. (1995). "Distribution of NMDA receptor subunit proteins NR2A, 2B, 2C and 2D in rat brain." Neuroreport **7**(1): 45-8.

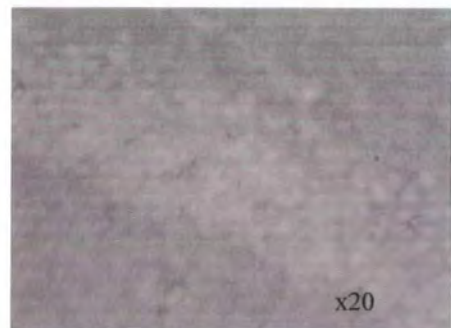
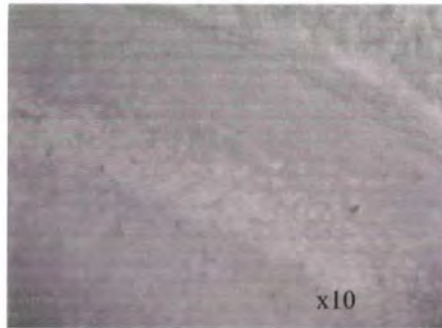
- Wenzel, A., Fritschy, J., Mohler, H., Benke, D. (1997). "NMDA receptor heterogeneity during postnatal development of the rat brain: differential expression of the NR2A, NR2B, and NR2C subunit proteins." J Neurochem **68**(2): 469-78.
- Wessell, R. H., Ahmed, S., Menniti, F., Dunbar, G., Chase, T., Oh, J. (2004). "NR2B selective NMDA receptor antagonist CP-101,606 prevents levodopa-induced motor response alterations in hemi-parkinsonian rats." Neuropharmacology **47**(2): 184-94.
- White, T. L. and S. L. Youngentob (2004). "The effect of NMDA-NR2B receptor subunit over-expression on olfactory memory task performance in the mouse." Brain Res **1021**(1): 1-7.
- Wilcock, G. K. and M. M. Esiri (1982). "Plaques, tangles and dementia. A quantitative study." J Neurol Sci **56**(2-3): 343-56.
- Williams, K. (1994). "Subunit-specific potentiation of recombinant N-methyl-D-aspartate receptors by histamine." Mol Pharmacol **46**(3): 531-41.
- Williams, K. (1995). "Pharmacological properties of recombinant N-methyl-D-aspartate (NMDA) receptors containing the epsilon 4 (NR2D) subunit." Neurosci Lett **184**(3): 181-4.
- Williams, J. M., Guevremont, D., Kennard, J., Mason-Parker, S., Tate, W., Abraham, W. (2003). "Long-term regulation of N-methyl-D-aspartate receptor subunits and associated synaptic proteins following hippocampal synaptic plasticity." Neuroscience **118**(4): 1003-13.
- Wong, T. P. (2002). "Aging of the Cerebral Cortex." McGill Journal of Medicine **6**: 104-113.

- Wyllie, D. J., Behe, P., Nassar, M., Schoepfer, R., Colquhoun, D. (1996). "Single-channel currents from recombinant NMDA NR1a/NR2D receptors expressed in *Xenopus* oocytes." Proc Biol Sci **263**(1373): 1079-86.
- Yoneda, Y., Ogita, K., Enomoto, R., Suzuki, T., Kito, S. (1991). "Identification and characterization of specific binding sites of [3H]spermidine in synaptic membranes of rat brain." Brain Res **563**(1-2): 17-27.
- Yoshimura, Y., Ohmura, T., Komatsu, Y. (2003). "Two forms of synaptic plasticity with distinct dependence on age, experience, and NMDA receptor subtype in rat visual cortex." J Neurosci **23**(16): 6557-66.
- Zhang, X. X. and W. X. Shi (2001). "Dynamic modulation of NMDA-induced responses by ifenprodil in rat prefrontal cortex." Synapse **39**(4): 313-8.
- Zhong, J., Carrozza, D., Williams, K., Pritchett, D., Molinoff, P. (1995). "Expression of mRNAs encoding subunits of the NMDA receptor in developing rat brain." J Neurochem **64**(2): 531-9.
- Zhou, M. and M. Baudry (2006). "Developmental changes in NMDA neurotoxicity reflect developmental changes in subunit composition of NMDA receptors." J Neurosci **26**(11): 2956-63.

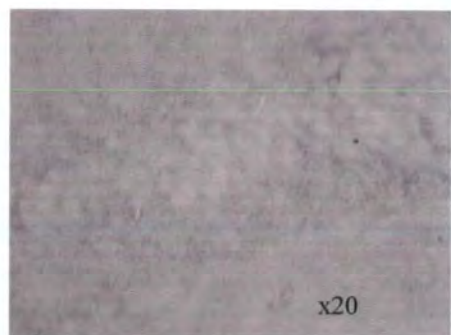
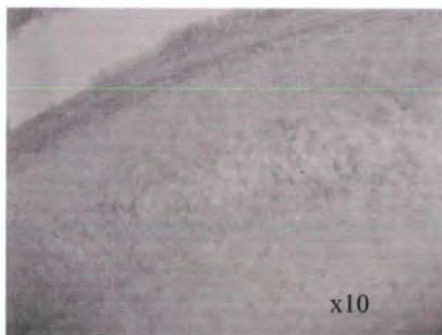
Appendix One: Chapter 3, Section 3.2.4 Continuation.

Additional Immunohistochemistry data using an in-house generated anti-NR2D antibody. The anti-NR2D antibodies were generated and characterised as described by Thompson *et al* (2002). The peptide corresponding to the amino acids 1307-1323 (LGTRRGSAHFSSLESEV) of the mouse NR2D subunit was conjugated to thyroglobulin by the glutaraldehyde method. The resultant conjugate was used to generate polyclonal antibodies in rabbits. See Chapter 3, section 3.2.4 for methods.

2D P21 CA1



2D P21 CA2



2D P21 CA3

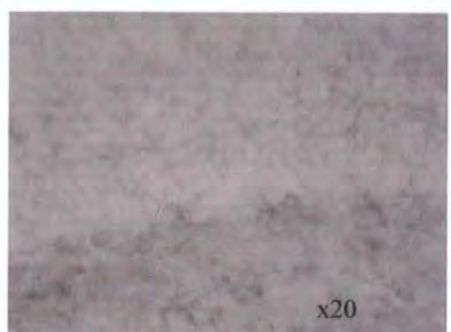
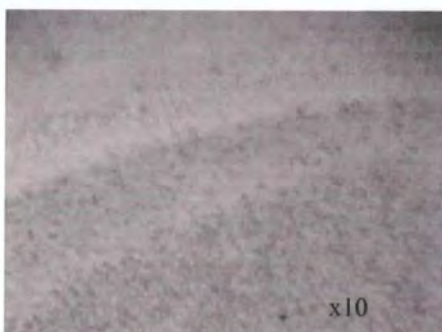


Figure 1 Immunohistochemical staining of P21 rat Hippocampal Formation using DAB against anti-NR2D antibody.

2D Adult CA1



2D Adult CA2



2D Adult CA3



Figure 2 Immunohistochemical staining of Adult rat Hippocampal Formation using DAB against anti-NR2D antibody.

2D P21 Thalamus



x10



x20

2D Adult Thalamus



x10

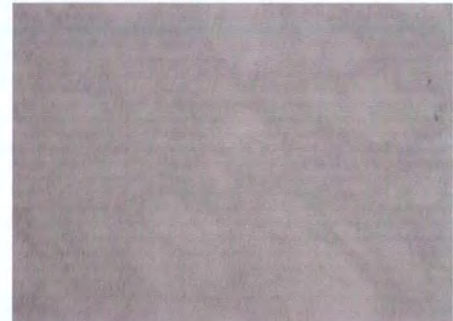


x20

2D Adult Striatum,



x10



x20

Figure 3 Immunohistochemical staining of P21 and Adult rat Thalamus and Striatum using DAB against anti-NR2D antibody.

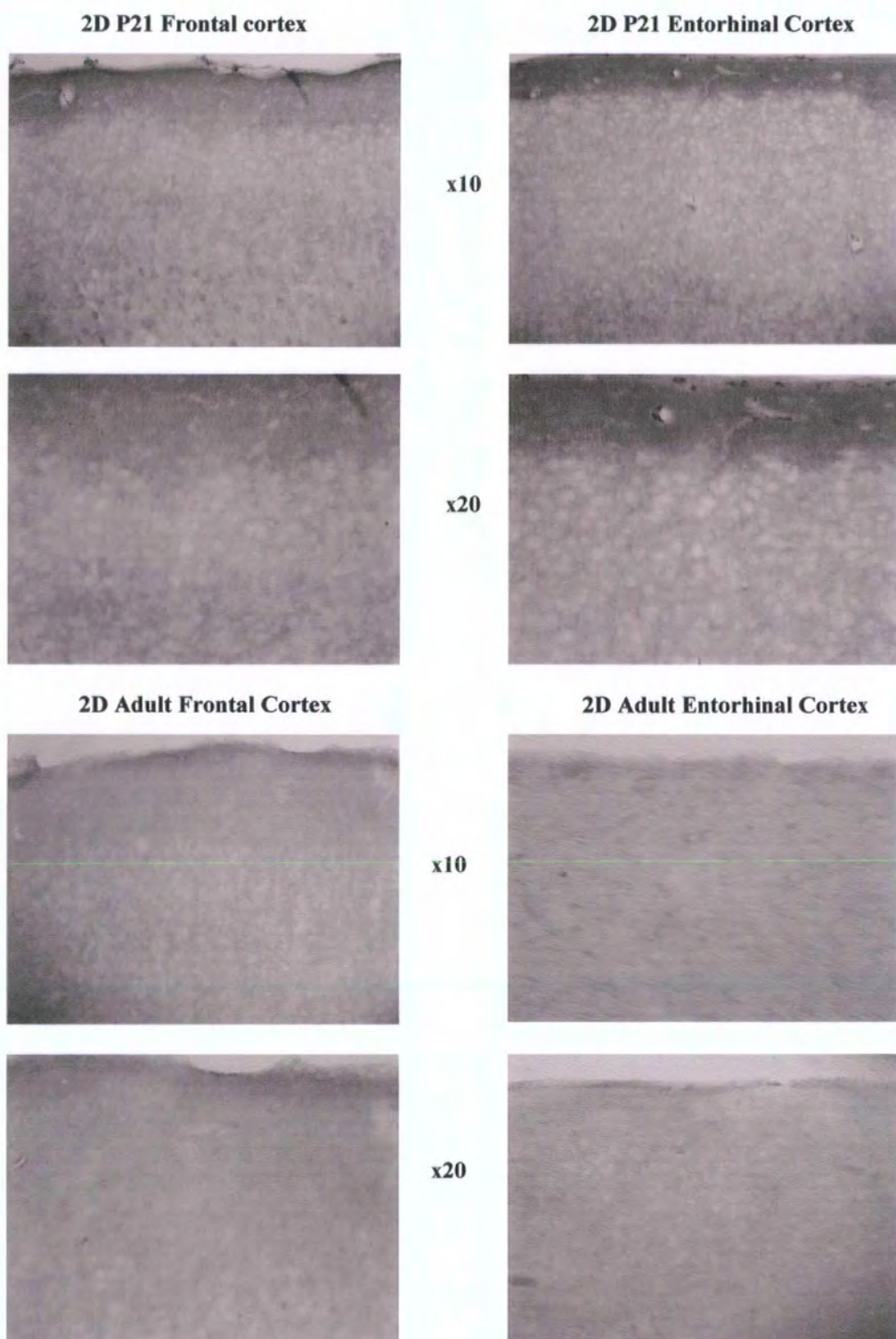


Figure 4 Immunohistochemical staining of P21 and Adult rat Frontal and Entorhinal Cortex using DAB against anti-NR2D antibody.

Publications and Conferences/Meetings Attended

1. **Neuroscience North East 2002** at University of Sunderland, December 2002.
2. **Neuroscience North East 2003** at University of Durham, December 2003.

Poster Presentation.

“Probing the NR2B subunit in the rodent and human CNS with novel defined pharmacological and immunological tools”.

3. **Molecular Biology of the Cell Forum.** Departmental meeting at University of Sunderland, March 2004.

Oral Presentation.

“Probing the NMDAR2B subunit in the mammalian brain”

4. **British Pharmacological Society, Summer Meeting.** Joint with the Danish Society for Pharmacology and Toxicology, at University of Bath. July 2004

Oral presentation.

“Probing the NR2B in the central mammalian nervous system: Further evidence for distinct NR2B ligands”

5. **Neuroscience North East 2004** at University of Newcastle, December 2004

Oral presentation

“Differential Pharmacological Properties of Structurally Distinct NMDAR2B Ligands”

6. **British Pharmacological Society (BPS)** at University of Newcastle, December 2004

Abstract (R Sheahan, M Lake, M Piggott and PL Chazot (2005) Br. J. Pharmacol (Suppl.) Newcastle meeting. Differential pharmacological properties of structurally distinct NR2B ligands).

Poster presentation

“Differential Pharmacological Properties of Structurally Distinct NMDAR2B Ligands”

7. British Neuroscience Association (BNA) 2005 at Durham University, September

Abstract (RL Sheahan, MA Piggott, M Lake, CL Thompson, PL Chazot (2005) BNA Postgraduate and Early Career conference, Durham).

Oral presentation

“Comparative autoradiographical analyses of Rodent and Human Brain using distinct NMDAR2B-selective ligands, [³H] Ro 25,6981 and [³H] CP-101,606”

8. British Pharmacological Society Imaging Special Interest Group Symposium, London, December 2005,

Oral Presentation

Given by PL Chazot CNS receptor imaging, Invited Symposium speaker, Presented some of our latest data funded by the PDS.

9. Fifth Forum of European Neuroscience, Vienna, Austria. July 2006.
Organised by FENS (Federation of European Neuroscience Societies).

Poster presented by P.L. Chazot

“Probing NMDAR2B subtypes in human ageing and dementias”

10. Third year Assessment to Biological Sciences Department, April 2006.

Oral Presentation

“Analyses of Rodent and Human Brain using distinct NMDAR2B-selective ligands, [³H]Ro 25,6981 and [³H]CP-101,606 “

Publications - Manuscripts in Preparation

1. R Sheahan, FC Shenton, D Burn, M Piggott and PL Chazot.

Probing the NMDAR2B receptor subtype in human ageing: tissue-dependent sex differences

2. R Sheahan, FC Shenton, D Burn, M Piggott and PL Chazot.

Detailed study of the NMDAR2B subtype in human Dementia with Lewy bodies and Parkinson's disease with Dementia

3. R Sheahan, FC Shenton, D Burn, M Piggott and PL Chazot.

Differential NMDAR2B profiles in human dementias

4. A Dougalis, G Lees, DT Monaghan, DE Jane and PL Chazot. Hippocampus.

Further definition of the NMDA receptor subtypes underlying hippocampal LTP and LTD

PROBING THE NR2B IN THE MAMMALIAN CENTRAL NERVOUS SYSTEM: FURTHER EVIDENCE FOR DISTINCT NR2B LIGANDS.

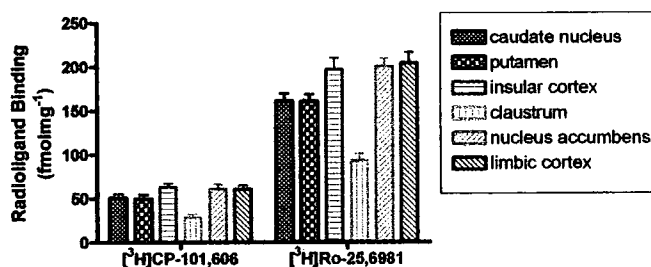
R.L. Sheahan¹, M. Lake^{1,2}, M. Piggott², and P.L. Chazot¹

¹School of Biological and Biomedical Sciences, Durham University, Durham, UK; ²MRC Unit, Newcastle General Hospital, Newcastle-upon-Tyne, UK

The N-methyl-D-aspartate (NMDA) receptor is a heteromeric ligand-gated ion channel comprising a range of subunits, namely NR1, NR2A-D and NR3A-B. The specific expression profile of the NR2B subunit in the brain, is developmentally and regionally regulated, and is involved in key processes such as learning, memory and motor coordination. There is clear evidence for different types of NR2B-containing receptors (NR1/2B, NR1/2B/2A, NR1/2B/2D) (Chazot, 2004). Previous studies in our laboratory have provided evidence that there are at least two classes of NR2B-selective compounds, one class which binds all NR1/NR2B-containing receptors (Ro 25,6981) and one which binds to just the dimeric NR1/NR2B receptor subtype (CP-101,606) (Chazot *et al.*, 2002). The aims of this study are to map the distinct NR1/NR2B-containing subtypes and in the murine and human brain using ligand autoradiography (Mutel *et al.*, 1998).

Both [³H] Ro 25,6981 and [³H] CP-101,606 specifically labelled mouse and human hippocampus, thalamus, striatum and cortex, consistent with our previous immunohistochemical studies (Thompson *et al.*, 2002). Notably, the number of specific [³H] Ro 25,6981 binding sites were consistently higher than [³H] CP-101,606 binding sites in both murine (not shown) and human brain structures (n = 16-26, p <0.0001) (Figure 1). These data provide further evidence that CP-101,606 labels a subset of NR2B-containing receptors.

Figure 1 Control human brain
Ligand autoradiography (mean
± SD for 16-26 samples)



Competition binding studies were used to determine the pharmacological properties of another NR2B ligand, ifenprodil using [³H] Ro 25,6981 binding to adult or P21 male Sprague-Dawley rat forebrain membranes. The assay was performed as described in Chazot *et al.*, 2002, except non-specific binding was defined by 100 μ M Ifenprodil. The competition curve for ifenprodil binding, using P21 membranes, displayed a pseudo Hill slope coefficient close to unity ($nH = -0.87 \pm 0.20$), with an IC_{50} value of $8.69 \pm 1.32 \mu M$. In contrast, the curve for ifenprodil binding using adult membranes was best fitted to a two-site fit model, with the $nH = 0.65 \pm 0.23$ (high affinity site, $EC_{50} = 0.25 \mu M$, $35 \pm 5\%$; low affinity site, $EC_{50} = 10.1 \mu M$, $63 \pm 5\%$). Therefore, we provide preliminary evidence that ifenprodil binds to more than one subtype of NR2B-containing receptors present in the adult forebrain, and that distinct populations of NR2B-containing receptors exist in young and mature rat forebrain.

Chazot, P.L. *et al.* (2002) *Neuropharmacol.* 42, p319-324

Chazot, P.L. (2004) *Current Medicinal Chemistry*, 10, p1241-1253

Mutel, V. *et al.* (1998) *Journal of Neurochemistry*, 70, 5, p2147-2155

Thompson, C.L. *et al.* (2002) *Molecular Brain Research*, 102, p55-61

This study was funded by Pfizer Inc (Japan)

